Branching control mechanisms in the model tree *Populus*: analyzing the role of strigolactones and *BRANCHED1*

Dissertation

for the award of the degree
"Doctor rerum naturalium"
of the Georg-August-Universität Göttingen

within the doctoral program "Molecular Biology of Cells"
of the Georg-August University School of Science (GAUSS)

submitted by

Merlin Muhr

from Herdecke, Germany

Göttingen, 2015

Thesis Committee

PD Dr. Thomas Teichmann
(Department of Plant Cell Biology, Georg-August-Universität Göttingen)
Prof. Dr. Andrea Polle
(Department of Forest Botany and Tree Physiology, Georg-August-Universität Göttingen)
Jun. Prof. Dr. Cynthia Gleason
(Department of Molecular Biology and Physiology, Georg-August-Universität Göttingen)

Members of the Examination Board

Referee: **PD Dr. Thomas Teichmann**
(Department of Plant Cell Biology, Georg-August-Universität Göttingen)

2nd Referee: **Prof. Dr. Andrea Polle**
(Department of Forest Botany and Tree Physiology, Georg-August-Universität Göttingen)

Further members of the Examination Board

Jun. Prof. Dr. Cynthia Gleason
(Department of Plant Molecular Biology and Physiology, Georg-August-Universität Göttingen)

Prof. Dr. Christiane Gatz
(Department of Plant Molecular Biology and Physiology, Georg-August-Universität Göttingen)

Prof. Dr. Stefan Jakobs
(Department of NanoBiophotonics, Max Planck Institute for Biophysical Chemistry, Göttingen)

Prof. Dr. Volker Lipka
(Department of Plant Cell Biology, Georg-August-Universität Göttingen)

Date of oral examination: 07.09.2015

Declaration

Hereby, I declare that this dissertation was undertaken independently and without any unauthorized aid.

I declare that this Ph.D. dissertation has not been presented to any other examining body either in its present or a similar form.

Furthermore, I also affirm that I have not applied for a Ph.D. or Dr. rer. nat. at any other higher school of education.

Göttingen, 14.07.2015

_____

Merlin Muhr

I. Table of Contents

II. List of Tables

III. List of Figures

IV. List of Abbreviations

:	Fused to (fusion of DNA sequences)
°C	Degrees Celsius
%	Percent
% (v/v)	Percent (volume/volume)
% (w/v)	Percent (weight/volume)
aa	Amino acid(s)
ABA	Abscisic acid
AM	Arbuscular mycorrhiza / Axillary meristem (depending on context)
amiRNA	artificial microRNA
AMP1	*ALTERED MERISTEM PROGRAM1*
Arabidopsis	*Arabidopsis thaliana*
A. thaliana	*Arabidopsis thaliana*
ATP	Adenosine triphosphate
bp	Base pair(s)
bHLH	basic helix-loop-helix
BLAST	Basic Local Alignment Search Tool
BR	Brassinosteroid
BRC1	*BRANCHED1*
CaMV 35S	Strong and constitutive 35S promoter from cauliflower mosaic virus
CCD	*CAROTENOID CLEAVAGE DIOXYGENASE*
CDS	Coding sequence
CK	Cytokinin
CKX	*CYTOKININ OXIDASE*
cm	Centimeter
CTP	Cytosine triphosphate
C_q	Quantification cycle
D	*DWARF*
DAD	*DECREASED APICAL DOMINANCE*
DAT	Days after treatment
DMSO	Dimethyl Sulfoxide
DNA	Deoxyribonucleic acid
DNase	Deoxyribonuclease
EDTA	Ethylenediaminetetraacetic acid
EF1	*ELONGATION FACTOR1*
EM	Ectomycorrhiza
EST	Expressed sequence tag
FC1	*FINE CULM1*

Fig.	Figure
GA	Gibberellic acid
Gent	Gentamicin
GFP	Green Fluorescent Protein
GR24	Synthetic SL analog
GTP	Guanosine triphosphate
GUS	β-glucuronidase
h	Hour(s)
HPLC-MS/MS	High-performance liquid chromatography - tandem mass spectrometry
IAA	Indole-3-acetic acid
IPT	*ISOPENTENYLTRANSFERASE*
JA	Jasmonic acid
Kan	Kanamycin
kb	Kilobases (1.000 bases)
l	Liter
LB	Luria Broth
m	Meter
M	Molar, mol/l
MAX1/2/3/4	*MORE AXILLARY GROWTH 1/2/3/4*
mg	Milligram
min	Minute(s)
ml	Milliliter
mm	Millimeter
mM	Millimolar
mRNA	messenger RNA
MS medium	Murashige & Skoog medium
µ	Micro
µg	Microgram
µl	Microliter
µm	Micrometer
µM	Micromolar
N	Nitrogen
ng	Nanogram
nm	Nanometer
NPA	1-N-naphthylphthalamic acid
nt	Nucleotide(s)
NTP	Nucleoside Triphosphate
ODx	Optical density at x nm wavelength

p.	Page
P	Phosphorus
PAR	Photosynthetically active radiation
PATS	Polar auxin transport stream
PCNA	*PROLIFERATING CELL NUCLEAR ANTIGEN*
Pc	*Populus* x *canescens*
PCR	Polymerase Chain Reaction
PEG	Polyethylene glycol
PIN1	*PIN-FORMED1*
Pt	*Populus trichocarpa*
P. x *can*	*Populus* x *canescens*
P. x *canescens*	*Populus* x *canescens*
qPCR	quantitative Polymerase Chain Reaction (real time PCR)
QTL	Quantitative trait locus
RAM	Root apical meristem
rcf	Relative centrifugal force (1 rcf is equivalent to 1 g = 9.81 m/s)
R/FR	Red/ far red ratio
Rif	Rifampicin
RMS	*RAMOSUS*
RNA	Ribonucleic acid
RNAi	RNA interference
RNase	Ribonuclease
rpm	Revolutions per minute
RT	Reverse Transcriptase
SA	Salicylic acid
SAM	Shoot apical meristem
SCF	Skp1—cullin—F-box protein complex
SD	Standard deviation
SDS	Sodium Dodecyl Sulphate
SL	Strigolactone
SLs	Strigolactones
SLB1/2	*STRIGOLACTONE BIOSYNTHESIS1/2*
SMS	Shoot multiplication signal
Spec	Spectinomycine
SPL14	*SQUAMOSA PROMOTER BINDING PROTEIN-LIKE 14*
SRC	Short rotation coppice
Tab.	Table
TAE	Tris-acetate-EDTA

Taq	*Thermus aquaticus*
TB1	*TEOSINTE BRANCHED1*
TCP	*TB1 CYCLOIDEA PCF*
T-DNA	Transferred DNA
TE	Tris-EDTA buffer
TF	Transcription factor
TPL	*TOPLESS*
Tris	Tris(hydroxymethyl)aminomethane
TTP	Thymidine triphosphate
UBQ	*UBIQUITIN*
UV	Ultraviolet
V	Volt
v/v	Volume (of solute) per volume (of solvent)
WT	Wild type
w/v	Weight (of solute) per volume (of solvent)
YEB	Yeast Extract Broth

V. Summary

Plants exhibit a large degree of phenotypic plasticity. Modifications of their genetically pre-defined body plan allow them to flexibly react to a wide range of environmental conditions. This includes changes in plant architecture, which are facilitated by the modular composition of the shoot. In the leaf axils of the primary stem, axillary buds are formed. Each of these buds has the potential to grow into a secondary stem, i.e. a branch. However, bud outgrowth is restricted and most buds are kept in a dormant state. To make the decision whether a bud is released from dormancy and grows into a branch, many endo- and exogenous factors are integrated in a complex network of hormones and transcription factors. This includes strigolactones (SLs), a novel class of phytohormones, which generally suppress bud outgrowth. The inhibitory effect of SLs is discussed to be mediated by flux modulation of the phytohormone auxin and/or regulation of other downstream targets directly within the bud. The most prominent example for a bud-specific SL-regulated gene is *BRANCHED1* (*BRC1*), whose transcript levels are positively influenced by SLs. It encodes a transcription factor which represses bud outgrowth, most likely by regulating cell cycling. SLs and *BRC1* were extensively studied in model species such as *Arabidopsis* (*Arabidopsis thaliana*), pea (*Pisum sativum*), petunia (*Petunia hybrida*) and rice (*Oryza sativa*). In contrast, our knowledge of the genes and pathways in woody perennial species, such as the model tree poplar (*Populus sp.*), is limited.

In this project, poplar orthologs of genes involved in SL biosynthesis (*MAX4*) and SL signaling (*MAX2*) were identified to investigate an anticipated role for SLs in controlling tree architecture. There are two orthologs each in poplar. To study their function, expression analysis was performed and transgenic lines were generated for amiRNA-mediated knockdowns of the individual orthologs, as well as simultaneous silencing of both. *MAX2* knockdowns were only partially successful and no phenotype could be observed, most likely due to a redundant function of the non-silenced ortholog. In contrast, *MAX4* double knockdowns were successful and typical SL-deficiency phenotypes were observed in the corresponding *amiMAX4-1+2* lines. This includes highly increased shoot branching, reduced plant height, reduced internode length and increased adventitious rooting. Direct quantification of SLs generally is difficult due to their low abundance, high instability and large diversity. Furthermore, standards and references for poplar SLs are not available, making measurements not feasible. Indirect evidence for SL-deficiency in *amiMAX4-1+2* plants was gathered instead, including successful complementation of the shoot phenotypes by grafting. Tree-specific aspects of bud

dormancy, especially winter dormancy, were also addressed. However, an influence of SLs could not be shown, indicating that SLs only appear to suppress bud outgrowth during the vegetative period.

As a downstream target of SLs and, therefore, another important component of branching control, a poplar *BRC1* ortholog was identified. This gene exhibited the typical expression patterns reported for other species and a significant down-regulation in the putatively SL-deficient *amiMAX4-1+2* lines. In addition, a poplar *BRC2* ortholog was found based on sequence and expression analysis. Both genes may control branching in poplar, integrating different environmental factors.

Taken together, the data generated in this study supports a role for SLs and *BRC1* as important regulators of bud outgrowth in poplar. The findings underline the high degree of conservation of fundamental processes involved in the control of plant architecture among a range of species, including trees. Beside of being a useful tool for discovering the role of SLs and *BRC1* in poplar, the highly branching lines generated in this project may be economically valuable for the use on short rotation coppices, where they may exhibit improved re-sprouting and canopy closure after coppicing.

VI. Zusammenfassung

Pflanzen verfügen über ein hohes Maß an phänotypischer Plastizität. Modifikationen ihres genetisch determinierten Aufbaus ermöglichen ihnen, flexibel auf ein breites Spektrum von Umwelteinflüssen zu reagieren. Dies umfasst Veränderungen der Pflanzenarchitektur, die durch den modularen Aufbau des Sprosses ermöglicht werden. In den Blattachseln des Primärsprosses werden Achselknospen angelegt. Jede einzelne dieser Knospen hat das Potenzial, zu einem Sekundärspross, d.h. einem Zweig, auszuwachsen. Der Knospenaustrieb wird jedoch reguliert und die meisten Knospen verbleiben in einem dormanten Status. Bei der Entscheidung, ob die Dormanz einer Knospe gebrochen wird und sie zu einem Zweig auswächst, spielen diverse endo- und exogene Faktoren eine Rolle, die in einem komplexen, aus Hormonen und Transkriptionsfaktoren bestehenden Regelnetz, integriert werden. Dieses umfasst Strigolactone (SL), eine neuartige Klasse von Phytohormonen, die im Allgemeinen den Knospenaustrieb hemmen. Es wird diskutiert, dass der inhibitorische Effekt der SL durch eine Modulation des Flusses des Phytohormons Auxin und/oder die Regulation anderer nachgelagerter Faktoren direkt in der Knospe herbeigeführt wird. Das bekannteste Beispiel für ein knospenspezifisches, SL-reguliertes Gen ist *BRANCHED1* (*BRC1*), dessen mRNA-Abundanz positiv von SL beeinflusst wird. Es codiert einen Transkriptionsfaktor der den Knospenaustrieb unterdrückt, was höchstwahrscheinlich über eine Regulation des Zellzyklus erfolgt. SL und *BRC1* wurden umfassend in Modellarten wie *Arabidopsis* (*Arabidopsis thaliana*), Erbse (*Pisum sativum*), Petunie (*Petunia hybrida*) und Reis (*Oryza sativa*) untersucht. Im Gegensatz dazu ist das Wissen über die Gene und Stoffwechselwege dieses Regelkreises in verholzten, ausdauernden Arten wie dem Modellbaum Pappel (*Populus sp.*), limitiert. In der vorliegenden Arbeit wurden Pappel-Orthologe von Genen, die an der SL-Biosynthese (*MAX4*) und der SL-Signaltransduktion (*MAX2*) beteiligt sind, identifiziert und auf eine vermutete Funktion in der Regulation der Baumarchitektur untersucht. Es existieren jeweils zwei Orthologe in der Pappel. Um ihre Funktion zu charakterisieren, wurden Expressionsanalysen durchgeführt und transgene Linien für amiRNA-vermittelte simultane oder einzelne *knock-downs* der beiden Orthologe erzeugt. *Knock-downs* von *MAX2* waren nur teilweise erfolgreich. Es konnte kein Phänotyp beobachtet werden, was höchstwahrscheinlich auf eine redundante Funktion des nicht herunterregulierten Orthologs zurückzuführen ist. *MAX4* Doppel-*Knock-downs* waren hingegen erfolgreich und es konnten typische SL-Mangelphänotypen in den entsprechenden *amiMAX4-1+2* Linien beobachtet werden. Diese umfassten eine erhöhte Sprossverzweigung, eine

Reduktion der Pflanzenhöhe, eine verkürzte Indernodienlänge sowie eine erhöhte Adventivbewurzelung. Durch ihre geringe Konzentration, hohe Instabilität und große Diversität ist die direkte Quantifizierung von SL sehr anspruchsvoll. Außerdem sind Standards und Referenzen für Pappel-SL nicht verfügbar, was direkte Messungen nicht durchführbar machte. Stattdessen wurden indirekte Hinweise auf SL-Mangel in den *amiMAX4-1+2* Pflanzen gesammelt. Ein Beispiel dafür ist die erfolgreiche Komplementation der Sprossphänotypen durch Pfropfung. Baumspezifische Aspekte der Knospendormanz, besonders die Winterdormanz, wurden ebenfalls untersucht. Ein Einfluss von SL konnte aber nicht nachgewiesen werden, was darauf hinweist, dass SL den Knospenaustrieb nur in der vegetativen Periode hemmen.

Als ein SL-reguliertes Zielgen und daher eine weitere wichtige Komponente der Verzweigungskontrolle wurde ein Pappel *BRC1* Ortholog identifiziert. Dieses Gen wies die typischen, in anderen Arten nachgewiesenen Expressionsmuster, sowie eine signifikant reduzierte Expression in den erzeugten *amiMAX4-1+2* Linien auf, welche wahrscheinlich reduzierte SL-Level haben. Zusätzlich wurde auf der Basis von Sequenz- und Expressionsanalysen ein Pappel *BRC2* Ortholog identifiziert. Beide Gene kontrollieren möglicherweise die Verzweigung in Pappeln und integrieren verschiedene Umwelteinflüsse.

Zusammengefasst legen die in diesem Projekt gewonnenen Daten eine Rolle von SL und *BRC1* als wichtige Regulatoren des Knospenaustriebs in Pappeln nahe. Die Ergebnisse machen deutlich, dass grundlegende Prozesse in der Kontrolle der Pflanzenarchitektur über ein breites Spektrum von Arten, einschließlich Bäumen, hoch konserviert sind. Abgesehen von ihrer Relevanz als Grundlage zur Erforschung der Rolle von SL und *BRC1* in Pappeln, sind die in diesem Projekt erzeugten stark verzweigten Linien möglicherweise wirtschaftlich für die Nutzung auf Kurzumtriebsplantagen interessant, auf welchen sie vermutlich über verbesserte Eigenschaften im Stockaustrieb nach der Ernte und im Kronenschluss verfügen.

1 Introduction

1.1 Plant architecture

Plants are sessile organisms. Their stationary lifestyle implies that they cannot change the location when environmental conditions become unfavorable, such as mobile organisms like most metazoan animals are able to do. Instead, plants possess a high degree of adaptivity, enabling them to cope with a wide range of environmental factors. To a large extent, this adaptivity is based on phenotypic plasticity: plants of the same genotype can exhibit enormously different phenotypes (Nicotra et al., 2010). The most obvious morphological adaptation to different growth conditions is a variation of plant architecture. There is a possible range from a plant bearing just the main shoot and no lateral branches to a highly ramified plant, possessing a large number of first- and higher-order branches. This flexible architecture is facilitated by the modular design of the plant shoot and a complex regulation of the branching process (McSteen and Leyser, 2005).

During embryogenesis, the bipolar apical-basal axis of the plant is determined by the formation of the shoot apical meristem (SAM) and the root apical meristem (RAM) as stem cell niches, giving rise to the primary shoot and root, respectively. The SAM establishes the shoot by iteratively and theoretically indeterminately initiating so-called phytomers during post-embryonic development. The phytomers can be regarded as the basic modules of the plant shoot and consist of an internode and a node with one or more attached leaves. In addition to the SAM (or primary meristem), so-called axillary meristems (or secondary meristems) are established in the leaf axils, i.e. at the adaxial side of the leaf bases. These meristems can produce buds, which have the potential to grow out and form a branch. A branch is a secondary growth axis, built in the same way as the primary shoot. Leaf axils of the branch also bear axillary buds and higher-order branching can occur, forming a complex structure (Bennett and Leyser, 2006; McSteen and Leyser, 2005; Sussex and Kerk, 2001). An illustration of the typical architecture of a dicotyledonous plant is shown in Fig. 1.1.

The branching process, outlined above, can be controlled at two levels: the formation of axillary meristems and subsequent regulation of their activity. There are many different mechanisms playing a role and especially bud outgrowth is influenced by numerous factors. In fact, many buds are arrested in a state of dormancy just after their formation. Endogenous factors such as the genetic background are integrated together with a large variety of exogenous conditions like the nutrient availability, damage, shading etc., to

decide whether a bud remains dormant or whether it becomes activated and grows into a lateral branch (Domagalska and Leyser, 2011). The underlying regulatory network allows the plant to flexibly adapt its genetically pre-defined body plan to the prevailing environmental conditions and react to changes. For example, as a response to loss of the shoot apex e.g. due to herbivory, axillary buds below the stump become activated and one or more lateral branches replace the lost shoot apex.

In the following chapters, the process of axillary bud development and the mechanisms regulating bud outgrowth are reviewed. The focus is on the action of hormones and transcription factors during bud outgrowth regulation. Strigolactones (SL) as recently identified hormones involved in this process, and their action, including an influence on the transcription factor *BRANCHED1* (*BRC1*), were a focus of this project. The special dormancy characteristics of perennial plants such as trees, and the economic significance of plant architecture, are discussed as well.

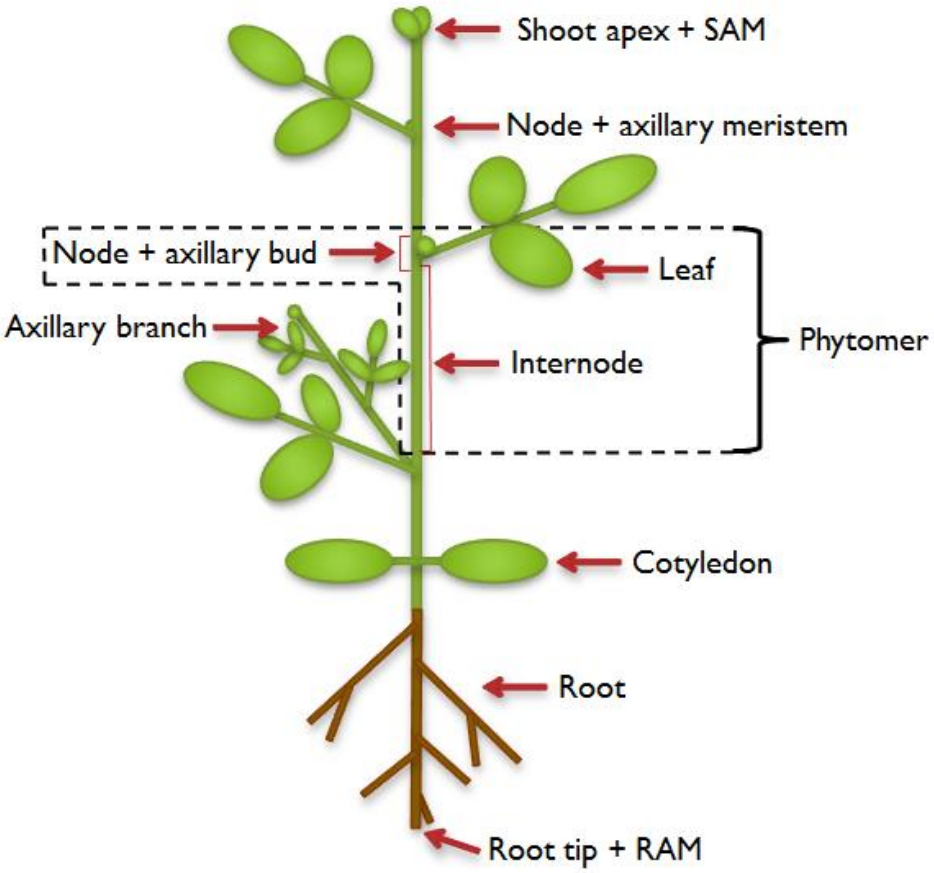

Fig. 1.1 Illustration of the typical architecture of a dicotyledonous plant. The primary shoot and root are established by the shoot and root apical meristems (SAM and RAM), respectively. The shoot is built as a consecutive arrangement of phytomers, which consist of an internode and a node with its attached leaf. In the leaf axils, axillary meristems are established and develop into axillary buds, which have the potential to grow out to form axillary branches. Image from Teichmann and Muhr (2015), modified.

1.2 Development of axillary meristems

The establishment of axillary meristems (AMs) in the leaf axils is an essential prerequisite for the formation of axillary buds and branches. When leaf primordia develop at the SAM, a boundary zone is formed between both structures as a region characterized by cells which are small, have stiff cell walls and exhibit a low dividing rate. In the center of this boundary zone, AMs develop (Janssen et al., 2014; Žádníková and Simon, 2014).

In the formation of the boundary zone, several factors were described to play a role. A local minimum of the growth-regulating phytohormone auxin in the boundary zone, caused by an altered distribution of the auxin efflux carrier protein PIN-FORMED1 (PIN1), appears to be important for the formation of AMs (Wang et al., 2014a, 2014b). Furthermore, brassinosteroids (BRs) as phytohormones involved in the regulation of cell growth and proliferation (Fridman and Savaldi-Goldstein, 2013), appear to play a major role as well. The transcription factor LATERAL ORGAN BOUNDARIES1 (LOB1) was shown to regulate BR levels in the boundary zone via the BR-inactivating enzyme PHYB ACTIVATION TAGGED SUPPRESSOR1 (BAS1), leading to the low cell size and proliferation rate observed in this zone (Bell et al., 2012). In addition, the growth-regulating phytohormone cytokinin (CK) is discussed to be involved in AM initiation (Wang et al., 2014b). Therefore, it appears that several hormones regulate the growth and division rate of cells in the boundary zone, keeping them in a slow-dividing and indeterminate state.

In addition to phytohormones, several transcriptions factors (TFs) were reported to be essential during the development of AMs. Except for LOB1 as described above, also the KNOXI transcription factor SHOOT MERISTEMLESS (STM) plays a role. STM is important for maintenance of the meristematic identity of the SAM (Long et al., 1996), but it is also expressed in the boundary zone (Long and Barton, 2000). Its expression requires the *Arabidopsis* GRAS domain transcription factor LATERAL SUPPRESSOR (LAS) (Greb et al., 2003). STM controls expression of the NAM-ATAF1/2-CUC2 (NAC) transcription factors CUP SHAPED COTYLEDONS1, 2, and 3 (CUC1, 2, and 3), which are essential for AM formation in *Arabidopsis* (Spinelli et al., 2011). Further transcription factors having important functions during AM development in *Arabidopsis* are the MYB transcription factor REGULATOR OF AXILLARY MERISTEMS1 (RAX1) (Keller et al., 2006) and the basic helix-loop-helix protein REGULATOR OF AXILLARY MERISTEM FORMATION (ROX) (Yang et al., 2012). While all genes mentioned above are *Arabidopsis* genes, numerous orthologs were described in other species, showing similar functions. It is discussed that many of the described factors act redundantly during formation of the boundary zone (Janssen et

al., 2014). They appear to be important in keeping the cells in this zone in a non-differentiated state, allowing them to develop into the AM.
Once established, the AM usually produces a few phytomers and then develops into an axillary bud (Bennett and Leyser, 2006; Stafstrom and Sarup, 2000). The bud can directly continue growth and form a branch, or its growth can be arrested. The resulting dormant bud can be activated at a later stage to resume growth, which is a tightly regulated process.

1.3 Regulation of axillary bud outgrowth

The outgrowth of axillary buds into lateral branches is regulated by a complex network involving hormones and transcription factors, integrating a multitude of endo- and exogenous factors which influence branching. In the following section, such factors are discussed. The three major hormones involved in bud outgrowth regulation are described along with BRANCHED1 (BRC1), a transcription factor playing a major role in integrating signals from different pathways in bud outgrowth control.

1.3.1 Endo- and exogenous factors influencing bud outgrowth

There are numerous factors having an impact on bud outgrowth. Undoubtedly, the genetic background has a major influence on plant architecture. Even within a given species, there are ecotypes, cultivars or varieties with low or high branch numbers. This becomes most evident in many cultivated species and often quantitative trait loci (QTL) are associated with this trait, for example in rice or willow (Cardoso et al., 2014; Salmon et al., 2014). In addition to the genetic background, also the position of a bud within a plant, which can be regarded as a "population" of competing buds, can play a role (Costes et al., 2014; White, 1979). A prominent example for the positional effect can be seen during apical dominance, a process in which the active apex suppresses outgrowth of axillary buds at the same shoot. When the apex is removed, usually one or few axillary buds grow out (Cline, 1997). These buds normally are the most apical buds, i.e. the ones closest to the decapitation site. The growing branches then re-establish apical dominance. Typically, buds which are located more basally, i.e. more distant from the decapitation site, will remain dormant. This indicates that the position of the bud can

decide about its fate. Beside of the genetic background and position effects, which both are endogenous factors, multiple exogenous factors significantly influence bud outgrowth. Such environmental factors can be biotic or abiotic or a linked combination of both, e.g. competition as a biotic factor will influence nutrient and light availability which are abiotic factors. For nutrients, especially the macronutrients nitrogen (N) and phosphorus (P), it is well-established that upon starvation, plants will suppress shoot growth and branching in favor of increased resource allocation to the root system, allowing the plant to scavenge a larger soil volume (Domagalska and Leyser, 2011). Shading by competing plants reduces the light red/far-red (R/FR) ratio and such a shift is detected by the phytochrome system, involving the photoreceptor phytochrome B (phyB). Branching then is repressed, allowing a resource allocation to the main shoot to outgrow competitors, known as the shade avoidance syndrome (Casal et al., 1986; Finlayson et al., 2010; González-Grandío et al., 2013; Pierik and Wit, 2014). Another environmental factor is removal of or damage to the apex, induced by herbivores, pathogens or harsh weather conditions. This will break apical dominance and induce bud outgrowth, as described above (Cline, 1997).
All factors, endogenous as well as exogenous ones, are integrated in a complex regulatory network of hormones and transcription factors to decide whether a bud stays dormant or grows out to form a branch.

1.3.2 Hormones in bud outgrowth regulation

There are three well-established major hormones playing a role in the regulation of bud outgrowth. Auxin and the recently identified strigolactones (SL) inhibit bud outgrowth, while cytokinin (CK) has a promoting effect. In the following paragraphs, the role of these hormones, as well as the extensive cross-talk between them, is outlined.

1.3.2.1 Auxin

Auxins, especially indole-3-acetic acid (IAA) as the most prominent representative of this class of phytohormones, are involved in many processes of plant development, including the regulation of branching (Ljung, 2013). Already early decapitation studies showed that a substance derived from the shoot apex is required for apical dominance (Thimann and Skoog, 1933), and this substance was soon shown to be auxin (Thimann and Skoog, 1934).

Auxin is mainly synthesized in young expanding leaves at the shoot apex (Ljung et al., 2001). It is transported basipetally in the so-called polar auxin transport stream (PATS), occurring in the xylem parenchyma cells and involving the action of PIN-FORMED (PIN) auxin efflux carrier proteins (Everat-Bourbouloux and Bonnemain, 1980; Gälweiler et al., 1998; Wisniewska et al., 2006). This transport is essential for the inhibitory action of auxin, as revealed by experiments with auxin transport inhibitors (Panigrahi and Audus, 1966). However, inhibition of bud outgrowth by auxin is not direct, as it was initially postulated (Thimann, 1937). Experiments with radiolabeled indole-3-acetic acid revealed that auxin transport is too slow to match bud outgrowth kinetics after decapitation. Furthermore, apex-derived auxin does not enter axillary buds (Booker et al., 2003; Brown et al., 1979; Hall and Hillman, 1975; Prasad et al., 1993) and the auxin concentration in axillary buds is not reduced after decapitation (Gocal et al., 1991). Therefore, the inhibitory effect of apically derived auxin appears to be indirect.

A simple possibility to explain this indirect action is provided by the second messenger model, which was already postulated by Snow (1937) as an alternative to the direct action model. According to the model, auxin influences a second messenger, which relays the inhibitory signal directly into the buds. By now, there is well-founded evidence supporting this model, and cytokinin and strigolactones are suggested to be second messengers of auxin (Fig. 1.2). In the case of cytokinin (CK), an auxin-mediated reduction of the hormone level would suppress bud outgrowth. This is implied by the fact that CK can act directly in the bud to promote its outgrowth, as revealed by studies with externally applied CK (Sachs and Thimann, 1967). Indeed, auxin can influence the CK pool by affecting CK biosynthesis and degradation, as discussed below (chapter 1.3.2.2, p. 10ff). As a consequence, also the local CK concentration in the buds may be regulated by auxin. Regarding CK as a second messenger, this would well explain the indirect action of auxin. However, the regulatory system is more complex: CK appears to be not the only second messenger of auxin, as there is evidence for strigolactones playing a similar role. Like CK, also SLs can have a direct effect on bud outgrowth. However, instead of promoting bud outgrowth, they have a suppressing effect when they are supplied to buds (Brewer et al., 2009). Therefore, an auxin-induced up-regulation of the SL pool would inhibit bud outgrowth. Indeed, auxin was shown to regulate the expression of SL biosynthesis genes, as discussed below (chapter 1.3.2.3, p. 11ff). The outcome of an auxin-mediated induction of SL as a second messenger is the same as a reduction of CK: both can relay the auxin signal into the bud and both effects will result in a suppression of bud outgrowth.

The findings discussed above provide well-founded support for the second messenger model. However, there appear to be additional effects involved in auxin-induced inhibition of bud outgrowth. An alternative model is based on the auxin canalization hypothesis (Sachs, 1981), which describes the differentiation of vascular tissue. According to the model, auxin is transported from a source to a sink, and a primary flux along a concentration gradient occurs in transport-competent cells. Auxin then modulates its own transport from the source to the sink via a positive feedback loop. This feedback occurs via the PIN-FORMED (PIN) auxin efflux carrier proteins, which are localized at the plasma membrane. This localization is polar and achieved by dynamic cycling (vesicle endo-and exocytosis) of PIN between the plasma membrane and an endosomal pool. Auxin induces PIN expression and inhibits PIN endocytosis, increasing the plasma membrane accumulation of its own transporter (Kleine-Vehn et al., 2011; Paciorek et al., 2005; Sauer et al., 2006; Vieten et al., 2005). This will enhance and concentrate, i.e. canalize, the initial auxin transport into special groups of cells (Sachs, 1981, 2000). Consecutively, these cells may develop into vascular tissue (De Smet and Jürgens, 2007). With respect to the influence of auxin transport during bud outgrowth regulation, it is assumed that not only the shoot apex, but also axillary buds are active auxin sources, as they contain young leaves which are typical sites of auxin production (Ljung et al., 2001). Auxin export may be important for the formation of a vascular connection between the bud and the main stem (Sachs, 1968), which actively transports auxin in the PATS basipetally to the root (Fig. 1.2). If the auxin gradient between the bud as a source and the stem as a sink is sufficient, an initial auxin flux can be established. Consequently, according to the canalization model, this initial flux will be enhanced and canalized. Ultimately, a vascular connection between the bud and the stem, i.e. a PATS connection of the bud to the main PATS in the stem, will form (Domagalska and Leyser, 2011). An implication from this model would be that exogenous auxin application to axillary buds would trigger outgrowth. However, this is not the case (Bayer et al., 2009). To explain this apparent contradiction, it is discussed that auxin export also plays a role for vascular patterning and development of the leaf primordia themselves. In this case, simple saturation of the bud with exogenous auxin would not simulate the more subtle auxin distribution pattern within the bud (Bayer et al., 2009).

Summarized, auxin export from the bud appears to be important for both, leaf development as well as a vascular connection of the bud to the main stem. However, a given bud is not the only auxin source in the plant. It competes with all other buds, and more importantly with the main apex as well as existing branches, for the main stem as a

shared auxin sink with limited capacity. If there is an active apex feeding auxin into the stem, the auxin level is high and the sink capacity will be saturated. As a result, an initial auxin flux from the axillary buds to the stem along a gradient cannot occur and the buds stay dormant. Upon decapitation, the apex as the main auxin source is removed, the auxin level in the stem is reduced and one or more buds can establish auxin export along a gradient. They will grow out to form branches with active apices, feeding auxin into the PATS. Consequently, the auxin level in the main stem is increased back to normal levels, preventing further buds from establishing a gradient and growing out (Domagalska and Leyser, 2011). Interestingly, axillary buds of pea (*Pisum sativum*) plants exhibited a polarization of PIN transporters and increased auxin export after decapitation, providing experimental evidence for the auxin canalization model during bud outgrowth regulation (Balla et al., 2011).

Summarized, there is experimental support for both, the second messenger model as well as the auxin transport canalization hypothesis. Possibly, both effects play a role, since they do not exclude each other. Auxin may regulate connection of axillary buds to the vascular system, and control sustained bud growth via CK and SL as well. There is evidence for an extensive cross-talk between the three hormones, as described in the following sections.

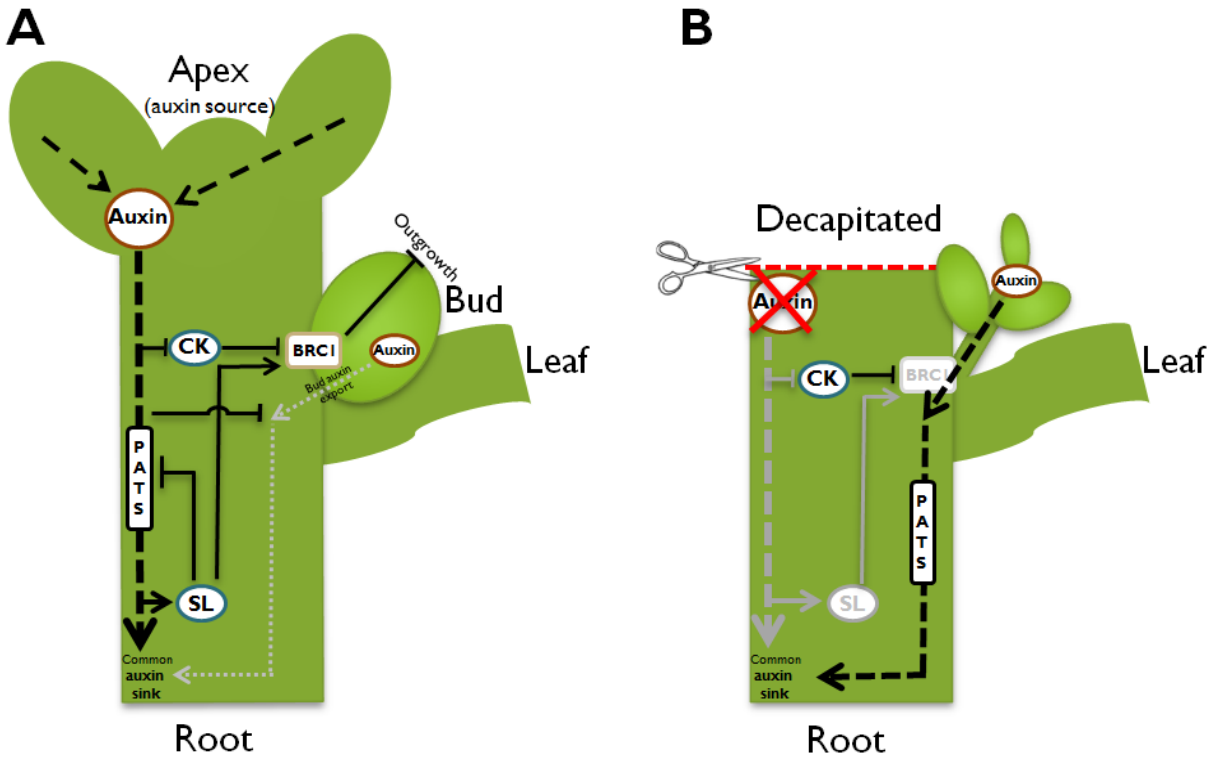

Fig. 1.2 Schematic illustration of models and hormonal pathways in bud outgrowth regulation. The major hormones involved in bud outgrowth control, auxin, cytokinin (CK) and strigolactone (SL), as well as the transcription factor BRANCHED1 (BRC1), are included. Auxin is mainly synthesized at the apex of an intact plant (A) and transported basipetally in the polar auxin transport stream (PATS) to the root, acting as an auxin sink. Auxin represses CK biosynthesis and promotes SL biosynthesis in the stem. Both hormones may relay the auxin signal directly into axillary buds (second messenger model), where they antagonistically regulate *BRC1* transcript levels. This indirect action of auxin enhances *BRC1* expression, leading to suppression of bud outgrowth. Auxin may also act by saturating the sink capacity of the stem (auxin transport canalization model). In addition to the apex, also axillary buds are active auxin sources, and the establishment of auxin export to the main stem acting as a shared auxin sink is suggested to be essential for vascular connection and outgrowth of the bud. However, high auxin levels in the stem, resulting from an active apex, prevent the establishment of an initial auxin flux (gray arrows, inactive pathway), thus suppressing bud outgrowth. SL can enhance this competition by inhibiting PATS via a depletion of PIN auxin efflux carriers from the plasma membrane of xylem parenchyma cells, further reducing the sink capacity of the stem and impeding the establishment of an initial auxin export from buds. After decapitation (B), the apex as the primary auxin source is lost. Furthermore, SL biosynthesis is reduced, dampening the inhibitory effect of SL on auxin transport in the PATS. Both effects increase the sink capacity of the stem, promoting the establishment of auxin export from buds and thus bud outgrowth (auxin transport canalization model). Also the promoting effect of SL on *BRC1* expression is dampened, while CK biosynthesis is de-repressed. Both lead to reduced *BRC1* expression, thus buds are released from outgrowth inhibition (second messenger model). Both models are not exclusive, and the effects may account for bud outgrowth regulation simultaneously. Image from Teichmann and Muhr (2015), modified.

1.3.2.2 Cytokinin

Cytokinins (hereafter referred to as cytokinin; CK) such as zeatin or kinetin are a class of phytohormones involved in many processes of plant development, with the most prominent role being an inducing effect on cytokinesis, hence the name. CK biosynthesis involves the activity of ISOPENTENYLTRANSFERASE (IPT) enzymes and takes place predominantly in the root, but also in other tissues, e.g. in nodal regions of the stem (Chen et al., 1985; Miyawaki et al., 2004; Nordström et al., 2004). Acropetal CK long-distance transport occurs in the transpiration stream, i.e. in the xylem (Kudo et al., 2010). As one of the three major hormones involved in branching control, cytokinin has a promoting effect on the outgrowth of axillary buds. This was shown for instance by experiments in which direct external application of CK on axillary buds triggered their outgrowth (Sachs and Thimann, 1964, 1967). The same effect was found when CK was locally overproduced in buds of transgenic plants, using an inducible promoter (Faiss et al., 1997). CK may act by influencing the expression of the transcription factor BRANCHED1 (BRC1), which is a negative regulator of bud outgrowth (see chapter 1.3.3, p. 19ff). This is supported by the finding that *BRC1* transcript levels were found to be reduced after application of CK to axillary buds (Braun et al., 2012; Dun et al., 2012).
As mentioned above, cytokinin levels are modified by auxin, and CK may act as a second messenger of auxin in bud outgrowth regulation (Fig. 1.2). Auxin can induce a decrease of the CK pool by down-regulation of *IPT* genes (Nordström et al., 2004; Tanaka et al., 2006). In addition, an auxin-induced up-regulation of *CYTOKININ OXIDASE* (*CKX*) genes, encoding enzymes which irreversibly inactivate CK, may cause a further reduction of CK levels (Shimizu-Sato et al., 2008). Decapitation studies provide additional support for the model. Expression of *IPT* genes in nodal areas of the stem is induced and CK levels in axillary buds are increased (in this chronological order) upon removal of the apex as an auxin source (Bangerth, 1994; Tanaka et al., 2006; Turnbull et al., 1997). This local regulation of CK in the stem and subsequent transport into the buds is discussed to be important for decapitation-induced bud outgrowth (Müller and Leyser, 2011). Summarized, there's well-founded evidence for an auxin-mediated control of CK as a promotor of bud outgrowth. However, it should be noted that the role of CK as a second messenger of auxin is questioned in a recent publication (Müller et al., 2015). Based on studies in *Arabidopsis ipt* mutants, which showed a normal decapitation-induced branching response, the authors postulate that CK rather plays a role in overriding apical dominance under conditions favoring branching. The down-regulation of CK biosynthesis by auxin is

discussed to be a control mechanism, preventing activation of too many buds by additional auxin from already activated ones. Thus, there may be feedback-regulation leading to hormonal balance, which could be modified by other factors (Müller et al., 2015). In addition to the regulation of CK by auxin, there appears to be extensive crosstalk between the hormones. In the bud, CK may influence auxin distribution. It was shown to modulate PIN1 expression and polarization, which may enhance auxin export from the bud (Kalousek et al., 2014). In addition, it is discussed that CK may induce local auxin biosynthesis in the young leaves within the bud (Müller and Leyser, 2011). Both effects would promote bud outgrowth according to the auxin transport canalization model.
Taking the available data together, the exact role and mode of action of CK is not fully resolved, but there appear to be different mechanisms. Together with auxin, CK forms a complex regulatory network. Another player in this system is the group of strigolactones, which further modify and extend the network.

1.3.2.3 Strigolactones

Strigolactones (SLs) are a class of hormones with an inhibitory effect on bud outgrowth. Since they are a major focus of this work, the current knowledge about SL is summarized below in more detail than it was done for the other hormones.
Like most phytohormones, SLs have multiple roles, with many of them only being discovered recently. SLs are found in root exudates of many plant species (Bouwmeester et al., 2007). The exudation matches well the first identified biological role of SL, an inducing effect on seed germination of the plant parasitic weed *Striga lutea* (Cook et al., 1966), hence the name strigolactone. Later, SLs were also found to induce spore germination and hyphal branching of arbuscular mycorrhiza (AM) fungi, which is important during mycorrhiza establishment (Akiyama et al., 2005; Besserer et al., 2006). Therefore, plants may exude SLs from their roots to attract this form of symbiosis, which is supported by the finding that SL-exudation into the soil is enhanced upon phosphate- and in some cases also nitrogen-starvation, conditions which promote mycorrhiza formation (Kohlen et al., 2011; López-Ráez et al., 2008; Yoneyama et al., 2007). This mechanism may be the original reason for SL exudation, and it may be exploited by parasitic weeds such as *Striga* and *Orobanche* which use SLs as a germination cue (Bouwmeester et al., 2007; Xie et al., 2010). Except for these roles as signaling molecules in the rhizosphere, SLs function as phytohormones within the plant as well. They were

suggested to promote leaf senescence (Ledger et al., 2010; Snowden et al., 2005; Woo et al., 2001) and to be important regulators during drought and salinity stress (Ha et al., 2014). Furthermore, SLs are implicated in the regulation of plant morphology and development: they were shown to promote internode elongation (de Saint Germain et al., 2013; Snowden et al., 2005) and secondary stem growth (Agusti et al., 2011). Additionally, SLs were reported to modulate root architecture: they suppress lateral root formation (Kapulnik et al., 2010; Ruyter-Spira et al., 2011) and adventitious rooting (Rasmussen et al., 2012), but promote root hair elongation (Kapulnik et al., 2010) and primary root growth (Ruyter-Spira et al., 2011). However, for this work, the most important role of SLs is their influence on shoot architecture. While the fundamental roles of auxin and cytokinin in bud outgrowth regulation were well-established for decades, the existence of an additional, third major hormone in branching control was suggested as well (Beveridge et al., 1997). This was based on the analysis of highly branched pea mutants (*ramosus* / *rms*), whose "bushy" phenotype could not be attributed to auxin or CK effects. Grafting studies revealed that the substance, later called "SMS" (shoot multiplication signal, Beveridge, 2006) is a mobile signal (Foo et al., 2001). It is transported acropetally in the shoot, and this transport was later postulated to occur in the xylem stream (Kohlen et al., 2011). The substance suppresses outgrowth of axillary buds, leading to the observed increased branching phenotype of mutant plants (Foo et al., 2001). Based on the analysis of further mutants and additional species (including *Arabidopsis more axillary growth* (*max*), petunia (*Petunia hybrida*) *decreased apical dominance* (*dad*) and rice (*Oryza sativa*) *dwarf / high tillering dwarf* (*d/htd*)), several genes involved in the biosynthesis and perception of the SMS were identified (reviewed in Beveridge, 2006; Waldie et al., 2014). Thus, large parts of the pathway were already known until finally, strigolactones or SL-derived compounds were found to be the elusive substance (Gomez-Roldan et al., 2008; Umehara et al., 2008). Following this breakthrough, the elucidation of the whole SL pathway gained increased attention and by now, large parts of SL biosynthesis are understood.

Structurally, SLs are terpenoid lactones consisting of a tricyclic lactone part (ABC ring structure), which is connected to the D-ring lactone (butenolide) by an enol-ether bridge (Zwanenburg et al., 2009). The D-ring appears to be crucial for biological activity (Boyer et al., 2012). There are numerous modifications to this basic structure found in the anticipated common SL precursor 5-deoxystrigol, making SLs a highly diverse group of hormones. Many natural SLs (>15) such as strigol, orobanchol or sorgolactone were already identified in different species and characterized for their biological activity (Xie et

al., 2010; Yoneyama et al., 2009; Zwanenburg et al., 2009). Beside of the identification of natural SLs, multiple synthetic analogs like GR24, GR7 or Nijmegen-1 were produced and characterized (Akiyama et al., 2010; Boyer et al., 2012; Xie et al., 2010; Zwanenburg and Mwakaboko, 2011; Zwanenburg et al., 2009). Most likely, more different variants of natural and synthetic SLs will be discovered in the future, although the identification of natural SLs is technically challenging since SL concentrations in plants are very low and the substances are highly unstable, especially in moist environments due to hydrolysis (Akiyama and Hayashi, 2006; Babiker et al., 1987; Mangnus and Zwanenburg, 1992; Xie et al., 2010; Yoneyama et al., 2009; Zwanenburg et al., 2009). The instability is suggested to be important for signaling in the rhizosphere, where concentration gradients play a role (Parniske, 2008).

In the following sections, SL biosynthesis and signaling will be discussed. The involved genes were identified by mutant analysis in several species and the nomenclature is not uniform, even within a given species. For simplicity reasons, common *Arabidopsis* nomenclature will be used here, although most genes were first described in other species. The corresponding gene names are compiled in Tab. 1.1. An illustration of the canonical SL pathway is shown in Fig. 1.3.

Tab. 1.1 Overview about components of the strigolactone pathway. Gene names in the commonly investigated species (*Arabidopsis*, pea, petunia and rice) are listed according to their activity in the SL pathway, starting from biosynthesis (green shading) via perception (blue shading) to downstream targets (red shading). The function of the corresponding protein is indicated and references are provided.

Arabidopsis	Pea	Petunia	Rice	Function	References
AtD27			*D27*	Isomerase	Waters et al., 2012a Lin et al., 2009
MAX3	*RMS5*	*DAD3*	*D17* (*HTD1*)	CCD7 carotenoid cleavage dioxygenase	Booker et al., 2004 Johnson et al., 2006 Ishikawa et al., 2005 Drummond et al., 2009
MAX4	*RMS1*	*DAD1*	*D10*	CCD8 carotenoid cleavage dioxygenase	Sorefan et al., 2003 Arite et al., 2007 Snowden et al., 2005
MAX1		*PhMAX1*	*SLB1*, *SLB2*	P450 cytochrome	Stirnberg et al., 2002 Drummond et al., 2011 Cardoso et al., 2014
AtD14		*DAD2*	*D14*	α/β hydrolase, SL receptor	Waters et al., 2012 Hamiaux et al., 2012 Arite et al., 2009
MAX2	*RMS4*	*PhMAX2A*	*D3*	F-box protein	Stirnberg et al., 2002 Johnson et al., 2006 Drummond et al., 2011 Ishikawa et al., 2005
SMXL7			*D53*	HSP101/ chaperonin-like protein, Class I Clp ATPase	Stanga et al., 2013 Jiang et al., 2013 Zhou et al., 2013

SL biosynthesis starts from an all-*trans*-β-carotene. This compound is isomerized to 9-*cis*-β-carotene via the action of the isomerase AtD27 (Lin et al., 2009; Waters et al., 2012a). Then, two consecutive cleavage steps are performed by CAROTENOID CLEAVAGE DIOXYGENASE enzymes (CCD7 and CCD8; MAX3 and MAX4 in *Arabidopsis*) to produce carlactone via a 9-*cis*-β-apo-10'-carotenal intermediate. Based on protein localization and gene expression data, it was shown that these steps take place in the plastids, predominantly in roots and hypocotyls (Alder et al., 2012; Booker et al., 2004; Sorefan et al., 2003). Carlactone, being the product of these reactions, was suggested to be a mobile intermediate of SL biosynthesis based on grafting experiments: a *max1* rootstock complemented the branching phenotype of *d27, max3* and *max4* scions, showing that MAX1 acts downstream of the aforementioned enzymes and utilizes a mobile substrate (Booker et al., 2005; Seto et al., 2014; Waters et al., 2012a). MAX1 is a cytochrome P450 monooxygenase, localized in the cytoplasm and predominantly expressed in tissues

associated to the vasculature (Booker et al., 2005). The product of the MAX1 reaction was found to be carlactonic acid. This compound is then further processed in a MAX1-independent reaction, yielding carlactonic acid methyl ester, which can directly interact with AtD14, a known SL receptor (Abe et al., 2014). Therefore, the whole pathway from the carotenoid precursor to at least one bioactive SL-like compound has been unraveled. However, the precise reactions leading to the high diversity of known SLs remain to be identified. Alternative pathways may also play a role, based on the finding that several SL biosynthesis mutants still have detectable levels of certain SL species (discussed in Waldie et al., 2014). With respect to their function, there appear to be SLs playing a major role as germination stimulants, while others seem to be involved predominantly in the regulation of bud outgrowth (Boyer et al., 2012).

Compared to SL biosynthesis, our knowledge of SL signaling is limited. Nevertheless, there were some recent breakthroughs in the field, such as the identification of the above-mentioned SL receptor D14 in rice. A loss-of-function mutation in *D14* and its orthologs in *Arabidopsis* (*AtD14*) and petunia (*DAD2*) causes increased branching, similar to the phenotype of SL biosynthesis mutants. However, the phenotype cannot be complemented by treatment with the synthetic SL analog GR24, indicating that D14 is involved in SL signaling rather than SL biosynthesis (Arite et al., 2009; Hamiaux et al., 2012; Waters et al., 2012b). D14 is an α/β hydrolase protein, which can directly bind GR24, as shown in petunia and rice (Hamiaux et al., 2012; Kagiyama et al., 2013). Although D14 possesses enzymatic activity and can hydrolyze GR24 after binding, the reaction is slow and the cleavage products are biologically inactive. These findings argue against a role of this reaction in generating a signal for downstream branching suppression, i.e. D14 is not involved in SL biosynthesis (Hamiaux et al., 2012; Nakamura et al., 2013; Zhao et al., 2013). The binding of GR24 and the hydrolysis reaction are discussed to rather have a role in modulating the activity of D14 as the SL receptor, e.g. by inducing a conformational change enabling the interaction with other components of SL signaling. Indeed, petunia DAD2 can bind PhMAX2A in the presence of GR24 in a dose-dependent manner, and the hydrolytic activity is required for this interaction (Hamiaux et al., 2012). The same was shown for rice D14 having increased affinity to D3 in the presence of GR24 (Jiang et al., 2013).

Thus, petunia PhMAX2A, rice D3, as well as their orthologs in *Arabidopsis* (MAX2) and pea (RMS4), are another component of the SL pathway. Mutants with defects in these genes exhibit highly increased branching, which cannot be complemented by grafting to a wild type rootstock or by GR24 treatment. This indicates that MAX2 is involved in SL signaling

as well (Beveridge et al., 1996; Drummond et al., 2011; Ishikawa et al., 2005; Stirnberg et al., 2002). MAX2 (formerly described as ORE9) is an F-box protein (Stirnberg et al., 2002; Woo et al., 2001). F-box proteins are generally involved in protein degradation. As part of an Skp1—cullin—F-box (SCF) E3 ubiquitin ligase complex, they are important for recognizing and recruiting substrate proteins for ubiquitination, i.e. marking them for proteasomal degradation (Ho et al., 2008). Notably, this also is a common feature of other plant hormonal signaling pathways, such as auxin, jasmonic acid (JA) or gibberellic acid (GA) signaling. The signaling chain finally leads to the degradation of transcription factors, inducing a transcriptional response of target genes (e.g. reviewed in Ho et al., 2008). MAX2 was indeed shown to be part of an SCF complex, and the F-box domain is essential for complex formation: a mutant of MAX2 lacking the F-box motif could not associate with ASK1 and AtCUL1, which are SCF core components (Stirnberg et al., 2007). Summarized, it appears that SL binds to D14 as the SL-receptor, enabling it to bind to MAX2. This binding appears to regulate the incorporation of MAX2-D14 into the SCF complex or to modulate its activity, i.e. substrate binding affinity. It should be noted that beside of activation by D14, also the karrikin receptor KAI2 can interact with MAX2 upon binding of karrikins, components found in the smoke of burnt plant material. Thus, there appear to be different pathways converging at MAX2, which is in line with the pleiotropic *max2* mutant phenotypes and different reported target proteins of the SCF^{MAX2} complex (reviewed in Waldie et al., 2014). Here, only relevant findings for the role of MAX2 and its targets in the SL-mediated suppression of bud outgrowth are discussed.

Identification of substrate proteins marked for degradation via the SCF^{MAX2} complex was an important step to further unravel the SL signaling chain. For the regulation of shoot branching, the EAR motif-containing rice D53 protein appears to be the most significant target. It interacts with D3 and D14 and it is degraded in an SL-dependent manner, which can be prevented by a gain of function mutation protecting it from degradation, leading to a highly branched phenotype (Jiang et al., 2013; Zhou et al., 2013). Interestingly, *D53* is a member of the rice *SMAX1-LIKE* (*SMAXL*) gene family. In *Arabidopsis*, *SMAXL7* is also discussed to be a candidate gene playing a role in shoot branching regulation downstream of *MAX2* (Stanga et al., 2013). However, the mode of action of *D53*/*SMXL7* is not fully understood. In rice, D53 interacts with the protein TPR2, related to TOPLESS (TPL) transcriptional co-repressor proteins. Thus, D53 may regulate the transcription of downstream genes (Jiang et al., 2013). An alternative hypothesis is that endocytosis of the auxin efflux carrier PIN1 could be inhibited by D53, since D53/SMAXL are chaperonin-like proteins which may sequester other proteins, i.e. prevent them from exerting their

normal function. If this is the case, SL-mediated degradation of D53 would increase PIN1 removal from the plasma membrane and thus dampen auxin transport (Waldie et al., 2014).

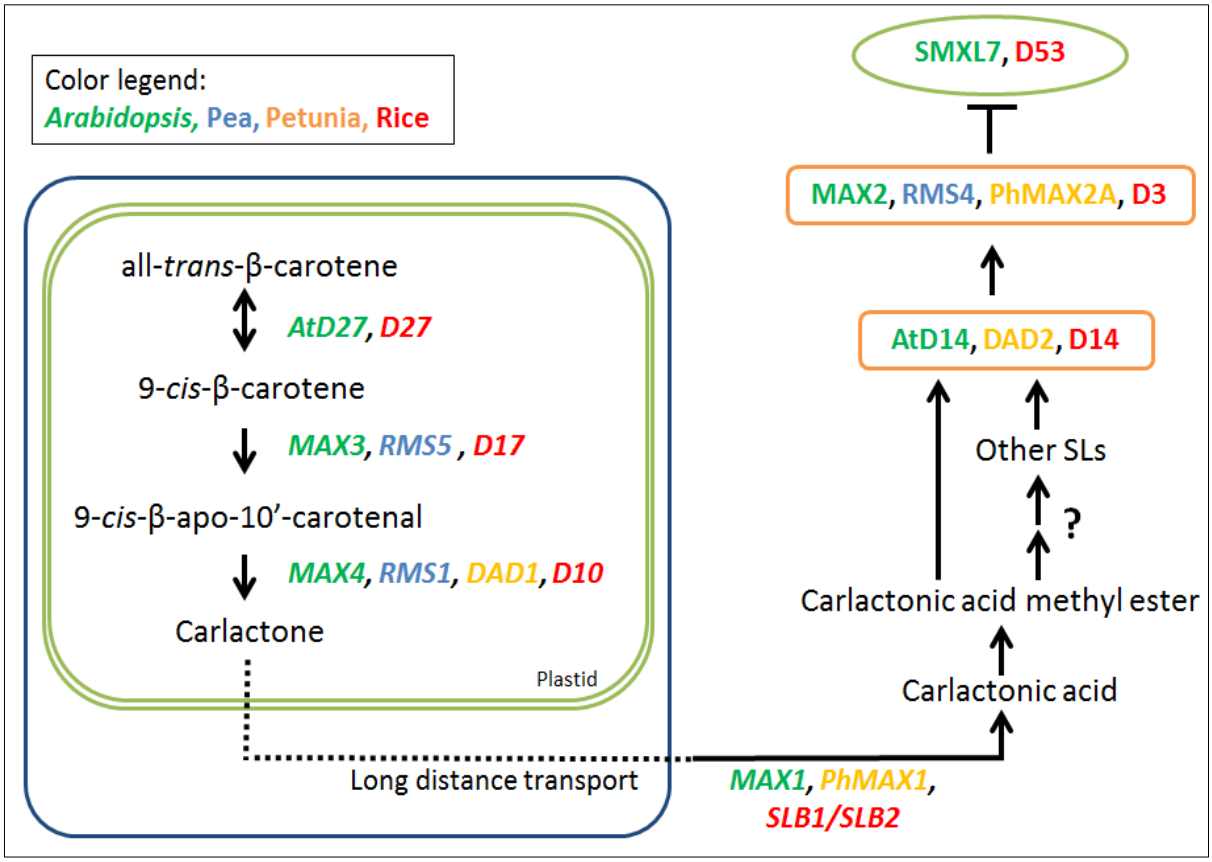

Fig. 1.3 Schematic illustration of known components of the strigolactone pathway. SL biosynthesis starts from a carotenoid precursor and leads to the formation of carlactonic acid methyl ester and other strigolactones, which are detected by D14. Binding induces complex formation with MAX2, inducing the degradation of target proteins. Known genes / proteins from different species are listed and marked with different colors. Schematic illustration adapted from Waters et al. (2012a).

Summarized, there are still many open questions and the exact SL signaling cascade remains elusive. Nevertheless, there are models trying to explain how SLs inhibit bud outgrowth. One is based on a direct action via the modulation of expression of the transcription factor BRC1, and the other model is based on the idea that SLs act indirectly by modulating auxin fluxes. Both models are discussed below.

As mentioned earlier, SLs can act directly in the bud. For instance, application of SL on axillary buds was shown to inhibit their outgrowth in *Arabidopsis* and pea (Brewer et al., 2009). An ultimate target of SLs during this direct action appears to be the transcription factor BRC1. SL-application increases *BRC1* expression and conversely, *BRC1* levels were reduced in SL-pathway mutants compared to the wild type (Braun et al., 2012; Dun et al.,

2012). Thus, BRC1 appears to be a downstream target of SLs, leading to an inhibition of bud outgrowth. The action of SL in the bud may be influenced by auxin, which utilizes SL as a second messenger (Fig. 1.2). This is supported by the finding that auxin modulates the SL level by inducing expression of the SL biosynthesis genes *MAX3* and *MAX4* in *Arabidopsis* (Hayward et al., 2009), as well as orthologous genes in other species such as rice and pea (Arite et al., 2007; Johnson et al., 2006). In addition, a depletion of auxin levels by decapitation or treatment with the auxin transport inhibitor 1-N-naphthylphthalamic acid (NPA), was found to reduce the expression of SL biosynthesis genes (Foo et al., 2005; Hayward et al., 2009; Johnson et al., 2006).

In addition to the direct action of SL appearing to be influenced by auxin, SL is also discussed to have an indirect mode of action. Interestingly, auxin is involved as well. Auxin transport rates in the stem of *Arabidopsis max* SL-pathway mutants were found to be enhanced, while auxin transport was reduced upon application of SL or an induction of SL biosynthesis. This matches well the observations that expression and plasma membrane accumulation of PIN auxin efflux carriers was increased in *max* mutants, whereas SL-treatment reduced PIN accumulation (Bennett et al., 2006; Crawford et al., 2010). These findings imply that SLs inhibit auxin transport by causing a depletion of PIN proteins (potentially via degradation of D53, as discussed above) from the plasma membrane, creating an interlocking feedback loop between both hormones. The inhibitory effect of reduced auxin transport on bud outgrowth may be explained by the auxin transport canalization model: reduced transport would lower the auxin sink capacity of the stem and prevent establishment of an initial auxin export from axillary buds (Crawford et al., 2010). SLs may also directly inhibit the establishment of an initial auxin export from axillary buds (canalization process), thereby preventing outgrowth (Waldie et al., 2014).

Summarized, strigolactones are phytohormones suppressing branching and there appear to be different modes of action. Most notably, there is extensive crosstalk with auxin, and both hormones influence each other.

1.3.2.4 Other hormones

Hormones in plants usually have multiple functions, depending on their spatio-temporal distribution and concentration. As outlined above, the three major hormones in bud outgrowth regulation, auxin, cytokinin and strigolactones, form a complex regulatory network which integrates various inputs to mediate a branching response. There is extensive cross-talk and its fine-tuning appears to be important during the regulation of bud outgrowth.

It should be noted that other phytohormones may play a role as well, modulating the regulatory network. Such a connection was for instance suggested for the strigolactone and brassinosteroid pathways (Wang et al., 2013). In addition, abscisic acid (ABA) was implicated to be involved in branching suppression upon shading (Reddy et al., 2013) and suggested to modulate SL biosynthesis (López-Ráez et al., 2010). Thus, the regulation of branching is based on a complex regulatory framework. It is likely that more interactions involved in the fine-tuning of the network will be identified in the future.

1.3.3 Transcription factors in bud outgrowth regulation: BRANCHED1

BRANCHED1 (BRC1) is a regulator implicated in the negative control of bud outgrowth, and it is classified as a TB1 CYCLOIDEA PCF (TCP) type transcription factor (Aguilar-Martínez et al., 2007; Finlayson, 2007). The TCP transcription factors are found in most investigated plant species and are known to control meristems and lateral organ development (Martín-Trillo and Cubas, 2010). Thus, they regulate many growth-related processes such as leaf development or shoot branching (Doebley et al., 1997; Palatnik et al., 2003).

The TCP gene family has several members discussed to result from gene duplications and subsequent diversification. The common feature of TCP transcription factors is the conserved TCP domain, containing a basic helix-loop-helix (bHLH) motif with a length of 59 amino acids. This domain is implicated in DNA binding and mediating protein-protein interactions (Cubas et al., 1999; Martín-Trillo and Cubas, 2010; Navaud et al., 2007). Based on differences in this domain, the TCP proteins are grouped into two classes (I and II). While class I is generally implicated in promoting growth and cell division, class II is discussed to have an inhibitory effect (Martín-Trillo and Cubas, 2010).

BRC1 encodes a class II TCP factor (CYC/TB1 sub-clade), correlating well with its role in inhibiting bud outgrowth. It was first identified in maize as *TEOSINTE BRANCHED1* (*Zea*

mays TB1; Doebley et al., 1997). Orthologs were described in other monocots such as rice *TEOSINTE BRANCHED1/FINE CULM1* (*Oryza sativa OsTB1/FC1*; Takeda et al., 2003) and sorghum *TEOSINTE BRANCHED1* (*Sorghum bicolor SbTB1*; Kebrom et al., 2006), as well as in dicots such as *Arabidopsis BRANCHED1* (*Arabidopsis thaliana AtBRC1*; Aguilar-Martínez et al., 2007; Finlayson, 2007), pea *BRANCHED1* (*Pisum sativum PsBRC1*; Braun et al., 2012) and tomato *BRANCHED1-LIKEb* (*Solanum lycopersicum SlBRC1b*; Martín-Trillo et al., 2011). Expression of *BRC1* and its orthologs in other species was found to be specific to dormant axillary buds, as shown in qPCR, Northern Blot, promoter-β-glucoronidase (GUS) fusion and *in situ* hybridization experiments. While expression levels were high in inactive axillary buds, *BRC1* expression was strongly reduced in active, growing buds, where tested. In other tissues, expression was not detectable or low. However, basal transcript levels were detected especially in floral and apical structures (Aguilar-Martínez et al., 2007; Braun et al., 2012; Doebley et al., 1997; Finlayson, 2007; Martín-Trillo et al., 2011; Minakuchi et al., 2010; Takeda et al., 2003).

BRC1 loss-of-function mutants were described to have significantly increased bud outgrowth, leading to a higher number of branches (see references above). Correspondingly, overexpression of *BRC1* orthologs resulted in reduced bud outgrowth in rice and wheat (Lewis et al., 2008; Takeda et al., 2003). Thus, *BRC1* is a negative regulator of bud outgrowth. Downstream targets of *BRC1* may be factors in the control of cell cycling, such as *PROLIFERATING CELL NUCLEAR ANTIGEN* (*PCNA*), whose expression is known to be controlled by TCP type transcription factors (reviewed in Müller and Leyser, 2011). Furthermore, comparative microarray experiments using wild type and *brc1* mutant buds revealed the regulation of genes associated with ribosomal and cell cycle functions. The same experiments also suggest a *BRC1*-dependent regulation of abscisic acid (ABA) related genes (González-Grandío and Cubas, 2014). ABA is a phytohormone connected to bud dormancy (Fedoroff, 2002). Thus, BRC1 appears to regulate dormancy-related hormonal signaling in addition to direct interference with the cell cycle.

Due to its function as a transcription factor involved in the suppression of bud outgrowth, *BRC1* is a potential molecular target of different pathways. Indeed, *BRC1* is discussed to be a central hub at which different branching pathways are integrated to make the decision whether a bud grows out or stays dormant (Aguilar-Martínez et al., 2007). For instance, *BRC1* transcript levels respond to shading-induced changes in the light red/far-red (R/FR) ratio. This ratio is sensed by the phytochrome system. Upon shading, branching is suppressed in favor of increased primary shoot growth as part of the so-called shade avoidance syndrome (Pierik and Wit, 2014). At high planting density, which is

a typical shade-inducing condition, *Arabidopsis BRC1* was found to be upregulated (Aguilar-Martínez et al., 2007). Furthermore, in *Arabidopsis* and sorghum, *BRC1/OsTB1* expression was increased at low R/FR conditions and in *phyB* mutants (González-Grandío et al., 2013; Kebrom et al., 2006). These findings indicate that BRC1 translates light signals into a bud outgrowth response. However, *BRC1* expression is regulated by additional factors, most importantly by cytokinin and strigolactones. The antagonistic regulatory effect of both hormones on *BRC1* fits well to their proposed role as second messengers of auxin acting directly in the buds, as described in the previous chapters.

CK application onto buds leads to reduced *BRC1* expression in pea and rice (Braun et al., 2012; Dun et al., 2012; Minakuchi et al., 2010). Conversely, *BRC1* transcript levels were slightly reduced in *Arabidopsis* mutants of *ALTERED MERISTEM PROGRAM1* (*AMP1*), which exhibit increased CK levels (Aguilar-Martínez et al., 2007; Helliwell et al., 2001). Thus, CK may promote bud outgrowth by negatively affecting *BRC1* expression. SL application, in contrast, was found to increase *BRC1* expression in pea (Braun et al., 2012; Dun et al., 2012), while *BRC1* transcript levels were reduced in *Arabidopsis* and pea SL pathway mutants (Aguilar-Martínez et al., 2007; Braun et al., 2012; Dun et al., 2012). Furthermore, rice *fc1* and pea *Psbrc1* mutants do not exhibit a reduction of bud outgrowth upon SL application anymore (Braun et al., 2012; Minakuchi et al., 2010). Thus, part of the SL action appears to be suppression of bud outgrowth by upregulating *BRC1* expression.

Interestingly, there appears to be a functional diversification upon *BRC1*-like genes. In *Arabidopsis*, there is a paralog of *BRC1* (*BRANCED2*; *BRC2*), which was reported to play a minor role in the regulation of bud outgrowth, too (Aguilar-Martínez et al., 2007; Finlayson, 2007). However, while *BRC1* transcript levels are reduced in SL pathway mutants, *BRC2* expression is not changed (Aguilar-Martínez et al., 2007). This indicates that *BRC1* is the major factor in relaying SL signals in *Arabidopsis*. Also in petunia, different *BRC1* orthologs were reported to have diversified in their function. While *PhTCP2* seems to be regulated by the R:FR response upon shading, *PhTCP3* (and to a lower extent *PhTCP1*) are discussed to be the major hub for the SL response. This includes the response to phosphorus limitation, a condition which increases SL levels (Drummond et al., 2015). A diversification of *BRC1* gene function is also conceivable in the model tree poplar. Due to the whole genome duplication event in the *Salicaceae* family (Tuskan et al., 2006), several *BRC1* orthologs may exist. While there are 24 *TCP* genes in *Arabidopsis*, 34 members of this family were found poplar (Navaud et al., 2007). Therefore, diversified functions or a high degree of redundancy are likely.

1.3.4 Bud outgrowth regulation in the perennial context

Our current knowledge about the regulation of bud outgrowth is largely based on studies of mostly herbaceous annual plants. The published data discussed in the previous chapters was predominantly generated using *Arabidopsis*, rice, pea and petunia as model systems. However, the perennial lifestyle of many plants found in temperate regions, such as the model tree poplar, requires a more complex regulation of bud activity. Most importantly, the harsh climatic conditions during winter require growth cessation in autumn as an adaptation strategy. Therefore, these species possess additional stages of dormancy and bud types, making them more complex systems to study.

In both, annual and perennial plants, dormant axillary buds exist during the growth phase. They are principally capable of growing out, but their outgrowth is suppressed by other parts of the plant. This "correlative inhibition" can for example be the result of an actively growing apex, suppressing outgrowth of the axillary buds below (apical dominance). The resulting growth inhibition is called paradormancy (Allona et al., 2008; Arora et al., 2003). Annual plants only possess this stage of dormancy. When the growing season ends and the conditions become unfavorable, they die back and only their seeds survive. In contrast, perennial plants possess two additional stages of dormancy, called eco- and endodormancy. When the environmental conditions become adverse and inhibit bud outgrowth at the end of the growing season, the buds initially enter ecodormancy. In this stage, they are principally still capable of growing out (Allona et al., 2008). Thus, ecodormancy is a reversible state of bud suppression. However, at a later time point, the buds undergo physiological adaptations, such as the production of a bud-scale, to survive winter. Short photoperiods and cold temperatures induce a deep state of dormancy, called endodormancy or winter dormancy. Then, even favorable conditions cannot trigger bud outgrowth until a certain chilling requirement (a cumulative time period of cold temperatures) is fulfilled. This reverts the buds to an ecodormant state and they can grow out when the conditions become favorable, if outgrowth is not prevented by paradormancy (Allona et al., 2008; Arora et al., 2003).

When dormancy is released and the buds become activated, they grow into branches. In temperate perennials, bud development and outgrowth may occur within the same growth season. However, both processes can also take place in subsequent seasons with an intervening period of winter dormancy. The formed branches are designated accordingly as sylleptic (bud development and outgrowth in the same season) or proleptic (bud outgrowth after winter dormancy) (Hallé et al., 1978; Remphrey and Powell, 1985).

Another interesting feature of temperate perennials is an additional type of dormant buds. In annual species, only dormant axillary buds can be found. The apical meristem does not form dormant buds: it either grows indeterminately or differentiates, for example into floral organs (Wang and Li, 2008). In contrast, temperate perennials cease growth of the apical meristem in autumn until resuming active growth in spring. During winter, the inactive apical meristem rests in a dormant apical bud (Arora et al., 2003).
Taken together, the additional bud types and dormancy stages make temperate perennial plants, including trees such as poplar, an interesting system to study bud outgrowth control mechanisms.

1.4 Economic significance of plant architecture

Plant architecture is a trait with a high economic significance. A striking example for this can be found in maize (*Zea mays* ssp. *mays*). While the anticipated wild maize ancestor teosinte (*Zea mays* ssp. *mexicana* and *Zea mays* ssp. *parviglumis*) has a high number of tillers (basal branches in grasses), the domesticated crop normally produces no tillers, but just a main shoot. This was reported to result from increased expression of the maize *BRC1* ortholog, *TB1* (Doebley et al., 1997). A similar finding was made in pearl millet (*Pennisetum glaucum*), in which QTL mapping exhibited a polymorphism in the *TB1* promoter (Remigereau et al., 2011). Also in low-tillering rice (*Oryza japonica*) cultivars, *TB1* is discussed to be regulated by the transcription factor *SQUAMOSA PROMOTER BINDING PROTEIN-LIKE 14* (*SPL14*), and this was correlated with the tiller number (Lu et al., 2013). Thus, *BRC1* orthologous genes were selected several times independently during crop domestication, indicating the prominent role of *BRC1* during bud outgrowth regulation in crop species. For monocot crops, an architectural ideotype was described, which includes a low number of tillers (Peng et al., 2008).
Also the SL pathway appears to be important for economically relevant aspects of plant architecture. In rice, *STRIGOLACTONE BIOSYNTHESIS1* and *2* (*SLB1* and *SLB2*), orthologs of the *Arabidopsis* SL biosynthesis gene *MAX1*, were identified during mapping of a tillering-relevant QTL (Cardoso et al., 2014). Additionally, SLs appear to regulate economically important aspects of plant architecture in trees. Fast-growing trees such as poplar (*Populus sp.*) or willow (*Salix sp.*) can be grown on so-called short rotation coppices (SRCs), which are harvested by coppicing in frequent intervals for bioenergy production. The rootstocks re-sprout after coppicing, and the re-sprouting efficiency is important. A

relevant QTL for this trait was reported to contain a willow ortholog of the *Arabidopsis* SL biosynthesis gene *MAX4* (Salmon et al., 2014). Furthermore, the SL pathway is discussed to be a promising target for the modification of branching patters in ornamental plants such as chrysanthemum (*Dendranthema grandiflorum*) (Liang et al., 2010).

Thus, *BRC1*-like genes, as well as genes of the SL pathway, play a role in controlling relevant traits of commercially produced plants and may be important targets for breeding programs. While a reduction of branching, especially a reduction of tiller numbers in monocots, is usually a favored trait (Wang and Li, 2008), also increased branching can be beneficial, as the aforementioned willow example shows. In addition to improved re-sprouting on SRCs, also the total biomass production may be enhanced. The crown architecture on plantations for bioenergy production is an important trait. A high degree of sylleptic branching leads to earlier canopy closure, which is particularly important during the establishment phase of a SRC. Thus, a high number of sylleptic branches was defined as part of a poplar ideotype on SRCs (Ceulemans et al., 1990; Scarascia-Mugnozza et al., 1989). Highly branched plants may have an increased leaf area index, enhancing light capture efficiency and photosynthesis, which in turn leads to higher biomass production (Broeckx et al., 2012; Ceulemans et al., 1990). Modifications of SL-pathway genes in poplar thus may improve plant architectural traits, similar to the findings made in willow.

1.5 Aim of the project

The aim of this project was the investigation of bud outgrowth control mechanisms in the model tree *Populus sp*. A focus was on the role of strigolactones, as well as poplar *BRC1* orthologs as potentially SL-responsive factors in bud outgrowth regulation.

About both, only little information can be found in the literature with respect to woody perennials. However, recent publications indicate that strigolactones are important branching regulators in tree species as well. Willow buds were shown to respond to SL treatment (Ward et al., 2013). Furthermore, a willow *MAX4* ortholog was found at an important QTL for re-sprouting behavior after coppicing, as mentioned above (Salmon et al., 2014). Interestingly, willow and poplar orthologs of genes involved in the strigolactone pathway were shown to be able to largely complement the increased branching phenotype of the corresponding *Arabidopsis* mutants (Czarnecki et al., 2014; Salmon et al., 2014; Ward et al., 2013). These findings indicate a high degree of

conservation of the SL pathway and provide strong hints that SLs play a similar role in trees compared to herbaceous annual plants, which were commonly investigated. However, the information from complementation data is rather indirect and *Arabidopsis* was used as a heterologous system. Although it is not a tree, kiwifruit (*Actinidia chinensis*) is a woody perennial as well. Its *MAX3 and MAX4* orthologs (*AcCCD7* and *AcCCD8*) were also shown to complement the corresponding *Arabidopsis* mutant phenotypes. Additionally, a RNAi-mediated knockdown of *AcCCD8* was shown to increase branching (Ledger et al., 2010), providing a more direct proof und underlining the importance of the significance of SLs in woody perennials.

However, willow and kiwifruit are non-model species. For willow, no whole genome sequence is available and it is not amenable to current genetic transformation techniques (Ward et al., 2013). In contrast, poplar is the model tree species. It is amenable to genetic transformation and vast genomic resources, including a whole genome sequence, are available. Therefore, poplar lines with modifications in the SL pathway would be a valuable resource to study the role of SLs in trees in more detail. The production of such plants was a major focus of this project. Beside of extensive phenotyping, the plants were to be used to study the role of SLs in tree-specific aspects of dormancy. Furthermore, it was a major aim to analyze the influence of SL deficiency on poplar *BRC1*. In *Arabidopsis* and other species, this major regulator of bud outgrowth is SL-responsive. However, a role for *BRC1* in trees has not been reported yet.

Beside of being a valuable platform for the investigation of SLs, *BRC1* and related factors in trees, manipulations of the SL pathway in poplar would modify the tree architecture. Poplar with altered branching patterns may be beneficial for the use on SRCs, as it was discussed for willow. Increased branching would enhance re-sprouting after coppicing and could positively influence the biomass yield due to early canopy closure (Broeckx et al., 2012; Salmon et al., 2014). It would result in a higher bark content of the stem biomass, as the surface area is increased relative to the stem volume. This would be an undesirable effect if the biomass is used as woodchips for energy production (increased alkali metal content). In contrast, it may be beneficial if the biomass is used for other purposes, such as a feedstock for industrial and pharmaceutical chemicals (Salmon et al., 2014).

1.6 Strategy

The strategy to obtain poplar lines with defects in SL biosynthesis and signaling was to identify poplar orthologs of known SL pathway genes by sequence and expression analysis. The identified genes were intended as targets for amiRNA-mediated knockdowns and the generated transgenic lines were to be investigated for corresponding phenotypes, with a focus on tree architecture.

Poplar *BRC1* orthologs were to be identified as well, based on sequence comparison and expression patterns, with a focus on tree-specific aspects of bud outgrowth regulation. Expression was to be analyzed in the generated poplar SL pathway knockdown lines to investigate the anticipated regulation of *BRC1* by SLs.

2 Materials and methods

In the following sections, all equipment and methods used in this work are stated. Standard media (e.g. LB) and routine methods (e.g. preparation of competent bacteria and transformation, nucleic acid extraction, polymerase chain reaction, gel electrophoresis) are based on well-established protocols, which are compiled in e.g. Sambrook and Russell (2000). The exact procedures are described in detail.

2.1 Equipment

Technical equipment used during this work is listed in Tab. 2.1. In the following chapters, only the device type is stated. The model and manufacturer names can be identified in the table.

Tab. 2.1 Technical equipment used during this work. The device type, model and manufacturing company are indicated.

Device type	Model	Manufacturer
Analytical scale	ED224S	Sartorius AG, Göttingen, Germany
Autoclave	Varioklav 135S	HP Medizintechnik GmbH, Oberschleißheim, Germany
Bead mill	TissueLyser LT	Qiagen AG, Hilden, Germany
Digital camera	DMC-FZ150	Panasonic Corporation, Kadoma, Japan
Electric power supply (for electrophoresis)	BluePower 500	Serva Electrophoresis GmbH, Heidelberg, Germany
Electrophoresis chamber	Sub-Cell GT	Bio-Rad Laboratories Inc., Hercules, U.S.A.
Electroporation device	BioRad MicroPulser	Bio-Rad Laboratories Inc., Hercules, U.S.A.
Freezer -80 °C	HFU 686 Basic	Thermo Electron LED GmbH, Lengenselbold, Germany
Gel documentation system	GenoPlex	VWR International GmbH, Darmstadt, Germany
Incubator	IPP500	Memmert GmbH & Co. KG, Schwabach, Germany
Laboratory centrifuge, cooled	Heraeus Fresco 17	Thermo Electron LED GmbH, Osterode, Germany
Laboratory centrifuge, cooled	Heraeus Multifuge 3SR+	Thermo Electron LED GmbH, Osterode, Germany
Laboratory scale	KERN 572	Kern & Sohn GmbH, Ballingen, Germany
Laboratory scale	ED62025-CW	Sartorius AG, Göttingen, Germany
Laboratory shaker	Laboshake RO500	C. Gerhardt GmbH & Co. KG, Königswinter, Germany

Device type	Model	Manufacturer
Laminar flow cabinet	S2020 1.8	Thermo Electron LED GmbH, Lengenselbold, Germany
Magnetic stirrer, heated	RH basic 2	IKA-Werke GmbH & Co. KG, Staufen, Germany
Microplate photometer	Infinite M200	Tecan Group AG, Männedorf, Switzerland
Microwave	R-26ST	Sharp Corporation, Osaka, Japan
pH-meter	inoLab pH720	WTW GmbH, Weilheim, Germany
Photometer	BioPhotometer plus	eppendorf AG, Hamburg, Germany
Plant growth cabinet	AR-66L/3	CLF Plant Climatics GmbH, Wertingen, Germany
Real-time thermocycler	CFX96 Real-Time PCR Detection System	Bio-Rad Laboratories Inc., Hercules, U.S.A.
Shaking incubator	New Brunswick Excella E24R	Eppendorf AG, Hamburg, Germany
Shaking incubator	New Brunswick Innova 44	Eppendorf AG, Hamburg, Germany
Stereo microscope	M165C	Leica Mikrosysteme GmbH, Wetzlar, Germany
Thermocycler	T100 Thermal Cycler	Bio-Rad Laboratories Inc., Hercules, U.S.A.
Thermomixer	Thermomixer comfort	Eppendorf AG, Hamburg, Germany
Ultrapure water system	Arium 611DI	Sartorius AG, Göttingen, Germany
UV transilluminator	2UV TFML-30	UVP LLC, Upland, U.S.A.
Vortex mixer	Vortex Genius 3	IKA-Werke GmbH & Co. KG, Staufen, Germany
Water bath, heated	WNB10	Memmert GmbH & Co. KG, Schwabach, Germany

2.2 Chemicals

Chemicals used during this work are listed in Tab. 2.2. The application of the corresponding component is indicated. In the following chapters, only the chemical names are stated. The manufacturer names can be identified in the table.

Tab. 2.2 Chemicals used during this work. The chemical name, supplier and application are indicated.

Chemical name	Supplier	Used for
2-mercaptoethanol	Carl Roth GmbH & Co. KG, Karlsruhe, Germany	RNA extraction
2-propanol	Carl Roth GmbH & Co. KG, Karlsruhe, Germany	DNA extraction
3‘,5‘-dimethoxy-4‘-hydroxyacetophenone	Sigma-Aldrich Corporation, St. Louis, U.S.A.	Poplar transformation, induction of Agrobacterium
Acetic acid	Carl Roth GmbH & Co. KG, Karlsruhe, Germany	TAE buffer

Chemical name	Supplier	Used for
Acetone	Carl Roth GmbH & Co. KG, Karlsruhe, Germany	Solvent
Agar (Difco)	Becton, Dickinson and Company, Sparks, U.S.A.	Bacterial growth media
Agar (Kobe I)	Carl Roth GmbH & Co. KG, Karlsruhe, Germany	Preparation of plant growth media
Agar (Plant)	Duchefa Biochemie B.V, Haarlem, The Netherlands	Preparation of plant growth media
Bromophenol blue	Merck KGaA, Darmstadt, Germany	Gel loading dye
$CaCl_2$	Merck KGaA, Darmstadt, Germany	Buffer solutions
Chloroform:Isoamylalcohol 24:1	AppliChem GmbH, Darmstadt, Germany	RNA extraction
Cefotaxime sodium	Duchefa Biochemie B.V, Haarlem, The Netherlands	Poplar transformation, elimination of Agrobacterium
Cetyltrimethylammonium bromide (CTAB)	Carl Roth GmbH & Co. KG, Karlsruhe, Germany	RNA extraction
Dimethyl sulfoxide (DMSO)	Carl Roth GmbH & Co. KG, Karlsruhe, Germany	Buffer solutions
Ethylenediaminetetraacetic acid (EDTA)	Carl Roth GmbH & Co. KG, Karlsruhe, Germany	Buffer solutions
Glycerol	Carl Roth GmbH & Co. KG, Karlsruhe, Germany	Bacterial -80 °C storage, gel loading buffer
Kanamycin sulphate monohydrate	Duchefa Biochemie B.V, Haarlem, The Netherlands	Poplar transformation, selective agent
KCl	Carl Roth GmbH & Co. KG, Karlsruhe, Germany	Buffer solutions
Meat extract (Lab-Lemco powder)	Oxoid Ltd., Basingstoke, U.K.	Bacterial growth media
Methyl jasmonate (JA)	Sigma-Aldrich Corporation, St. Louis, U.S.A.	Leaf JA treatment
Murashige & Skoog medium including vitamins	Duchefa Biochemie B.V, Haarlem, The Netherlands	Preparation of plant growth media
$MgSO_4$	Sigma-Aldrich Corporation, St. Louis, U.S.A.	Growth media, buffer solutions
NaCl	VWR International GmbH, Darmstadt, Germany	Growth media, buffer solutions
Orange G	Carl Roth GmbH & Co. KG, Karlsruhe, Germany	Gel loading dye
PEG-1450	Sigma-Aldrich Corporation, St. Louis, U.S.A.	Poplar bud hormone treatment solution
Peptone (Bacto)	Becton, Dickinson and Company, Sparks, U.S.A.	Bacterial growth media
Plant agar	Duchefa Biochemie B.V, Haarlem, The Netherlands	Preparation of plant growth media
Pluronic F-68	Thermo Fisher Scientific Inc., Waltham, U.S.A.	Poplar transformation, surfactant

Chemical name	Supplier	Used for
Polyvinylpyrrolidon K30 (PVP K30)	Carl Roth GmbH & Co. KG, Karlsruhe, Germany	RNA extraction
rac-GR24	Chiralix B.V., Nijmegen, The Netherlands	Poplar treatment (synthetic strigolactone analog)
Sucrose	Duchefa Biochemie B.V, Haarlem, The Netherlands	Preparation of plant and bacterial growth media
Sodium dodecyl sulphate (SDS)	Merck KGaA, Darmstadt, Germany	Buffer solutions
Thidiazuron	Duchefa Biochemie B.V, Haarlem, The Netherlands	Poplar transformation, growth regulator
Ticarcillin disodium / Clavulanate potassium	Duchefa Biochemie B.V, Haarlem, The Netherlands	Poplar transformation, elimination of Agrobacterium
Tris	Carl Roth GmbH & Co. KG, Karlsruhe, Germany	Buffer solutions
Tween-20	Carl Roth GmbH & Co. KG, Karlsruhe, Germany	Poplar bud hormone treatment solution
Yeast extract (Bacto)	Becton, Dickinson and Company, Sparks, U.S.A.	Bacterial growth media

2.3 Oligonucleotides

Oligonucleotides were designed using the Geneious software (Kearse et al., 2012) and synthesized by Life Technologies Inc. (Carlsbad, U.S.A). The lyophilized oligonucleotides were dissolved in 10 mM Tris-HCl pH 8.0 buffer solution to a final concentration of 100 µM. From these stocks, working stocks were prepared as a 1:10 dilutions with sterile water (10 µM final concentration). Oligonucleotides were used for amplification of genes for cloning and sequencing, diagnostic PCR to screen for correct bacteria and plant transformants, as well as quantitative PCR for expression analysis. All oligonucleotides used in this work are listed in Tab. 2.3.

Tab. 2.3 Oligonucleotides used during this work. Number and name of the oligonucleotide, the sequence and the purpose are indicated.

Oligonucleotide name	Sequence 5'-3'	Purpose
8 PtMAX4-1_F	CACCATGGCTTCCTTGGCATTTTCC	Cloning of P. x can MAX4-1
9 PtMAX4-1_R	TTATTTCTTTGGCACCCAGCATC	Cloning of P. x can MAX4-1
10 PtMAX4-2_F	CACCATGGTTTCTGATCAGTATGAGAGCAA	Cloning of P. x can MAX4-2
11 PtMAX4-2_R	TTACTTCTTCGGCACCCAGC	Cloning of P. x can MAX4-2
12 PtMAX4-1+2_seq1	ACCGCCAAATCGAATCGGAG	Sequencing of P. x can MAX4 orthologs
13 PtMAX4-1+2_seq2	GGATGGGTCCACTCGTTTCC	Sequencing of P. x can MAX4 orthologs
18 EF1_F	AAGCCATGGGATGATGAGAC	qPCR reference gene

Oligonucleotide name	Sequence 5'-3'	Purpose
19 EF1_R	ACTGGAGCCAATTTTGATGC	qPCR reference gene
22 M13_F	CGTTGTAAAACGACGGCCAGT	Sequencing of inserts in pENTR/D-TOPO.
23 M13_R	CAGGAAACAGCTATGACCATG	Sequencing of inserts in pENTR/D-TOPO.
24 MAX4-1+2_partial_F1	CACCCGATGGCTATGCCACATTAGTC	Cloning of P. x can MAX4 orthologs
25 MAX4-1+2_partial_F2	CACCACACTGGCGTGGTCAAGCTC	Cloning of P. x can MAX4 orthologs
26 MAX4-1+2_partial_R1	CCCAGCATCCATGTAATCCATA	Cloning of P. x can MAX4 orthologs
34 PtMAX4-1+2_seq3R	TAAGCCTCCGATTCGATTTG	Sequencing of P. x can MAX4 orthologs
35 PtMAX4-1+2_seq4	GAGCATGGGAAAGGAATGG	Sequencing of P. x can MAX4 orthologs
36 PtMAX4-1+2_seq5R	AGGGTGTTGGGGAAGTTAC	Sequencing of P. x can MAX4 orthologs
39 PtMAX2-1_F	CACCGTCTTCAACAATACAGGCC	Cloning of P. x can MAX2-1
40 PtMAX2-1_R	ATGATCATTATTCGTTTAGAAAG	Cloning of P. x can MAX2-1
41 PtMAX2-2_F	CACCCCGTGTGTGCTCTCTCTC	Cloning of P. x can MAX2-2
42 PtMAX2-2_F2	CACCATGGCTGCTACCATGAAC	Cloning of P. x can MAX2-2
43 PtMAX2-2_R	GGAAAAAAAAAACTCAGATCAG	Cloning of P. x can MAX2-2
44 PtMAX2-1_F2	CACCATGGCTAAAAAATTTAACACTAATG	Cloning of P. x can MAX2-1
45 PtMAX2-1_R2	TCAATCAGGAATCGCACG	Cloning of P. x can MAX2-1
46 PtMAX2-2_R2	TCAGTCGAGGATCTGACG	Cloning of P. x can MAX2-2
47 PtMAX2-1_seq1	GGATTCAAGTCCCATGAG	Sequencing of P. x can MAX2 orthologs
48 PtMAX2-2_seq1	CAATCACTGCAGCTTGTC	Sequencing of P. x can MAX2 orthologs
49 Ptc-miR408_F	CAAGGGGAAGCGTGTTCC	Amplification/sequencing of amiRNA backbone.
50 Ptc-miR408_R	TGTCCTCAAAGGACGTTTGTC	Amplification/sequencing of amiRNA backbone.
51 pK7WG_F (RB)	GCGGGAAACGACAATCTG	Sequencing of inserts in pK7WG.
53 pK7WG(2)_R (T35S)	TTGCGGACTCTAGCATGG	Sequencing of inserts in pK7WG(2).
64 ami*MAX2-1_F	ATAGTACCCTCGGGTTTCG	Diagnostic PCR.
65 ami*MAX2-2_F	CACGTTAACTGCCCCATC	Diagnostic PCR.
66 ami*MAX2-1+2_F	CAACCGTGGGAAGTCTATTATG	Diagnostic PCR.
67 ami*MAX4-1_F	GAAACGGATATGCTCTGTTATG	Diagnostic PCR.
68 ami*MAX4-2_F	TCACACACGACAAACTTAGATG	Diagnostic PCR.
69 ami*MAX4-1+2_F	CGACAGGTTCATATTTCCTTTG	Diagnostic PCR.
70 SpecR_F	TAGCTTCAAGTATGACGGGC	Diagnostic PCR.
71 SpecR_R	CGGTTCGTAAGCTGTAATGC	Diagnostic PCR.
85 KanR_F2	GCTTGGGTGGAGAGGCTATT	Diagnostic PCR.
86 KanR_R2	TCAAGAAGGCGATAGAAGGC	Diagnostic PCR.
93 PcMAX2-1_qPCR_F	GCCCGTGGGAGAGGTTTTAT	qPCR
94PcMAX2-1_qPCR_R	CAATGTCCTGTGGAGGCCAA	qPCR

Oligonucleotide name	Sequence 5'-3'	Purpose
95 PcMAX2-2_qPCR_F	TGGCTGGCCTGTATGATTGT	qPCR
96 PcMAX2-2_qPCR_R	CACGCTGTGATGGTTTGTGC	qPCR
97 PcMAX4-1_qPCR_F	TAGAGAAGCTCCGTCTACAAAATCT	qPCR
98 PcMAX4-1_qPCR_R	AATTTCCCATGTCGACTCCCG	qPCR
99 PcMAX4-2_qPCR_F	TTGGAGAGGCTGAGGCTACA	qPCR
100 PcMAX4-2_qPCR_R	GGGCTCCCATCCAAAGGAAT	qPCR
111 PcUBQ_qPCR_F	GTCCACCCTCCATTTGGTCC	qPCR reference gene
112 PcUBQ_qPCR_R	GGTCTTTCCTGTGAGCGTCT	qPCR reference gene
118 Potri.008G115800_qPCR_F	GCTTCCAGGTGGGACAAACT	qPCR
119 Potri.008G115800_qPCR_R	TGGTGGTAGCTTCATGTTCGT	qPCR
120 Potri.010G130200_qPCR_F	ATTTCATGACCACCCCGCAT	qPCR
121 Potri.010G130200_qPCR_R	GGCTTTCTTCAACATGGGCG	qPCR
122 Potri.012G059900_qPCR_F	TGCACAACACTGGAACTCCT	qPCR
123 Potri.012G059900_qPCR_R	TGCATGCCTGATCCCATGTC	qPCR
124 Potri.015G050500_qPCR_F	AGTGGAGTCCCTCTCTTCCC	qPCR
125 Potri.015G050500_qPCR_R	AGGCCTCATGATCCCATGTTT	qPCR
126 Potri.017G112000_qPCR_F	AGCTCTCACCACTCACTTGC	qPCR
127 Potri.017G112000_qPCR_R	GCAGATGGCCTCAACTTCCT	qPCR

2.4 Vectors and plasmids

The vectors and plasmids used in this work are listed in Tab. 2.4.

For sequencing of the candidate genes, the corresponding *P.* x *canescens* gene was cloned into pENTR/D-TOPO (Life Technologies Inc., Carlsbad, U.S.A.) and plasmid DNA was sequenced.

The amiRNA constructs were obtained in the vector pUC57 (cloned by GenScript USA Inc., Piscataway, U.S.A.) and transferred into the binary Gateway destination vector pK7WG2 (VIB, Gent, Belgium) for transformation of plant material. A vector map of pK7WG2 is shown in Appendix Fig. 7.1 (p. 150).

Tab. 2.4 Vectors and plasmids used during this work. The vector name, as well as the insert type and the purpose of use are indicated.

Vector	Insert	Purpose
pENTR/D-TOPO	-	Gateway entry vector
pENTR/D-TOPO	PxMAX4-1 (partial)	Sequencing of P. x can MAX4-1 (partial).
pENTR/D-TOPO	PxMAX4-2 (partial)	Sequencing of P. x can MAX4-2 (partial).
pENTR/D-TOPO	PxMAX2-1	Sequencing of P. x can MAX2-1.
pENTR/D-TOPO	PxMAX2-2	Sequencing of P. x can MAX2-2.
pUC57	amiMAX2-1	Hosting synthesized amiRNA construct.
pUC57	amiMAX2-2	Hosting synthesized amiRNA construct.
pUC57	amiMAX2-1+2	Hosting synthesized amiRNA construct.
pUC57	amiMAX4-1	Hosting synthesized amiRNA construct.

Vector	Insert	Purpose
pUC57	amiMAX4-2	Hosting synthesized amiRNA construct.
pUC57	amiMAX4-1+2	Hosting synthesized amiRNA construct.
pK7WG2	-	Gateway destination vector
pK7WG2	amiMAX2-1 #1	amiRNA expression destination construct.
pK7WG2	amiMAX2-2 #4	amiRNA expression destination construct.
pK7WG2	amiMAX2-1+2 #6	amiRNA expression destination construct.
pK7WG2	amiMAX4-1 #7	amiRNA expression destination construct.
pK7WG2	amiMAX4-2 #9	amiRNA expression destination construct.
pK7WG2	amiMAX4-1+2 #11	amiRNA expression destination construct.
pK7WG2	GUS	GUS control construct, for testing poplar transformation.

2.5 Plants

2.5.1 Plant material

The female *Populus* x *canescens* (Aiton) Sm. clone INRA 717-1B4 was used as a wild type reference in all experiments carried out during this work. *Populus* x *canescens* is a natural poplar hybrid also known as *Populus tremula* x *Populus alba* or gray poplar. It is amenable to genetic transformation and was used as a host for the production of transgenic amiRNA lines for targeted knockdowns of genes involved in the strigolactone pathway (*amiMAX4* and *amiMAX2* lines).

2.5.2 Plant culture media, vessels and substrates

Poplar stem cuttings were routinely propagated in an *in vitro* culture system. As culture vessels, 580 ml glass jars (WECK-Sturzglas Rundrand 100, J.WECK GmbH u. Co. KG, Wehr, Germany) were used. For improved gas exchange, a Paramoll N260/200 fleece ring (Mank GmbH, Dernbach, Germany) was placed between the jar and the lid. The jars were sealed with Micropore surgical tape (3M GmbH, Neuss, Germany) to prevent contamination.
As standard growth medium in the *in vitro* culture, half-strength Murashige & Skoog (½ MS) medium containing vitamins (Duchefa Biochemie B.V, Haarlem, The Netherlands), supplemented with 20 g/l sucrose (Duchefa Biochemie B.V, Haarlem, The Netherlands) and solidified with agar (Kobe I agar, Carl Roth GmbH & Co. KG, Karlsruhe, Germany), was used.
When potted plants for growth in soil were required, young, *in vitro* grown plants (about 6 cm tall) were transferred to plastic pots containing substrate (Fruhstorfer Erde Typ T25, HAWITA Gruppe GmbH, Vechta, Germany) supplemented with 5 % (v/v) washed screed sand (0/8 mm) to prevent excess moisture. Plants were fertilized with a compound fertilizer (WUXAL, AGLUKON Spezialdünger GmbH & Co. KG, Düsseldorf, Germany) when necessary and transferred to bigger pots containing fresh substrate (Fruhstorfer Erde Typ T, HAWITA Gruppe GmbH, Vechta, Germany) roughly every 6 weeks.

2.5.3 Plant growth conditions

The *in vitro* culture vessels were placed in a growth cabinet (AR-66L/3, CLF Plant Climatics GmbH, Wertingen, Germany) or a growth chamber (Johnson Controls, Milwaukee, U.S.A.). A day/night period of 16/8 hours was maintained. The temperature was 22 °C (18 °C during the dark phase in the growth chamber). For lighting, fluorescent tubes (840 and Fluora, OSRAM GmbH, München, Germany) were adjusted to a light flux of 70-80 µE PAR. The relative humidity was adjusted to 60 %.

After the transfer of plants from the *in vitro* culture to pots with substrate, the pots were placed on a plastic tray covered with a transparent lid to increase the relative humidity. For acclimatization of the plants to standard conditions in the growth chamber, the lid was lifted successively over the course of two weeks and removed afterwards. Plants were grown in the growth chamber to a size of about 10-50 cm and then transferred to a greenhouse, if required.

In the greenhouse, a minimum temperature of 22/14 °C (day/night) was maintained by heating. Natural daylight was supplemented with metal halide lamps (HQI-TS 250W/D, OSRAM GmbH, München, Germany) to maintain a 16 h photoperiod.

Some plants were also grown at outdoor conditions as indicated.

If required, greenhouse- and outdoor-grown plants were treated with insecticides and fungicides.

2.6 Bacteria

During this work, *Escherichia coli* (*E. coli*) strains DH5α or TOP10 were used as hosts for molecular cloning and propagation of plasmids. *Agrobacterium tumefaciens* strain GV3101 pMP90 was used as a vector for genetic transformation of poplar.

2.6.1 Bacterial growth media and growth conditions

E. coli was grown at 37 °C in liquid LB medium (10 g/l tryptone, 5 g/l yeast extract, 5 g/l NaCl) or on solid LB plates (additional 15 g/l agar, poured into Petri dishes). *A. tumefaciens* was cultivated at 28 °C in liquid YEB medium (5 g/l beef extract, 5 g/l peptone, 5 g/l sucrose, 1 g/l yeast extract, 2 mM $MgSO_4$) or on solid YEB plates (additional 15 g/l agar, poured in Petri dishes). If required, the appropriate antibiotics were added according to Tab. 2.5. Liquid cultures were grown in plastic culture tubes or Erlenmeyer flasks under constant shaking (180 rpm).

For long-term storage of bacteria, glycerol was added to a fresh liquid culture to a final concentration of 25 % (v/v) and aliquots were stored in a cryogenic vial (Corning Inc., Corning, U.S.A.) at -80 °C.

Tab. 2.5 Antibiotics used during this work for selection of bacteria. The concentration of the stock solutions and the final concentration for bacterial selection, as well as the manufacturer, are indicated.

Antibiotic	Stock	Manufacturer	[Final] *E. coli*	[Final] *Agrobacterium*
Carbenicillin	100 mg/ml in H_2O	Duchefa	100 µg/ml	50 µg/ml
Gentamicin	25 mg/ml in H_2O	Roth		25 µg/ml
Kanamycin	50 mg/ml in H_2O	Roth	50 µg/ml	
Rifampicin	50 mg/ml in DMSO	Duchefa		50 µg/ml
Spectinomycine	100 mg/ml in H_2O	Duchefa	100 µg/ml	100 µg/ml

2.6.2 Competent cells and transformation

The production and transformation of competent bacterial cells used during this work is described below.

For cloning purposes, chemically competent *E. coli* DH5α were prepared. For pENTR/D-TOPO cloning, the chemically competent *E. coli* TOP10 cells provided with the pENTR/D-TOPO cloning kit (Life Technologies Inc., Carlsbad, U.S.A.) were used instead. Electro-competent *A. tumefaciens* GV3101 pMP90 were prepared for transformation with binary destination vectors.

2.6.2.1 Chemically competent E. coli cells and transformation

For the preparation of chemically competent *E. coli* cells, a starter culture of the strain DH5α was inoculated from -80 °C storage in 5 ml LB medium and incubated overnight at 37 °C under constant shaking. 200 ml of fresh LB medium were inoculated with 2 ml of the starter culture and grown in a shaking incubator at 37 °C until the culture reached an OD_{600} of 0.3 – 0.5. The cells were harvested by centrifugation for 10 min at 3450 rcf and 4 °C. The supernatant was discarded and the cells were resuspended in 200 ml ice-cold 100 mM $CaCl_2$. After incubation for 25 min on ice, the cells were harvested by centrifugation (as previously) and the supernatant was discarded. The pellet was resuspended in 8 ml ice-cold 100 mM $CaCl_2$ and ice-cold glycerol was added to a final concentration of 15 % (v/v). After incubation for one hour on ice, 100 µl aliquots were prepared, snap-frozen in liquid nitrogen and stored at -80 °C.

For transformation of competent *E.* coli, the appropriate amount of DNA (100 ng purified plasmid DNA or 1-2 µl of LR reaction) was added to an aliquot of competent cells previously thawed on ice. After 20 min incubation on ice, a heat-shock was performed for 45 s at 42 °C in a water bath. The cells were immediately cooled for 2 min on ice and 400 µl of LB medium (no antibiotics) were added. After incubation at 37 °C for one hour in a shaking incubator, the cells were plated on LB medium containing the appropriate antibiotics and incubated overnight at 37 °C. Individual colonies were picked, re-streaked on fresh LB medium plates and successful transformation was confirmed by colony PCR.

2.6.2.2 Electro-competent A. tumefaciens cells and transformation

For the preparation of electro-competent *A. tumefaciens* cells, a starter culture of strain GV3101 pMP90 was inoculated in 20 ml YEB medium (containing rifampicin and gentamicin) and incubated overnight at 28 °C under constant shaking. A 400 ml YEB rifampicin gentamicin culture was inoculated with the starter culture and grown in a shaking incubator at 28 °C until the culture reached an OD_{600} of 0.3 - 0.6. The cells were harvested by centrifugation for 10 min at 4.000 rcf and 4 °C. The supernatant was discarded. The cells were resuspended in 400 ml ice-cold sterile water and pelleted again by centrifugation (as previously). This washing step was repeated once with 200 ml ice-cold sterile water. The pellet was then washed once in 16 ml ice-cold 10 % glycerol and finally resuspended in 8 ml ice-cold glycerol. 50 µl aliquots were prepared, snap-frozen in liquid nitrogen and stored at -80 °C.

For transformation of electro-competent *A. tumefaciens*, the appropriate amount of DNA (100 ng of purified plasmid DNA) was added to an aliquot of competent cells previously thawed on ice. The mixture was transferred into an electroporation cuvette. An electric pulse (pre-defined program mode “Agr”) was applied using a Bio-Rad MicroPulser electroporation device. 800 µl YEB medium (no antibiotics) were added immediately and the mixture was incubated at 28 °C under constant shaking for two hours before plating on YEB medium containing the appropriate antibiotics (rifampicin, gentamicin and spectinomycine in case of transformation with pK7WG2-based destination clones). Plates were incubated at 28 °C for 2 days. Individual colonies were picked, re-streaked on fresh YEB medium plates and successful transformation was confirmed by colony PCR.

2.7 DNA extraction

2.7.1 Plasmid DNA extraction

Plasmid DNA was extracted from *E. coli* which was used as a cloning host and for propagation of plasmids. 4 ml liquid LB medium containing the appropriate antibiotics were inoculated with the bacterial strain and incubated overnight in a shaking incubator. The cells were collected by centrifugation and plasmid DNA was extracted using the NucleoSpin Plasmid Kit (Macherey-Nagel GmbH & Co. KG, Düren, Germany) according to the manufacturer's instructions. The DNA concentration was measured using a spectrophotometer and plasmid DNA was stored at -20 °C.

2.7.2 Plant DNA extraction

For high-purity DNA extraction using plant material, the DNeasy Plant Mini Kit (Qiagen AQ, Hilden, Germany) was used according to the manufacturer's instructions.
For the extraction of DNA for analytical PCR, e.g. from leaf material of *in vitro* grown *P.* x *canescens* plants to check their transgenic status, a quick DNA preparation protocol was used.

Extraction buffer	0.2 M Tris-HCl pH 8.0
	1.25 M NaCl
	0.025 M EDTA
	0.5 % (w/v) SDS
TE buffer	10 mM Tris-HCl pH 8.0
	1 mM EDTA

Up to 100 mg of plant material were collected in a 2 ml plastic tube containing a 5 mm stainless steel bead (Qiagen AG, Hilden, Germany). The material was snap-frozen in liquid nitrogen and stored at -80 °C if required. The tissue was disrupted at 50 Hz for 2x1 minute using the Qiagen TissueLyser LT. The following steps were carried out at room temperature. 300 µl of extraction buffer were added, the mixture was thoroughly mixed by vortexing and incubated for one minute. After centrifugation at 17.000 rcf for five minutes, the supernatant was transferred to a new tube, mixed thoroughly with 300 µl

2-propanol and incubated for five minutes. After centrifugation at 17.000 rcf for five minutes, the supernatant was discarded. The pellet was air-dried and resuspended in 100 µl TE buffer. The DNA concentration was measured using a spectrophotometer and samples were stored at -20 °C.

2.8 Sequencing of plasmid DNA

For sequencing of plasmids, 600-1200 ng purified plasmid DNA were mixed with 30 pmol (3 µl of a 10 µM stock) sequencing primer (see chapter 2.3; p. 30f) and adjusted with sterile water to a final volume of 12 µl. If required, several reactions with different sequencing primers were performed to cover the full length of the region of interest. The samples were delivered to SEQLAB GmbH (Göttingen, Germany) using the Barcode Economy Run Service.
Sequences were downloaded as files in the ".ab1" format and analyzed using the Geneious Software (Kearse et al., 2012).

2.9 Polymerase chain reaction (PCR)

Polymerase Chain Reaction (PCR) was performed for DNA amplification. This was done for the initial amplification of genes for cloning, as well as for analytical amplification such as colony PCR to check for bacterial colonies harboring the correct plasmid or to monitor the transgenic status of transformed plants. For cloning purposes, a proofreading DNA polymerase (Phusion Hot Start II, Thermo Fisher Scientific Inc., Waltham, U.S.A.) was used to reduce the mutation rate. For analytical PCR, a standard *Taq* DNA polymerase (DreamTaq DNA polymerase, Thermo Fisher Scientific Inc., Waltham, U.S.A.) was used. The PCR reaction mixtures were prepared as a master mix, if applicable, according to the DNA polymerase manufacturer's instructions. As buffers, the solutions provided with the polymerase were used. Oligonucleotides (chapter 2.3; p. 30f) were added from a 10 µM working stock. A dNTP mixture (10 mM each) was prepared from 100 mM dATP, dTTP, dCTP and dGTP (Thermo Fisher Scientific Inc., Waltham, U.S.A.) and added to the appropriate final concentration. As template, purified DNA was used at the recommended concentration. For colony PCR, a small fraction of a bacterial colony was resuspended in sterile water and directly used as template.

The reaction mixes were prepared in a volume of 25 µl or 50 µl in 200 µl single PCR tubes, 8-well stripes or 96-well plates. Reactions were performed in a thermocycler instrument according to the recommendations of the DNA polymerase manufacturer.
PCR products were checked by agarose gel electrophoresis for purity and correct size. Products were purified for downstream processing either directly or as an excised band from an agarose gel using the NucleoSpin Gel and PCR Clean-up kit (Macherey-Nagel GmbH & Co. KG, Düren, Germany).

2.10 Agarose gel electrophoresis

Loading dye 6x	10 mM Tris-HCl pH 8.0
	60 % (v/v) glycerol
	60 mM EDTA
	0.03 % (w/v) Orange G
	0.03 % (w/v) Bromophenol blue
TAE buffer 50x	2 M Tris
	1 M acetic acid
	50 mM EDTA

Agarose gel electrophoresis was performed for the analysis of DNA and RNA length, purity and integrity. Agarose gels (typically 1 % agarose) were prepared by dissolving the agarose (LE agarose, Biozym Scientific GmbH, Hessisch Oldendorf, Germany) in the appropriate amount of 1x TAE buffer by heating in a microwave oven. One drop of 0.025 % ethidium bromide solution (Carl Roth GmbH & Co. KG, Karlsruhe, Germany) was added per 50 ml of gel prior to polymerization. The gel was placed in an electrophoresis chamber and covered with 1x TAE buffer. The samples were mixed with 6x loading dye (1x final concentration) and loaded into the gel pockets next to a DNA size standard (GeneRuler DNA ladder 50bp, 100bp or 1kb, Thermo Fisher Scientific Inc., Waltham, U.S.A.). Gels were run at 90-120 V for the appropriate time and documented on a gel documentation system.

2.11 Cloning of *P.* x *canescens MAX* ortholog candidate genes

Since the sequence of the *P.* x *canescens MAX* ortholog candidate genes was unknown but required for amiRNA design, the genes were amplified from *P.* x *canescens* genomic DNA by PCR using a proofreading DNA polymerase. The PCR products were checked for the correct size by agarose gel electrophoresis, purified from the gel using a purification kit and cloned into the vector pENTR/D-TOPO using the pENTR/D-TOPO Cloning Kit (Life Technologies Inc., Carlsbad, U.S.A.). Correct clones were identified by colony PCR, plasmid DNA was extracted and the cloned insert was sequenced.

2.12 amiRNA design

For the design of artificial microRNA (amiRNA) constructs to specifically target the messenger RNAs (mRNAs) of the selected candidate genes for degradation, the WMD3 Web MicroRNA Designer tool (http://wmd3.weigelworld.org/cgi-bin/webapp.cgi) (Schwab et al., 2006) was used. The *P. trichocarpa* reference sequences of the target genes were used as input, and the corresponding amiRNA sites were designed using default settings. The highest-ranked amiRNAs (best fit to target(s) and low probability of off-targets, based on *P. trichocarpa* genome sequence information) were considered. Since the design was based on the *P. trichocarpa* target gene reference sequences, the target sites of the amiRNAs were confirmed in the corresponding *P.* x *canescens* sequences. The latter were obtained by cloning and sequencing of the candidate genes.

There are two copies each of *MAX4* and *MAX2* in poplar which may be functionally redundant. Hence, amiRNAs for individual and simultaneous silencing were designed. The miRNA and miRNA* sites of the endogenous poplar microRNA precursor ptr-miR408 (Lu et al., 2005) were replaced with the designed sequences to obtain candidate-gene specific amiRNAs. The amiRNA constructs were designed with flanking Gateway *attL* sites to facilitate direct cloning into the Gateway destination vector pK7WG2.

An overview about the amiRNA and amiRNA* sites designed and used in this work to engineer amiRNAs specific for silencing of the intended SL-pathway genes is shown in Tab. 2.6. An example sequence of a full-length amiRNA construct designed and used in this work is given in Appendix Fig. 7.2 (p. 151).

Tab. 2.6 Overview about the amiRNA and amiRNA* sequences designed and used during this work. The target genes are indicated together with the corresponding sites leading to amiRNA specificity. Sequences are noted in 5'-3' orientation.

Target gene(s)	amiRNA sequence	amiRNA* sequence
MAX4-1	TTAACAGTGCATATCCGTCTC	GAAACGGATATGCTCTGTTAT
MAX4-2	TTCTAAGATTGTCGTGTGCGA	TCACACACGACAAACTTAGAT
MAX4-1 + MAX4-2	TAAGGAATTATGAACCTGCCG	CGACAGGTTCATATTTCCTTT
MAX2-1	TTCGAAAGCCGAGGGTACCAT	ATAGTACCCTCGGGTTTCGAT
MAX2-2	TAGATGGCGCAGTTAACGCGA	TCACGTTAACTGCCCCATCTT
MAX2-1 + MAX2-2	TTAATAGTCTTCCCACGGCTG	CAACCGTGGGAAGTCTATTAT

2.13 Synthesis and cloning of amiRNA constructs

The amiRNA constructs used in this work were based on the endogenous poplar microRNA precursor ptr-miR408 (Lu et al., 2005) and designed as described in chapter 2.12 (p. 42f). In order to circumvent laborious cloning procedures, the constructs were designed with flanking *attL* sites and ordered as synthetic DNA constructs in the pUC57 vector from GenScript (Piscataway, U.S.A.). The constructs were then directly transferred into the binary Gateway destination vector pK7WG2 by performing a LR reaction.

2.14 LR reaction (Gateway cloning)

The Gateway system features quick recombination of DNA sequences via *att* sites, allowing the shuttling of an insert flanked with these sites from one vector to another. Frequently, so-called LR reactions are carried out to transfer an insert present in a Gateway entry or donor vector (flanking *attL1* and *attL2* sites) into a Gateway destination vector (*attR1* and *attR2* sites). In this work, the cloning of the insert into an entry or donor vector was omitted for cloning of the amiRNA constructs. The constructs were synthesized directly with flanking *attL* sites, allowing immediate recombination with the binary destination vector pK7WG2.

The LR reactions were carried out using the Invitrogen Gateway LR clonase II enzyme mix (Life Technologies Inc., Carlsbad, U.S.A.) according to the manufacturer's instructions. Usually, incubation time was extended from 1 hour to overnight for enhanced yield, as

recommended. 1 µl of the reaction mixture was directly used for the transformation of competent *E. coli* cells.

2.15 Genetic transformation of *P.* x *canescens* plants

Co-incubation medium	2,2 g/l MS medium incl. vitamins 20g/l sucrose 7 g/l plant agar pH adjusted to 5.8
Selection medium	2,2 g/l MS medium incl. vitamins 20g/l sucrose 7 g/l plant agar 0.01 % (w/v) Pluronic F-68 0.0022 mg/l Thidiazuron 150 mg/l Cefotaxime 200 mg/l Ticarcillin Clavulanate 50 mg/l Kanamycin pH adjusted to 5.8
Rooting medium	2,2 g/l MS medium incl. vitamins 20g/l sucrose 7 g/l plant agar 150 mg/l Cefotaxime 200 mg/l Ticarcillin Clavulanate 50 mg/l Kanamycin pH adjusted to 5.8

P. x *canescens* was transformed using *A. tumefaciens* as a vector according to a transformation protocol adopted from Tobias Brügmann (AG Fladung, Thünen Institute of Forest Genetics, Großhansdorf, Germany). All steps were carried out under sterile conditions.

All transformations were performed using *Agrobacterium tumefaciens* strain GV3101 pMP90, harboring the amiRNA construct in the binary vector pK7WG2, which contains a

kanamycin resistance gene (*NEOMYCIN PHOPHOTRANSFERASE II*) for plant selection. The appropriate *Agrobacterium* strain was streaked out from -80 °C storage on YEB plates containing antibiotics, and cultivated as described (see chapter 2.6.1; p. 36ff). From this fresh culture, a 4 ml liquid culture (same medium) was inoculated and incubated overnight. This starter culture was used to inoculate 100 ml liquid YEB medium (pre-warmed to 28 °C, no antibiotics for rapid growth of the bacteria) as the main culture. The main culture was incubated under standard conditions and the optical density at 600 nm (OD_{600}) was measured frequently. When it reached 0.25 to 0.8, 3‘,5‘-dimethoxy-4‘-hydroxyacetophenone (acetosyringone) was added to a final concentration of 20 µM and the culture was further incubated for 30 minutes to induce the bacteria.

In parallel to the bacterial culture, the plant material was prepared. For the transformation, approx. 6 weeks old *P.* x *canescens* wild type plants grown *in vitro* under standard conditions (see chapter 2.5.2; p. 34ff), were used. These plants have little lignification, making them easier to process and regeneration efficiency is higher compared to older plants. Whole shoots were harvested and the leaves and shoot tips were discarded. If required, the stems were stored in liquid ½ MS medium for several hours before cutting into small explants (approx. 3-8 mm) using a scalpel blade.

The explants were transferred into the *Agrobacterium* main culture and incubated for 30 minutes in a shaking incubator at 120 rpm and 28 °C. After this inoculation step, the explants were retrieved from the bacterial culture using a sieve. Excess liquid was removed by blotting on filter paper and the explants were distributed in Petri dishes containing co-incubation medium. These plates were then incubated for three days at 25 °C in the dark to allow the bacteria to overgrow the explants and transform the plant cells.

For removal of *Agrobacterium*, the explants were collected and washed 1x in sterile water, 3x in 400 µg/ml ticarcillin clavulanate and 1x in sterile water (in this order). Each washing step was carried out in an Erlenmeyer flask for five minutes under manual shaking and the explants were retrieved using a sieve. After the last washing step, excess liquid was removed by blotting on filter paper, and the explants were distributed in Petri dishes containing selection medium (including kanamycin). As a control for regeneration efficiency, the same medium without kanamycin was used.

The plates were placed in a growth cabinet at approx. 10 µE lighting. Regenerates developed after 2-6 weeks and were transferred into culture vessels containing rooting medium for further growth. The light intensity was increased to approx. 20 µE. If required, the regenerates were subsequently transferred to fresh rooting medium every

four weeks. When shoots emanated from the regenerates, cuttings were made and placed on rooting medium. Rooted cuttings were sampled (leaves) and the transgenic status was tested by PCR. To avoid false-positive results from bacteria persisting in the plant tissue, a second PCR was performed to exclude this possibility (PCR against the spectinomycine resistance gene on the vector backbone of pK7WG2, used for bacteria selection).

Confirmed transgenic lines received a line number, were adapted to standard *in vitro* cultivation conditions (increased light intensity) and propagated. An illustration of the transformation procedure is given in Fig. 2.1.

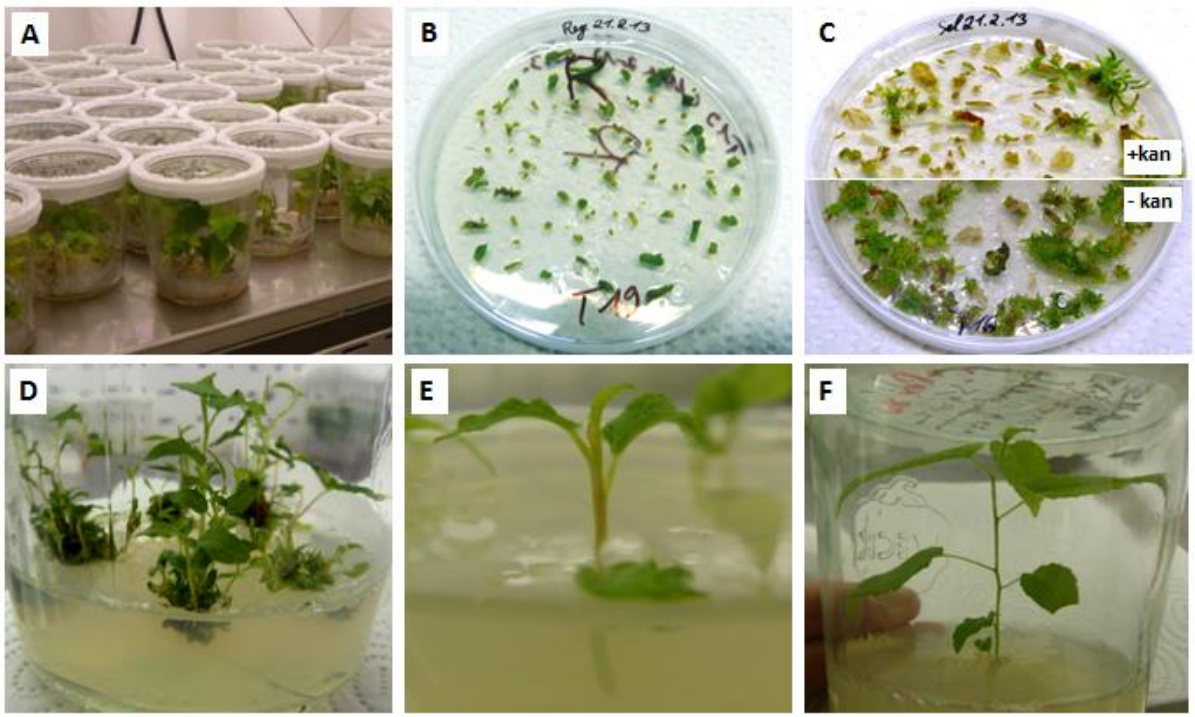

Fig. 2.1 Illustration of the genetic transformation of poplar. *P.* x *canescens* wild type plants grown *in vitro* (A) serve as a starting material for the transformation. After co-incubation with *A. tumefaciens*, the explants are arranged on the appropriate medium (B). After 4-6 weeks, regenerates develop (C). After further cultivation, the regenerates start to produce shoots (D) which are used to prepare cuttings (E). Rooted cuttings (F) are analyzed by PCR and transgenic plants are assigned with a line number.

2.16 Gene expression analysis

For gene expression analysis, quantitative PCR (qPCR) was performed. Total RNA was extracted from various plant tissues and used for synthesis of complementary DNA (cDNA) by *in vitro* reverse transcription. The cDNA was used for quantification by qPCR.

2.16.1 RNA extraction

Total RNA was extracted from plant tissues using the innuPREP Plant RNA Kit (Analytik Jena AG, Jena, Germany) or a CTAB-based extraction protocol ("pine method") (Chang et al., 1993). The detailed protocols are outlined in the following sections.
For poplar leaf material, the RNA extraction kit was a reliable and fast option and was used if only this tissue type was tested. For other tissue types, the performance of the kit was insufficient and the CTAB-based protocol was used instead. For high quality RNA extraction from axillary buds, a combination of both protocols was required, as suggested by Ruttink et al. (2007). In this case, the samples were initially processed according to the CTAB-based protocol. After LiCl precipitation, the samples were used as starting material for RNA extraction using the kit.
After RNA extraction, the RNA concentration was determined using a spectrophotometer. If required, RNA integrity was monitored on a 1 % agarose gel.

2.16.1.1 RNA extraction using the innuPREP Plant RNA Kit

For leaf material, the innuPREP Plant RNA Kit was highly effective and therefore used if only this tissue type was tested, as for the expression analysis of the poplar *MAX2* orthologs in transgenic *amiMAX2* lines (see chapter 3.7.1; p. 91ff).
Up to 100 mg of leaf material were collected in a 2 ml plastic tube containing a 5 mm stainless steel bead (Qiagen AG, Hilden, Germany). The material was snap-frozen in liquid nitrogen and stored at -80 °C if required. The tissue was disrupted at 50 Hz for 3x1 minute using the Qiagen TissueLyser LT. 450 µl lysis solution PL (supplied with the kit) were added and the mixture was incubated for 10 min in a Thermomixer at 1.400 rpm and room temperature. The following steps were carried out according to the manufacturer's

instructions. RNA samples were eluted in 50 µl RNase-free water. Samples were stored at -80 °C.

2.16.1.2 RNA extraction using a CTAB-based protocol

A CTAB-based protocol (Chang et al., 1993) was used for poplar tissues (roots, bark, developing xylem, wood, axillary buds) for which the kit-based RNA extraction did not yield sufficiently high RNA quality and quantity.

Isolation buffer	2 % (w/v) CTAB
	2 % (w(v) PVP K30
	25 mM EDTA
	2 M NaCl
	100 mM Tris-HCl pH 8.0
SSTE buffer	0.5 % (w/v) SDS
	1 mM EDTA
	1 M NaCl
	10 mM Tris-HCl pH 8.0

The plant material was harvested, snap-frozen in liquid nitrogen and stored at -80 °C, if required. The tissue was disrupted by manual grinding using a mortar and pestle, cooled with liquid nitrogen. 1.5 ml isolation buffer and 30 µl 2-mercaptoethanol were mixed, heated to 65 °C in a water bath and added to 200 mg of the plant material. The sample was briefly mixed and incubated for 15 min at 65 °C prior to incubation for 15 min under shaking at 160 rpm and room temperature. 1.5 ml chloroform:isoamylalcohol (24:1) were added. After shaking for 15 min at 160 rpm and room temperature, the samples were centrifuged for 15 min at 17.000 rcf. The aqueous (upper) phase was transferred to a new tube and 1.5 ml chloroform:isoamylalcohol (24:1) were added. After shaking for 15 min at 160 rpm and room temperature, the samples were centrifuged for 15 min at 17.000 rcf. The aqueous phase was transferred to a new tube and the volume was determined. The 0.3-fold volume of 8 M LiCl (4 °C) was added and the RNA was precipitated overnight on ice.

The samples were centrifuged for 40 min at 4 °C and 17.000 rcf and the supernatant was discarded. For extraction of RNA from poplar buds, at this step the processing was continued using the RNA extraction kit as described above, starting with the addition of buffer PL. For all other tissues, extraction was continued according to the CTAB-based protocol by dissolving the pellet in 100 µl SSTE buffer (pre-warmed to 65 °C) in a Thermomixer at 42 °C and 850 rpm. 100 µl chloroform:isoamylalcohol (24:1) were added, the sample was mixed by vortexing and centrifuged for 5 min 17.000 rcf and room temperature. The aqueous phase was transferred to a new tube. The chloroform:isoamylalcohol extraction was repeated once and after transfer of the aqueous phase to a new tube, 200 µl ethanol (96 %, ice-cold) were added and the RNA was precipitated for at least 2 h on ice. The samples were centrifuged for 40 min at 4 °C and 17.000 rcf and the supernatant was discarded. The pellet was washed with 400 µl of 70 % ethanol. The samples were centrifuged at 4 °C and 17.000 rcf and the supernatant was discarded. The pellet was air-dried at 37 °C and resuspended in 20 µl RNase-free water. Samples were stored at -80 °C.

2.16.2 cDNA synthesis (reverse transcription)

Complementary DNA (cDNA) was prepared by reverse transcription of total RNA using the Fermentas RevertAid H Minus First Strand cDNA Synthesis Kit (Thermo Fisher Scientific Inc., Waltham, U.S.A.). The obtained cDNA was used as template DNA for quantification by qPCR.

Prior to cDNA synthesis, a DNase I treatment was performed to eliminate possible contaminations by genomic DNA. The following components (provided with the kit or purchased separately from the same manufacturer) were added to an RNase-free tube:

Total RNA	up to 1 µg
10X Reaction Buffer with $MgCl_2$	1 µl
DNase I	1 µl (1 u)
RNase Inhibitor RiboLock	0.5 µl (10 u)
Water, nuclease-free	to 10 µl

The samples were incubated for 30 min at 37 °C and the reaction was terminated by adding 1 µl 50 mM EDTA and incubation for 10 min at 65 °C.

For cDNA synthesis, the following reagents were added:

5X Reaction Buffer	4 µl
Oligo $(dT)_{18}$ primer	1 µl
RiboLock RNase Inhibitor (20 u/µl)	0.5 µl (10 u)
10 mM dNTP Mix	2 µl
RevertAid H Minus Reverse Transcriptase	1 µl (200 u)
Water, nuclease-free	to 20 µl

The mixture was incubated for 60 min at 42 °C and the reaction was terminated by incubation for 5 min at 70 °C. The product of the reaction was stored at -80 °C.
The cDNA quality was tested by standard PCR using intron-spanning primers, which reveal genomic DNA contamination.

2.16.3 quantitative PCR (qPCR)

Quantitative PCR (qPCR) was performed for analysis of the expression of a gene of interest relative to a reference gene. As reference genes, poplar *UBIQUITIN* (*UBQ*; Potri.001G418500) or poplar *ELONGATION FACTOR 1* (*EF1*; Potri.001G224700) were used (Regier and Frey, 2010).
The reaction setup was done using the SsoFast EvaGreen Supermix (Bio-Rad Laboratories Inc., Hercules, U.S.A.), containing all required components except for primers and template. Primers were added to a final concentration of 500 nM each. Reaction mixes were prepared as master mixes for each primer pair and distributed in 96 well plates (Multiplate clear, Bio-Rad Laboratories Inc., Hercules, U.S.A.). As template, 6 µl of a 1:10 dilution of the cDNA were added to gain a final reaction volume of 15 µl. For each reaction, three technical replicates were made. Reactions for different target genes in the same sample were always performed on the same 96 well plate.
The reaction was performed according to the recommendations in the SsoFast EvaGreen Supermix protocol on a CFX96 Real-Time PCR Detection System (Bio-Rad Laboratories Inc., Hercules, U.S.A.).
Data analysis was done using the Bio-Rad CFX Manager software (Bio-Rad Laboratories Inc., Hercules, U.S.A.) and Microsoft Excel (Microsoft Corporation, Redmond, U.S.A.). Generally, the quantification cycle (C_q) was determined for all samples and the average of

the three technical replicates was calculated. The cycle number difference between the target and reference genes (ΔC_q[target-reference]) was calculated and the relative expression was determined according to the formula $2^{-\Delta Cq}$. The average and standard deviation of the relative expression were calculated for all biological replicates and different sample types were compared.

2.17 Phenotyping of architectural plant traits

The transgenic lines generated during this work were phenotyped for architectural traits to investigate the impact of the gene knockdowns on plant architecture. Therefore, plants were transferred from the *in vitro* culture to pots and grown in a growth chamber, a greenhouse or under outdoor conditions as described (see chapter 2.5; p. 33ff). *P.* x *canescens* wild type plants were always grown and evaluated in parallel.

At an appropriate size (e.g. about 1.5 m shoot height for 3 months old greenhouse-grown plants), plants were photographed and the shoot height as well as the stem base diameter were measured. The number of nodes was counted and the number of branches and their position was recorded. In addition to this basic phenotyping, additional parameters were determined for several lines. The shoot was separated into stem and leaves (separately for the main stem and branches), and the corresponding biomass was determined by weighing. Beside this determination of the fresh weight, also the dry weight was measured after drying of the samples at 60 °C for an appropriate time (until they did not lose weight anymore). The root system was accessed by washing off the culture substrate. Excess water was removed using a salad spinner. The roots were photographed and the fresh and dry weight was determined as well.

If required, samples were taken for RNA extraction and expression analysis. Leaves and buds were always harvested from a defined position (defined number of nodes counted from the apex). Bark, developing xylem and wood were sampled at the stem base just above the soil level. The bark was peeled off manually. Developing xylem was then scraped from the stem with a scalpel blade. The remaining tissue was cut into small pieces using secateurs and taken as a wood sample. From the root system, young, white/gray-colored tissue was collected. All samples were snap-frozen in liquid nitrogen and stored at -80 °C until processing.

2.18 Poplar leaf JA-treatment

To confirm the jasmonic acid (JA) induced up-regulation of the expression of Potri.004G182100 which was used as JA-marker gene, *P.* x *canescens* wild type leaves from plants grown in a growth chamber (6 weeks old after potting) were detached and placed in a glass container containing wet filter paper to increase the moisture and to prevent wilting of the leaves. Methyl jasmonate (95 %) was pipetted on dry filter paper (1 µl per 1 l of container volume) and placed in the glass container. A mock-treatment without methyl jasmonate was performed. The leaves were collected after 22 hours, snap-frozen in liquid nitrogen and stored at -80 °C.

2.19 Poplar GR24 treatments

Treatments with the synthetic strigolactone analog rac-GR24 (Chiralix B.V., Nijmegen, The Netherlands) were performed to test the effect of the hormone on *P.* x *canescens* wild type stem cuttings bearing one or two axillary buds (one- and two-node-assays). Furthermore, application of the hormone directly to dormant buds was tested in intact wild type and transgenic *amiMAX4-1+2* plants. In the latter, complementation of the increased branching phenotype was tested.

2.19.1 GR24 treatment of *P.* x *canescens* stem cuttings

Stem cuttings bearing one or two nodes (including the buds; the leaves were removed) were prepared from young *in vitro* grown *P.* x *canescens* plants. Cuttings from different plants were randomized and placed on standard ½ MS medium containing 5 µM GR24 or the same volume of acetone (0.05 % final concentration) which was used as solvent for GR24 as mock control. Bud outgrowth was defined as the unfolding of the first leaf and monitored daily.

In one-node-assays, the single bud grows out in virtually all cuttings. Therefore, the average time until bud outgrowth was calculated. In two-node-assays, not all buds grow out. Therefore, the percentage of outgrown buds was calculated at a defined time point.

2.19.2 GR24 treatment of axillary buds

Bud treatment solution	1 % (w/v) PEG-1450
	6.25 % (v/v) ethanol
	0.0125 % (v/v) Tween-20
	0.05 % (v/v) acetone

Plants grown *in vitro* were potted and acclimatized to growth chamber conditions. Bud treatment was started 3 weeks after potting and done twice a week, i.e. every 3-4 days. The first treatment was applied at freshly grown (after potting) buds at node 4 counted from the apex, while node 1 was counted as the most apical node bearing a young, unfolded and expanding leaf. Bud treatment solution was prepared according to Dun et al. (2009) with modifications recommended by C. Beveridge (University of Queensland, Brisbane, Australia; personal communication). 6 µl of bud treatment solution containing 5 µM GR24 were pipetted directly on the buds. As mock control, 6 µl of bud treatment solution containing no GR24 (but acetone which was used as a solvent for GR24), were applied. The treatment was repeated twice for the same buds at the following treatment time points, i.e. the second and third treatment were done after 3-4 days each. While the plants grew, new buds reaching the position at node 4 counted from the apex were included in the treatment over the course of the experiment and the solution was applied three times in total as well. In total, axillary buds at 10-15 consecutive nodes were treated per plant. The time point of bud outgrowth was recorded for each individual bud and the time from the first treatment until outgrowth was calculated.

2.20 Poplar grafting

Grafting of poplar was carried out to combine rootstocks and scions (shoots) of different genotypes (wild type and amiRNA lines) and to analyze the resulting plant architecture.
Young, approx. 6 cm tall plants grown from cuttings propagated *in vitro* were potted and acclimatized to growth chamber conditions for 2.5 weeks. For the graft-combination of different genotypes (and self-grafted controls within the same genotype), a wedge-grafting technique was used. The stem of the rootstock was cut horizontally approx. 4-5 cm above the soil level using a clean scalpel blade. The stump was sliced vertically in the middle, about 5 mm deep. The scion was prepared by cutting the apex of a suitable plant/genotype at a length of approx. 2-3 cm. All leaves >1 cm were removed to reduce transpiration and the stump of the scion was sliced to form a wedge shape. The scion was carefully inserted into the sliced stump of the rootstock, ensuring as much direct contact of the tissues as possible. A 1 cm long piece of silicone tube (1.5/3.5 mm Ø; Carl Roth GmbH & Co. KG, Karlsruhe, Germany) was sliced longitudinal and wrapped around the graft union to stabilize it mechanically. To prevent drying of the graft union, it was wrapped in Parafilm M laboratory film (Bemis Inc., Neenah, U.S.A.). A photograph of a grafted plant is shown in Fig. 2.2 A.
The grafted plants were placed in a tray with sufficient water and covered with a transparent plastic lid to maintain high humidity. Plants were further cultivated in a growth chamber. For the first day after grafting, the plants were kept entirely dark, and shading was successively removed over the course of one week. Then the humidity was reduced by stepwise lifting of the tray hood, as routinely done for acclimatization of plants potted from the *in vitro* culture. Shoots developing from axillary buds at the rootstock (below the graft union) due to initial release from apical dominance were removed using a scalpel blade. After 2-3 weeks, the plants formed a stable graft union. The Parafilm and silicone tube were removed. A close-up photograph of the graft union after healing is shown in Fig. 2.2 B. Further cultivation was done under standard conditions.
For interstock grafting, the grafting procedure was repeated. When the graft union of the first grafting step was completely healed, another grafting step was performed by cutting of the rootstock 1-2 cm above to first graft union and inserting a new scion. Therefore, the scion of the first grafting step was turned into the interstock.

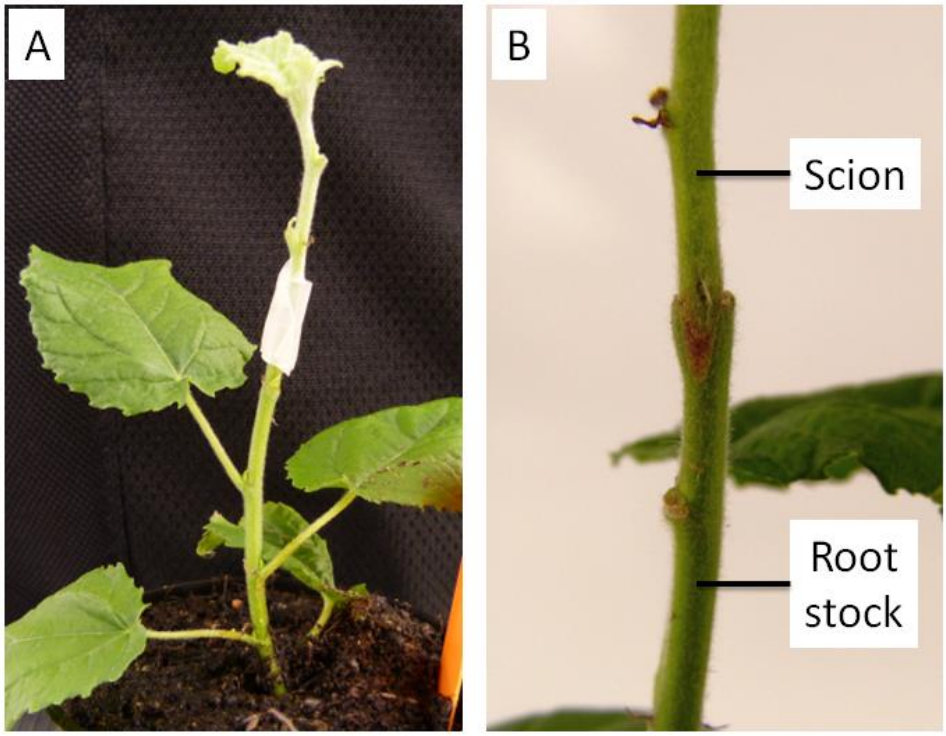

Fig. 2.2 Photographs of grafted poplar plants. Poplar plant directly after grafting. The grafting site is stabilized with a silicone tube and Parafilm (A). Close-up of the graft union after healing (B).

3 Results

3.1 Identification of branching-relevant poplar SL-pathway genes

To study the strigolactone (SL) pathway in poplar, candidate genes were selected based on published data. In *Arabidopsis* and other species, knockout mutants of the genes in this pathway exhibit highly increased branching (Seto and Yamaguchi, 2014). In this study, the genes *MORE AXILLARY GROWTH4* (*MAX4*) and *MORE AXILLARY GROWTH2* (*MAX2*) were chosen for analysis in poplar. *MAX4* is involved in SL biosynthesis (Sorefan et al., 2003) and *MAX2* participates in SL signaling (Stirnberg et al., 2007) in *Arabidopsis*.

To identify poplar orthologs of *MAX4* and *MAX2*, a BLAST (Basic Local Alignment Search Tool) analysis was performed. The *Arabidopsis* protein sequences taken from TAIR (The Arabidopsis Information Resource; www.arabidopsis.org) (Lamesch et al., 2011) were used as a query to search for similar sequences in a poplar translated nucleotide database (TBLASTN search) on Phytozome (www.phytozome.org) (Goodstein et al., 2012). For both candidate genes, two poplar orthologs each with high ranks in the BLAST analysis were identified (Tab. 3.1). The presence of two orthologs was expected, since a whole genome duplication occurred in the *Salicaceae* family, which comprises poplar (Tuskan et al., 2006). The genes identified here were also described in a recent publication as poplar orthologs of the *Arabidopsis MAX* genes and were shown to be able to (partially) complement the mutant phenotypes in *Arabidopsis* (Czarnecki et al., 2014). The corresponding annotation from this publication is included in (Tab. 3.1).

Protein sequence alignments based on *in silico* translations of the *Arabidopsis MAX* genes and their poplar orthologs were done using the Geneious Software (Kearse et al., 2012), showing a high degree of conservation (Appendix Fig. 7.3 and Fig. 7.4, p. 152).

Tab. 3.1 Overview about the selected SL pathway candidate genes. *Arabidopsis MAX4* and *MAX2*, as well as their corresponding poplar orthologs, are shown. The names of the poplar orthologs as used in this work are indicated together with the gene names used in a recent publication (Czarnecki et al., 2014). Gene IDs are indicated as they can be found in the TAIR (for *Arabidopsis*) and Phytozome databases (for poplar).

Gene name (this work)	Gene name (Czarnecki *et al.*, 2014)	Species	Gene ID	Length CDS [bp]	Length genomic [bp]	Length protein [aa]
AtMAX4		*A. thaliana*	At4G32810	1713	3258	570
PtMAX4-1	*PtrMAX4b*	*P. trichocarpa*	Potri.006G238500	1674	5367	557
PtMAX4-2	*PtrMAX4a*	*P. trichocarpa*	Potri.018G044100	1674	3953	557
AtMAX2		*A. thaliana*	At2G42620	2082	2329	693
PtMAX2-1	*PtrMAX2b*	*P. trichocarpa*	Potri.011G066700	2016	3198	671
PtMAX2-2	*PtrMAX2a*	*P. trichocarpa*	Potri.014G142600	2106	2890	701

3.2 Sequencing of *MAX* genes in *Populus* x *canescens*

In 2006, a poplar whole genome sequence was published (Tuskan et al., 2006). However, the species used in the sequencing project was *Populus trichocarpa* (black cottonwood), which is not well amenable to genetic transformation. In contrast, *Populus* x *canescens* (gray poplar, a natural poplar hybrid) is well-transformable using *Agrobacterium tumefaciens* as a vector. Established transformation protocols are available (e.g. as described by Filichkin et al., 2006), making it a suitable species for projects requiring the generation of transgenic poplar plants. Therefore, *P.* x *canescens* was also used in this work.

In this project, targeted gene knockdowns using artificial microRNAs (amiRNAs) were carried out. This method can be used for knocking down genes with high specificity, but it requires precise knowledge of the target sequence. Since no whole genome sequence is available for *P.* x *canescens* and also expressed sequence tag (EST) data could not be found, the target genes intended to be knocked down were cloned and sequenced.

Clones were obtained for all *P.* x *canescens MAX4* and *MAX2* orthologs, although for *MAX4*, only a truncated version could be successfully cloned. PCR using the forward primer initially designed for full-length amplification of both *MAX4* orthologs did not yield any amplicon. This is most likely due to sequence variations at this site between *P. trichocarpa* and *P.* x *canescens*, combined with the fact that primer design was based on the *P. trichocarpa* sequence information. Therefore, an alternative forward primer within the predicted coding sequence (CDS) was designed and used for successful cloning of a truncated version of the gene.

The obtained clones were sequenced and compared to the *P. trichocarpa* reference sequences. The DNA and protein sequence identities are shown in Tab. 3.2. Both values were very high (≥97.6 %), as expected for species from the same genus. However, differences on the single nucleotide level had to be considered for amiRNA design.

Alignments of all *MAX* gene sequences from *P. trichocarpa* and *P.* x *canescens* are shown in Appendix Fig. 7.5 - Fig. 7.8 (p. 153f). For *MAX4-1* and *MAX4-2*, the obtained *P.* x *canescens* sequences from a genomic clone were manually spliced according to the annotations from *P. trichocarpa* in order to show only relevant sequence data, and aligned to the *P. trichocarpa* reference CDS sequences. The introns are removed during mRNA processing and are not suited as targets for amiRNA. For *MAX2-1* and *MAX2-2*, manual editing was not necessary since these genes do not contain introns.

Tab. 3.2 Sequence and protein identity of *P.* x *canescens* (*Pc*) *MAX4* and *MAX2* orthologs compared to the corresponding *P. trichocarpa* reference sequence.

Gene	DNA sequence identity [%]	Protein sequence identity [%]
PcMAX4-1	98.5	97.9
PcMAX4-2	98.5	98.9
PcMAX2-1	98	98.1
PcMAX2-2	97.6	99

Based on the obtained sequence data, artificial microRNAs were designed as described in chapter 2.12 (p. 42f). Since there are two highly similar orthologs of *MAX4* and *MAX2* in poplar (designated *MAX4-1* and *MAX4-2* as well as *MAX2-1* and *MAX2-2*), amiRNAs for silencing of individual *MAX* orthologs (*amiMAX4-1* and *amiMAX4-2* as well as *amiMAX2-1* and *amiMAX2-2*), and simultaneous silencing of both orthologs (*amiMAX4-1+*2 and *amiMAX2-1+2*), were designed. Individual silencing was performed based on the idea that the two orthologs may be functionally different, and unraveling these possible functions would be an interesting example of gene diversification. However, also similar functions were likely based on the knowledge of the highly similar sequences. This would lead to redundancy, masking the effect of individual knockdowns. Thus, simultaneous silencing of both orthologs was done as well to produce a knockdown phenotype.

3.3 Expression pattern of *MAX* genes in wild type poplar

To investigate the expression patterns of the selected SL pathway candidate genes in poplar, publicly available microarray data from *Populus balsamifera* was evaluated. Additionally, qPCR expression analysis was performed for different tissues of *Populus* x *canescens*, the species used during this work.

3.3.1 Expression pattern of *MAX* genes in *P. balsamifera* (poplar eFP browser)

For an initial overview about the expression patterns of the poplar *MAX* candidate genes, the web-based tool *Populus* electronic Fluorescent Pictograph (eFP) browser (http://bar.utoronto.ca/efppop/cgi-bin/efpWeb.cgi) (Wilkins et al., 2009) was used. This tool allows to access transcript abundance data from an Affymetrix Poplar Genome Array experiment carried out with different *Populus balsamifera* tissues, including young and mature leaves, roots and developing xylem. The output of the web tool is a graphical illustration of the transcript abundance as shown in Fig. 3.1 for the poplar *MAX4* orthologs and in Fig. 3.2 for the *MAX2* orthologs. Generally, expression of the candidate genes was low when compared to the reference gene *UBIQUITIN* (*UBQ*; Potri.001G418500), for example. This gene had a fluorescence readout of approximately 30.000 units for example in the roots, while readouts for the *MAX* genes were well below 2.000 units.

For *MAX4-1*, the strongest signal was found in roots, while it was very weak in all other tissues. Absolute values for *MAX4-2* were very low, with the highest expression in male catkins (Fig. 3.1). For *MAX2-1* and *MAX2-2*, absolute values were higher and a more uniform expression pattern was found for both genes. Expression was rather high in roots and developing xylem, as well as young leaves (Fig. 3.2).

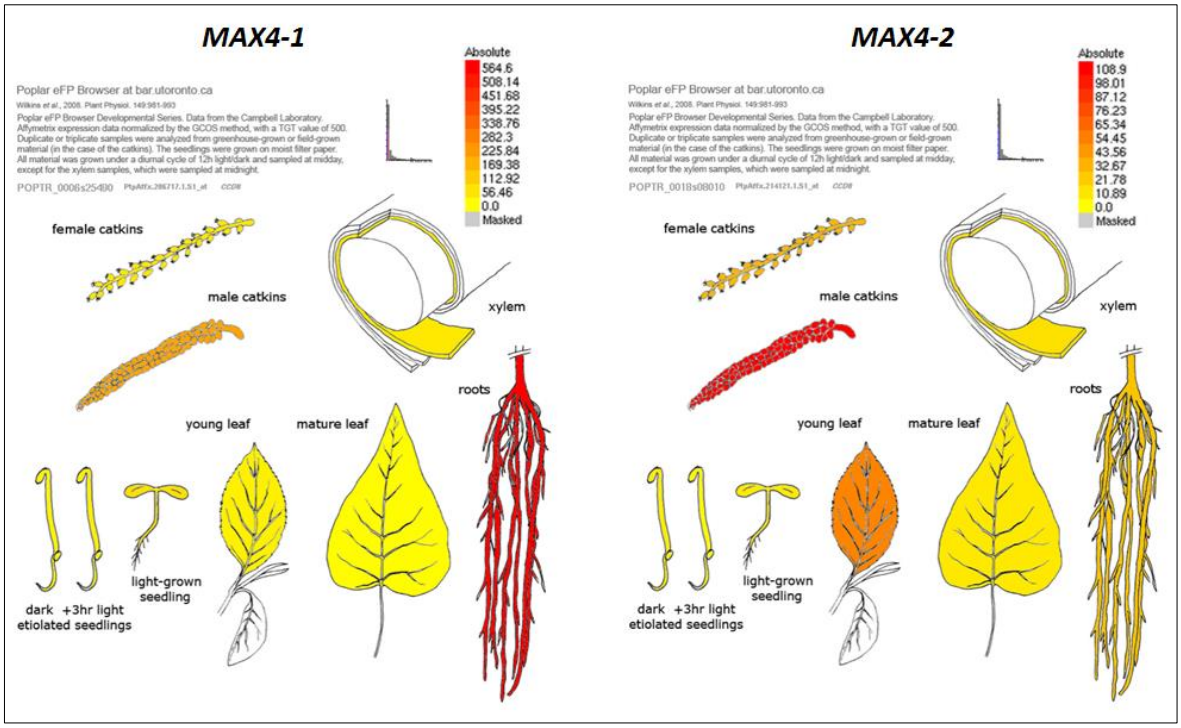

Fig. 3.1 ***Populus* eFP browser expression data for *MAX4-1* and *MAX4-2* in different tissues.** Yellow color indicates low transcript abundance, while red color represents high transcript levels. Note the respective absolute fluorescence readout scale at the top.

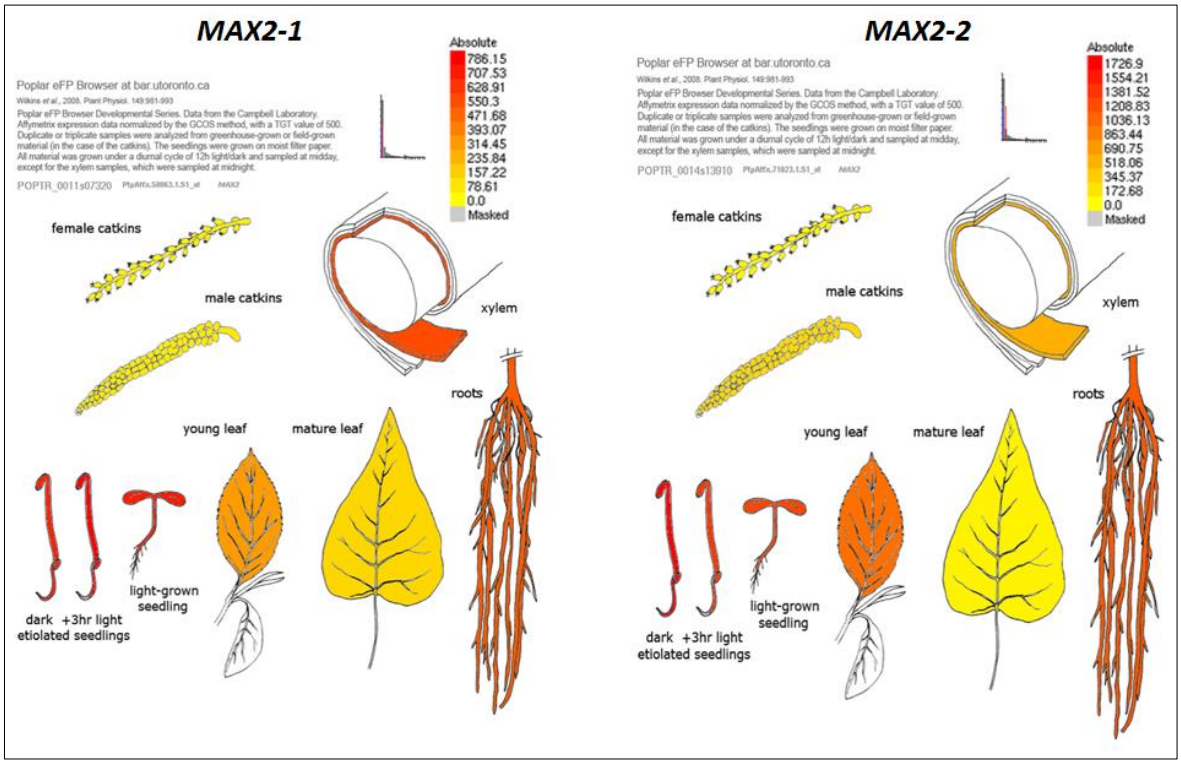

Fig. 3.2 ***Populus* eFP browser expression data for *MAX2-1* and *MAX2-2* in different tissues.** Yellow color indicates low transcript abundance, while red color represents high transcript levels. Note the respective absolute scale at the top. Note the respective absolute fluorescence readout scale at the top.

3.3.2 Expression pattern of *MAX* genes in *P.* x *canescens*

The poplar eFP browser data shown in the previous section is based on *P. balsamifera* samples. For expression analysis of the selected SL-pathway genes in *P.* x *canescens*, the species used in this work, a qPCR experiment was performed.

Whole *in vitro* grown wild type plants were dissected into leaves, roots and stems and the expression levels of the candidate genes relative to *UBIQUITIN* (*UBQ*, Potri.001G418500) were determined. The obtained expression data is shown in Fig. 3.3. Expression of *MAX4-1* and *MAX4-2* was extremely low and could only be detected in roots and stems. *MAX2-1* and *MAX2-2* transcript levels were very low in roots. In leaves and stems, expression was also low, but considerably higher compared to *MAX4* and well-detectable.

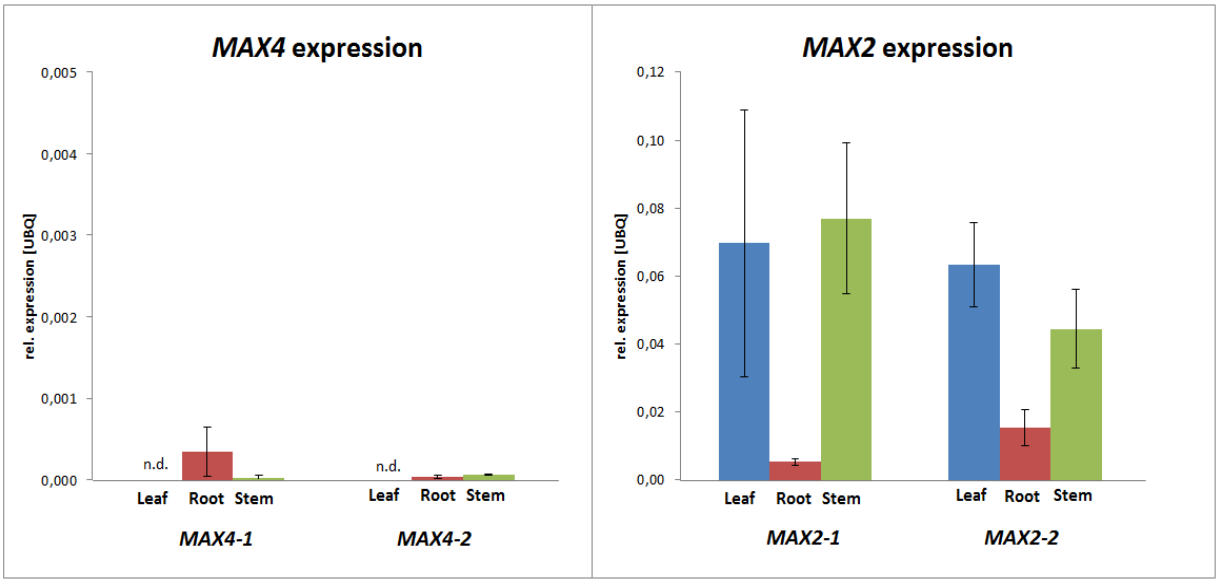

Fig. 3.3 Expression of *P.* x *canescens MAX4* and *MAX2* orthologs in different tissues of *in vitro* grown WT plants. Expression levels were normalized against the reference gene *UBQ*. n=3 pools of tissue from 3 individual plants each. Error bars indicate standard deviation.

For a more detailed analysis, greenhouse-grown wild type plants (4.5 months old) were separated into leaves, roots, dormant axillary buds, wood, bark as well as developing xylem, and subjected to qPCR analysis. As for *in vitro* grown plants, the expression levels of the candidate genes relative to *UBQ* were determined.

Also in the greenhouse-grown plants, expression of *MAX4-1* and *MAX4-2* was generally very low. Transcripts of both genes could not be detected in leaves, dormant axillary buds and bark. Expression was extremely low in roots and developing xylem, but significantly higher in the wood samples (stem tissue without bark and developing xylem) (Fig. 3.4).

Expression of *MAX2-1* and *MAX2-2* was also low relative to the reference gene, but transcripts from these genes could be detected in all tested tissues. Expression appeared to be highest in leaves and lowest in roots (Fig. 3.5).

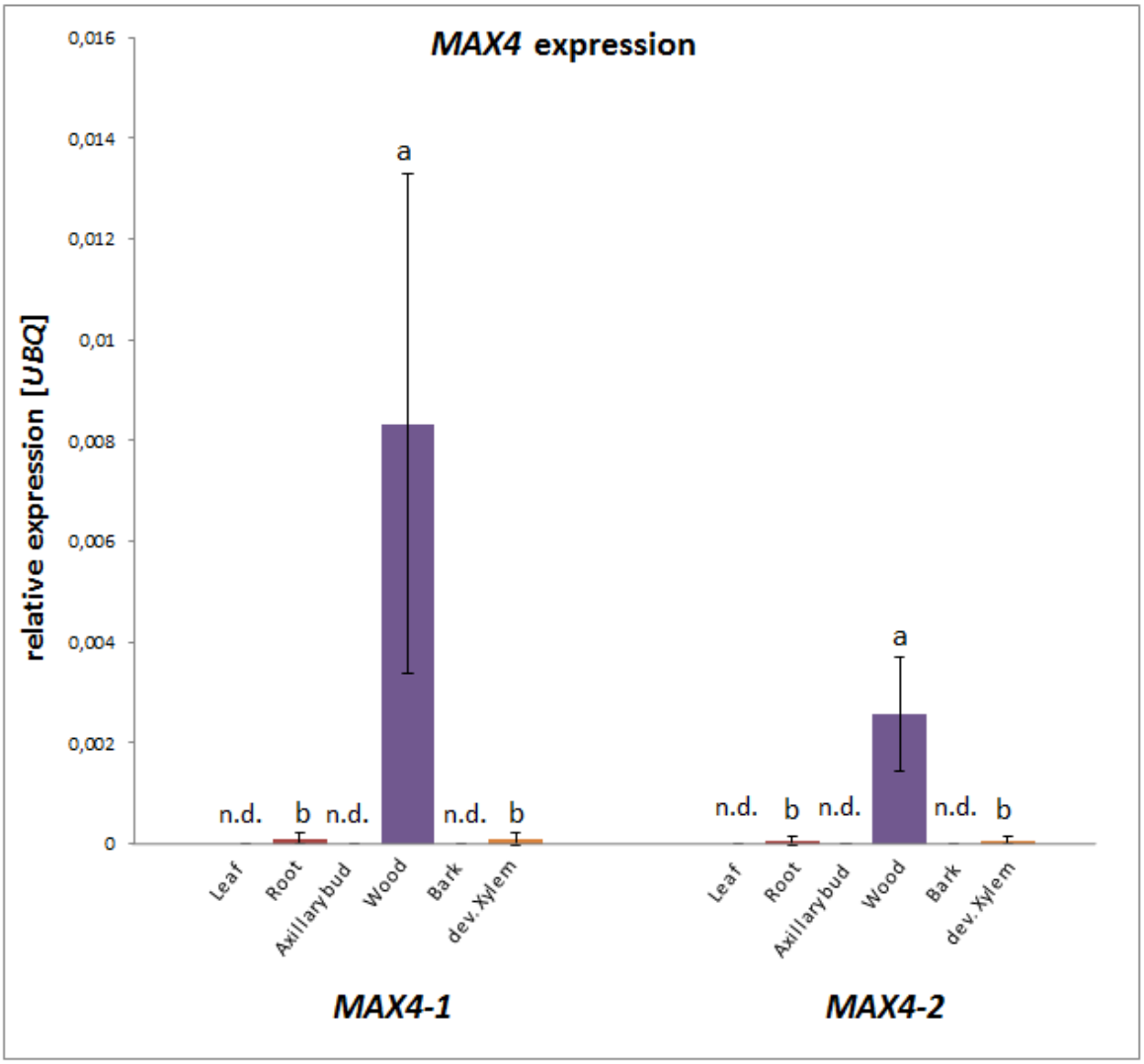

Fig. 3.4 Expression of *P.* x *canescens MAX4* orthologs in different tissues of greenhouse-grown WT plants. Expression relative to the reference gene *UBQ* was determined. The data was subjected to a Shapiro-Wilk normality test and a Kruskal-Wallis One Way Analysis of Variance on Ranks (ANOVA). For pairwise multiple comparison, a Tukey Test was performed. Differences with $p<0.05$ ($n=6$) were considered as significant. Error bars indicate standard deviation.

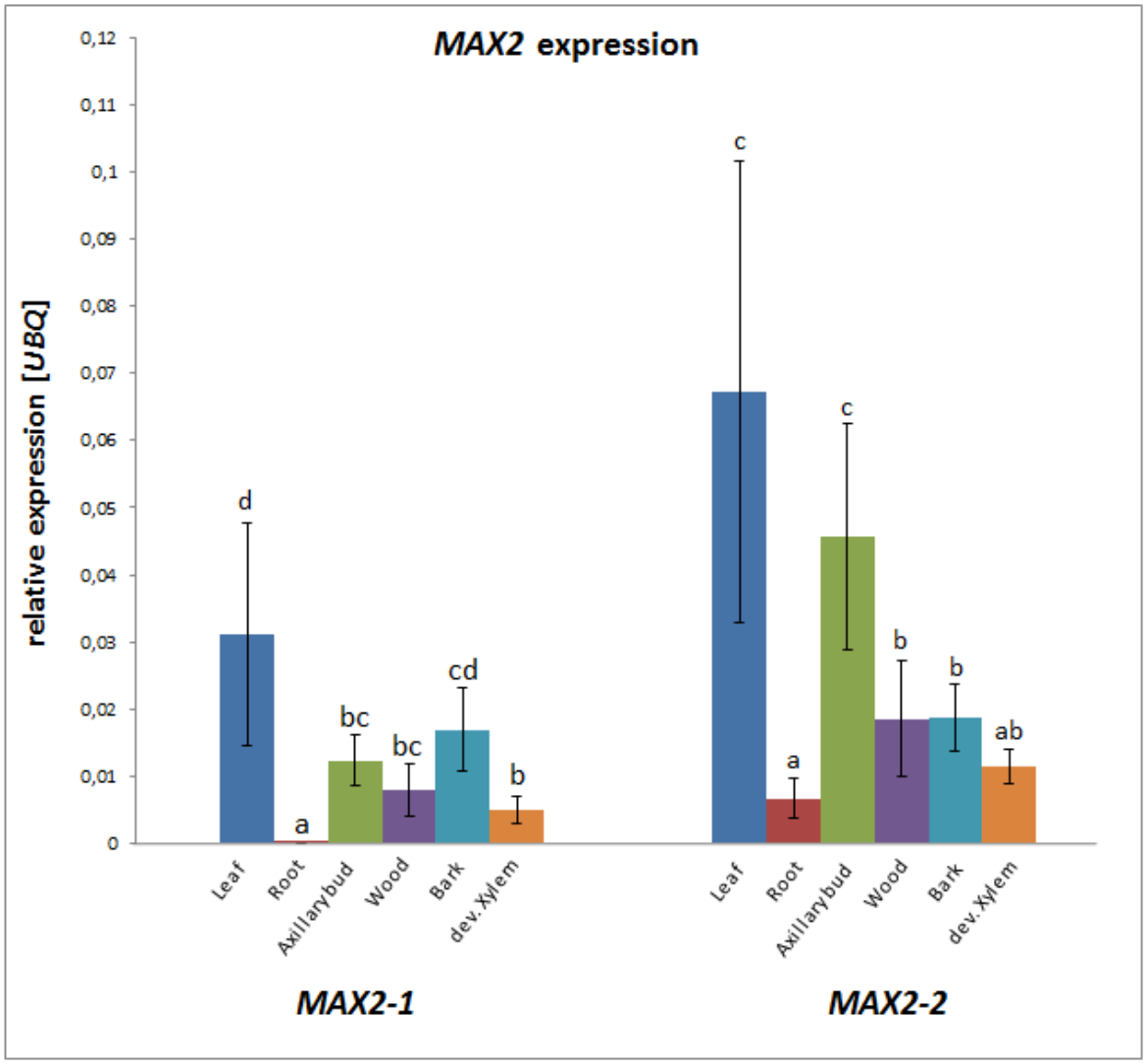

Fig. 3.5 Expression of *P.* x *canescens MAX2* orthologs in different tissues of greenhouse-grown WT plants. Expression relative to the reference gene *UBQ* was determined. The data was subjected to a Shapiro-Wilk normality test and a Kruskal-Wallis One Way Analysis of Variance on Ranks (ANOVA). For pairwise multiple comparison, a Tukey Test was performed. Differences with $p<0.05$ (n=6) were considered as significant. Error bars indicate standard deviation.

3.4 Generation of *MAX4* and *MAX2* knockdown (*amiMAX*) lines

For testing the significance of the SL pathway in poplar, orthologs of the SL biosynthesis gene *MAX4* und the SL signaling gene *MAX2* were identified (see chapter 3.1; p. 56ff) and selected for amiRNA-mediated knockdowns. This required the generation of transgenic plants, harboring the amiRNA constructs.

The genetic transformation of *P.* x *canescens* was successful and for all constructs (individual as well as simultaneous knockdown of the *MAX4* and *MAX2* orthologs, six constructs in total), 12-14 independent transgenic lines were obtained each. An overview about these lines is given in Appendix Tab. 7.1 (p.155). Most of the *MAX4* knockdown lines and some of the *MAX2* knockdown lines were grown under greenhouse conditions for phenotyping, as discussed below.

3.5 Target gene expression analysis and phenotyping: *amiMAX4* lines

For an initial characterization of the *MAX4* knockdown (*amiMAX4*) lines generated in this work, transcript levels of the target genes were assayed by qPCR and compared to the expression in wild type plants to confirm efficient knockdowns. Furthermore, the plants were phenotyped for architectural and biomass traits.

3.5.1 Target gene expression analysis in *amiMAX4* lines

For a confirmation of successful targeting of the poplar *MAX4* genes by the amiRNA constructs, expression analysis was performed. The prerequisite for showing a successful knockdown is well-detectable expression in the wild type. Thus, for the characterization of knockdown efficiency, qPCR analysis was performed using wood samples from greenhouse-grown plants, which exhibit sufficient *MAX4* expression (Fig. 3.4). Expression analysis was focused on representative *amiMAX4-1+2* double knockdown lines which showed a robust branching phenotype as revealed during phenotyping (see below, chapter 3.5.2.1; p. 66ff).

The reference gene used for the wood sample qPCR experiments was *ELONGATION FACTOR1* (*EF1*, Potri.001G224700) instead of *UBIQUITIN* (*UBQ*, Potri.001G418500) which was used for normalization in other qPCR experiments. This was done because there were

stability problems with *UBQ* when the samples were stored and extracted at different time points. In contrast to *UBQ*, *EF1* exhibited higher stability.

Compared to the wild type (*P.* x *canescens*), the tested representative *amiMAX4-1+2* lines (T14 #4A; T14 #6A; T22 #5A) expectedly showed significantly reduced transcript levels for both *MAX4* orthologs (*MAX4-1* and *MAX4-2*) (Fig. 3.6 A and B). A replication of this experiment with lines T14 #4A and T22 #5A, and an additional line showing a milder branching phenotype (T22 #13A), was done (Appendix Fig. 7.9; p. 155). The significant, simultaneous down-regulation of the target genes *MAX4-1* and *MAX4-2* was confirmed in all tested lines and the knockdown was therefore successful.

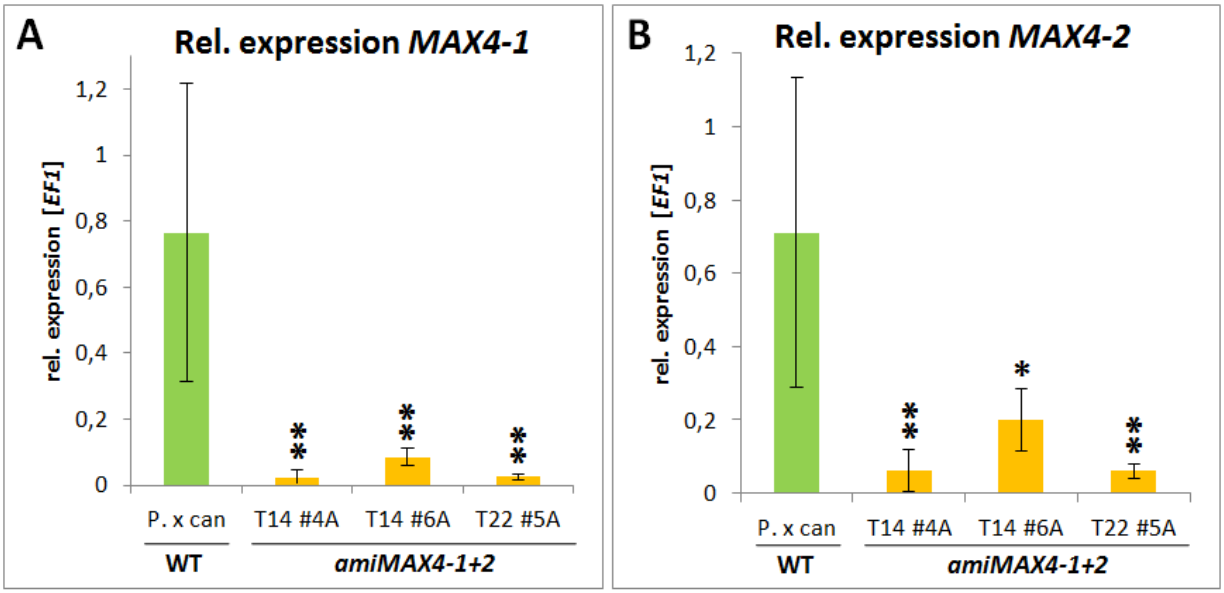

Fig. 3.6 Expression analysis of *MAX4-1* (A) and *MAX4-2* (B) in representative *amiMAX4-1+2* lines. Expression levels were analyzed in the *P.* x *canescens* wild type and three representative *MAX4-1+2* double knockdown lines. Expression was normalized against the reference gene *EF1*. n= 3-7. Error bars indicate standard deviation. Asterisks indicate significant differences compared to the wild type (*P.* x *can*) according to Student's *t*-test. One and two asterisks indicate $p<0.05$ and $p<0.01$, respectively.

3.5.2 Architectural phenotyping of *amiMAX4* lines

The *amiMAX4* lines generated in this project were evaluated by detailed phenotyping. A focus was put on the shoot architecture, but also biomass parameters were measured. Additionally, adventitious rooting and bud break in spring were investigated.

3.5.2.1 Shoot architecture of amiMAX4 lines

Based on published data for *Arabidopsis*, petunia, rice and pea (Arite et al., 2007; Snowden et al., 2005; Sorefan et al., 2003), an increased shoot branching phenotype was expected when genes of the SL pathway were knocked down. To test this hypothesis, the transgenic poplar *MAX4* individual and simultaneous knockdown lines (*amiMAX4-1*, *amiMAX4-2* and *amiMAX4-1+2*) were grown for phenotyping of shoot architectural traits. Three months old, greenhouse-grown plants were analyzed. Measured parameters were the number, position and length of branches, the plant height, the number of nodes, as well as the stem base diameter. Based on the number of nodes and the plant height, the average internode length was calculated.

Fig. 3.7 - Fig. 3.11 and Appendix Fig. 7.10 (additional lines, p. 156) show shoot architectural traits of *amiMAX4-1*, *amiMAX4-2* and *amiMAX4-1+2* plants compared to *P.* x *canescens* wild type control plants, and Fig. 3.12 shows the habitus of representative *P.* x *canescens* wild type and *amiMAX4-1+2* plants. In total, 10-13 lines per genotype were scored for shoot architectural traits.

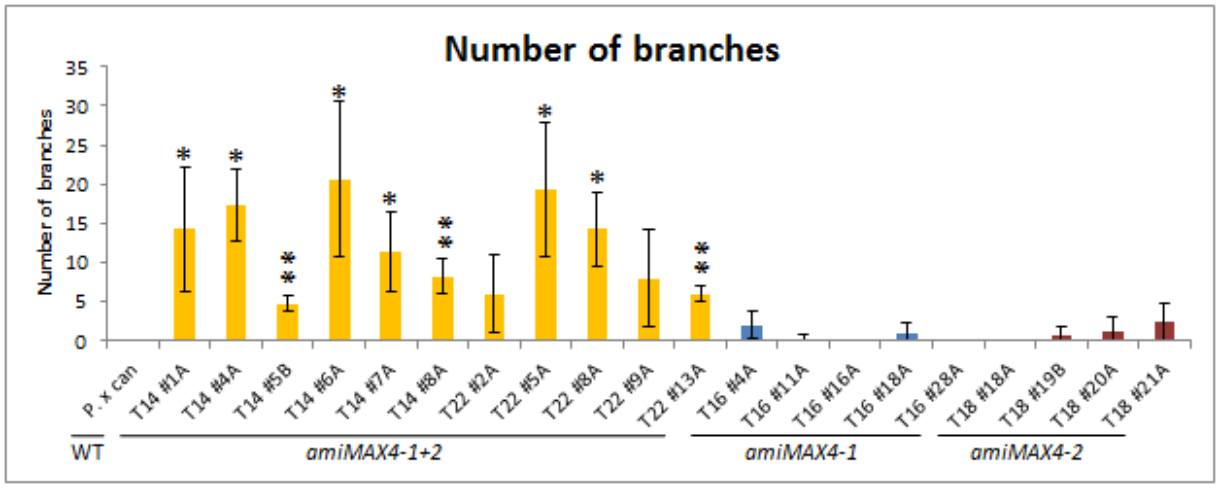

Fig. 3.7 **Branching phenotype of *amiMAX4* lines.** The number of branches was counted in greenhouse-grown plants. In this experiment, the *P.* x *canescens* wild type (left) did not produce any branches. n= 3-8. Error bars indicate standard deviation. Asterisks indicate significant differences compared to the wild type (*P.* x *can*) according to Student's *t*-test. One and two asterisks indicate $p<0.05$ and $p<0.01$, respectively.

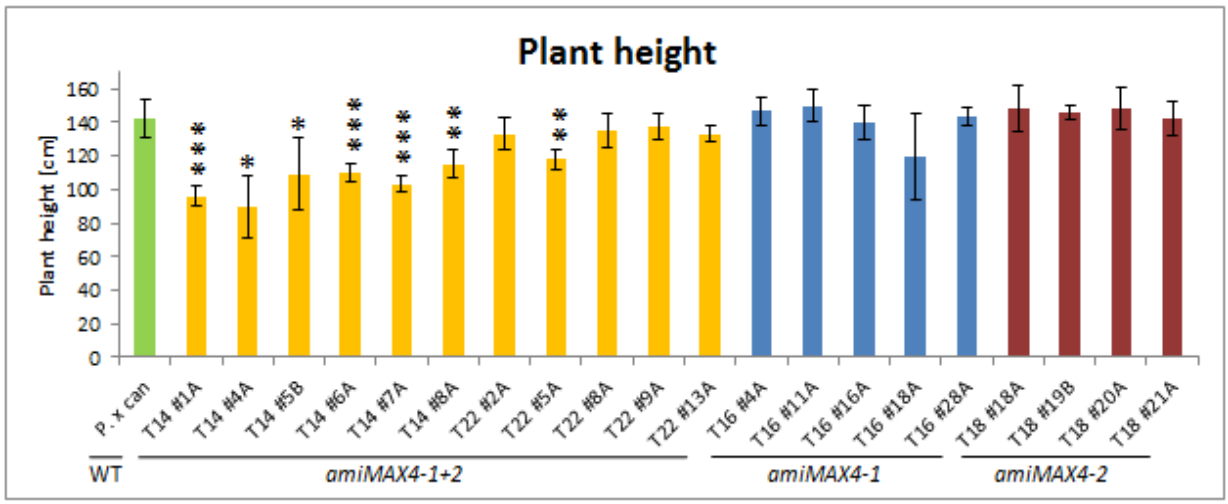

Fig. 3.8 **Plant height of *amiMAX4* lines.** The height was measured from the soil surface to the apex in greenhouse-grown plants. n= 3-8. Error bars indicate standard deviation. Asterisks indicate significant differences compared to the wild type (*P.* x *can*) according to Student's *t*-test. One, two and three asterisks indicate $p<0.05$, $p<0.01$ and $p<0.001$, respectively.

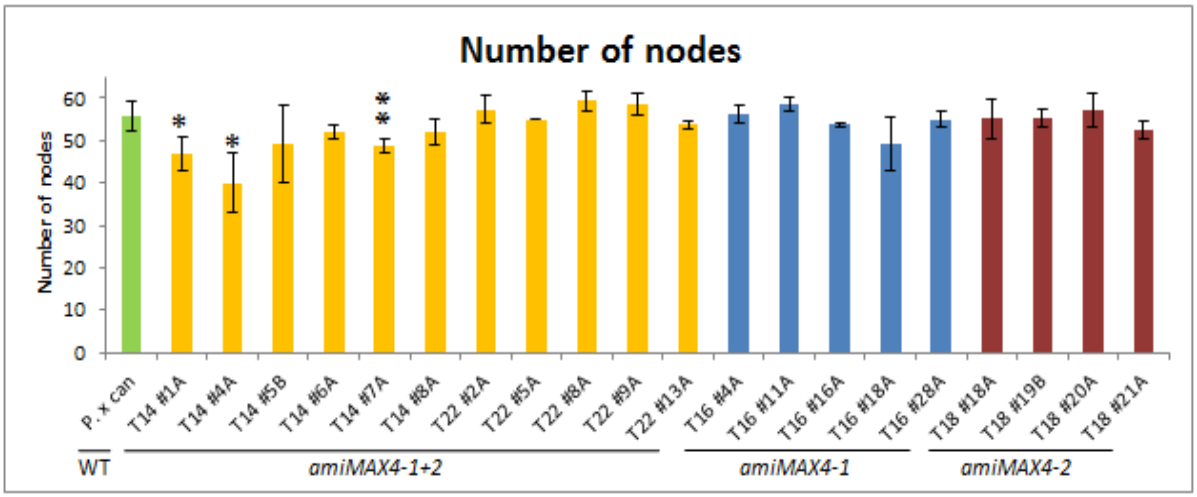

Fig. 3.9 **Number of nodes of *amiMAX4* lines.** The number of nodes was counted from the stem base (soil surface level) to the apex in greenhouse-grown plants. n= 3-8. Error bars indicate standard deviation. Asterisks indicate significant differences compared to the wild type (*P.* x *can*) according to Student's *t*-test. One and two asterisks indicate p<0.05 and p<0.01, respectively.

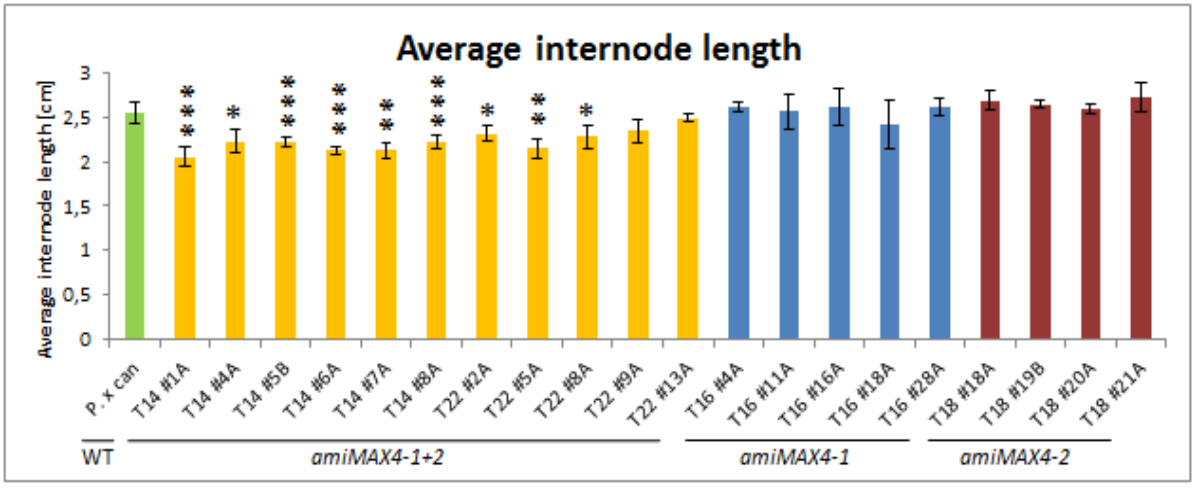

Fig. 3.10 **Average internode length of *amiMAX4* lines.** The average internode length was calculated based on the plant height and the number of nodes of greenhouse-grown plants. n= 3-8. Error bars indicate standard deviation. Asterisks indicate significant differences compared to the wild type (*P.* x *can*) according to Student's *t*-test. One, two and three asterisks indicate p<0.05, p<0.01 and p<0.001, respectively.

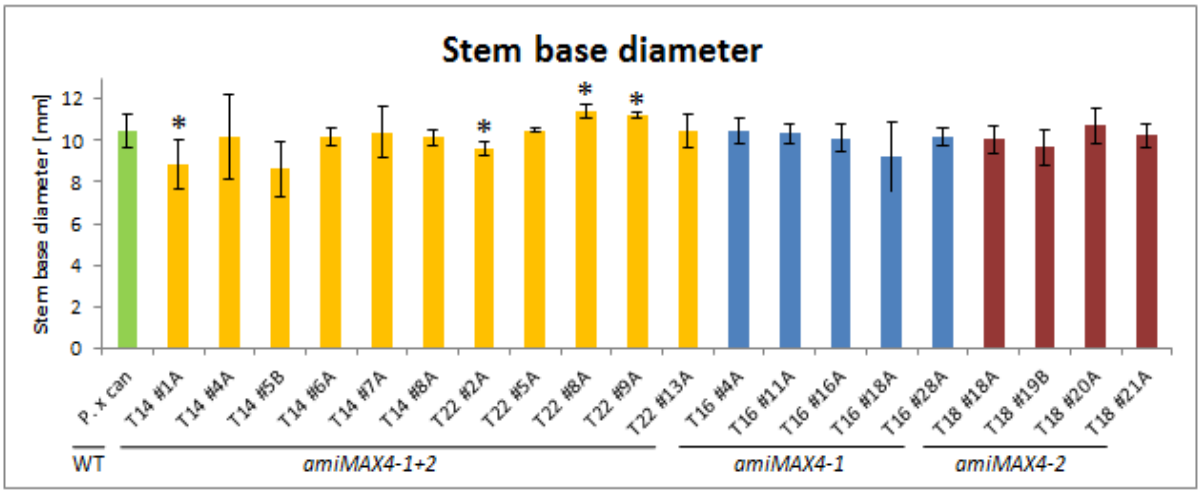

Fig. 3.11 Stem base diameter of *amiMAX4* lines. The stem base diameter was measured directly above the soil level in greenhouse-grown plants. n= 3-8. Error bars indicate standard deviation. Asterisks indicate significant differences compared to the wild type (*P.* x *can*) according to Student's *t*-test. One asterisk indicates $p<0.05$.

Fig. 3.12 Habitus of *P.* x *canescens* wild type and *amiMAX4-1+2* (T14 #4A) plants. The photograph was taken for representative specimen. Plants were 3.5 months old and grown under greenhouse conditions.

In the *MAX4* double knockdown lines (*amiMAX4-1+2*), which are putatively deficient in SL biosynthesis due to the successful knockdown of both *MAX4* orthologs, significant shoot architectural phenotypes were observed. In contrast, all measured parameters did not significantly differ between *MAX4* individual knockdown lines (*amiMAX4-1* and *amiMAX4-2*) and the *P.* x *canescens* wild type control. Therefore, only the observations made for *amiMAX4-1+2* plants are described in the following section in detail.

The most prominent phenotype exhibited by the *amiMAX4-1+2* lines was highly increased branching compared to the wild type (Fig. 3.7 and Appendix Fig. 7.10 A, p. 156), leading to a "bushy" appearance of the plants (Fig. 3.12).

The plant height was found to be reduced in most lines compared to the wild type (Fig. 3.8 and Appendix Fig. 7.10 B, p. 156). However, this phenotype was less drastic compared to the branching phenotype, and not present in all lines. Despite of this reduction in the plant height, the number of nodes was not significantly changed in most lines (Fig. 3.9 and Appendix Fig. 7.10 C, p. 156). Based on the plant height and the number of nodes, the average internode length was calculated. Consistent with the reduced height and a similar number of nodes in most *amiMAX4-1+2* lines, the average internode length was significantly reduced compared to the wild type (Fig. 3.10 and Appendix Fig. 7.10 D, p. 156). The stem base diameter was significantly changed in some *amiMAX4-1+2* lines compared to the *P.* x *canescens* wild type, although there is no clear trend visible as the measured diameter was increased in some lines and reduced in others (Fig. 3.11 and Appendix Fig. 7.10 E, p. 156).

For confirmation of the phenotypes, the evaluation of architectural traits was done in another replicate for representative lines. The phenotypes were reproducible, as shown in Appendix Fig. 7.11 (p. 157). Especially the number of branches, the plant height and the average internode length showed exactly the same significant changes. The number of nodes and the stem base diameter were less stable parameters and showed some fluctuation among the different lines.

For testing of the stability of the observed phenotypes under different growth conditions, the representative *amiMAX4-1+2* lines T14 #4A and T22 #5A were grown together with the *P*. x *canescens* wild type in a controlled environment growth chamber (two replicates, Appendix Fig. 7.12 and Fig. 7.13; p. 158) and under outdoor conditions (Appendix Fig. 7.14; p. 160). For the latter, the phenotypes were scored in winter after the first growing season. Overall, the phenotypes were stable. Especially the significantly increased number of branches, the reduced plant height and the reduced average internode length in *amiMAX4-1+2* lines, were highly reproducible phenotypes.

3.5.2.2 Biomass traits of amiMAX4 lines

For selected *amiMAX4* lines, biomass traits of greenhouse-grown plants were determined in two replicates (Fig. 3.13 and Appendix Fig. 7.15, p. 161). The fresh and dry weight of roots and the shoot was measured. The shoot was separated into the stem (including branches) and leaves.

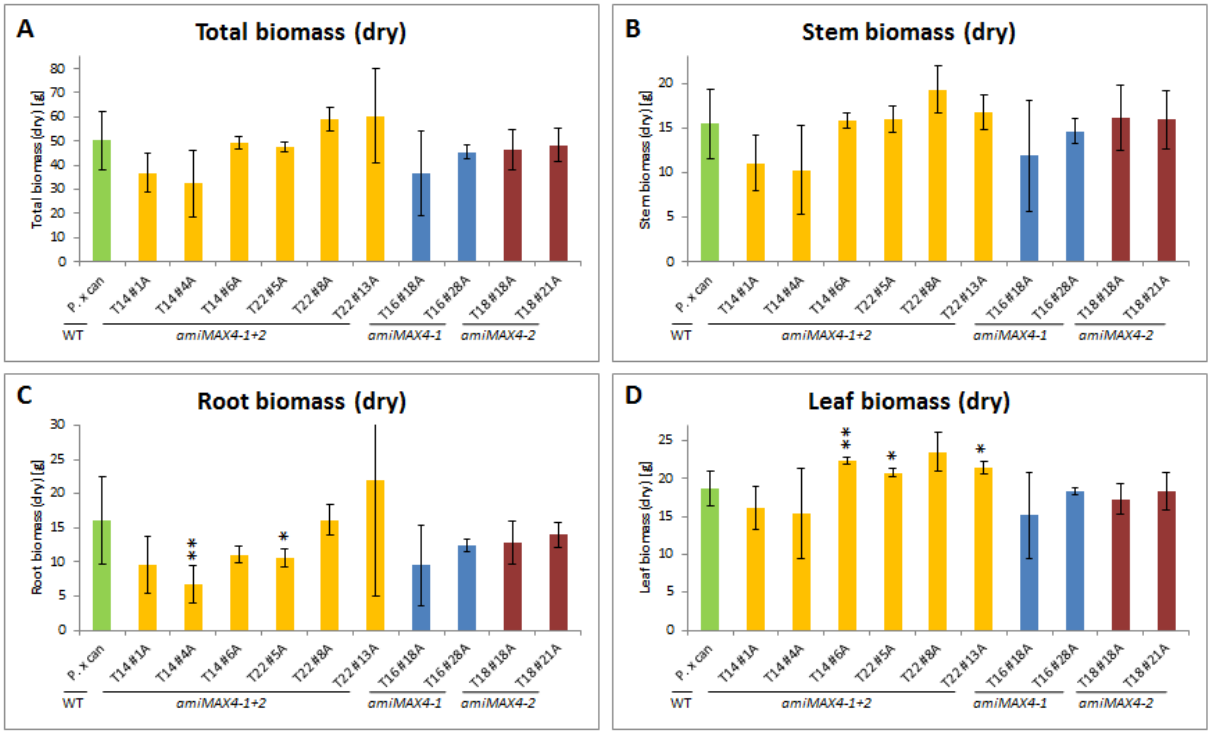

Fig. 3.13 **Biomass parameters of selected *amiMAX4* lines.** The total dry biomass of the plants (A), as well as the separate dry weights of the stem (including branches) (B), the roots (C) and the leaves (including leaves from the branches) (D), was determined. n= 3-8. Error bars indicate standard deviation. Asterisks indicate significant differences compared to the wild type (*P.* x *can*) according to Student's *t*-test. One and two asterisks indicate $p<0.05$ and $p<0.01$, respectively.

For the total dry biomass, a minor reduction was observed in the *amiMAX4-1+2* lines T14 #1A and T14 #4A (Fig. 3.13 A), and this was found to be significant in a replication of the experiment (Appendix Fig. 7.15 A; p. 161). However, other *amiMAX4-1+2* lines exhibited a similar or even higher (by trend, not significant) total dry weight compared to the *P.* x *canescens* wild type, so there is no general tendency for total biomass changes among all *amiMAX4-1+2* lines. The *amiMAX4-1* and *amiMAX4-2* single knockdown lines did not exhibit any obvious total biomass changes in both replicates as well (Fig. 3.13 A and Appendix Fig. 7.15 A; p. 161). When the dry biomass was evaluated for stems, roots and leaves separately (Fig. 3.13 B-D), no clear changes were observed, too. Apparent

significant changes for the root and leaf biomass in some *amiMAX4-1+2* lines (Fig. 3.13 C and D) were not entirely reproducible (Appendix Fig. 7.15 C and D; p. 161).

Summarized, there appears to be no consistent change of biomass parameters in the *amiMAX4* lines in three months old plants. However, for some *amiMAX4-1+2* lines, the dry weight was reduced by trend. These lines tend to be the ones with strong shoot architectural phenotypes (Fig. 3.7 - Fig. 3.11; p. 67).

3.5.2.3 Root architecture of amiMAX4-1+2 lines: adventitious rooting

Adventitious rooting is a trait which is influenced by strigolactones. SL pathway mutants of *Arabidopsis* and pea were shown to produce more adventitious roots, consequently SL appears to suppress this process (Rasmussen et al., 2012). Therefore, adventitious rooting was expected to be increased in the poplar *amiMAX4-1+2* lines as well, if they are indeed SL-deficient. To investigate this hypothesis, stem cuttings of *in vitro* grown *P.* x *canescens* wild type and *amiMAX4-1+2* (representative lines T14 #4A and T22 #5A) plants were prepared and cultivated under standard *in vitro* conditions as described in chapter 2.5 (p. 33ff). Adventitious roots were counted.

The number of adventitious roots was found to be significantly increased in the putatively SL-deficient *amiMAX4-1+2* lines T14 #4A and T22 #5A compared to the *P.* x *canescens* wild type (Fig. 3.14). The results were reproducible in a second replicate (Appendix Fig. 7.16, p. 162).

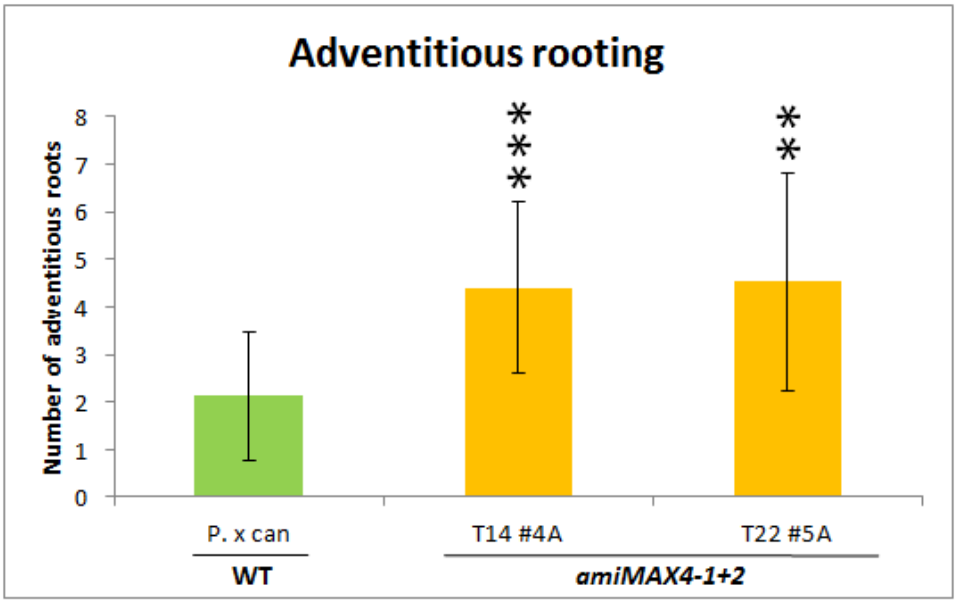

Fig. 3.14 Adventitious rooting in representative *amiMAX4-1+2* lines. The number of adventitious roots was counted for *in vitro* grown cuttings of the representative *amiMAX4-1+2* lines T14 #4A and T22 #5A, as well as the *P.* x *canescens* wild type. Cuttings were 8 weeks old. n=15. Error bars indicate standard deviation. Asterisks indicate significant differences compared to the wild type (*P.* x *can*) according to Student's *t*-test. Two and three asterisks indicate $p<0.01$ and $p<0.001$, respectively.

3.6 Detailed characterization of *amiMAX4-1+2* lines

The poplar *MAX4-1* and *MAX4-2* double knockdown lines (*amiMAX4-1+2*) exhibited successful silencing of the target genes, coinciding with architectural phenotypes which are typically observed in SL-deficient plants (chapter 3.5.2, p. 65ff). For further characterization of these lines, additional experiments were performed. The expression of SL-responsive marker genes was monitored and the shoot architectural phenotypes were complemented in a grafting study. Strigolactone treatment experiments were performed, including a complementation experiment. An anticipated role of SLs during bud break in spring was investigated and a possible crosstalk with the jasmonic acid (JA) pathway was addressed. The results of these experiments are described in the following chapters.

3.6.1 Expression of SL-regulated marker genes in *amiMAX4-1+2* lines

Direct quantification of SL-levels in the putatively SL-deficient poplar *amiMAX4-1+2* lines generated in this project relative to the *P.* x *canescens* wild type would confirm their expected SL deficiency. However, SL quantification is technically extremely challenging. The abundance of SLs generally is very low and they are highly unstable (Xie et al., 2010; Yoneyama et al., 2009). Furthermore, there appear to be structurally different and even less stable SLs in poplar compared to previously investigated species such as *Arabidopsis* (Koichi Yoneyama, Utsunomiya University, Tochigi, Japan, personal communication). References and standards, which are required for direct measurements or poplar SLs, are not available yet.

For these reasons, indirect confirmation of SL-deficiency in the *amiMAX4-1+2* lines was carried out. A frequently used possibility is the analysis of marker gene expression. Two SL-regulated marker genes were identified based on literature data: *MORE AXILLARY GROWTH3* (*MAX3*) (Hayward et al., 2009; Mashiguchi et al., 2009) and *BRANCHED1* (*BRC1*) (Aguilar-Martínez et al., 2007; Braun et al., 2012). The expression of the poplar *MAX3* and *BRC1* orthologs in the *amiMAX4-1+2* lines was expected to be changed compared to the wild type, if the *amiMAX4-1+2* lines are indeed SL-deficient.

3.6.1.1 MAX3 expression in amiMAX4-1+2 lines

MAX3 was identified as a SL-responsive marker gene based on published data. There is a *MAX2*-dependent negative feedback-regulation in the SL-pathway in *Arabidopsis*, acting on both *CAROTENOID CLEAVAGE DIOXYGENASE* (*CCD*) genes which are involved in SL biosynthesis (*MAX3* and *MAX4*) (Mashiguchi et al., 2009). The authors of this study reported a >2-fold increase of *MAX3* transcript levels in a *max4* mutant relative to the wild type, due to release from negative feedback. In another study, a 6- to 10-fold increase of *MAX3* expression in hypocotyls of *max1, max2* and *max4* mutants was reported (Hayward et al., 2009).

Based on these findings, a poplar ortholog of *MAX3* was selected as a promising, SL-regulated marker gene. A BLAST analysis was performed as described for the identification of the poplar *MAX4* and *MAX2* orthologs (see chapter 3.1; p. 56ff). Only one gene (Potri.014G056800) was found to be a clear poplar *MAX3* ortholog, although two copies were likely to be detected due to the whole genome duplication in the *Salicaceae* family, as described for *MAX4* and *MAX2*. However, the identification of only one poplar *MAX3* ortholog is in agreement with a recently published characterization of the poplar *MAX* genes (Czarnecki et al., 2014).

Expression of poplar *MAX3* was investigated in wood samples of representative *amiMAX4-1+2* lines relative to the wild type. As reported for *Arabidopsis max4* and pea *rms1* mutants, increased transcript levels of Potri.014G056800 were expected. The results of the expression analysis are shown in Fig. 3.15.

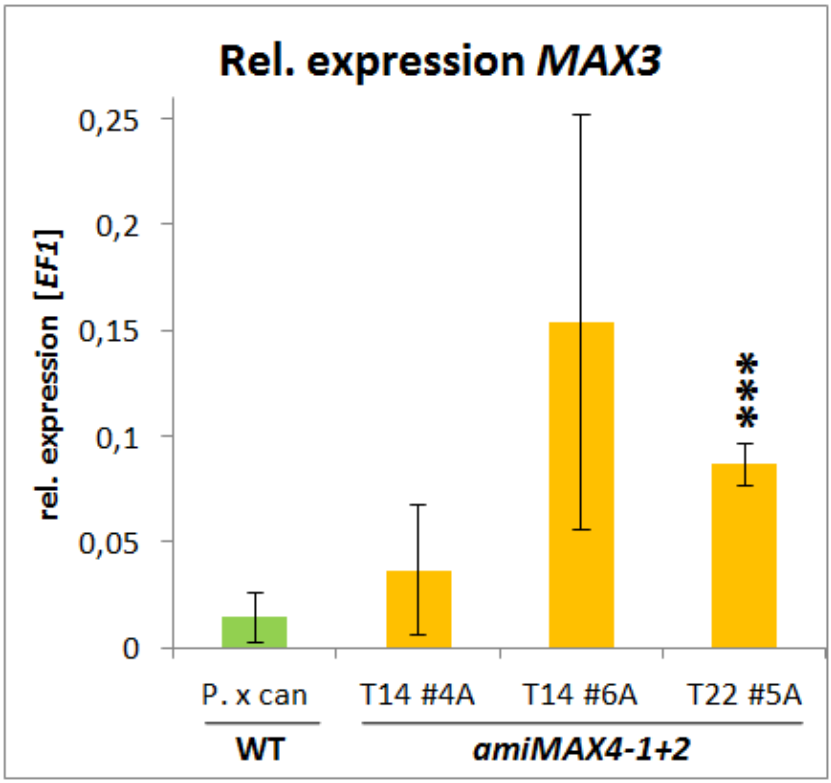

Fig. 3.15 **Expression analysis of *MAX3* in representative *amiMAX4-1+2* lines.** Expression levels were analyzed in the *P.* x *canescens* wild type and three representative *amiMAX4-1+2* double knockdown lines. Expression was normalized against the reference gene *EF1*. n= 3-7. Error bars indicate standard deviation. Asterisks indicate significant differences compared to the wild type (*P.* x *can*) according to Student's *t*-test. Three asterisks indicate p<0.001.

The relative expression of the poplar *MAX3* ortholog was increased in all tested *amiMAX4-1+2* lines by trend, but this was only significant in line T22 #5A. In a repetition of the experiment, no significant expression changes compared to the wild type were found in this line (Appendix Fig. 7.17; p. 162). Therefore, no reproducible significant upregulation of *MAX3* transcript levels could be detected in the tested *amiMAX4-1+2* lines, even though there appears to be a trend. The error range was high, making it difficult to judge small differences in expression.

3.6.1.2 BRC1 expression in amiMAX4-1+2 lines

Arabidopsis BRC1 encodes a transcriptional regulator being discussed to play a central role in bud outgrowth control. The closely related gene *BRC2* was also reported to have a minor function in this process (Aguilar-Martínez et al., 2007; Finlayson, 2007). In *Arabidopsis* SL pathway mutants, including the SL-deficient *max4-1* mutant, *BRC1* is significantly down-regulated on the transcript level, while expression of *BRC2* is not changed (Aguilar-Martínez et al., 2007). Also in the pea *rms1* mutant (equivalent to *Arabidopsis max4-1*), a 10-fold reduction of *PsBRC1* transcript was reported (Braun et al., 2012). Therefore, a poplar ortholog of *BRC1* appeared to be a promising marker gene for SL-deficiency. However, such a poplar gene has not been described yet. In this project, Potri.012G059900 was identified as a likely functional *BRC*-like ortholog. Also a putative *BRC2* ortholog (Potri.010G130200) was found (see chapter 3.8, p. 95ff). The expression of these genes was investigated by qPCR in representative *amiMAX4-1+2* lines and compared to the *P*. x *canescens* wild type.

Since expression of both genes was found to be largely specific to dormant axillary buds in the wild type (Fig. 3.29), this tissue type was harvested from 3.5 months old, greenhouse-grown *P.* x *canescens* wild type and *amiMAX4-1+2* plants after they were phenotyped for architectural traits (Appendix Fig. 7.11; p. 157). Dormant axillary buds were taken from nodes 15-30 counted from the plant apex. In *amiMAX4-1+2* plants, not all positions could be sampled because branches already grew out frequently.

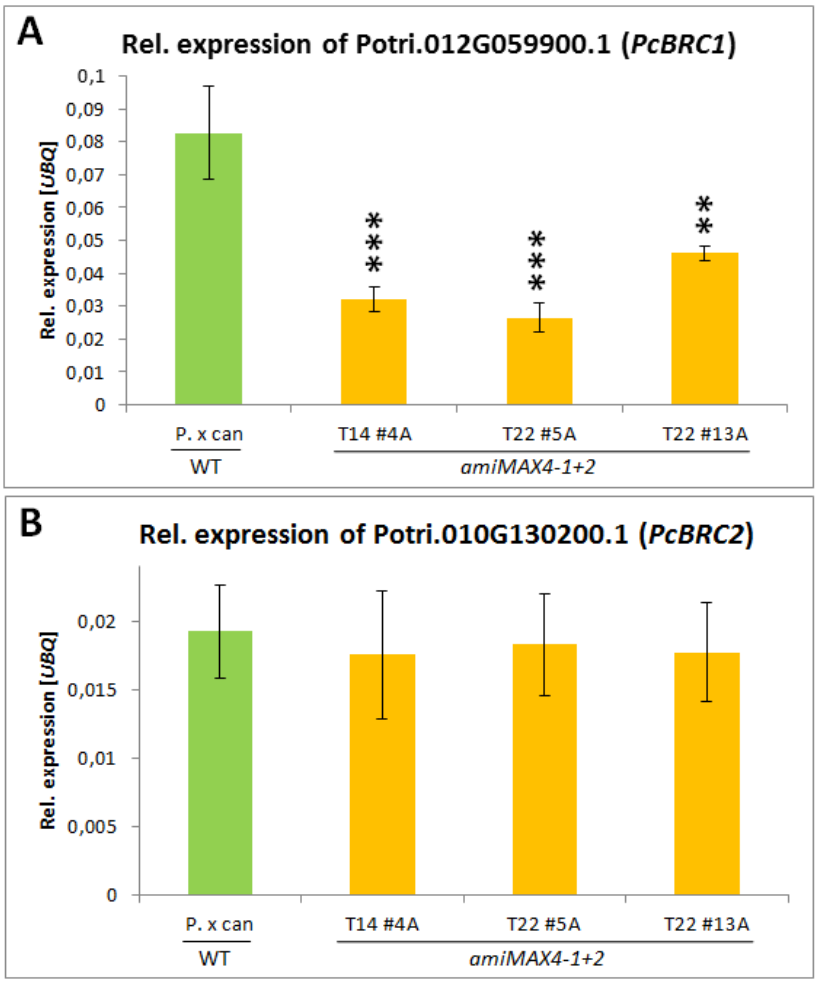

Fig. 3.16 **Expression of putative *P.* x *canescens BRC1* (A) and *BRC2* (B) orthologs in dormant axillary buds of greenhouse-grown plants.** Expression was determined in the *P.* x *canescens* wild type and three representative *amiMAX4-1+2* double knockdown lines. Expression was normalized against the reference gene *UBQ*. n= 4-5. Error bars indicate standard deviation. Asterisks indicate significant differences compared to the wild type according to Student's *t*-test. Two and three asterisks indicate $p<0.01$ and $p<0.001$, respectively.

As revealed by the expression analysis, Potri.012G059900 (*PcBRC1*) transcript levels were significantly reduced in the *amiMAX4-1+2* lines (Fig. 3.16 A). This reduction was less severe in line T22 #13A, which consistently showed milder architectural phenotypes (see chapter 3.5.2; p. 65ff). Therefore, Potri.012G059900 seems to be down-regulated in the *amiMAX4-1+2* lines as expected for a poplar *BRC1* ortholog in SL-deficient plants. This regulation appears to correlate with the strength of the architectural phenotype.

In contrast to *PcBRC1*, transcript levels of the putative poplar *BRC2* ortholog Potri.010G130200 were not changed in all tested *amiMAX4-1+2* lines compared to the wild type (Fig. 3.16 B), similar to the observations made in *Arabidopsis* (Aguilar-Martínez et al., 2007).

The experiment was replicated and the results were confirmed. While there was no significant difference in the amount of detected transcripts of Potri.010G130200 in the *amiMAX4-1+2* lines T14 #4A and T22 #5A compared to the wild type, Potri.012G059900 was significantly down-regulated (Appendix Fig. 7.18; p. 163).

3.6.2 Complementation of *amiMAX4-1+2* phenotype: grafting

The *amiMAX4-1+2* lines generated in this project are expected to be SL-deficient. If this is the case, the typically observed phenotypes, especially increased branching and a reduced internode length, should be rescued in an *amiMAX4-1+2* scion grafted to a wild type rootstock. The rootstock can synthesize SLs, which are transported acropetally into the scion where they were expected to completely suppress the SL-deficiency phenotypes. This was already successfully shown for the petunia *dad1-1* mutant (Napoli, 1996), the pea *rms1* mutant (Foo et al., 2001) and the *Arabidopsis max4-1* mutant (Sorefan et al., 2003).

For the complementation by grafting, the *P.* x *canescens* wild type as well as the representative poplar *amiMAX4-1+2* lines T14 #4A and T22 #5A were used. Beside of self-grafted controls (rootstock and scion from different individuals of the same genotype), *amiMAX4-1+2* scions were combined with wild type rootstocks and vice versa. Grafting was performed three weeks after potting of *in vitro* grown plants, using a wedge-grafting technique (see chapter 2.20, p. 54ff). After healing of the graft union (roughly 1 month), the plants were grown for 2 months in a greenhouse until evaluation of architectural traits was done.

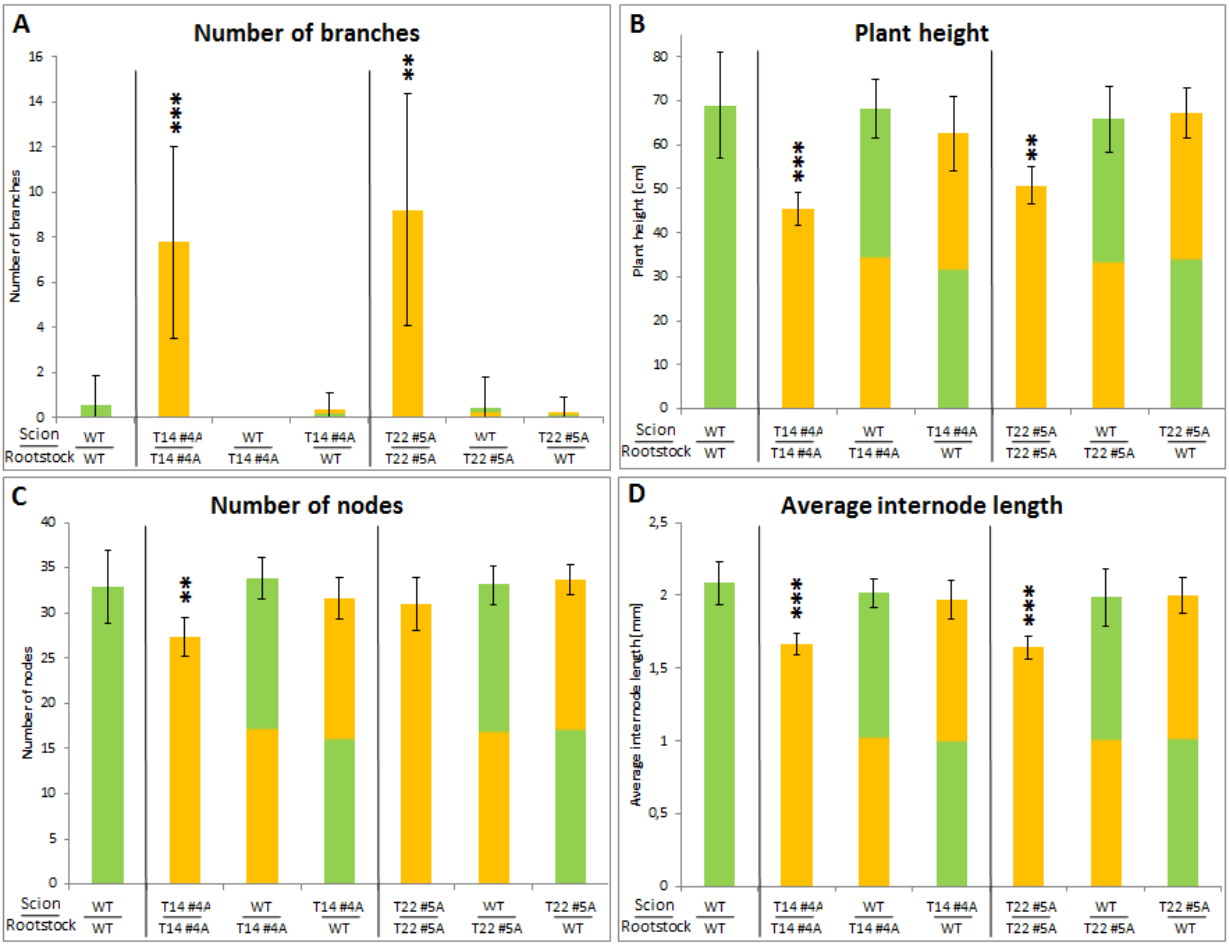

Fig. 3.17 **Architectural traits of grafted poplar plants.** For grafting, the *P.* x *canescens* wild type, as well as the representative *amiMAX4-1+2* lines T14 #4A and T22 #5A, were used. The upper label indicates the genotype of the scion, while the lower label specifies the genotype of the rootstock. The genotypes are also highlighted by the coloring of the bars (wild type green and knockdown line yellow). The number of branches (A), the plant height (B), the number of nodes (C) and the average internode length (D) were determined for greenhouse-grown plants. n= 8-9. Error bars indicate standard deviation. Asterisks indicate significant differences compared to the wild type (*P.* x *canescens*) according to Student's *t*-test. Two and three asterisks indicate p<0.01 and p<0.001, respectively.

The architectural traits of the grafted poplar plants are shown in Fig. 3.17. The self-grafted control plants exhibited the normal phenotypes as observed previously in non-grafted plants (see chapter 3.5.2.1; p. 66ff). Briefly, *amiMAX4-1+2* plants showed significantly increased branching, a reduced plant height, a reduced number of nodes (T14 #4A only) and a reduced internode length, when compared to the *P.* x *canescens* wild type. However, none of these typical phenotypes of SL-deficient plants could be observed when an *amiMAX4-1+2* scion was grafted on a wild type rootstock. No significant differences were found for all measured parameters compared to self-grafted wild type control plants. Also for the inversed control (wild type scion grafted on an *amiMAX4-1+2* rootstock), no significant differences compared to wild type plants were

observed. Consequently, a wild type rootstock can fully complement the architectural phenotype of an *amiMAX4-1+2* scion and an *amiMAX4-1+2* rootstock does not have any influence on the phenotype of a wild type scion.

In petunia and pea, also interstock grafting experiments were performed (Napoli, 1996; Foo et al., 2001). In these experiments, a wild type interstock fragment inserted into the stem of SL-deficient mutants was shown to be sufficient to complement the mutant phenotype of the scion. In this work, interstock grafting was performed as well. Although the replicate number was low and a self-interstock-grafted control of *amiMAX4-1+2* line T14 #4A was not included due to limited plant material, this experiment provides a hint that also in poplar, a small (approx. 1 cm) wild type interstock stem segment can rescue the typically observed *amiMAX4-1+2* phenotypes. The number of branches, the plant height, the number of nodes and the average internode length (Appendix Fig. 7.19 A-D; p. 164) of *amiMAX4-1+2* line T14 #4A plants supplemented with a wild type interstock, were comparable to the corresponding parameters measured for wild type self-interstock-grafted plants. The same was observed for wild type plants bearing a T14 #4A interstock.

3.6.3 GR24 treatment of wild type and *amiMAX4-1+2* plants

Generally, strigolactones are known to suppress bud outgrowth. For experiments to manipulate SL-levels, the synthetic strigolactone analog rac-GR24 (hereafter referred to as GR24) is routinely used. In this project, it was tested whether this substance is active in bud outgrowth inhibition in poplar. Stem cuttings (one or two nodes) were used to supply GR24 through the growth medium and bud outgrowth dynamics were monitored.
Furthermore, it was tested whether direct application of GR24 on axillary buds can rescue the branching phenotype of the putatively SL-deficient *amiMAX4-1+2* lines generated in this project.

3.6.3.1 GR24 treatment of wild type and amiMAX4-1+2 stem cuttings

To test whether the synthetic strigolactone GR24 is functional in poplar and can inhibit bud outgrowth, experiments using stem cuttings were performed. For a so-called one-node-assay, *P.* x *canescens* wild type stem cuttings bearing one node (i.e. one axillary bud) were prepared from *in vitro* grown plants. The cuttings were placed on standard growth medium (1/2 MS agar medium) supplemented with GR24 (in acetone, 5 µM final concentration) or the same amount of solvent only (Mock, 0.05 % acetone final concentration). Since stem cuttings lack apical dominance (no apex present in the cutting), the single bud grows out in virtually all cuttings. The time point of bud outgrowth (defined as unfolding of the first leaf) was recorded for each cutting and the days until bud outgrowth were calculated. If GR24 is active in suppressing bud outgrowth in this assay, buds of treated cuttings were expected to grow out later.

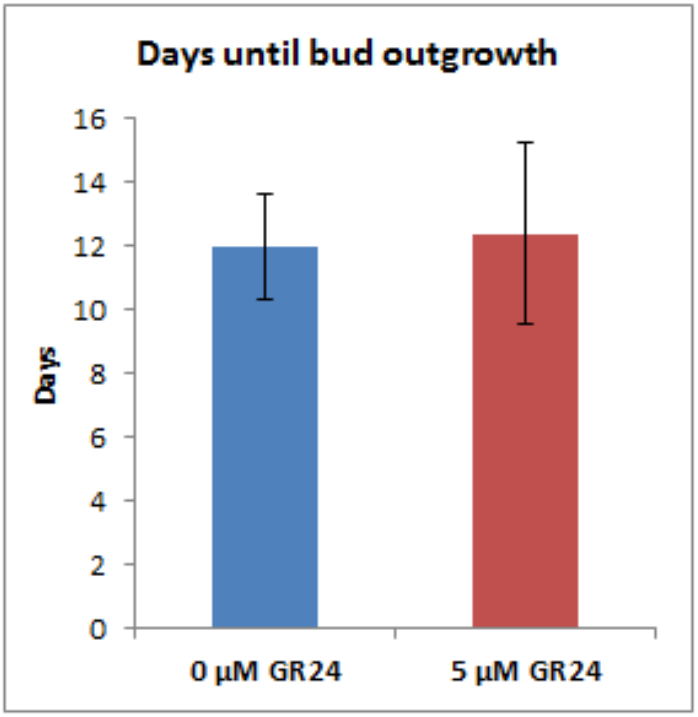

Fig. 3.18 One-node-assay. Bud outgrowth rate of *P.* x *canescens* wild type stem cuttings after 5 µM GR24 treatment. The time point from preparation of the cuttings until outgrowth of their bud on medium containing no (0 µM) or 5 µM GR24 was recorded. n=19-22. Error bars indicate standard deviation. A Student's *t*-test did not result in any significant difference between mock- and GR24-treated cuttings.

However, bud outgrowth was not delayed in GR24-treated cuttings compared to the mock-treated control in two independent experiments (Fig. 3.18 and Appendix Fig. 7.20; p. 165). Interestingly, this is in agreement with observations made in other species, in which basally supplied GR24 alone failed to suppress bud outgrowth in one-node-assays. For example, even a 20 µM GR24 treatment (4-fold more than used in this work) did not delay bud outgrowth in *Arabidopsis* one-node stem segments (Crawford et al., 2010). Similar observations were made in chrysanthemum and willow (Liang et al., 2010; Ward et al., 2013). Only with auxin applied simultaneously to the apex, an additional inhibitory effect of GR24 was reported in these studies. This indicates the importance of a competing auxin source for SLs to take effect, which may be explained by the canalization model (see discussion chapter 4.4.3.1, p. 115ff).

Notably, a second bud is sufficient as such an auxin source, as shown in the same studies: in two-node assays, GR24 was able to inhibit bud outgrowth without additional auxin supply. While this effect was observed for both buds in *Arabidopsis* (Crawford et al., 2010), it was more specific for the lower bud in the case of chrysanthemum and willow (Liang et al., 2010; Ward et al., 2013).

To test whether GR24 can suppress bud outgrowth in a two-node-assay in poplar, appropriate cuttings were prepared from *in vitro* grown plants. In addition to the *P.* x *canescens* wild type, the representative *amiMAX4-1+2* lines T14 #4A and T22 #5A were included in this experiment. The cuttings were cultivated in the same way as in the one-node-assay on medium containing solvent only (Mock) or 5 µM GR24. The time point of outgrowth was monitored for each bud individually. Since not all buds grow out in this assay, the bud outgrowth rate in percent was calculated 10 days after preparation of the cuttings instead of determining the time point of bud outgrowth.

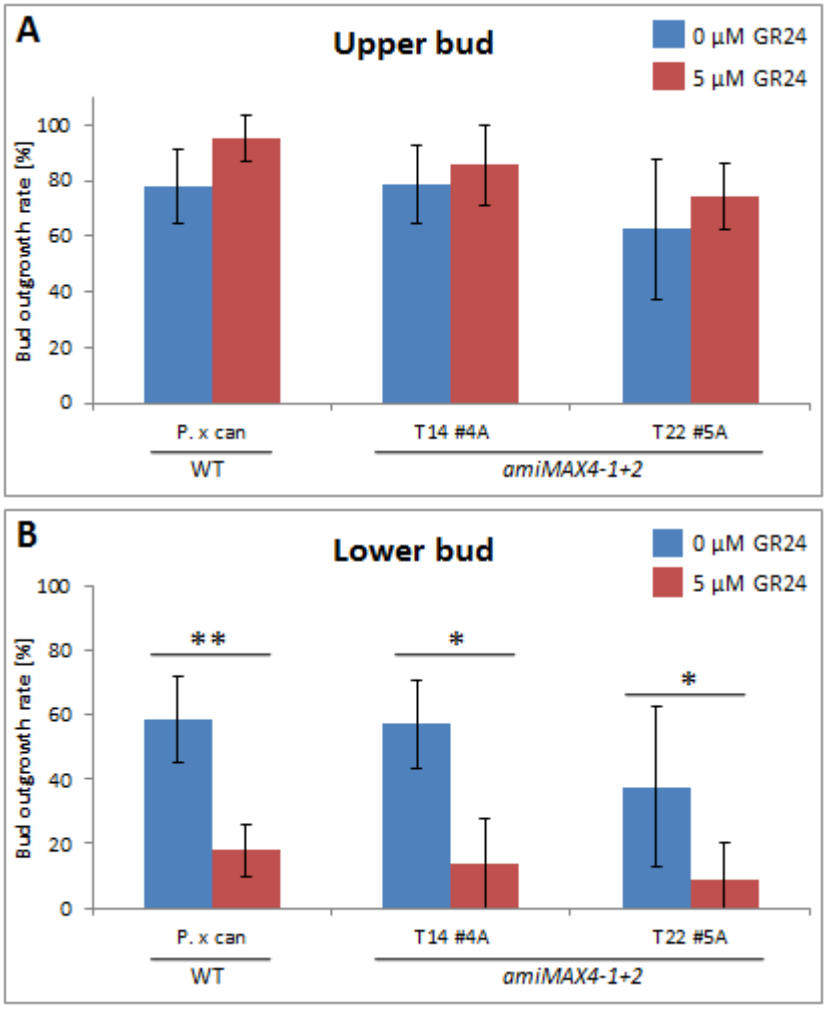

Fig. 3.19 Two-node-assay. Bud outgrowth rates of *P.* x *canescens* wild type and *amiMAX4-1+2* stem cuttings after 5 µM GR24 treatment. Cuttings bearing two nodes were prepared and placed on medium containing no (0 µM) or 5 µM GR24. The percentage of outgrown buds 10 days after preparation of the cuttings was determined separately for the upper (A) and lower buds (B). n=3 culture vessels containing 7-8 cuttings each. Error bars indicate standard deviation. Asterisks indicate significant differences between MOCK- and GR24-treated cuttings according to Student's *t*-test. One and two asterisks indicate $p<0.05$ and $p<0.01$, respectively.

When comparing mock- and GR24-treated cuttings, poplar two-node stem cuttings exhibited similar dynamics as previously reported in chrysanthemum and willow: while outgrowth of the upper bud was not significantly changed (Fig. 3.19 A), activation of the lower bud was strongly suppressed (Fig. 3.19 B). Generally, wild type and *amiMAX4-1+2* cuttings showed the same regulation. There were no significant differences in the bud outgrowth rates between the genotypes at both bud positions within a given treatment.

3.6.3.2 GR24 treatment of buds in wild type and amiMAX4-1+2 plants

External supply of SLs to plants which are defective in SL biosynthesis is expected to complement their increased branching phenotype. This was shown experimentally with GR24 fed to the vasculature or supplied directly onto the surface of axillary buds. For example, a single external application of 10 µl 100 nM GR24 directly to axillary buds of pea *rms1-10* (equivalent to *max4*) mutant plants strongly inhibited bud outgrowth (Gomez-Roldan et al., 2008). Furthermore, 5 µM GR24 supplied every third day for 20 days to the rosette axillary buds of *Arabidopsis* strongly suppressed branching in the *max4-1* mutant (Gomez-Roldan et al., 2008). If the poplar *amiMAX4-1+2* lines generated in this project are impaired in SL-biosynthesis and therefore are SL-deficient, their branching phenotype should be complemented as well by external application of SL.
Therefore, external application of GR24 directly on axillary buds of the representative *amiMAX4-1+2* lines T14 #4A and T22 #5A as well as *P.* x *canescens* wild type plants, was tested for suppression of bud outgrowth. 6 µl of a 5 µM GR24 solution (see chapter 2.19.2; p. 53f) were applied directly to axillary buds and the time from the first treatment until bud outgrowth (defined as unfolding of the first leaf of the developing branch) was recorded. The percentage of growing buds at 7, 10, 14 and 17 days after treatment (DAT) was calculated.

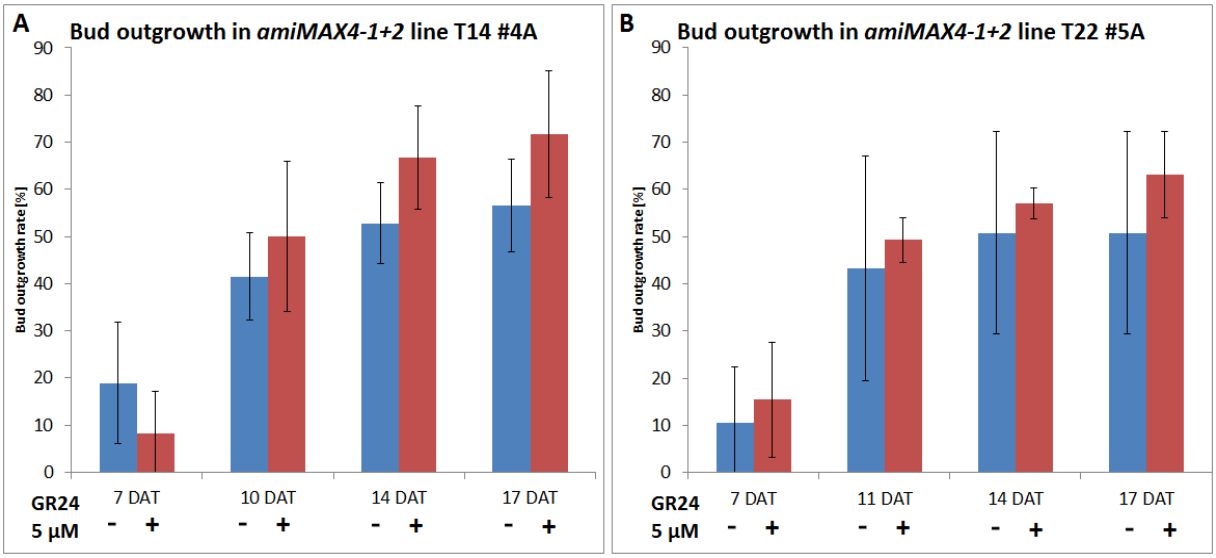

Fig. 3.20 **Bud outgrowth rates in *amiMAX4-1+2* lines T14 #4A (A) and T22 #5A (B) after GR24 treatment.** The bud outgrowth rates in % at 7, 10, 14 and 17 days after the first treatment (DAT) are shown after application of a mock (-) or 5 µM GR24 (+) solution. n=5 plants. Per plant, 10-15 nodes were treated and bud outgrowth was observed. Error bars indicate standard deviation. A Student's *t*-test did not result in any significant differences in outgrowth between the mock- and GR24-treated buds at the corresponding time points.

P. x *canescens* wild type control plants did not exhibit any bud outgrowth after mock- and GR24 treatments. All treated buds remained dormant over the course of the experiment (data not shown). Fig. 3.20 shows the bud outgrowth rates in *amiMAX4-1+2* lines T14 #4A and T22 #5A after mock- and GR24 treatments. During the course of time, generally more buds grew out, which is a frequently observed phenotype in these lines. However, there were no significant differences between mock- and GR24-treated buds at a given time point. Interestingly, although this is not significant, the GR24-treated buds exhibited increased outgrowth rates by trend compared to the mock-treated controls. This is in contrast to the expected reduction in bud outgrowth by GR24 treatment, as it was reported for SL-deficient *Arabidopsis* and pea mutant plants (Gomez-Roldan et al., 2008).

3.6.4 Spring bud break in *amiMAX4-1+2* lines

For the analysis of the effects of SL-deficiency on bud outgrowth, annual species (e.g. *Arabidopsis*, pea and rice) or species not undergoing winter dormancy (e.g. petunia), have been frequently used as described in chapter 1.3.2.3 (p. 11ff). In contrast, poplar is a perennial model species from temperate regions, and it has to survive harsh winters. This lifestyle requires further stages of dormancy. In addition to paradormancy (bud

outgrowth is suppressed by other parts of the plant, see chapter 1.3.4 (p. 22ff) for a discussion of the different dormancy stages) which can be found in annual species as well, poplar buds enter a deep state of dormancy during winter, called endodormancy (or winter dormancy). Thus, poplar features an additional stage of dormancy, and bud break after winter dormancy occurs in spring.

To test a possible influence of SL-deficiency on the spring outgrowth behavior of endodormant buds, bud break was investigated in the putatively SL-deficient *amiMAX4-1+2* poplar lines generated during this project. The representative *amiMAX4-1+2* lines T14 #4A und T22 #5A were transferred to outdoor conditions in summer 2014, together with *P.* x *canescens* wild type plants as a reference. The plants exhibited the typically observed phenotypes of *amiMAX4-1+2* lines, including increased branching rates (Appendix Fig. 7.14, p. 160). Bud break was monitored after the first period of winter dormancy. At a given time point (20.04.2015), the length of the expanding lateral buds or branches was measured at the 10 most apical nodes in all lines. Compared to the wild type, the bud length in the *amiMAX4-1+2* line T14 #4A was significantly increased, indicating earlier bud break (Fig. 3.21). However, there were no significant changes in bud length in line T22 #5A compared to the wild type.

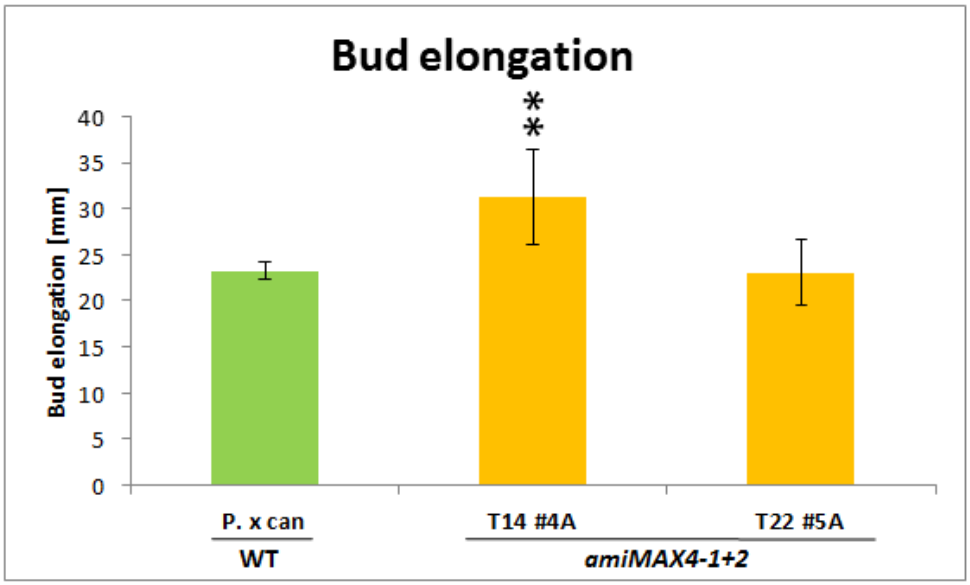

Fig. 3.21 **Bud elongation during bud break in spring in representative *amiMAX4-1+2* lines and the *P.* x *canescens* wild type.** At a given time point in spring (20.01.2015), the average bud/branch length was measured for the 10 most apical axillary buds of each plant. n= 4-8 plants. Error bars indicate standard deviation. Asterisks indicate significant differences compared to the wild type (*P.* x *can*) according to Student's *t*-test. Two asterisks indicate p<0.01.

3.6.5 Analysis of possible JA-crosstalk in *amiMAX4-1+2* lines

Hormonal regulation in plants is complex and there is a large extent of crosstalk between different hormonal pathways, for example during plant development or the defense against pathogens (Depuydt and Hardtke, 2011; Derksen et al., 2013). Recently, such a crosstalk between strigolactones and jasmonic acid (JA) was reported (Torres-Vera et al., 2014). Jasmonic acid is an important regulator of plant defense against necrotrophic pathogens like the fungi *Alternaria alternata* and *Botrytis cinerea*. The authors of the study found that a tomato (*Solanum lycopersicum*) *Slccd8* (*MAX4* ortholog) RNAi line, which only has a residual SL level of 5 % compared to the wild type, is more susceptible towards these pathogens. They report a significant reduction of the JA level in leaves (HPLC-MS/MS data), which coincides with a 4-fold reduction of expression of the JA-marker gene *PinII*. Therefore, they hypothesize the existence of a crosstalk between SL and JA and therefore postulate a role for SL in plant defense (Torres-Vera et al., 2014).
To investigate whether such a crosstalk is also present in poplar, a JA-regulated poplar marker gene was identified based on literature data. Transcript levels of the predicted chitinase gene Potri.004G182100 (POPTR_0004s18880) were shown to be upregulated in *P. trichocarpa* roots after JA-treatment (Plett et al., 2014). To investigate whether this regulation can also be found in leaves of *P.* x *canescens* wild type plants, detached leaves of plants grown in a growth chamber were treated with methyl jasmonate (JA) for 24 hours and expression of Potri.004G182100, compared to a mock-treated control, was monitored. After JA-treatment, Potri.004G182100 was highly upregulated (approx. 365-fold) (Fig. 3.22 A), making it a suitable marker gene for monitoring JA-levels.

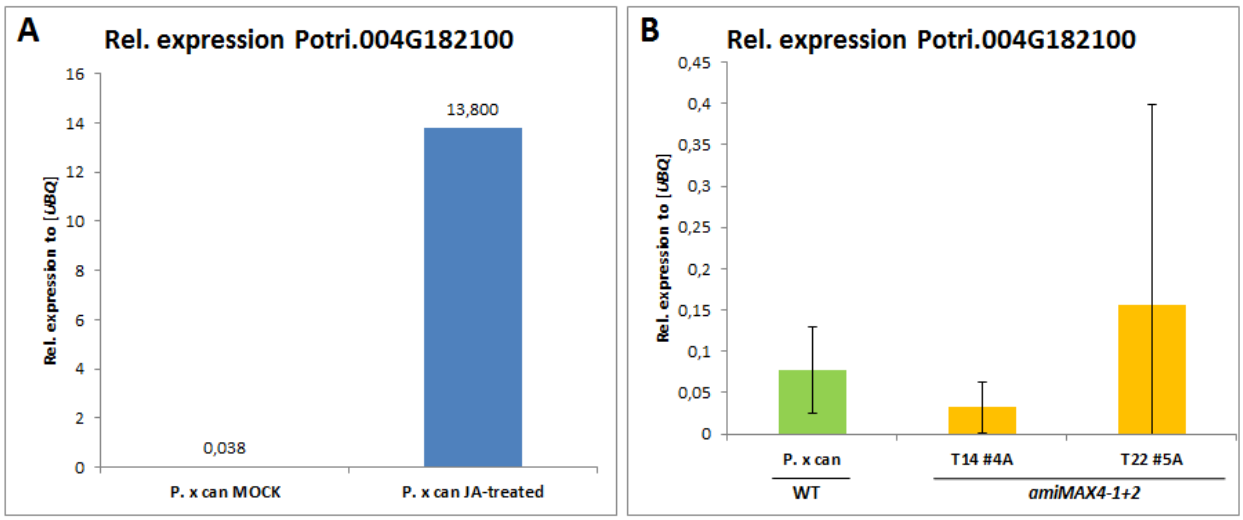

Fig. 3.22 **Relative expression of the JA-marker gene Potri.004G182100.** Expression was normalized against the reference gene *UBQ*. A: Relative expression after mock- and JA-treatment. n= 1 pool of 4 leaves from 2 individual plants. B: Relative expression in leaves of *P.* x *canescens* wild type plants and the representative *amiMAX4-1+2* lines T14 #4A and T22 #5A. n= 3-4. Error bars indicate standard deviation. A Student's *t*-test did not result in any significant differences between the *amiMAX4-1+2* lines compared to the wild type.

For testing whether the expression of the selected JA-marker gene is changed in the putatively SL-deficient representative *amiMAX4-1+2* lines T14 #4A and T22 #5A relative to the wild type, leaf samples were harvested from 1.5 months old greenhouse-grown plants and assayed by qPCR. Compared to the *P.* x *canescens* wild type, there was no significant change in the expression level of Potri.004G182100 in the tested *amiMAX4-1+2* lines (Fig. 3.22 B). Also no trend could be observed. While the average expression level was lower in line T14 #4A relative to the wild type, it was slightly increased in line T22 #5A. Since the tested highly JA-responsive marker gene was not regulated in the *amiMAX4-1+2* lines, also the JA-level in leaves of these lines presumably is not changed, contrasting the data reported for the tomato RNAi line (Torres-Vera et al., 2014).

The authors of the aforementioned study also reported significantly reduced salicylic acid (SA) levels in the tested tomato *Slccd8* line, based on HPLC-MS/MS experiments. However, they could not observe any changes in expression of the SA-marker gene *PR1a* and conclude that the change in the hormonal level is not sufficient to modify the SA-response (Torres-Vera et al., 2014). In *P. trichocarpa*, the genes *PtrWRKY60* (Potri.018G019700) and *PtrWRKY89* (Potri.006G109100) were previously shown to be transcriptionally upregulated in leaves specifically after SA-treatment (Jiang et al., 2014). Expression of these marker genes was also investigated in the same poplar *amiMAX4-1+2* lines and compared to the wild type as described above. No significant changes of the SA-

responsive marker could be shown in the *amiMAX4-1+2* lines compared to the wild type (see Appendix Fig. 7.21; p. 165), indicating that crosstalk between SL and SA is unlikely.

3.7 Target gene expression analysis and phenotyping: *amiMAX2* lines

In addition to *MAX4*, the *MAX2* knockdown (*amiMAX2*) lines generated during this project were assayed by qPCR for target gene expression levels relative to the wild type for an initial characterization. Several lines were also phenotyped for architectural traits.

3.7.1 Target gene expression analysis in *amiMAX2* lines

For expression analysis of the target genes in the *amiMAX2* lines, leaves of *in vitro* grown plants appeared to be a suited tissue. Unlike the poplar *MAX4* orthologs, of which transcripts were barely detectable in this material, *MAX2-1* and *MAX2-2* were expressed at a low, but well-detectable level in leaves of wild type plants (Fig. 3.3). This tissue type was therefore used for expression analysis in the *MAX2* knockdown lines instead of wood samples which were used to check the knockdown efficiency in the *amiMAX4* lines, as described above.

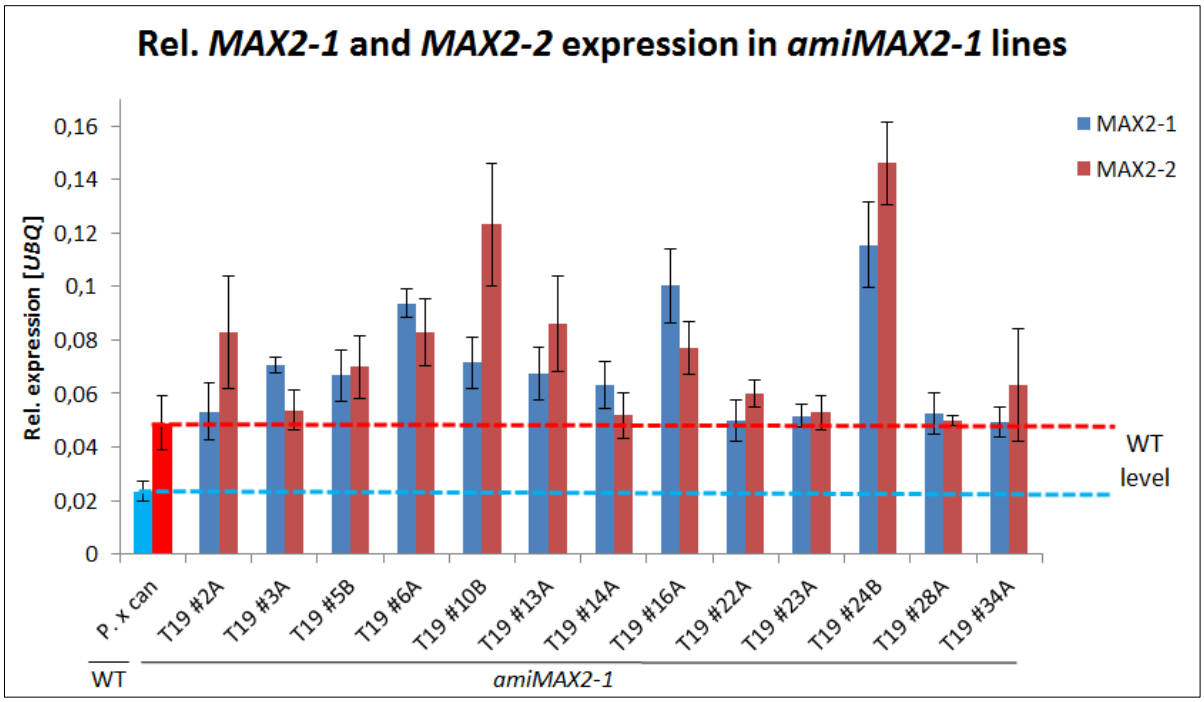

Fig. 3.23 **Expression analysis of *MAX2-1* and *MAX2-2* in transgenic poplar *amiMAX2-1* lines.** Expression levels were normalized against the reference gene *UBQ*. The relative expression levels of both *MAX2* genes in the wild type (left) are marked as dashed lines. n= 1 pool of leaves from 3 *in vitro* grown plants. Error bars indicate standard deviation of 3 technical replicates during qPCR. For the wild type, average and standard deviation were calculated for 13 replicates (pools of leaves from 3 plants each).

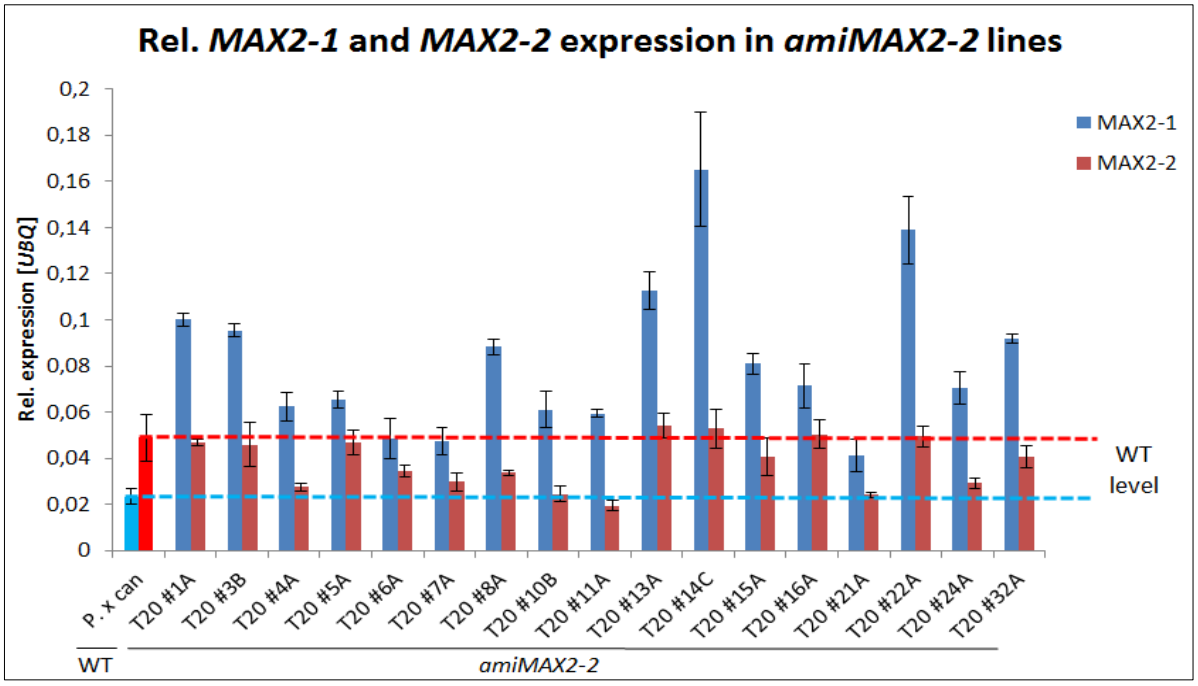

Fig. 3.24 **Expression analysis of *MAX2-1* and *MAX2-2* in transgenic poplar *amiMAX2-2* lines.** Expression levels were normalized against the reference gene *UBQ*. The relative expression levels of both *MAX2* genes in the wild type (left) are marked as dashed lines. n= 1 pool of leaves from 3 *in vitro* grown plants. Error bars indicate standard deviation of 3 technical replicates during qPCR. For the wild type, average and standard deviation were calculated for 13 replicates (pools of leaves from 3 plants each).

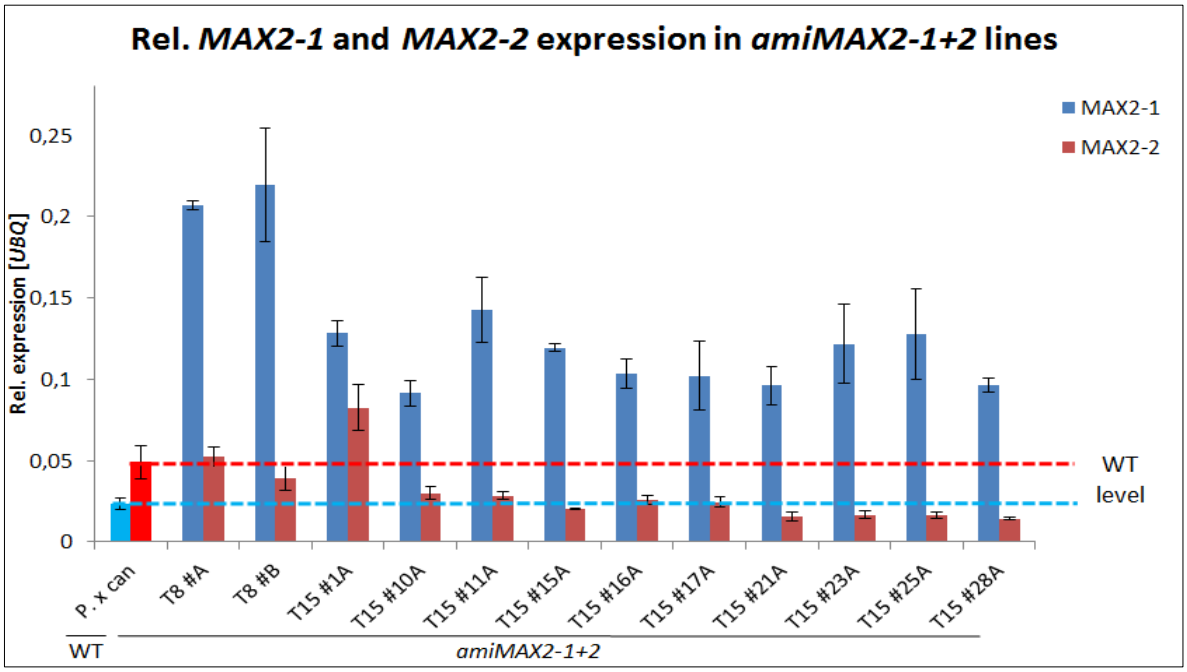

Fig. 3.25 **Expression analysis of *MAX2-1* and *MAX2-2* in transgenic poplar *amiMAX2-1+2* lines.** Expression levels were normalized against the reference gene *UBQ*. The relative expression levels of both *MAX2* genes in the wild type (left) are marked as dashed lines. n= 1 pool of leaves from 3 *in vitro* grown plants. Error bars indicate standard deviation of 3 technical replicates during qPCR. For the wild type, average and standard deviation were calculated for 13 replicates (pools of leaves from 3 plants each).

In the *amiMAX2-1* lines (Fig. 3.23), no reduction of *MAX2-1* transcript levels was found. This was unexpected, since the amiRNA was designed to target transcripts of this gene for degradation. In contrast, *MAX2-1* expression was increased in most knockdown lines compared to wild type plants. Interestingly, the same effect was observed for *MAX2-2*, which was not targeted by the amiRNA.

In most *amiMAX2-2* lines (Fig. 3.24), transcript levels of *MAX2-2* were considerably reduced compared to the wild type. This was expected, because *MAX2-2* was supposed to be targeted by the amiRNA. However, at the same time, *MAX2-1* levels unexpectedly were increased in most lines compared to the expression level of this gene in the *P.* x *canescens* wild type.

A similar pattern was observed in the *amiMAX4-1+2* lines (Fig. 3.25), in which both orthologs were intended to be down-regulated by the amiRNA. In most lines, *MAX2-2* expression was found to be reduced as expected, but *MAX2-1* levels were increased.

Overall, the knockdown appeared to be successful for *MAX2-2* in *amiMAX2-2* and *amiMAX2-1+2* lines. However, at the same time, *MAX2-1* transcript levels were increased. Since technical problems during qPCR are unlikely to cause this consistent effect, and the plants did not exhibit any branching phenotype (see chapter 3.7.1, p. 91ff), an in-depth expression analysis using more replicates or other tissues was not performed.

3.7.2 Architectural phenotyping of *amiMAX2* lines

As for a knockdown of the poplar orthologs of the SL biosynthesis gene *MAX4*, also a knockdown of the poplar *MAX2* orthologs (putatively involved in SL signaling) was expected to lead to highly increased branching, based on literature data for other plant species (see discussion in chapter 1.3.2.3; p. 11ff). Although the knockdown of the poplar *MAX2* orthologs was only partially successful as shown above (chapter 3.7.1, p. 91ff) and reduced transcript levels were only found for *MAX2-2*, a possible specialization of the different orthologs was considered. Potentially, also a knockdown of only one ortholog could then lead to an observable phenotype. Therefore, transgenic poplar *MAX2* individual and simultaneous knockdown lines were grown for phenotyping under greenhouse conditions for an assessment of shoot architectural traits.

3.7.2.1 *Shoot architecture of amiMAX2 lines*

For phenotyping of shoot architectural traits of the *amiMAX2* lines, 3.5 months old plants (after potting of the *in vitro* grown cuttings) grown under greenhouse conditions, were analyzed. Several parameters were measured: the number, position and length of branches, the plant height, the number of nodes, as well as the stem base diameter. Based on the number of nodes and the plant height, the average internode length was calculated. The architectural traits of *amiMAX2-1*, *amiMAX2-2* and *amiMAX2-1+2* plants compared to the wild type are shown in Fig. 3.26.

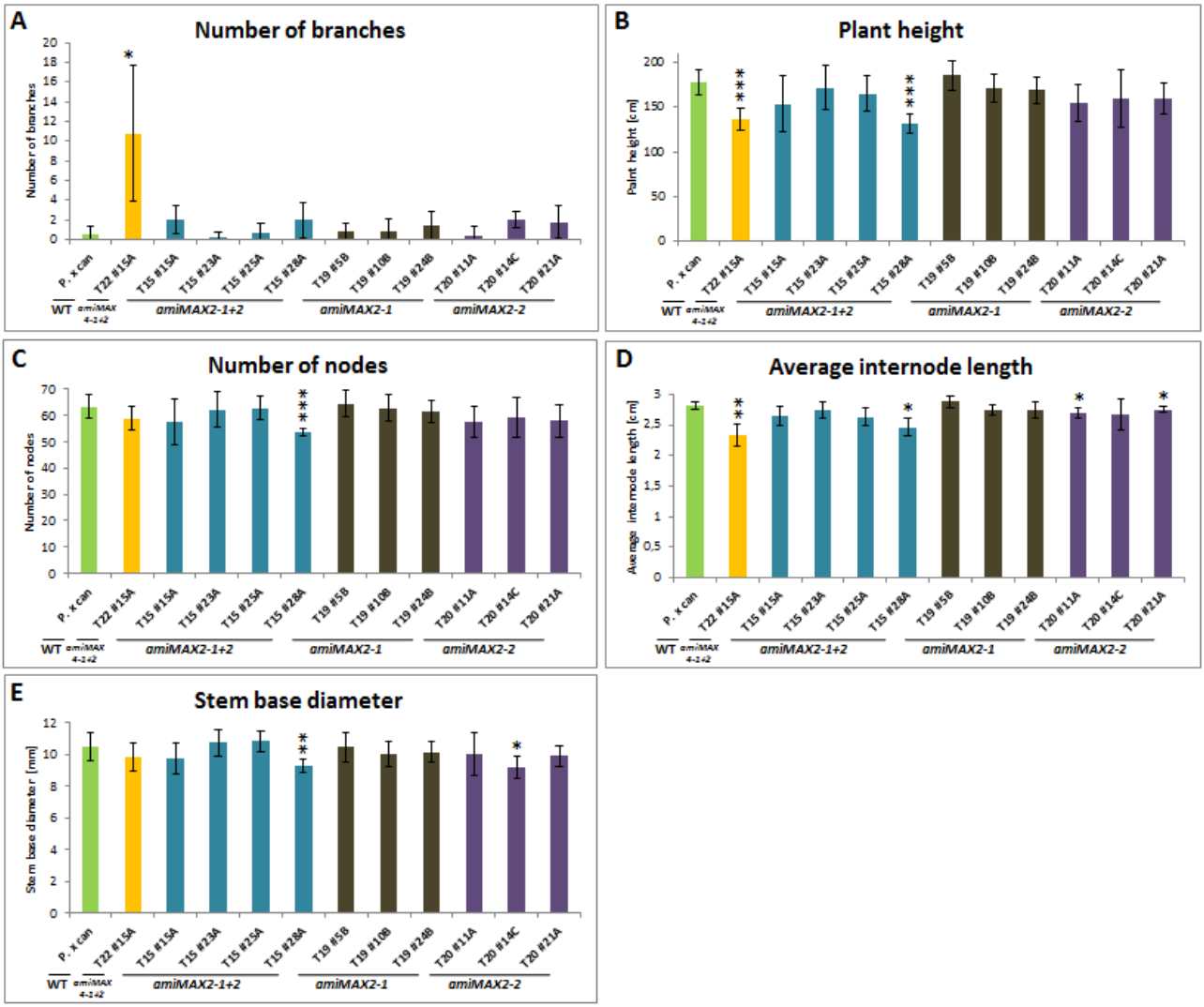

Fig. 3.26 **Architectural traits of *amiMAX2* lines.** The number of branches (A), the plant height (B), the number of nodes (C), the average internode length (D) and the stem base diameter (E) of selected *amiMAX2* lines were determined for greenhouse-grown plants. *amiMAX4-1+2* line T22 #15A was included as a control showing the typical phenotype of an SL-deficient plant. n = 4-10. Error bars indicate standard deviation. Asterisks indicate significant differences compared to the wild type (*P.* x *can*) according to Student's *t*-test. One, two and three asterisks indicate $p<0.05$, $p<0.01$ and $p<0.001$, respectively.

In the *amiMAX4-1+2* double knockdown line T22 #15A which was included as a control, branching was highly increased, the plant height and the average internode length were significantly reduced, and the number of nodes as well as the stem base diameter were not changed, as observed previously for this genotype (Fig. 3.26 A-E and chapter 3.5.2.1, p. 66ff). However, with respect to these parameters, the tested *amiMAX2* lines largely did not differ from the *P.* x *canescens* wild type control. Only *amiMAX2-1+2* line T15 #28A appeared to have a generally reduced growth phenotype (reduced plant height, number of nodes, average internode length and stem base diameter). However, it did not exhibit increased branching, as it was observed for *amiMAX4-1+2* lines and expected for plants in which SL signaling is impaired.

3.7.2.2 Biomass traits of amiMAX2 lines

Because the investigated *amiMAX2* lines grown under greenhouse conditions did not exhibit any phenotype significantly different from the *P*. x *canescens* wild type (see above), biomass parameters were not recorded.

3.8 Identification and characterization of poplar *BRANCHED1* orthologs

Arabidopsis BRANCHED1 (*AtBRC1*) and its orthologs in many other species, including monocots like rice and dicot species such as pea, were reported to be central regulators of bud outgrowth. This regulation includes the integration of signals from the SL-pathway, together with other factors such as cytokinin (Aguilar-Martínez et al., 2007; Finlayson, 2007; Minakuchi et al., 2010; Braun et al., 2012). Both hormones, SL and CK, control *BRC1* expression antagonistically (Dun et al., 2012).

Since *BRC1* was reported to be a key element in branching control and its transcript levels are SL-responsive in the investigated species, it may be a target of strigolactones in poplar as well. For this reason, putative poplar *BRC1* orthologs were identified and their expression was analyzed. Transcript levels of the candidate genes were monitored in dormant and growing buds as well as other tissue types of wild type plants. Furthermore, expression was investigated in dormant buds of representative, putatively SL-deficient *amiMAX4-1+2* lines, as well as dormant buds of outdoor-grown wild type plants at different developmental stages including winter dormancy.

3.8.1 Identification of poplar *BRC1* candidate genes by sequence analysis

As described for the identification of the poplar *MAX* gene orthologs (chapter 3.1, p. 56ff), a TBLASTN search was performed in the database Phytozome (www.phytozome.org) using the *Arabidopsis* BRC1 protein sequence taken from the TAIR database (www.arabidopsis.org) as query.

Generally, among the BRC1 orthologs in different species, there is a high sequence similarity in the TCP domain, while other parts of the protein are less conserved. Beside of *AtBRC1*, there is a similar gene named *AtBRC2* in *Arabidopsis*, which also plays a minor role in branching control (Aguilar-Martínez et al., 2007). The presence of two paralogous genes in *Arabidopsis*, combined with a whole genome duplication event in the *Salicaceae* family (Tuskan et al., 2006), suggested that more than one *BRC1*-like gene may exist in the poplar genome. Considering these findings, it is difficult to identify a true functional poplar *BRC1* ortholog based on simple sequence similarity. However, candidate genes were identified. For this purpose, the 10 highest-ranked results from the BLAST search were used to build a *ClustlW* alignment of the sequences, which was then used for building a phylogenetic tree using the neighbor joining method and default settings,

including the bootstrap test of phylogeny. The analysis was done using the MEGA 5.2 software (Tamura et al., 2011).

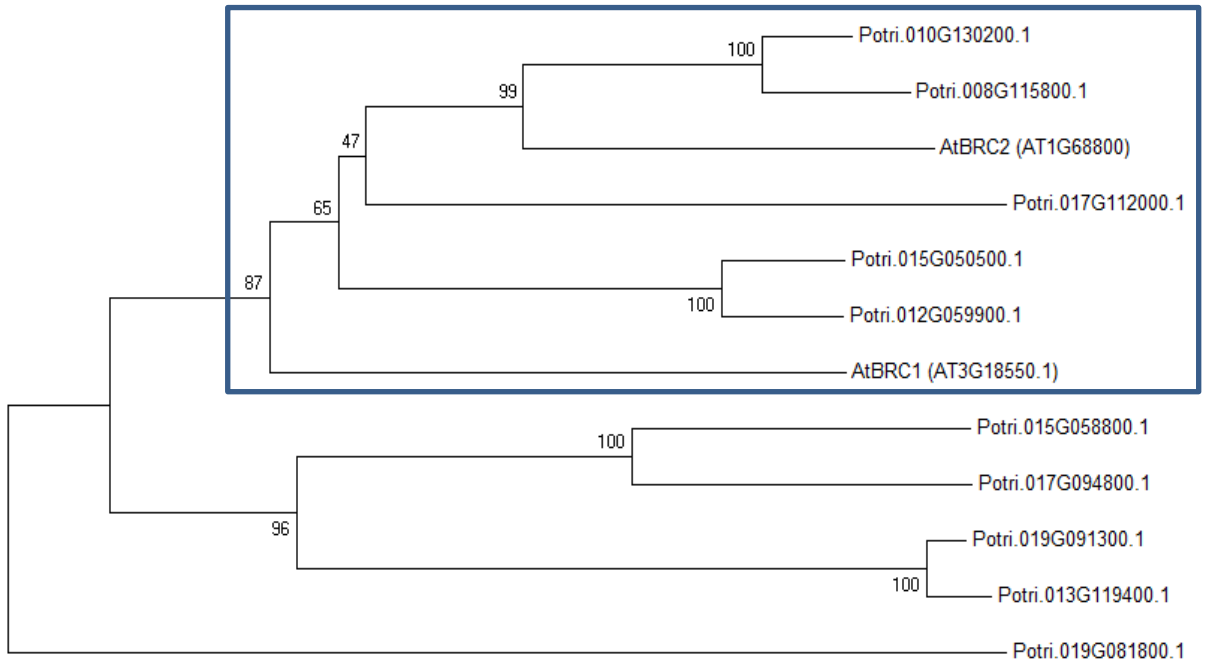

Fig. 3.27 **Phylogenetic tree of putative poplar *BRC1* orthologs.** The 10 highest-ranked candidate genes identified in a TBLASTN search against the AtBRC1 protein sequence were used to build a phylogenetic tree in the MEGA5.2 software, using a *ClustlW* alignment and the neighbor joining method. In the analysis, AtBRC2 was included. The part of the tree including the selected candidate genes is highlighted. Numbers indicate bootstrap values (1.000 replications) as calculated by the software.

Based on the phylogenetic tree (Fig. 3.27), five candidate genes were selected as putative *AtBRC1* and *AtBRC2* orthologs (highlighted in Fig. 3.27). There are two pairs of genes clustering closely together: Potri.010G130200 and Potri.008G115800 as well as Potri.015G050500 and Potri.012G059900. These clusters are possibly the result of the aforementioned whole genome duplication event in the *Salicaceae* family (Tuskan et al., 2006). The two genes each therefore appear to be closely related duplicates (paralogs), which is supported by the high bootstrap values. The fifth gene (Potri.017G112000) does not cluster together with any of the other genes.

Based on the phylogenetic tree, it is not possible to assign any of the candidate genes clearly as an *AtBRC1* ortholog. However, the Potri.010G130200 and Potri.008G115800 cluster stands close to *AtBRC2* and the bootstrap value is high, indicating that these two genes are most likely orthologs of *AtBRC2*. The Potri.015G050500 and Potri.012G059900 cluster appears to be closer related to *AtBRC1*, although the low bootstrap values do not permit a clear classification. There is also the fifth candidate gene, Potri.017G112000, for

which no clear assignment is possible. Due to these uncertainties and because the phylogenetic analysis does not necessarily allow a judgment about the functionality of the genes, all five genes were regarded as putative functional poplar orthologs of *AtBRC1*. Possibly, even a poplar gene showing a higher similarity to *AtBRC2* could be one or even the only functional *BRC1* ortholog, and should be further analyzed. Tab. 3.3 provides an overview about the selected candidate genes.

Tab. 3.3 Overview about the *Arabidopsis BRC* genes and their putative poplar orthologs. *Arabidopsis BRC1* and *BRC2* and their corresponding poplar orthologs, identified by a BLAST analysis, are shown. The poplar orthologs were named according to their corresponding chromosome numbers.

Gene	Species	Gene ID	Length CDS [bp]	Length genomic [bp]	Length protein [aa]
AtBRC1	*A. thaliana*	At3G18550	1302	1836	433
AtBRC2	*A. thaliana*	At1G68800	1071	1475	356
PtBRC1-8	*P. trichocarpa*	Potri.008G115800	1362	2222	453
PtBRC1-10	*P. trichocarpa*	Potri.010G130200	1419	1456	472
PtBRC1-12	*P. trichocarpa*	Potri.012G059900	1185	2185	394
PtBRC1-15	*P. trichocarpa*	Potri.015G050500	1209	1726	402
PtBRC1-17	*P. trichocarpa*	Potri.017G112000	1125	2033	374

3.8.2 Expression of poplar *BRC1* candidate genes in dormant vs. growing WT buds

For a functional poplar *BRC1* ortholog, expression in dormant axillary buds was expected. The transcript level should be reduced when the buds start to grow out, as it was observed in *Arabidopsis* (Finlayson, 2007). Therefore, greenhouse-grown *P.* x *canescens* wild type plants were sampled. Dormant axillary buds (size: 2-3 mm) were harvested and the plants were decapitated to induce outgrowth of the remaining buds. Three additional bud developmental stages were harvested according to their status: slightly swollen (size: 3-5 mm), swollen (size: 5-8 mm) and growing (size: 8-20 mm).

The expression of the selected *BRC1* ortholog candidate genes was monitored in these samples by qPCR.

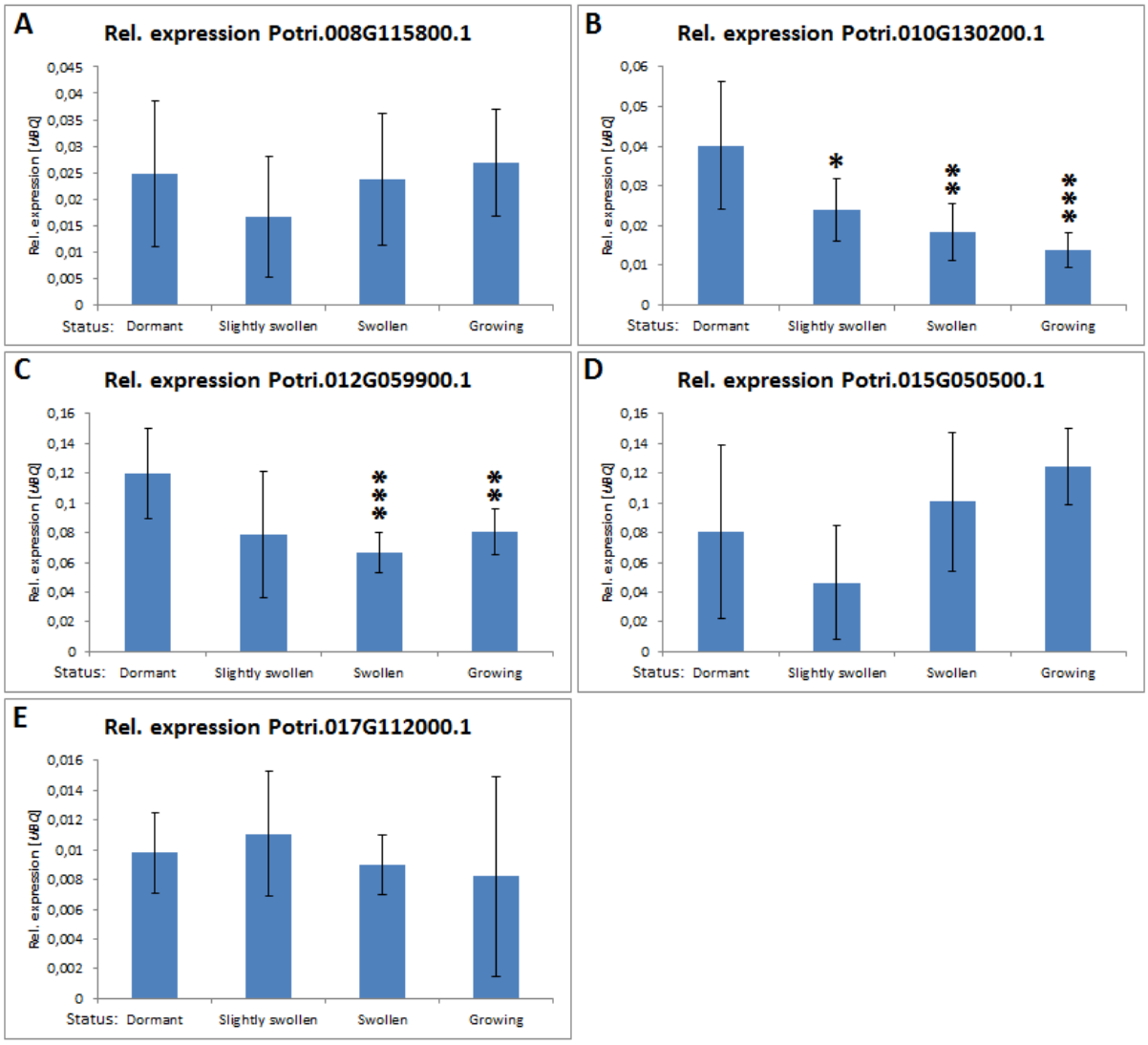

Fig. 3.28 Expression of putative *P.* x *canescens BRC1* ortholog candidate genes in dormant and growing buds. Expression levels of the candidate genes Potri.008G115800 (A), Potri.010G130200 (B), Potri.012G059900 (C), Potri.015G050500 (D) and Potri.017G112000 (E) relative to the reference gene *UBQ* were determined in dormant, slightly swollen, swollen and growing buds of *P.* x *canescens* wild type plants. n= 4-10. Error bars indicate standard deviation. Asterisks indicate significant differences compared to dormant buds according to Student's *t*-test. One, two and three asterisks indicate $p<0.05$, $p<0.01$ and $p<0.001$, respectively.

Expression levels of the candidate genes Potri.008G115800, Potri.015G050500 and Potri.017G112000 were not significantly changed in swollen or growing axillary buds compared to dormant buds (Fig. 3.28 A, D and E). Therefore, these genes do not show the expected reduction of transcript levels when the buds grow out. However, two candidate genes exhibited this expected regulation. Potri.010G130200 already had significantly reduced transcript levels in only slightly swollen buds compared to dormant buds (Fig. 3.28 B). The transcript levels were found to decrease further when the bud grew out. The regulation was gradual from dormant over slightly swollen and swollen to growing buds,

with the latter exhibiting the lowest expression. For Potri.012G059900, also a significant reduction of transcript levels was observed in swollen and growing compared to dormant axillary buds (Fig. 3.28 C). However, the trend was not as obvious as for Potri.010G130200.

Summarized, two candidate genes showed the expected regulation: Potri.010G130200 and Potri.012G059900. The first appears to be a rather close ortholog of *AtBRC2*, while the latter appears to be closer related to *AtBRC1* based on the phylogenetic analysis (Fig. 3.27).

3.8.3 Expression of poplar *BRC1* candidate genes in different WT tissues

Beside of a rather high expression level in dormant axillary buds and a down-regulation in growing buds, expression of a functional poplar *BRC1* ortholog was expected to be low or undetectable in other tissues, as it was observed in *in situ* hybridization, qPCR and promoter-GUS fusion experiments in maize (Hubbard et al., 2002), rice (Takeda et al., 2003), *Arabidopsis* (Aguilar-Martínez et al., 2007; Finlayson, 2007) and pea (Braun et al., 2012). Therefore, expression of the candidate genes was tested in different tissues of greenhouse-grown *P.* x *canescens* wild type plants. Since Potri.017G112000 could not be clearly assigned during the phylogenetic analysis (Fig. 3.27) and did not show any regulation in outgrowing buds (Fig. 3.28), this gene was excluded from further analysis.

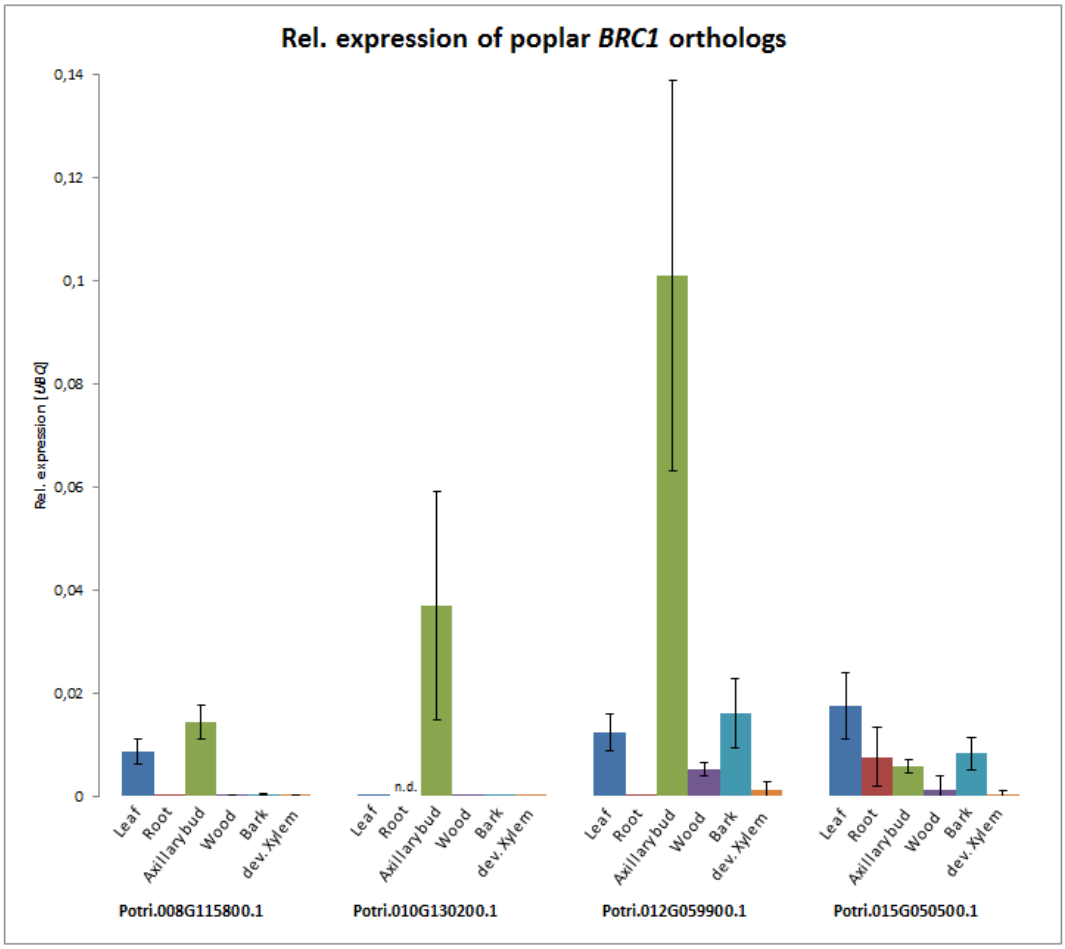

Fig. 3.29 Expression of poplar *BRC1* ortholog candidate genes in different tissues. Expression was monitored in leaves, roots, axillary buds, wood, bark and developing xylem of 3.5 months old, greenhouse-grown *P.* x *canescens* wild type plants. Expression was determined relative to the reference gene *UBQ*. n=4. Error bars indicate standard deviation.

Potri.010G130200 exhibited the expected expression pattern during previous analysis of dormant and outgrowing axillary buds (Fig. 3.28 B). Also in the different tissues tested here, this gene showed the typical expression pattern of a *BRC1* ortholog: transcripts were well-detectable in dormant axillary buds, while no or only minor expression was found in all other tested tissues (Fig. 3.29). The other candidate gene showing the expected reduction of transcript levels in outgrowing buds, Potri.012G059900 (Fig. 3.28 C), exhibited the highest expression in dormant axillary buds. However, low to moderate transcript levels were also detectable in other tissues. Potri.008G115800 was only moderately expressed in dormant axillary buds. While almost no transcripts of this gene were detected in roots, wood, bark and developing xylem, there also was moderate expression in leaves. For Potri.015G050500, expression was generally low to moderate, but not specific to any tissue.

3.8.4 Expression of poplar *BRC1* candidate genes in *amiMAX4-1+2* lines

The expression analysis in various tissues of wild type *P.* x *canescens* plants resulted in the identification of two poplar candidate genes showing the expression pattern which was expected for a functional *BRC1* ortholog (see chapter 3.8.2 and 3.8.3; p. 98f). Based on the phylogenetic analysis (chapter 3.8.1, p. 96ff), Potri.010G130200, the best candidate identified in the expression analysis, can be regarded as an ortholog of *AtBRC2*. Potri.012G059900, which was also a promising candidate, appears to be more closely related to *AtBRC1* (Fig. 3.27).

Another important feature of a functional *BRC1* ortholog is an induction of expression by strigolactones. In SL pathway (*max*/*rms*) mutants of *Arabidopsis* and pea, *BRC1* levels were, therefore, found to be reduced. In contrast, *BRC2* expression was not altered in *Arabidopsis max* mutants (Aguilar-Martínez et al., 2007; Braun et al., 2012). The same regulation was expected for functional poplar *BRC1* and *BRC2* orthologs in the putatively SL-deficient *amiMAX4-1+2* knockdown lines generated in this project. Therefore, expression of the most promising candidate genes Potri.010G130200 and Potri.012G059900 was monitored in dormant buds of representative *amiMAX4-1+2* lines relative to the wild type.

The results are described in chapter 3.6.1.2 (p. 76ff), where the identified *BRC*-like genes were used as marker genes for SL-deficiency. As expected for a *BRC2* ortholog, expression of Potri.010G130200 was not altered in the tested *amiMAX4-1+2* lines (Fig. 3.16 B and Appendix Fig. 7.18 B; p. 163), arguing against a regulation of this gene by SLs. However, transcript levels of Potri.012G059900 were significantly reduced in all tested lines compared to the wild type (Fig. 3.16 A and Appendix Fig. 7.18 A; p. 163), as anticipated for a functional poplar *BRC1* ortholog.

3.8.5 Expression of poplar *BRC1* and *BRC2* during winter dormancy

In contrast to annual and herbaceous species such as *Arabidopsis* and pea, which were frequently used in previous studies to investigate the role of *BRC1* in bud outgrowth regulation, poplar is a perennial, woody species. Instead of only seeds, the whole plant survives the cold winters found in temperate climates. The adaptation strategy involves growth cessation during autumn, when even the shoot apical meristems form dormant buds. This results in an additional type of dormant buds. Along with the axillary buds, they

enter a deep state of dormancy (winter dormancy or endodormancy), i.e. there also is an additional stage of dormancy which is not found in annual plants. The different stages of dormancy are discussed in chapter 1.3.4 (p. 22ff).

Winter dormancy in poplar as a model system therefore offered the opportunity to study expression of *BRC1* in more detail compared to frequently investigated species. Also the identified putative poplar *BRC2* ortholog was included in the expression analysis. Dormant axillary and apical buds were harvested from approx. 3 years old, outdoor-grown *P.* x *canescens* wild type trees during endodormancy in winter (27.01.2014) and during bud break in spring. For the latter, swollen buds (outer layers already breaking, turning green, 01.04.2014) and outgrown buds (leaves starting to unfold, 06.04.2014) were sampled. In addition and as a reference sample for paradormant (dormancy during growth period) buds from the same trees, axillary buds were sampled 08.09.2014. Decapitation was done to release buds from apical dominance and thus to induce bud outgrowth for obtaining additional reference samples. However, this was not successful. The time point was at the end of the growing season and the buds may have already entered an ecodormant state.

Photographs of representative buds at the different time points of harvesting are shown in Fig. 3.30.

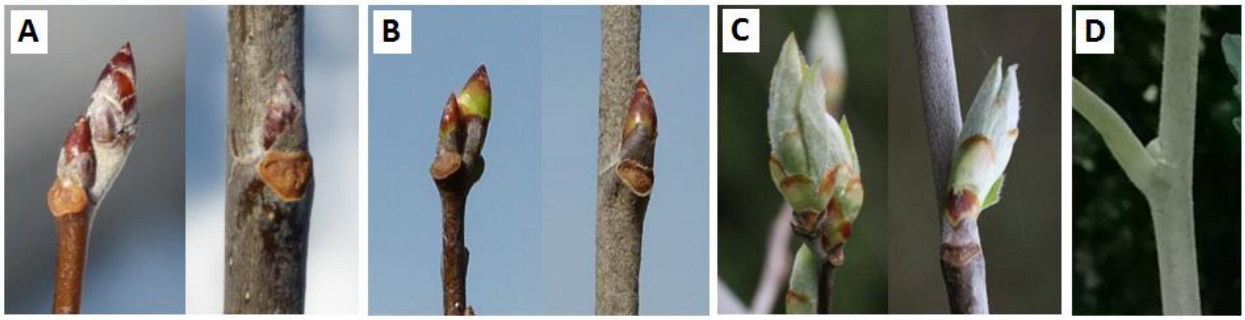

Fig. 3.30 Photographs of representative *P.* x *canescens* buds at the different harvesting time points. Endodormant apical (left) and axillary buds (right) were harvested during winter (A). The corresponding swollen (B) and growing buds (C) were sampled in spring. During the growing season, also paradormant axillary buds were sampled (D).

All collected samples were used for expression analysis of the poplar *BRC1* and *BRC2* ortholog candidate genes Potri.012G059900 and Potri.010G130200 and the results are shown in Fig. 3.31.

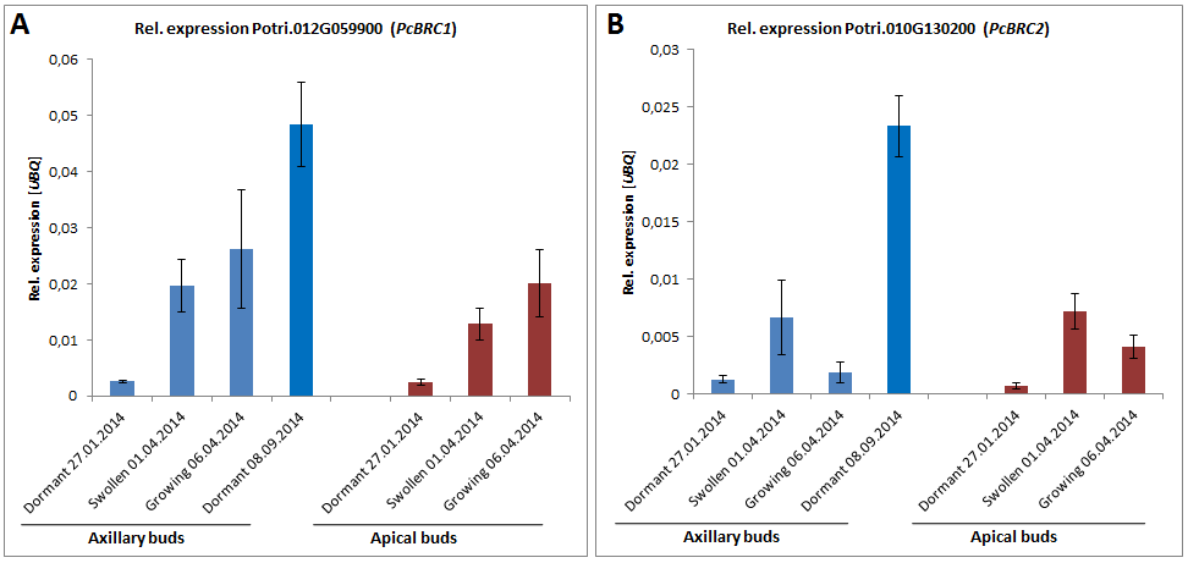

Fig. 3.31 Expression of putative poplar *BRC1* and *BRC2* orthologs in axillary and apical buds at different developmental stages. Expression of *PcBRC1* (Potri.012G059900; A) and *PcBRC2* (Potri.010G130200; B) was monitored in dormant and growing axillary (blue) as well as apical buds (red) from approx. 3 years old, outdoor-grown *P.* x *canescens* wild type plants. Buds were sampled at different time points: during winter dormancy, bud break in spring and during the growth period. Note: dormant apical buds do not exist during the growth period, but only during winter dormancy. Expression levels were normalized against the reference gene *UBQ*. n=4-5. Error bars indicate standard deviation.

Unexpectedly, Potri.012G059900 (*PcBRC1*) transcript levels were low in axillary and apical buds sampled during winter and then increased in swollen buds in spring (Fig. 3.31 A). In growing buds of both types, there was a further increase in expression by trend. The highest relative expression level was observed in para- or ecodormant buds sampled during the growing season. The expression level reached approximately half of the level found in paradormant axillary buds of greenhouse-grown plants (Fig. 3.28 C).

Similar to Potri.012G059900, transcript levels of Potri.010G130200 (*BcBRC2*) were increased in swollen axillary and apical buds compared to the corresponding bud types during winter dormancy (Fig. 3.31 B). The expression level then dropped slightly in growing buds of both types. Expression was also highest in dormant axillary buds during the growing season (para- or ecodormant), almost reaching the same expression level relative to *UBQ* as it was observed in paradormant axillary buds of greenhouse-grown wild type plants (Fig. 3.28 B).

With respect to the different bud types, there were no major differences. Overall, expression levels and patterns of both genes in apical buds were very similar to the patterns found in axillary buds, as described above. This indicates that there is no differential expression.

4 Discussion

For an investigation of the significance of strigolactones in the model tree poplar, candidate genes involved in SL biosynthesis (*MAX4*) and SL signaling (*MAX2*) were selected based on studies in other species. The corresponding poplar orthologs were identified and their expression was investigated in different tissues of *P*. x *canescens* wild type plants. To analyze their role in poplar, loss of function lines (amiRNA mediated gene silencing) were generated and phenotyped for several SL-related traits. The results are discussed in the following chapters, starting from the identification of the candidate genes, followed by a confirmation of knockdown efficiency and a discussion of the observed architectural phenotypes. Lines, in which both poplar *MAX4* orthologs were knocked down (*amiMAX4-1+2*), showed robust SL deficiency phenotypes. Additional experiments were done with these lines for characterization of SL-related traits. These include complementation of the phenotypes by grafting, expression analysis of SL-related marker genes, an investigation of possible crosstalk with the JA pathway and GR24-treatment experiments.

A second focus was the transcription factor *BRC1* as a SL-regulated component of bud outgrowth regulation. The identification of putative functional poplar *BRC1* orthologs is discussed. The expression pattern of poplar *BRC1* candidate gene was monitored in different tissues, especially in buds. Tree-specific aspects of dormancy were addressed. Expression of poplar *BRC1* was also investigated in putatively SL-deficient *amiMAX4-1+2* lines, which were expected to have reduced transcript levels.

4.1 Identification of poplar *MAX* orthologs and sequencing

For each of the two SL pathway candidate genes, *MAX4* and *MAX2*, two orthologs were identified in poplar (*MAX4-1* and *MAX4-2*; *MAX2-1* and *MAX2-2*). The presence of two paralogs (genes resulting from a duplication event within a given species) is common for many genes in poplar. It can be explained by a duplication event, in which almost the entire genome was doubled. The duplication was estimated to have occurred 8-13 million years ago (Tuskan et al., 2006), which is very recent on an evolutionary scale, especially for organisms with long generation times such as trees. Thus, a high degree of conservation among the paralogs was expected. Indeed, cloning and sequencing of the genes revealed high sequence identity (see alignments in Appendix Fig. 7.3 and Fig. 7.4, p.

152). Such conservation made redundancy effects likely and was the reason for the design of amiRNA constructs which targeted both paralogs simultaneously. Recently, a characterization of the poplar SL pathway genes was published (Czarnecki et al., 2014). This study confirmed the correct identification of poplar *MAX* genes in this work. It showed that both copies could complement the corresponding *Arabidopsis* mutant branching phenotypes, which is a strong indication for functional redundancy. Yet, it does not prove redundancy directly, as *Arabidopsis* is a heterologous system. Complementation was only partial and not equally effective for the two paralogs (Czarnecki et al., 2014), which may be interpreted as a hint for a somewhat different function. Furthermore, expression patterns of the two paralogs in poplar were not found to be identical (see chapter 3.3, p. 59f; and discussion below) and pointed to a diversification, since spatiotemporal expression patterns play an important role for the gene function. Additionally, although the paralogs are highly similar on the sequence level, even minor differences, e.g. changes leading to alterations at binding sites for interaction partners or substrates, can have a large impact on the function of the encoded proteins. To resolve such possible diversification, individual knockdowns of the poplar paralogs were attempted, too.

4.2 Expression pattern of *MAX* genes in wild type poplar

Expression of the identified poplar *MAX* genes was monitored in *P.* x *canescens* wild type plants (see chapter 3.3.2, p. 61f).

Transcript levels of the poplar *MAX4* orthologs were found to be extremely low in young, *in vitro* grown plants. The highest expression was observed for *MAX4-1* in roots (Fig. 3.3, p. 61), which matches the eFP browser data (Fig. 3.2, p. 60). Transcripts of both genes were also detectable in stems, while no expression was found in leaves (Fig. 3.3, p. 61). This overall pattern was expected, since *MAX4* in other species is known to be expressed at low levels, and expression occurs predominantly in root tips and nodal areas of the stem (Arite et al., 2007; Liang et al., 2010; Snowden et al., 2005; Sorefan et al., 2003). Accordingly, no or only basal *MAX4* expression was found in developing xylem, leaves, axillary buds and bark, when the expression pattern was investigated in 4.5 months old greenhouse-grown plants (Fig. 3.4, p. 62). Interestingly, in these plants, only minor amounts of *MAX4* transcripts were detectable in the roots. In contrast, transcripts were readily detectable in the stem (wood, no bark). It is unclear why expression shifted from

the root to the stem as the major site of *MAX4* expression in plants grown under greenhouse conditions compared to *in vitro* grown plants. Such a tissue-specific shift of *MAX4* expression depending on the growth conditions and/or plant age has not been tested or reported for other species. Nonetheless, it is known that the stem as a site for SL biosynthesis is sufficient, and the root is not required. This was shown by grafting experiments in *Arabidopsis*, pea and petunia, in which wild type scions were grafted onto *MAX* mutant rootstocks, still exhibiting WT-like architecture (Foo et al., 2001; Napoli, 1996; Sorefan et al., 2003). In petunia, even a small wild type interstock stem fragment was sufficient to rescue the mutant phenotype of a *max4* scion grafted onto a *max4* rootstock (Foo et al., 2001). Also in this work, grafting studies using *amiMAX4-1+2* lines showed the same outcome (see chapter 3.6.2 (p. 79ff); and discussion below). Thus, it appears that the root is not required for biosynthesis of SLs acting in the stem.

Expression profiling was done for the poplar *MAX2* orthologs as well (chapter 3.3.2, p. 61f). *MAX2* is known to be an important component of SL signaling. Thus, it was expected to be expressed in tissues where SLs are perceived. SLs are discussed to be involved in the regulation of auxin transport in the PATS in xylem parenchyma cells (canalization model), and there may also be a local mode of action within the buds (second messenger model) (see chapter 1.3.2.3, p. 11ff). Thus, a pattern of broad expression can be expected. Indeed, *MAX2* expression was previously reported to occur in almost all tested plant organs of *Arabidopsis*, pea, petunia and rice, particularly in the vasculature of various tissues (Drummond et al., 2011; Ishikawa et al., 2005; Johnson et al., 2006; Stirnberg et al., 2007). This was also implied in poplar (*P. balsamifera*) by microarray (eFP browser) data (Fig. 3.2, p. 60) and confirmed in this work by qPCR in *P.* x *canescens* (Fig. 3.5, p. 63). Thus, the expression pattern matched published data and points to a role for *MAX2* in poplar, similar to the function described in other species.

4.3 Target gene expression analysis and phenotyping: *amiMAX4* lines

4.3.1 Target gene expression analysis in *amiMAX4* lines

Individual knockdowns (*amiMAX4-1* and *amiMAX4-2* lines) were carried out to resolve a potential diversification of gene functions, while simultaneous knockdowns of both poplar orthologs (*amiMAX4-1+2* lines) were done to overcome likely redundancy effects. A successful knockdown was expected to reduce the transcript levels of the target genes.

Since *MAX4* is involved in SL biosynthesis, silencing would most likely result in SL deficiency, in turn leading to alterations in architectural phenotypes. For the investigation of knockdown efficiency, plants had to be grown under greenhouse-conditions to obtain wood samples. Samples from other tissues or younger plants were not suited, because *MAX4* was only sufficiently expressed in this tissue type in wild type plants (Fig. 3.4, p. 62). At the time point of sampling, plants were tall and old enough to exhibit typical phenotypes. Thus, architectural phenotyping was done before expression analysis. Based on the obtained data, expression analysis was only performed for several representative *amiMAX4-1+2* lines. Individual *MAX4* knockdown lines (*amiMAX4-1* and *amiMAX4-2*) did not exhibit architectural phenotypes and were excluded from expression analysis.
As expected for lines showing typical SL-deficiency phenotypes (see discussion below), all tested *amiMAX4-1+2* lines exhibited a significant down-regulation of both target genes (Fig. 3.6, p. 65). Thus, the knockdown was successful.

4.3.2 Architectural phenotyping of *amiMAX4* lines

While *amiMAX4-1+2* double knockdown lines exhibited strong changes in architectural traits, there were no significant differences between single knockdown lines (*amiMAX4-1* and *amiMAX4-2*) and the *P.* x *canescens* wild type (chapter 3.5.2, p. 65ff). Thus, the discussion of architectural phenotypes in the following paragraphs focuses on the *amiMAX4-1+2* lines.

4.3.2.1 Shoot architecture of amiMAX4 lines

MAX4 is involved in SL biosynthesis. Loss of function mutations and RNAi-mediated silencing led to typical SL-deficiency phenotypes in *Arabidopsis*, pea, petunia, rice, tomato and kiwifruit. The most prominent phenotype is highly increased shoot branching (Arite et al., 2007; Kohlen et al., 2012; Ledger et al., 2010; Snowden et al., 2005; Sorefan et al., 2003).
The absence of this phenotype in poplar *MAX4* single knockdown lines (see chapter 3.5.2, p. 65ff) may be explained by the high degree of conservation between both poplar *MAX4* orthologs (see alignment in Appendix Fig. 7.3, p. 152), making redundancy likely. This is supported by the finding that both can at least partially complement the *Arabidopsis max4* mutant phenotypes (Czarnecki et al., 2014). Loss of function of one copy could then

be masked by the activity of the other paralog. Such a redundancy effect may be enhanced by the negative feedback control mechanism present in the SL pathway, acting on *MAX4* (Mashiguchi et al., 2009). Via release from negative feedback, knockdown of one *MAX4* paralog may induce compensatory upregulation of the other, functionally redundant gene. Another explanation for the absence of a phenotype in the *MAX4-1* and *MAX4-2* lines would be unsuccessful knockdown of the target genes by the amiRNA constructs. This cannot be ruled out, as expression analysis of the target genes was not done in individual knockdown lines.

In contrast to the *MAX4* single knockdown lines, *amiMAX4-1+2* double knockdown lines revealed a robust increased branching phenotype in almost all tested lines, which was reproducible and stable under different conditions. This is remarkable, since it is the first direct implication for a regulation of branching processes by SLs in trees in a way similar to the mechanisms observed in other species. Thus, it underlines the high degree of conservation of fundamental control mechanisms.

For an in-depth characterization, other architectural phenotypes were investigated in the *amiMAX4* lines. Compared to the wild type, the plant height was reduced in *amiMAX4-1+2* lines, which is a common phenotype of SL-deficient mutants (Arite et al., 2007; Snowden et al., 2005; Sorefan et al., 2003). The reduced plant height is a consequence of a reduced internode length, while the number of nodes is not changed in most *amiMAX4-1+2* lines (Fig. 3.9 and Fig. 3.10, p. 68). The reduced internode length also is a typical sign of SL deficiency: SLs were reported to stimulate internode elongation by controlling cell division, leading to a reduced internode length in SL-deficient pea and petunia mutants (de Saint Germain et al., 2013; Snowden et al., 2005). Interestingly, such a reduction was not observed in kiwifruit *MAX4* knockdown lines (Ledger et al., 2010). Like poplar, kiwifruit is a woody perennial species. The presence of the phenotype in the poplar *amiMAX4-1+2* lines indicates conservation of this function in woody perennials, which may be lost specifically in kiwifruit.

Summarized, shoot architectural phenotyping revealed typical SL-deficiency related symptoms in poplar *amiMAX4-1+2* lines. Thus, there are strong hints that the knockdown of both *MAX4* orthologs indeed led to reduced SL levels.

4.3.2.2 Biomass traits of amiMAX4 lines

During phenotyping, also biomass traits of poplar *amiMAX4* lines were investigated. Although SL-deficient plants are frequently described to have a reduced height compared to wild type plants, there are no reports addressing the biomass. The branches may compensate for the reduction of primary shoot growth. In this work, the biomass was determined separately for stems, leaves and roots of *amiMAX* lines and compared to the *P.* x *canescens* wild type (see chapter 3.5.2.2, p. 70ff). However, no major differences were observed in *amiMAX4* lines compared to the *P.* x *canescens* wild type. Although there were some significant differences in few lines with respect to the root and leaf dry weight, this was not consistent. Also for the total biomass, no significant differences were observed in any of the tested lines (Fig. 3.13, p. 71). Thus, a reduction of growth in the primary shoot is entirely compensated by biomass of the branches and appears to result from resource allocation to this part of the plant. Although pea SL pathway mutants with manually removed axillary buds were reported to still be shorter than wild type plants, suggesting that the reduced internode length is independent of increased branching, such a redistribution of resources is discussed to play a role: when buds were removed, increased leaf growth and stem thickening was observed in wild type and SL mutant plants (de Saint Germain et al., 2013). Thus, SL deficiency triggers increased branching, but resource allocation is an SL-independent process.
Summarized, SL-deficiency appears not to influence total biomass, but only the biomass distribution within the plant appears to be changed as a secondary effect.

4.3.2.3 Root architecture of amiMAX4 lines: adventitious rooting

In addition to their role in shoot architecture, SLs were reported to have profound effects on the root architecture. In this work, adventitious rooting was addressed. SLs appear to have an inhibitory effect on this developmental process: while GR24 treatment inhibited adventitious rooting, *Arabidopsis* and pea SL pathway mutants were reported to produce increased numbers of adventitious roots (Rasmussen et al., 2012).
The putatively SL-deficient poplar *amiMAX4-1+2* lines generated in this project showed increased numbers of roots growing from stem cuttings, too (Fig. 3.14, p. 73). This provides further evidence for the anticipated SL-deficiency in these lines. Additionally, it underlines the role of SLs in adventitious root formation in trees, in which such a function has not been studied yet. Also in kiwifruit, which is the only woody perennial for which

putatively SL-deficient lines (*MAX4* knockdown) were generated, adventitious rooting was not addressed (Ledger et al., 2010).
Taken together, the findings strongly suggest that the role of SLs in adventitious root formation is conserved in trees, and provides further evidence for SL deficiency in the generated *amiMAX4-1+2* lines.

4.4 Detailed characterization of *amiMAX4-1+2* lines

Since the generated poplar *amiMAX4-1+2* lines exhibited typical phenotypes of SL-deficient plants, they were characterized in detail. Direct quantification of SLs to prove SL-deficiency was not feasible (see explanation in chapter 3.6.1, p. 74f). Although this may become feasible in the future, in this project, further indirect proof was collected instead in addition to the typical architectural phenotypes described above. For this purpose, the expression of SL-responsive marker genes was monitored and the shoot architectural phenotypes were complemented by grafting. Furthermore, exogenous treatment with synthetic SL (GR24) was done in wild type and *amiMAX4-1+2* stem segments to test its effect on poplar; and buds of *amiMAX4-1+2* plants were treated with GR24 in another complementation approach.
Since the experiments provide strong support for the anticipated SL deficiency in the generated lines, a recently suggested crosstalk of the SL pathway with jasmonic acid (JA) was investigated. Furthermore, an anticipated influence of SL deficiency on the time point of bud break after winter dormancy was studied.

4.4.1 Expression of SL-regulated marker genes in *amiMAX4-1+2* lines

The expression of known SL-responsive genes was employed as an indicator for SL-deficiency in the *amiMAX4-1+2* lines. *MAX3* was chosen since it is negatively feedback-regulated by SLs in *Arabidopsis* and pea, along with other SL biosynthesis genes (Hayward et al., 2009; Johnson et al., 2006; Mashiguchi et al., 2009; de Saint Germain et al., 2013). In contrast, *BRC1* is positively regulated by SLs (Aguilar-Martínez et al., 2007; Braun et al., 2012).

4.4.1.1 MAX3 expression in amiMAX4-1+2 lines

In *Arabidopsis max* and pea *rms* SL biosynthesis and signaling loss of function mutants, a moderate (2 to 10-fold) increase in *MAX3*/*RMS5* expression was reported. This is due to release of *MAX3*/*RMS5* from negative feedback in these plants (Hayward et al., 2009; Johnson et al., 2006; Mashiguchi et al., 2009; de Saint Germain et al., 2013; Waters et al., 2012a). Thus, the poplar *MAX3* ortholog Potri.014G056800 (identified by sequence comparison, also reported in Czarnecki et al. (2014)) appeared to be a suitable marker for SL deficiency. However, regulation could not be clearly shown in stem samples of the tested representative poplar *amiMAX4-1+2* lines. Although transcript levels were increased by trend compared to the *P.* x *canescens* wild type, this was only significant in one line. The increase was approx. 2-fold in this line (Fig. 3.15, p. 76), but it was not reproducible in a repetition of the experiment.

There are several possible explanations for the failure to show *MAX3* feedback regulation in poplar. The variation among the biological replicates was high, potentially obscuring a rather subtle effect. In the above-mentioned studies, the regulation was sometimes observed to be only 2-fold, even in full loss-of-function mutants, which are either SL-deficient or have defects in SL signaling. Although the tested poplar lines show typical SL-deficiency phenotypes, expression analysis of the target genes (*MAX4-1* and *MAX4-2*) revealed residual transcript levels (Fig. 3.6, p. 65). Thus, it is likely that the plants are not fully SL-deficient and rather have reduced SL levels. This may not be sufficient to cause release of the SL biosynthesis genes, including *MAX3*, from negative feedback. An alternative explanation would be the absence of negative feedback regulation of *MAX3* in poplar. Although the SL pathway appears to be generally conserved among species, rice *D17* (*HTD1*, *MAX3* ortholog) transcript levels were not increased in SL pathway mutant lines compared to the wild type (Arite et al., 2007). Thus, there seems to be no negative feedback regulation of this gene in rice, and this may be the case in poplar as well.

However, the finding that *D17* is not regulated in rice does not generally connote absence of negative feedback in the SL pathway in this species. Negative feedback rather may target other genes in SL biosynthesis. Interestingly, *D10* (*MAX4* ortholog) transcript levels were found to be increased in SL pathway mutants (Arite et al., 2007). Thus, rice is an example for a species in which the *MAX3* ortholog is not subject to negative feedback, while the *MAX4* ortholog is regulated. Further studies showed that *MAX4* orthologs are also regulated in other species in addition to *MAX3*: *MAX4*/*RMS1*/*DAD1* transcript levels were increased in *Arabidopsis*, pea and petunia SL pathway mutants (Hayward et al.,

2009; Johnson et al., 2006; Mashiguchi et al., 2009; Snowden et al., 2005; Waters et al., 2012a). This regulation may also be present in poplar, but it could not be tested since *MAX4* was the knockdown target.

4.4.1.2 BRC1 expression in amiMAX4-1+2 lines

Transcript levels of the bud outgrowth regulating transcription factor BRC1 were reported to be significantly reduced in *Arabidopsis* and pea SL pathway mutants, including SL-deficient *max4*/*rms1* lines (Aguilar-Martínez et al., 2007; Braun et al., 2012). Thus, poplar *BRC1* orthologs appeared to be suited marker genes for SL-deficiency in the *amiMAX4-1+2* lines. Since poplar *BRC1* has not been described yet, candidate genes for functional orthologs were identified (see chapter 3.8, p. 95ff; and discussion chapter 4.6, p. 122ff). A down-regulation of transcript levels of these genes in *amiMAX4-1+2* knockdown lines compared to the *P.* x *canescens* wild type was expected. Indeed, expression of the gene Potri.012G059900 was significantly reduced in axillary buds of the tested representative *amiMAX4-1+2* lines (Fig. 3.16, p. 78). Therefore, this finding provides further proof for SL-deficiency in these lines.

4.4.2 Complementation of *amiMAX4-1+2* phenotype: grafting

The shoot architectural phenotypes of SL-deficient mutants can be complemented by grafting of a mutant scion onto a wild type rootstock, as shown in *Arabidopsis*, pea and petunia (Foo et al., 2001; Napoli, 1996; Sorefan et al., 2003). In this work, this was successfully done for representative *amiMAX4-1+2* lines as well. While self-grafted control plants exhibited the typical SL-deficiency phenotypes (increased shoot branching as well as reduced plant height and internode length), the phenotypes were rescued when the transgenic scions were grafted onto a wild type rootstock (Fig. 3.17, p. 80). This indicates that a mobile, graft-transmittable signal can complement the phenotype, providing further evidence for SL-deficiency in the poplar knockdown lines generated in this project.

From studies in other species, it is known that also a wild type scion grafted onto a mutant rootstock exhibits a WT-like phenotype. This indicates that the root as site of SL production is not required for normal shoot architecture, and local biosynthesis in the shoot is sufficient (see references above). As shown in Fig. 3.17 (p.80), also *P.* x *canescens*

wild type scions, grafted onto an *amiMAX4-1+2* rootstocks, had a WT-like phenotype. This indicates that also in poplar, local SL biosynthesis in the shoot is sufficient for normal plant architecture. This is supported by expression analysis in wild type *P.* x *canescens* plants grown under greenhouse conditions, revealing that *MAX4* expression was extremely low and hardly detectable in roots (chapter 4.2, p. 106ff). However, this appears to be contradicting regarding the successful complementation of the *amiMAX4-1+2* shoot architectural phenotypes by a wild type rootstock. In this experiment, the complementing substance (SL) must be rootstock-derived. This apparent ambiguity may be explained by the fact that the rootstock, for technical reasons, also contained the basal part of the stem (approx. 5 cm, see photograph Fig. 2.2, p. 55). SL production in this tissue is likely to be sufficient, since small interstock stem pieces, inserted into the shoot of pea and petunia SL biosynthesis mutant plants by grafting, were shown to mediate full complementation of architectural phenotypes (Foo et al., 2001; Napoli, 1996). This was also tested in this work. Although the replicate number was too low for statistical analysis, the experiments indicate that *amiMAX4-1+2* plants bearing an approx. 1 cm short wild type interstock fragment exhibited the same shoot architecture as self-grafted wild type control plants (Appendix Fig. 7.19, p. 164). Thus, the basal stem fragment of the rootstock can be regarded as sufficient for full complementation of the architectural phenotype of the scion, even though the poplar *MAX4* genes are not significantly expressed in the roots.

4.4.3 GR24 treatment of wild type and *amiMAX4-1+2* plants

In addition to providing endogenous SLs from wild type tissues by grafting, another possibility to complement the phenotype of SL-deficient plants is exogenous application of SLs, such as the synthetic SL analog GR24. Since the use of GR24 was not reported for poplar yet, the effect of this substance on *in vitro* grown *P.* x *canescens* wild type and *amiMAX4-1+2* stem cuttings was tested in one- and two-node-assays. In an attempt to complement the enhanced bud outgrowth phenotype of *amiMAX4-1+2* lines, GR24 was applied directly to axillary buds of intact plants grown in a climate chamber.

4.4.3.1 GR24 treatment of wild type and amiMAX4-1+2 stem cuttings

To test whether the synthetic SL analog GR24 is functional in poplar and effective in inhibiting bud outgrowth, its effect on *in vitro* grown stem cuttings was monitored. For this purpose, the hormone was applied basally via the growth medium, from which it can be taken up. Such uptake of bud outgrowth modifying substances (e.g. cytokinin) into stem cuttings has already been proven in *Arabidopsis* (Chatfield et al., 2000) and GR24 treatment assays were successfully used in *Arabidopsis*, chrysanthemum and willow (Crawford et al., 2010; Liang et al., 2010; Ward et al., 2013). In accordance with the data reported in these studies, also treatment of poplar wild type stem cuttings bearing one bud (one-node-assay) with 5 µM GR24 did not inhibit bud outgrowth (Fig. 3.18, p. 83; and Appendix Fig. 7.20, p. 165). This finding appears odd since GR24 is an inhibitor of bud outgrowth, but may be explained by the auxin transport canalization model. According to the model, SLs act by inhibiting auxin transport, reducing the sink capacity of the stem. This in turn impedes the establishment of an initial auxin export from the buds as a prerequisite for outgrowth. To be effective, the proposed mechanism requires a competing auxin source in addition to the bud itself, which is not present in one-node stem segments. Thus, there is no competition, which could be enhanced by GR24 modulating auxin transport. Accordingly, providing auxin apically is expected to enable GR24 to inhibit bud outgrowth in a one-node-assay. Indeed, this was shown in *Arabidopsis*, chrysanthemum and willow (Crawford et al., 2010; Liang et al., 2010; Ward et al., 2013).

Although the discussed explanation of the absence of an inhibitory effect of basally supplied GR24 in one-node-assays using the auxin canalization model is appealing, it should be noted that it is questioned in a recent publication (Brewer et al., 2015). In pea, very similar findings were made with an experimental setup similar to the one used in the publications mentioned above (“split plate assay”, first described in Chatfield et al., 2000): basal GR24 was only effective in inhibiting bud outgrowth in a one-node-assay if auxin was supplied apically. However, an effect of basal GR24 alone without apical auxin was observed in a slightly different experimental setup (“open tube assay”) (Brewer et al., 2015). Both assays are principally very similar and the authors do not provide an explanation for this contradictive finding. Therefore, it remains to be elucidated which conditions caused the contrasting results and whether different mechanisms are active.

In addition to apical auxin supply in one-node-assays, also a second bud was expected to be sufficient as a competing auxin source, suppressing outgrowth of the other bud.

Modulation of auxin fluxes by basally supplied GR24 could then directly take effect without any further auxin treatment. Indeed, this was confirmed in two-node-assays in *Arabidopsis*, chrysanthemum and willow (Crawford et al., 2010; Liang et al., 2010; Ward et al., 2013). To test the effect of GR24 on bud outgrowth in poplar stem segments bearing two nodes, corresponding cuttings were made from *in vitro* grown plants treated in the same way as done in the one-node-assay. As expected, GR24 significantly inhibited bud outgrowth in the two-node-assay (Fig. 3.19, p. 84). This proves that GR24 is functional and can be perceived as a SL in poplar. Furthermore, the experiment shows that also in this species, in an experimental setup which differs slightly from the standard "split plate assay", an additional auxin source than a given individual bud itself is required for the inhibitory effect of GR24 on bud outgrowth. A second bud is sufficient for this purpose. Interestingly, the competing auxin source apparently needs to be apical relative to the inhibited bud in poplar. This is suggested by the finding that only the lower bud was inhibited by GR24, while outgrowth of the upper bud was not significantly changed (Fig. 3.19, p. 84). This observation was also made in chrysanthemum and willow (Liang et al., 2010; Ward et al., 2013). Since poplar and willow are closely related members of the *Salicaceae* family, a similar mode of action in poplar can be expected. Notably, there appear to be differences between more distantly related species. In *Arabidopsis*, also the upper bud was reported to be affected, indicating that also a basal auxin source can inhibit outgrowth of a more apical bud (Crawford et al., 2010; Prusinkiewicz et al., 2009).

In the two-node-assay carried out in this work, representative *amiMAX4-1+2* lines were included in addition to the *P.* x *canescens* wild type. The knockdown lines exhibit enhanced bud outgrowth compared to the wild type in intact plants (see chapter 3.5.2.1, p. 66ff), which may also be seen in stem cuttings. If this was the case, GR24 was expected to complement this phenotype, i.e. provide direct proof for SL-deficiency in the *amiMAX4-1+2* lines. However, no significant differences were observed in the bud outgrowth rates of wild type and *amiMAX4-1+2* cuttings within a given treatment (mock or GR24). This may be explained by the fact that stem cuttings lack an active apex (i.e. they are decapitated), which appears to immediately release both buds from dormancy. Therefore, the enhanced bud outgrowth phenotype of the *amiMAX4-1+2* lines cannot be seen in this experimental setup. Since *amiMAX4-1+*2 lines are impaired in SL biosynthesis, but not SL signaling, they exhibit a WT-like reaction to GR24 treatment.

Summarized, GR24 was shown to be a functional SL in poplar, suppressing branching as reported for other species. However, with the assay used here, complementation of the branching phenotype of the *amiMAX4-1+2* lines could not be shown. For this purpose, a

different assay is required, in which a difference between the wild type and the knockdown lines can be seen in the mock control.

4.4.3.2 GR24 treatment of buds in wild type and amiMAX4-1+2 plants

In the previous experiment, GR24 was shown to be a functional SL in poplar. To test whether the increased branching phenotype of the *amiMAX4-1+*2 lines generated in this work can be complemented by GR24, buds of intact plants were treated. These plants possess an active apex as a major auxin source. Therefore, GR24 is expected to be active in suppressing bud outgrowth, similar to two-node assays or one-node assays with apically supplied auxin. In pea and *Arabidopsis*, direct external application of GR24 onto axillary buds of SL-deficient plants has already been shown to complement their increased branching phenotype (Gomez-Roldan et al., 2008). A similar rescue of the phenotype in the poplar *amiMAX4-1+2* lines would directly confirm SL deficiency as the reason for increased bud outgrowth.

For this experiment, the plants were grown in a climate chamber to a size of up to 50 cm. *P.* x *canescens* wild type plants did not produce branches under these conditions. Therefore, an inhibitory effect of GR24 treatment could not be observed. In contrast, the *amiMAX4-1+2* plants exhibited a high degree of bud outgrowth in the mock-treated control (Fig. 3.20, p. 86), which is the typical phenotype observed in these lines without treatment. However, GR24 application unexpectedly did not reduce the bud outgrowth rate, i.e. the increased branching phenotype was not complemented. The reason for this failure is unclear, but may be technical. For example, the amount of GR24 supplied to the buds may not be sufficient. However, this is unlikely, since 6 µl of a 5 µM GR24 solution were applied three times in total over the course of 10-11 days in this experiment. In contrast, a single application of only 10 µl 100 nM GR24 was effective in suppressing bud outgrowth in the pea *rms1* (*MAX4* ortholog) mutant (Gomez-Roldan et al., 2008). Thus, the absolute amount of applied GR24 was 90-fold (30-fold amount applied three times) higher in this work and should have been sufficient in suppressing or at least delaying bud outgrowth. Another possibility would be that the solution did not penetrate poplar buds sufficiently. In this work, the treatment solution was composed in the same way as a solution which was successfully used in pea (Gomez-Roldan et al. (2008) and C. Beveridge, personal communication). However, the permeability of poplar buds may be different. Thus, the solution should be optimized for poplar bud treatments. As an alternative to

local application of the solution onto axillary buds, GR24 may also be directly fed to the vascular system of the main stem, using a method which was successfully applied in pea (Dun et al., 2012; Gomez-Roldan et al., 2008).

It should be noted that, unexpectedly, GR24 treatment appeared to enhance bud outgrowth slightly compared to mock treatment. Although this effect was not significant, it was highly consistent at different time points and in the two different lines used for this experiment (Fig. 3.20, p. 86). If this effect is genuine, it would argue against insufficient penetration of the buds by the GR24 solution. Interestingly, SLs are discussed to be able to enhance bud outgrowth, depending on the SL concentration and the auxin transport status in the plant. For instance, GR24 was shown to promote bud outgrowth in *Arabidopsis tir3* mutants (reduced auxin transport) when supplied at certain concentrations. However, this effect was not reported in *Arabidopsis* wild type and *max* mutant plants (Shinohara et al., 2013). Thus, the apparent promoting effect of GR24 in *amiMAX4-1+2* poplar lines upon direct treatment of buds observed here, cannot be explained by these findings. Increased bud outgrowth upon application of GR24 to buds of intact SL-deficient plants would also contradict the observations made in *Arabidopsis* and pea (Gomez-Roldan et al., 2008). It would imply differential regulation in poplar, which is unlikely. Hence, the non-significant trend observed here may be simply a technical artifact.

4.4.4 Spring bud break in *amiMAX4-1+2* lines

Strigolactones are well-known for their role in suppressing bud outgrowth, i.e. consolidating dormancy. There are different states of dormancy, as described in chapter 1.3.4 (p. 22ff). So far, only the role of SLs in enhancing the paradormant state of buds during the growing season was studied, since routinely used branching model plants belong to annual species. These plants do not survive winter, and therefore lack winter dormancy (endodormancy). It was conceivable that SLs also stabilize endodormancy or ecodormancy, and bud break in spring appeared to be a suitable occasion to study this possible role. For this analysis, SL-deficient plants are required. So far, *MAX4* knockdown kiwifruit lines were the only reported putatively SL-deficient temperate perennial plants, but bud break in spring was not studied (Ledger et al., 2010). Thus, spring bud break was investigated in the poplar *amiMAX4-1+2* lines generated in this project. Representative lines and the *P.* x *canescens* wild type were grown under outdoor conditions and the bud elongation during bud break after the first winter was measured (Fig. 3.21, p. 87). It was expected that SL-deficient plants would exhibit earlier bud break, leading to more elongated buds.

Indeed, buds of the *amiMAX4-1+2* line T14 #4A were significantly more elongated at a defined time point compared to the wild type, supporting the hypothesis. However, this phenotype was not reproducible. In the second representative *amiMAX4-1+2* line T22 #5A, no difference was observed. Hence, even though the experiment provides a hint for a role of SLs in consolidating ecodormancy, a conclusion cannot be drawn. A repetition of the experiment, including more lines, would be required.

4.4.5 Analysis of possible JA-crosstalk in *amiMAX4-1+2* lines

Pathogens have a tremendous impact on plants, and the JA-pathway counteracts a wide range of herbivorous and necrotrophic pests and pathogens (Campos et al., 2014; Pieterse et al., 2012). Recently, crosstalk between strigolactones (SLs) and the jasmonic acid (JA) pathway was reported, based on infection studies using SL-deficient tomato lines. The plants exhibited reduced JA-levels as well as reduced JA-marker gene expression and were more susceptible to the tested necrotrophic fungal pathogens *Alternaria alternata* and *Botrytis cinerea* (Torres-Vera et al., 2014). An interference of SLs with the JA pathway appears to be another critical role for SLs as phytohormones regulating various aspects in plant development.

Since other functions of SLs, most notably their role in controlling branching, are highly conserved among plant species, SL-JA crosstalk was expected to be present in poplar as well. A strongly JA-responsive marker gene was identified in poplar and its expression was monitored in representative *amiMAX4-1+2* lines compared to the *P.* x *canescens* wild type. As discussed in the previous chapters, there is well-founded evidence for SL-deficiency in these lines. Based on the published data (Torres-Vera et al., 2014), a reduction of JA-levels in the SL-deficient plants was expected, which should be observable by marker gene expression analysis. However, such regulation was not found (Fig. 3.22, p. 89). Thus, the reported crosstalk could not be confirmed in poplar.

This is in line with observations of *amiMAX4-1+2* lines grown under outdoor conditions. Under these conditions, the plants were highly challenged by numerous pathogens, such as *Chrysomela sp.* leaf beetles. An impaired JA-response due to SL deficiency would be expected to result in increased infestation of *amiMAX4-1+2* plants with such pathogens compared to the wild type. However, although it was not quantified, there were no indications of higher susceptibility.

Thus, the artificial conditions (infection and monitoring of disease symptoms at detached leaves) used by Torres-Vera et al. (2014) may have led to artificial results, or the mode of regulation is not conserved in poplar.

4.5 Target gene expression analysis and phenotyping: *amiMAX2* lines

As discussed for *MAX4,* also the SL-signaling gene *MAX2* was a target gene in this work. The corresponding loss of function mutants in many herbaceous species, including *Arabidopsis*, pea, petunia and rice, are characterized by increased branching (Drummond et al., 2011; Ishikawa et al., 2005; Johnson et al., 2006; Stirnberg et al., 2002). There are two *MAX2* orthologs in poplar, designated *MAX2-1* and *MAX2-2* in this work and also identified by Czarnecki et al. (2014) as *MAX2b* and *MAX2a*, respectively. Individual knockdowns (*amiMAX2-1* and *amiMAX2-2* lines), as well as simultaneous knockdowns of both orthologs (*amiMAX2-1+2* lines), were intended. Since increased branching was expected in the knockdown lines, architectural phenotyping was done.

4.5.1 Target gene expression analysis in *amiMAX2* lines

To investigate knockdown efficiency, expression of both *MAX2* orthologs was monitored in the generated transgenic *amiMAX2* lines. Upon knockdown of an individual ortholog, a reduction of its transcript level was expected, while expression of the second ortholog should not be changed. However, this was not the case. In contrast, *MAX2-1* expression appeared to be increased in *amiMAX2-1* lines relative to the *P.* x *canescens* wild type. Interestingly, also *MAX2-2* expression was increased (Fig. 3.23, p. 91). The reason for this up-regulation is unclear. The amiRNA construct may not be functional and the *MAX2-1* target mRNA may not be degraded. However, this should not lead to increased expression, especially for the non-targeted gene *MAX2-2*. The only conceivable theory would be that *MAX2-1* expression normally is under negative control of unknown factors. An initial reduction of transcript levels by the amiRNA may lead to release from this negative control. This release may over-compensate a low level of amiRNA-mediated degradation, leading to increased net transcript levels. *MAX2-1* and *MAX2-2* may be redundant and under the same negative control, which would explain increased *MAX2-2* transcript levels, although this gene was not targeted. At least redundancy is very likely, since both poplar *MAX2* orthologs were already successfully used to complement the *Arabidopsis max2* mutant phenotype partially (Czarnecki et al., 2014).

When *MAX2-2* levels were assayed in *amiMAX2-2* lines, a reduction was observed relative to the wild type (Fig. 3.24, p. 92). Thus, silencing was successful in the case *MAX2-2*.

Notably, *MAX2-1* expression was increased in these lines, which may be explained by redundancy and a compensatory up-regulation of *MAX2-1* upon silencing of *MAX2-2*.
In *amiMAX2-1+2* lines, similar expression patterns were found as in *amiMAX2-2* lines. Although both orthologs were targeted, only the *MAX2-2* knockdown was successful and the transcript levels were reduced. In contrast, *MAX2-1* expression was increased (Fig. 3.25, p. 91). The amiRNA construct apparently did successfully target *MAX2-2*, but not *MAX2-1*. As discussed above, both genes may be redundant and *MAX2-1* may be up-regulated to compensate for reduced *MAX2-2* levels.

4.5.2 Architectural phenotyping of *amiMAX2* lines

As described above, *MAX2* knockdowns were only partially successful. Nevertheless, several lines of the three genotypes (single and double knockdowns) were grown under greenhouse-conditions for architectural phenotyping. Although there appears to be redundancy among the orthologs, there still may be a certain degree of specialization and diversification, which was expected to possibly result in visible phenotypes. However, no phenotypes were observed: the recorded architectural parameters did not significantly differ between *amiMAX2* and *P.* x *canescens* wild type plants (Fig. 3.26, p. 94). Only the *amiMAX2-1+2* line T15 #28A exhibited significantly reduced growth in all measured traits. However, all other lines of the same genotype did not exhibit this defect, and the branching level of this line was WT-like. Since increased branching was expected as a typical phenotype of plants impaired in SL-signaling, the reduced growth phenotype appears to be coincidental and may be the result of a random gene knockout at the insertion locus of the T-DNA.
Taken together, an interruption of SL signaling by knockdowns of the poplar *MAX2* orthologs was not successful, making further analysis of SL signaling in the generated lines impossible. Other amiRNA constructs should be designed for successful simultaneous targeting of *MAX2-1* and *MAX2-2*, which most likely would result in SL-insensitive poplar lines.

4.6 Identification and characterization of poplar *BRANCHED1* orthologs

For an investigation of the role of *BRC1* in poplar as a woody perennial species, three genes were identified as likely poplar *BRC1* orthologs. However, a clear assignment was not possible (Fig. 3.27, p. 97). Only two genes (Potri.015G050500 and Potri.012G059900) unambiguously clustered together and likely result from the whole genome duplication in poplar (Tuskan et al., 2006), i.e. they are paralogs. A third gene, Potri.017G112000, was similar to *BRC1*, but it was distinct to Potri.015G050500 and Potri.012G059900 and there appears to be no paralog of this gene.

In addition to *BRC1*, another closely related TCP gene, *BRC2*, was described to play a minor role in branching regulation in *Arabidopsis* (Aguilar-Martínez et al., 2007). Due to this function, it was conceivable that a poplar ortholog of *BRC2* may also play a role in branching regulation, and it could have evolved even a major role. Thus, *BRC2* was considered as well, and two poplar orthologs (most likely being paralogs), Potri.008G115800 and Potri.010G130200, were clearly identified (Fig. 3.27, p. 97).

In total, five poplar *BRC1*/*BRC2* candidate genes were found (Tab. 3.3, p. 98). The identification of a gene showing characteristics of a functional *BRC1* ortholog is discussed in the following paragraphs.

4.6.1 Expression of poplar *BRC1* candidate genes in wild type plants

Expression analysis of the five identified poplar *BRC1*-like candidate genes was performed with the aim to identify a functional poplar *BRC1* ortholog. For a functional ortholog, high expression was expected in dormant axillary buds. In contrast, transcript levels were expected to be reduced in outgrowing buds, as it was reported for *Arabidopsis BRC1* (Finlayson, 2007). Indeed, two candidate genes fulfilled these criteria in poplar bud samples: Potri.012G059900 and Potri.010G130200 (Fig. 3.28, p. 99). According to the sequence analysis, Potri.012G059900 is a putative *BRC1* ortholog, while Potri.010G130200 is closely related to *Arabidopsis BRC2*. As noted above, both genes have one highly similar paralog each (Potri.015G050500 and Potri.008G115800, respectively) (Fig. 3.27, p. 97). However, the paralogs were not significantly regulated in outgrowing buds (Fig. 3.28, p. 99). This indicates that only one of the two closely related copies appears to have retained the typical expression pattern. After the presumed gene duplication, the other copy may have lost its original function and may either be non-

functional or have attained a different, unknown role. Potri.017G112000, which appeared to be a third *BRC1* ortholog, also exhibited no regulation (Fig. 3.28, p. 99).

In addition to dormant and outgrowing buds, expression of the candidate genes was monitored in different tissues of *P.* x *canescens* wild type plants. Potri.017G112000 was omitted from this analysis, since it could not be clearly assigned based on sequence analysis and it was not regulated in growing compared to dormant axillary buds. Expression of a functional poplar *BRC1* ortholog was expected to be largely specific to axillary buds, based on expression data published for *Arabidopsis* and other herbaceous species (Aguilar-Martínez et al., 2007; Braun et al., 2012; Finlayson, 2007; Hubbard et al., 2002; Takeda et al., 2003). Indeed, the putative *BRC1* ortholog Potri.012G059900 was highly expressed in dormant axillary buds in this experiment as well. Although moderate expression was observed in other tissues than buds, this corresponds to the typical expression pattern in *Arabidopsis*, in which Northern Blot and qPCR data revealed low *BRC1* levels in various tissues (Aguilar-Martínez et al., 2007; Finlayson, 2007). In contrast, the Potri.012G059900 paralog Potri.015G050500 can be ruled out as functional poplar *BRC1*. In addition to the absence of down-regulation in growing compared to dormant axillary buds, expression of this gene was not tissue-specific. It was found to be highly expressed in leaves, roots and bark (Fig. 3.29, p. 101).

In addition to Potri.012G059900, the close *BRC2* ortholog Potri.010G130200 also exhibited the expected expression. Transcript levels were specifically found in axillary buds, but not in other tissues. In contrast, its paralog Potri.008G115800 was expressed in leaves, too (Fig. 3.29, p. 101). This indicates that also for these two paralogs, only one appears to fulfil the anticipated function in bud outgrowth regulation.

Taking the expression data in different tissues and dormant/growing buds together, Potri.012G059900 appeared to be a promising candidate for a functional poplar *BRC1* ortholog, while Potri.010G130200 appears to be a functional *BRC2* ortholog. Both may regulate bud outgrowth in poplar. In the following discussion, Potri.012G059900 will be called *PcBRC1* (*P.* x *canescens BRANCHED1*), while Potri.010G130200 is designated *PcBRC2*.

4.6.2 Expression of poplar *BRC1* candidate genes in *amiMAX4-1+2* lines

A significant feature of *Arabidopsis BRC1* and its pea and petunia orthologs is its positive regulation by SLs. Correspondingly, *BRC1* transcript levels were found to be reduced in SL pathway mutants (Aguilar-Martínez et al., 2007; Braun et al., 2012; Drummond et al., 2015) and expression was increased after GR24 treatment (Braun et al., 2012). Therefore, reduced expression was expected for poplar *BRC1* in axillary buds of the putatively SL-deficient *amiMAX4-1+2* lines generated in this project. Indeed, transcript levels of *PcBRC1* were significantly lower in the tested representative lines relative to the wild type (Fig. 3.16, p. 78). This corroborates that *PcBRC1* is a functional poplar ortholog. Furthermore, the obtained data provide additional proof for SL-deficiency in the *amiMAX4-1+2* lines, as discussed in chapter 4.4.1.2 (p. 113ff). Poplar *BRC1* appears to be regulated by SLs, which highlights the high degree of conservation of the SL pathway and its downstream targets in trees.

In contrast to *BRC1*, *Arabidopsis BRC2* transcript levels were reported to be unchanged in *max* SL pathway mutants, arguing against a regulation of this gene by SLs (Aguilar-Martínez et al., 2007). This observation was also made in this work for poplar *BRC2*, which was not found to be differentially expressed in wild type and *amiMAX4-1+*2 plants (Fig. 3.16, p. 78). However, the exact function of *PcBRC2* is not clear. Although it appears to be non-responsive to the SL level, its highly bud-specific expression and down-regulation in outgrowing buds suggest an involvement in bud outgrowth regulation as well. Potentially, it integrates signals from different pathways. This idea is supported by observations made in other species. In *Arabidopsis*, *BRC1* and *BRC2* both are regulated in dependence of the planting density (Aguilar-Martínez et al., 2007) and play a role in the branching response upon changes in the light R:FR ratio (Finlayson et al., 2010). A diversification was also found in petunia, which possesses three *BRC1*-like genes (*PhTCP1* – *PhTCP3*). *PhTCP1* and *PhTCP2* are closely related to *AtBRC2*. While *PhTCP3* and to a lower extent *PhTCP1* appear to be regulated by SLs, *PhTCP2* is not regulated in the SL-signaling mutant *dad2*. Nevertheless, expression of all three genes, including *PhTCP2*, is R:FR responsive (Drummond et al., 2015).

Summarized, there appears to be a possible diversification of *BRC1*-like gene function at least in some species. Regulation by SLs appears to be rather specific to *BRC1*, while other pathways, most notably R:FR signaling, seem to regulate *BRC2* as well. Thus, also poplar *BRC2* may be important for suppression of bud outgrowth, but it possibly is regulated by other factors than SLs. In addition to the light conditions, another factor may be cytokinin,

which is known to negatively regulate *BRC1* in *Arabidopsis* buds (Braun et al., 2012; Dun et al., 2012) and may also regulate *BRC2* in poplar. In terms of bud outgrowth suppression, the combined expression of *PcBRC1* and *PcBRC2* may be required to keep the bud in a dormant state. Different factors would simultaneously act on the pool of *PcBRC1* and *PcBRC2* transcripts. There may be a certain threshold, which needs to be exceeded for stable maintenance of dormancy. Once the combined *PcBRC1* and *PcBRC2* transcript level drops below the threshold, bud outgrowth may be triggered. This simple model (illustrated in Fig. 4.1) would explain how different factors, which differentially act on the *BRC* genes, may be integrated in the decision whether a bud stays dormant or grows into a branch. This model also implies that either a very strong individual stimulus, or a combination of weak inputs, could trigger bud outgrowth.

To test whether poplar *BRC1* and *BRC2* respond to branching-regulating factors other than SLs, expression of both genes should be monitored at different growth conditions, e.g. a modification of planting density or altered light quality. Furthermore, single and double knockdown lines could be generated for detailed analysis of the influence of *PcBRC1* and *PcBRC2* on tree architecture.

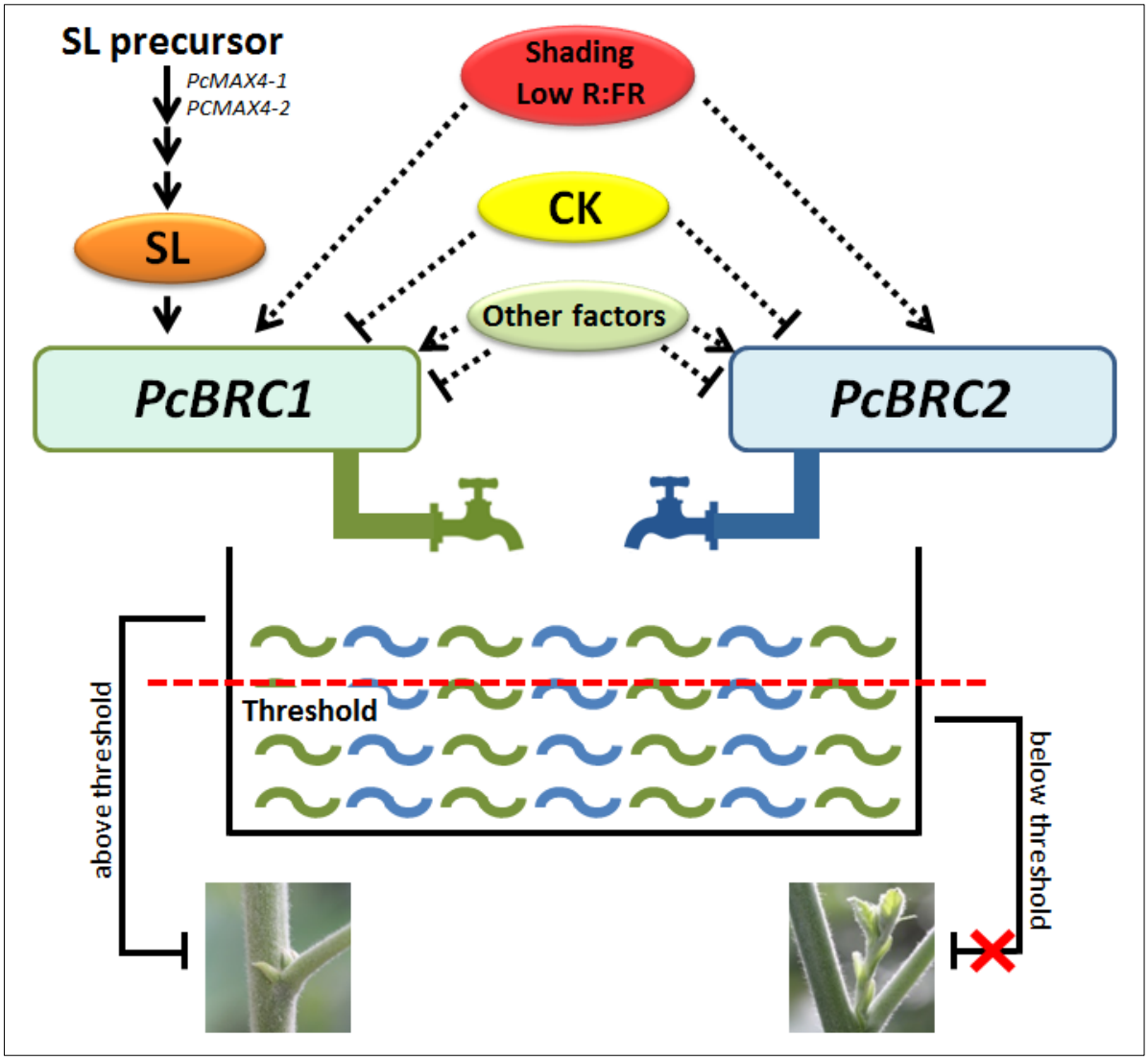

Fig. 4.1 Tentative model for the action of poplar *BRC1* and *BRC2* in bud outgrowth regulation. Multiple factors may influence the combined pool of *PcBRC1* (green) and *PcBRC2* (blue) transcripts. Strigolactones (SL), synthesized via the action of *PcMAX4-1*/*PcMAX4-2* and other enzymes, positively regulate *PcBRC1*, but not *PcBRC2*. Hypothetical other modes of regulation, indicated by dashed lines, may modify transcription of one or both genes, too. Based on findings in other species, shading and a low R:FR ratio are expected to positively regulate BRC gene expression, while cytokinin (CK) most likely has a negative effect. Additional factors may also play a role. There may be a certain threshold for the *PcBRC1*/*PcBRC2* transcript pool, which has to be exceeded for consolidation of bud dormancy. If the transcript level drops below this hypothetical threshold, inhibition of bud outgrowth would be abolished and a branch could be formed.

4.6.3 Expression of poplar *BRC1* and *BRC2* during winter dormancy

As discussed above, poplar *BRC1* and *BRC2* orthologs were identified in this project. Since the role of these genes has not been addressed in woody perennial species yet, a possible involvement of poplar *BRC1*-like genes in tree-specific aspects of bud dormancy (discussed in chapter 1.3.4, p. 22ff) was investigated.

To test a possible role during endodormancy (winter dormancy), buds were sampled in winter and during bud break (swollen and growing buds) in spring and expression of *PcBRC1* and *PcBRC2* was investigated. However, the obtained data does not support a role for these genes during endodormancy. Their transcript levels were extremely low in dormant buds sampled in winter, while expression was increased in swollen and growing buds in spring (Fig. 3.31, p. 104). If they played a role as a suppressor of bud outgrowth during winter, the opposite pattern would be expected: high expression during winter and low expression in growing buds in spring. As a control, expression in paradormant axillary buds was monitored during the growing season and found to be highly increased compared to the other time points (Fig. 3.31, p. 104), which corresponds to the role of *BRC1*-like genes in maintaining dormancy during the vegetative period. Thus, the function of both genes appears to be limited to controlling paradormancy, as discussed above. During endodormancy, other unknown mechanisms may suppress bud outgrowth, making high *BRC1* levels dispensable. For instance, it is discussed that a simple isolation of the meristem from growth-inducing substances (e.g. gibberellins) may be sufficient to maintain dormancy (Rohde and Bhalerao, 2007).

Since dormant apical buds are a specific feature of temperate perennial plants, they were sampled at the same time points in addition to axillary buds. Expression of *PcBRC1* and *PcBRC2* was monitored to investigate a possible differential regulation between both bud types. However, no obvious differences were found at any given sampling time point (Fig. 3.31, p. 104). Hence, there appears to be no differential regulation with respect to *BRC1*/*BRC2*.

4.7 Economic significance of the SL pathway in poplar

In this work, the significance of the SL pathway and its downstream target *BRC1* in the regulation of bud outgrowth in trees was addressed. The pathway appears to be conserved in woody perennial species, and putatively SL-deficient poplar lines with increased branching phenotypes were obtained. These lines are a valuable resource for studying various aspects of SLs in trees, since no mutants are available. In addition, poplar with modified tree architecture may be advantageous for commercial use on short rotation coppices.

Increased branching, such as it is observed in the *amiMAX4-1+2* lines, leads to higher bark content. This may be beneficial for using the plant material as a feedstock for industrial and pharmaceutical chemicals (Salmon et al., 2014). Also the total biomass yield, which is a critical agronomical trait, could be positively influenced. High bud outgrowth rates may result in enhanced re-sprouting from the rootstock after coppicing, as well as better light interception as a result of early canopy closure (Broeckx et al., 2012; Ceulemans et al., 1990; Scarascia-Mugnozza et al., 1989). Increased biomass production relative to the wild type could not be detected in the *amiMAX4-1+2* lines generated in this project (Fig. 3.13, p. 71). However, only young, greenhouse-grown plants were used for the measurements. At this developmental stage, the branches were just being formed and did not have sufficient time to develop to make a major contribution to biomass production. In contrast, trees on plantations are grown for several years and the branches may have a significant impact, especially those formed in the first growing season. Thus, biomass production should be tested in a field trial, also considering different planting densities. In addition to increased branching, the *amiMAX4-1+2* lines exhibited other phenotypes such as increased adventitious rooting. Short rotation coppices are established using stem cuttings, and proper adventitious rooting is critical for this form of vegetative propagation. Therefore, this appears to be a beneficial phenotype.

In contrast, there are also undesired traits in SL-deficient plants. If the biomass is processed as a fuel for energy production, which currently is the predominant application of poplar grown on short rotation coppices, the elevated bark content in highly branching lines is disadvantageous due to increased pollutant emissions (Salmon et al., 2014). For this application, a reduction of branching should be pursued using different approaches. Also the reduced plant height and reduced internode elongation in SL-deficient plants are rather undesired traits. However, it may be possible to eliminate such traits, since there are many different SLs and they may function in different processes. Using synthetic SLs,

such specificity was already shown. For example, the SL analog compound “23” was reported to have an extremely low inducing effect on germination of seeds of the parasitic weed *Orobanche ramosa* compared to GR24 (10.000 times lower). In contrast, it was shown to have an even stronger inhibitory effect on pea bud outgrowth than GR24. Combined, this implies that compound “23” has a highly specific mode of action in controlling bud outgrowth compared to GR24, showing that different SLs can specifically control different processes. Furthermore, there are hints that structurally different SLs also have differential activity on hyphal branching of arbuscular mycorrhiza fungi. Thus, hyphal branching, parasitic weed germination, as well as bud outgrowth suppression, are discussed to possibly rely on different perception systems (Boyer et al., 2012). It is conceivable that there are also specialized SLs for the control of endogenous processes in the plant other than shoot branching, such as internode elongation or root branching. Once the complex biosynthesis steps leading to the large variety of SLs are elucidated, specific steps may be modified in order to produce the desired phenotypes, while avoiding less favorable traits. Therefore, modifications in the SL pathway appear to be a promising target for improving the tree architecture for commercial purposes.

5 Outlook

In this work, the roles of the phytohormone striolactone and the transcription factor BRC1 during bud outgrowth regulation were addressed in the model tree *Populus*. Based on the material and results generated in this work, further research may be carried out to discover additional aspects of branching regulation in trees. Promising perspectives are outlined in the following sections.

5.1 Confirmation of SL deficiency in *amiMAX4-1+2* lines

Direct quantification of SLs to confirm deficiency in the poplar *amiMAX4-1+2* lines was not feasible, as discussed above. As an alternative, bioassays could be performed. They make use of arbuscular mycorrhiza fungi such as *Gigaspora gigantea* and root parasitic weeds like *Orobanche ramosa* as biosensors for SLs (Buee et al., 2000; Matusova et al., 2005). In addition to direct measurements and bioassays, another possibility to prove SL deficiency could be complementation of the observed phenotypes by delivery of GR24 via the vascular system, using a vascular feeding method which was successfully applied in pea by Gomez-Roldan et al. (2008) and Dun et al. (2012). Furthermore, a hydroponics system may be established, such as described by Boyer et al. (2012).

5.2 Further phenotyping of *amiMAX4-1+2* lines

In addition to an effect on adventitious rooting (Rasmussen et al., 2012) which was quantified and confirmed in representative poplar *amiMAX4-1+2* lines in this work, SLs were reported to influence other aspects of root architecture (Kapulnik et al., 2010; Ruyter-Spira et al., 2011). Thus, a detailed analysis of the root system may be done in poplar *amiMAX4-1+2* lines to study the significance of SLs in shaping the root architecture of trees.

Another phenotype found in SL-deficient *Arabidopsis* and pea mutants was reduced cambial activity, leading to reduced secondary growth. In contrast, secondary growth was increased by GR24 treatment in *Arabidopsis* and *Eucalyptus* (*E. globulus*). Based on this data, the regulation of cambium activity by SLs is discussed to be conserved among

species, including trees (Agusti et al., 2011). Therefore, cambial activity and wood anatomy may be investigated in the poplar *amiMAX4-1+2* lines, too.

5.3 Auxin transport in *amiMAX4-1+2* lines

SLs are well-known for their effect on auxin fluxes. They promote removal of PIN auxin efflux carriers from the plasma membrane, leading to an inhibition of auxin transport. While GR24 treatment dampened auxin transport in *Arabidopsis*, SL pathway mutants showed increased auxin flux rates (Bennett et al., 2006; Crawford et al., 2010). Thus, auxin transport may be studied in poplar *amiMAX4-1+2* lines to investigate whether this effect is conserved in trees.

5.4 Mycorrhiza status of *amiMAX4-1+2* lines

A further interesting trait to investigate in the putatively SL-deficient poplar lines generated in this work is their mycorrhiza status. Most land plants establish mycorrhiza as an important symbiotic relationship with fungi, improving the nutrient and water supply of the plant. There are different types of mycorrhiza, most notably endomycorrhiza (including arbuscular mycorrhiza, AM) and ectomycorrhiza (EM) (Kadereit et al., 2014). For the establishment of AM, SLs are known to be an important factor (Akiyama et al., 2005; Buee et al., 2000). However, a role for SLs in establishment of EM could not be shown yet. GR24 treatment did not have an effect on hyphal branching of four different EM fungi (Steinkellner et al., 2007). Nonetheless, there may be other important pathways regulated by SLs. In the AM fungus *Rhizophagus irregularis*, short-chain chitin oligomers are synthesized and discussed to be signals involved in the communication with the host plants. Interestingly, their synthesis is significantly increased upon GR24 treatment (Genre et al., 2013), and such an effect may also be found in EM fungi. Additionally, EM fungi may react to other SLs than AM fungi, i.e. sensing tree-specific SLs. Therefore, treatment with tree-specific SLs, yet to be identified, may induce a response in EM fungi species.

Another possibility to investigate an influence of SLs is to directly assess the mycorrhiza status of SL-deficient plants relative to the wild type. However, frequently studied SL-deficient model species are not colonized by EM fungi, hindering the investigation of a

conceivable involvement of SLs in EM interactions in the past. As suggested by Garcia et al. (2015), “generation of *ccd7* and *ccd8* knockout or knockdown tree lines should allow a direct investigation of this hypothesis”. With the poplar *amiMAX4-1+2* lines generated in this project, such *ccd8* knockdown trees now are available.

5.5 Further characterization of poplar *BRC1* and *BRC2*

In this work, poplar *BRC1* and *BRC2* orthologs were identified. The apparent regulation of *PcBRC1* by SLs (chapter 3.8.4, p. 102ff) suggests that this component of bud outgrowth regulation is conserved in trees. To confirm their function, both poplar *BRC* genes could be used in an experiment to complement the corresponding *Arabidopsis* mutant phenotype, similar to the experiments reported for the poplar *MAX* genes (Czarnecki et al., 2014). Furthermore, knockdowns could be performed in poplar. The availability of loss-of-function lines would facilitate comprehensive testing of the hypotheses for the mode of action of poplar *BRC1* and *BRC2*, summarized in the model shown in Fig. 4.1 (p. 127).

PcBRC2 expression was found in axillary buds while transcripts were hardly detectable in any other of the tested tissues (chapter 3.8.3, p. 100ff), suggesting that activity of the *PcBRC2* promoter is highly bud-specific. This may be further tested with a promoter-reporter fusion (such as *proPcBRC2:GUS*) and the promoter may be used as a tool for bud-specific gene expression (e.g. *IPT* and *CKX* genes to manipulate cytokinin levels) to further analyze mechanisms in bud outgrowth regulation. Furthermore, it may also be useful for biotechnological approaches to specifically modify bud outgrowth without causing pleiotropic effects.

6 References

Abe, S., Sado, A., Tanaka, K., Kisugi, T., Asami, K., Ota, S., Kim, H.I., Yoneyama, K., Xie, X., Ohnishi, T., et al. (2014). Carlactone is converted to carlactonoic acid by MAX1 in Arabidopsis and its methyl ester can directly interact with AtD14 in vitro. Proc. Natl. Acad. Sci. *111*, 18084–18089.

Aguilar-Martínez, J.A., Poza-Carrión, C., and Cubas, P. (2007). Arabidopsis BRANCHED1 acts as an integrator of branching signals within axillary buds. Plant Cell *19*, 458–472.

Agusti, J., Herold, S., Schwarz, M., Sanchez, P., Ljung, K., Dun, E.A., Brewer, P.B., Beveridge, C.A., Sieberer, T., Sehr, E.M., et al. (2011). Strigolactone signaling is required for auxin-dependent stimulation of secondary growth in plants. Proc. Natl. Acad. Sci. *108*, 20242–20247.

Akiyama, K., and Hayashi, H. (2006). Strigolactones: Chemical Signals for Fungal Symbionts and Parasitic Weeds in Plant Roots. Ann. Bot. *97*, 925–931.

Akiyama, K., Matsuzaki, K., and Hayashi, H. (2005). Plant sesquiterpenes induce hyphal branching in arbuscular mycorrhizal fungi. Nature *435*, 824–827.

Akiyama, K., Ogasawara, S., Ito, S., and Hayashi, H. (2010). Structural requirements of strigolactones for hyphal branching in AM fungi. Plant Cell Physiol. *51*, 1104–1117.

Alder, A., Jamil, M., Marzorati, M., Bruno, M., Vermathen, M., Bigler, P., Ghisla, S., Bouwmeester, H., Beyer, P., and Al-Babili, S. (2012). The Path from β-Carotene to Carlactone, a Strigolactone-Like Plant Hormone. Science *335*, 1348–1351.

Allona, I., Ramos, A., Ibáñez, C., Contreras, A., Casado, R., and Aragoncillo, C. (2008). Molecular control of winter dormancy establishment in trees: a review. Span. J. Agric. Res. *6*, 201–210.

Arite, T., Iwata, H., Ohshima, K., Maekawa, M., Nakajima, M., Kojima, M., Sakakibara, H., and Kyozuka, J. (2007). DWARF10, an RMS1/MAX4/DAD1 ortholog, controls lateral bud outgrowth in rice. Plant J. Cell Mol. Biol. *51*, 1019–1029.

Arite, T., Umehara, M., Ishikawa, S., Hanada, A., Maekawa, M., Yamaguchi, S., and Kyozuka, J. (2009). d14, a strigolactone-insensitive mutant of rice, shows an accelerated outgrowth of tillers. Plant Cell Physiol. *50*, 1416–1424.

Arora, R., Rowland, L.J., and Tanino, K. (2003). Induction and Release of Bud Dormancy in Woody Perennials: A Science Comes of Age. HortScience *38*, 911–921.

Babiker, A.G.T., Hamdoun, A.M., Rudwan, A., Mansi, N.G., and Faki, H.H. (1987). Influence of soil moisture on activity and persistence of the strigol analogue GR 24. Weed Res. *27*, 173–178.

Balla, J., Kalousek, P., Reinöhl, V., Friml, J., and Procházka, S. (2011). Competitive canalization of PIN-dependent auxin flow from axillary buds controls pea bud outgrowth. Plant J. *65*, 571–577.

Bangerth, F. (1994). Response of cytokinin concentration in the xylem exudate of bean (Phaseolus vulgaris L.) plants to decapitation and auxin treatment, and relationship to apical dominance. Planta *194*, 439–442.

Bayer, E.M., Smith, R.S., Mandel, T., Nakayama, N., Sauer, M., Prusinkiewicz, P., and Kuhlemeier, C. (2009). Integration of transport-based models for phyllotaxis and midvein formation. Genes Dev. *23*, 373–384.

Bell, E.M., Lin, W., Husbands, A.Y., Yu, L., Jaganatha, V., Jablonska, B., Mangeon, A., Neff, M.M., Girke, T., and Springer, P.S. (2012). Arabidopsis lateral organ boundaries negatively regulates brassinosteroid accumulation to limit growth in organ boundaries. Proc. Natl. Acad. Sci. U. S. A. *109*, 21146–21151.

Bennett, T., and Leyser, O. (2006). Something on the Side: Axillary Meristems and Plant Development. Plant Mol. Biol. *60*, 843–854.

Bennett, T., Sieberer, T., Willett, B., Booker, J., Luschnig, C., and Leyser, O. (2006). The Arabidopsis MAX Pathway Controls Shoot Branching by Regulating Auxin Transport. Curr. Biol. *16*, 553–563.

Besserer, A., Puech-Pagès, V., Kiefer, P., Gomez-Roldan, V., Jauneau, A., Roy, S., Portais, J.-C., Roux, C., Bécard, G., and Séjalon-Delmas, N. (2006). Strigolactones Stimulate Arbuscular Mycorrhizal Fungi by Activating Mitochondria. PLoS Biol *4*, e226.

Beveridge, C.A. (2006). Axillary bud outgrowth: sending a message. Curr. Opin. Plant Biol. *9*, 35–40.

Beveridge, C.A., Ross, J.J., and Murfet, I.C. (1996). Branching in Pea (Action of Genes Rms3 and Rms4). Plant Physiol. *110*, 859–865.

Beveridge, C.A., Symons, G.M., Murfet, I.C., Ross, J.J., and Rameau, C. (1997). The rms1 Mutant of Pea Has Elevated Indole-3-Acetic Acid Levels and Reduced Root-Sap Zeatin Riboside Content but Increased Branching Controlled by Graft-Transmissible Signal(s). Plant Physiol. *115*, 1251–1258.

Booker, J., Chatfield, S., and Leyser, O. (2003). Auxin Acts in Xylem-Associated or Medullary Cells to Mediate Apical Dominance. Plant Cell *15*, 495–507.

Booker, J., Auldridge, M., Wills, S., McCarty, D., Klee, H., and Leyser, O. (2004). MAX3/CCD7 Is a Carotenoid Cleavage Dioxygenase Required for the Synthesis of a Novel Plant Signaling Molecule. Curr. Biol. *14*, 1232–1238.

Booker, J., Sieberer, T., Wright, W., Williamson, L., Willett, B., Stirnberg, P., Turnbull, C., Srinivasan, M., Goddard, P., and Leyser, O. (2005). MAX1 encodes a cytochrome P450 family member that acts downstream of MAX3/4 to produce a carotenoid-derived branch-inhibiting hormone. Dev. Cell *8*, 443–449.

Bouwmeester, H.J., Roux, C., Lopez-Raez, J.A., and Bécard, G. (2007). Rhizosphere communication of plants, parasitic plants and AM fungi. Trends Plant Sci. *12*, 224–230.

Boyer, F.-D., Germain, A. de S., Pillot, J.-P., Pouvreau, J.-B., Chen, V.X., Ramos, S., Stévenin, A., Simier, P., Delavault, P., Beau, J.-M., et al. (2012). Structure-Activity Relationship Studies of Strigolactone-Related Molecules for Branching Inhibition in Garden Pea: Molecule Design for Shoot Branching. Plant Physiol. *159*, 1524–1544.

Braun, N., Germain, A. de S., Pillot, J.-P., Boutet-Mercey, S., Dalmais, M., Antoniadi, I., Li, X., Maia-Grondard, A., Signor, C.L., Bouteiller, N., et al. (2012). The Pea TCP Transcription Factor PsBRC1 Acts Downstream of Strigolactones to Control Shoot Branching. Plant Physiol. *158*, 225–238.

Brewer, P.B., Dun, E.A., Ferguson, B.J., Rameau, C., and Beveridge, C.A. (2009). Strigolactone Acts Downstream of Auxin to Regulate Bud Outgrowth in Pea and Arabidopsis. Plant Physiol. *150*, 482–493.

Brewer, P.B., Dun, E.A., Gui, R., Mason, M., and Beveridge, C.A. (2015). Strigolactone inhibition of branching independent of polar auxin transport. Plant Physiol. http://dx.doi.org/10.1104/pp.15.00014.

Broeckx, L.S., Verlinden, M.S., Vangronsveld, J., and Ceulemans, R. (2012). Importance of crown architecture for leaf area index of different Populus genotypes in a high-density plantation. Tree Physiol. *32*, 1214–1226.

Brown, B.T., Foster, C., Phillips, J.N., and Rattigan, B.M. (1979). The indirect role of 2,4-D in the maintenance of apical dominance in decapitated sunflower seedlings (Helianthus annuus L.). Planta *146*, 475–480.

Buee, M., Rossignol, M., Jauneau, A., Ranjeva, R., and Bécard, G. (2000). The Pre-Symbiotic Growth of Arbuscular Mycorrhizal Fungi Is Induced by a Branching Factor Partially Purified from Plant Root Exudates. Mol. Plant. Microbe Interact. *13*, 693–698.

Campos, M.L., Kang, J.-H., and Howe, G.A. (2014). Jasmonate-Triggered Plant Immunity. J. Chem. Ecol. *40*, 657–675.

Cardoso, C., Zhang, Y., Jamil, M., Hepworth, J., Charnikhova, T., Dimkpa, S.O.N., Meharg, C., Wright, M.H., Liu, J., Meng, X., et al. (2014). Natural variation of rice strigolactone biosynthesis is associated with the deletion of two MAX1 orthologs. Proc. Natl. Acad. Sci. *111*, 2379–2384.

Casal, J.J., Sanchez, R.A., and Deregibus, V.A. (1986). The effect of plant density on tillering: The involvement of R/FR ratio and the proportion of radiation intercepted per plant. Environ. Exp. Bot. *26*, 365–371.

Ceulemans, R., Stettler, R.F., Hinckley, T.M., Isebrands, J.G., and Heilman, P.E. (1990). Crown architecture of Populus clones as determined by branch orientation and branch characteristics. Tree Physiol. *7*, 157–167.

Chang, S., Puryear, J., and Cairney, J. (1993). A simple and efficient method for isolating RNA from pine trees. Plant Mol. Biol. Report. *11*, 113–116.

Chatfield, S.P., Stirnberg, P., Forde, B.G., and Leyser, O. (2000). The hormonal regulation of axillary bud growth in Arabidopsis. Plant J. *24*, 159–169.

Chen, C.M., Ertl, J.R., Leisner, S.M., and Chang, C.C. (1985). Localization of cytokinin biosynthetic sites in pea plants and carrot roots. Plant Physiol. *78*, 510–513.

Cline, M. (1997). Concepts and terminology of apical dominance. Am. J. Bot. *84*, 1064–1064.

Cook, C.E., Whichard, L.P., Turner, B., Wall, M.E., and Egley, G.H. (1966). Germination of Witchweed (Striga lutea Lour.): Isolation and Properties of a Potent Stimulant. Science *154*, 1189–1190.

Costes, E., Crespel, L., Denoyes, B., Morel, P., Demene, M.-N., Lauri, P.-E., and Wenden, B. (2014). Bud structure, position and fate generate various branching patterns along shoots of closely related Rosaceae species: a review. Plant Biophys. Model. *5*, 666.

Crawford, S., Shinohara, N., Sieberer, T., Williamson, L., George, G., Hepworth, J., Müller, D., Domagalska, M.A., and Leyser, O. (2010). Strigolactones enhance competition between shoot branches by dampening auxin transport. Development *137*, 2905–2913.

Cubas, P., Lauter, N., Doebley, J., and Coen, E. (1999). The TCP domain: a motif found in proteins regulating plant growth and development. Plant J. *18*, 215–222.

Czarnecki, O., Yang, J., Wang, X., Wang, S., Muchero, W., Tuskan, G.A., and Chen, J.-G. (2014). Characterization of MORE AXILLARY GROWTH genes in Populus. PloS One *9*, e102757.

Depuydt, S., and Hardtke, C.S. (2011). Hormone Signalling Crosstalk in Plant Growth Regulation. Curr. Biol. *21*, 365–373.

Derksen, H., Rampitsch, C., and Daayf, F. (2013). Signaling cross-talk in plant disease resistance. Plant Sci. Int. J. Exp. Plant Biol. *207*, 79–87.

De Smet, I., and Jürgens, G. (2007). Patterning the axis in plants – auxin in control. Curr. Opin. Genet. Dev. *17*, 337–343.

Doebley, J., Stec, A., and Hubbard, L. (1997). The evolution of apical dominance in maize. Nature *386*, 485–488.

Domagalska, M.A., and Leyser, O. (2011). Signal integration in the control of shoot branching. Nat. Rev. Mol. Cell Biol. *12*, 211–221.

Drummond, R.S.M., Martínez-Sánchez, N.M., Janssen, B.J., Templeton, K.R., Simons, J.L., Quinn, B.D., Karunairetnam, S., and Snowden, K.C. (2009). Petunia hybrida CAROTENOID CLEAVAGE DIOXYGENASE7 Is Involved in the Production of Negative and Positive Branching Signals in Petunia. Plant Physiol. *151*, 1867–1877.

Drummond, R.S.M., Sheehan, H., Simons, J.L., Martínez-Sánchez, N.M., Turner, R.M., Putterill, J., and Snowden, K.C. (2011). The Expression of Petunia Strigolactone Pathway Genes is Altered as Part of the Endogenous Developmental Program. Front. Plant Sci. *2*, 115.

Drummond, R.S.M., Janssen, B.J., Luo, Z., Oplaat, C., Ledger, S.E., Wohlers, M.W., and Snowden, K.C. (2015). Environmental Control of Branching in Petunia. Plant Physiol. *168*, 735–751.

Dun, E.A., Hanan, J., and Beveridge, C.A. (2009). Computational Modeling and Molecular Physiology Experiments Reveal New Insights into Shoot Branching in Pea. Plant Cell *21*, 3459–3472.

Dun, E.A., Germain, A. de S., Rameau, C., and Beveridge, C.A. (2012). Antagonistic Action of Strigolactone and Cytokinin in Bud Outgrowth Control. Plant Physiol. *158*, 487–498.

Everat-Bourbouloux, A., and Bonnemain, J.-L. (1980). Distribution of labelled auxin and derivatives in stem tissues of intact and decapitated broad-bean plants in relation to apical dominance. Physiol. Plant. *50*, 145–152.

Faiss, M., Zalubìlová, J., Strnad, M., and Schmülling, T. (1997). Conditional transgenic expression of the ipt gene indicates a function for cytokinins in paracrine signaling in whole tobacco plants. Plant J. Cell Mol. Biol. *12*, 401–415.

Fedoroff, N.V. (2002). Cross-Talk in Abscisic Acid Signaling. Sci. Signal. *2002*, re10.

Filichkin, S.A., Meilan, R., Busov, V.B., Ma, C., Brunner, A.M., and Strauss, S.H. (2006). Alcohol-inducible gene expression in transgenic Populus. Plant Cell Rep. *25*, 660–667.

Finlayson, S.A. (2007). Arabidopsis Teosinte Branched1-like 1 regulates axillary bud outgrowth and is homologous to monocot Teosinte Branched1. Plant Cell Physiol. *48*, 667–677.

Finlayson, S.A., Krishnareddy, S.R., Kebrom, T.H., and Casal, J.J. (2010). Phytochrome Regulation of Branching in Arabidopsis1[W][OA]. Plant Physiol. *152*, 1914–1927.

Foo, E., Turnbull, C.G., and Beveridge, C.A. (2001). Long-distance signaling and the control of branching in the rms1 mutant of pea. Plant Physiol. *126*, 203–209.

Foo, E., Bullier, E., Goussot, M., Foucher, F., Rameau, C., and Beveridge, C.A. (2005). The Branching Gene RAMOSUS1 Mediates Interactions among Two Novel Signals and Auxin in Pea. Plant Cell *17*, 464–474.

Fridman, Y., and Savaldi-Goldstein, S. (2013). Brassinosteroids in growth control: how, when and where. Plant Sci. Int. J. Exp. Plant Biol. *209*, 24–31.

Gälweiler, L., Guan, C., Müller, A., Wisman, E., Mendgen, K., Yephremov, A., and Palme, K. (1998). Regulation of Polar Auxin Transport by AtPIN1 in Arabidopsis Vascular Tissue. Science *282*, 2226–2230.

Garcia, K., Delaux, P.-M., Cope, K.R., and Ané, J.-M. (2015). Molecular signals required for the establishment and maintenance of ectomycorrhizal symbioses. New Phytol. 10.1111/nph.13423.

Genre, A., Chabaud, M., Balzergue, C., Puech-Pagès, V., Novero, M., Rey, T., Fournier, J., Rochange, S., Bécard, G., Bonfante, P., et al. (2013). Short-chain chitin oligomers from arbuscular mycorrhizal fungi trigger nuclear Ca2+ spiking in Medicago truncatula roots and their production is enhanced by strigolactone. New Phytol. *198*, 190–202.

Gocal, G.F.W., Pharis, R.P., Yeung, E.C., and Pearce, D. (1991). Changes after Decapitation in Concentrations of Indole-3-Acetic Acid and Abscisic Acid in the Larger Axillary Bud of Phaseolus vulgaris L. cv Tender Green. Plant Physiol. *95*, 344–350.

Gomez-Roldan, V., Fermas, S., Brewer, P.B., Puech-Pagès, V., Dun, E.A., Pillot, J.-P., Letisse, F., Matusova, R., Danoun, S., Portais, J.-C., et al. (2008). Strigolactone inhibition of shoot branching. Nature *455*, 189–194.

González-Grandío, E., and Cubas, P. (2014). Identification of gene functions associated to active and dormant buds in Arabidopsis. Plant Signal. Behav. *9*, e27994.

González-Grandío, E., Poza-Carrión, C., Sorzano, C.O.S., and Cubas, P. (2013). BRANCHED1 promotes axillary bud dormancy in response to shade in Arabidopsis. Plant Cell *25*, 834–850.

Goodstein, D.M., Shu, S., Howson, R., Neupane, R., Hayes, R.D., Fazo, J., Mitros, T., Dirks, W., Hellsten, U., Putnam, N., et al. (2012). Phytozome: a comparative platform for green plant genomics. Nucleic Acids Res. *40*, D1178–D1186.

Greb, T., Clarenz, O., Schafer, E., Muller, D., Herrero, R., Schmitz, G., and Theres, K. (2003). Molecular analysis of the LATERAL SUPPRESSOR gene in Arabidopsis reveals a conserved control mechanism for axillary meristem formation. Genes Dev. *17*, 1175–1187.

Ha, C.V., Leyva-González, M.A., Osakabe, Y., Tran, U.T., Nishiyama, R., Watanabe, Y., Tanaka, M., Seki, M., Yamaguchi, S., Dong, N.V., et al. (2014). Positive regulatory role of strigolactone in plant responses to drought and salt stress. Proc. Natl. Acad. Sci. *111*, 851–856.

Hall, S.M., and Hillman, J.R. (1975). Correlative inhibition of lateral bud growth in Phaseolus vulgaris L. timing of bud growth following decapitation. Planta *123*, 137–143.

Hallé, F., Oldeman, R.A.A., and Tomlinson, P.B. (1978). Tropical trees and forests: an architectural analysis. Springer-Verl. pp. 441.

Hamiaux, C., Drummond, R.S.M., Janssen, B.J., Ledger, S.E., Cooney, J.M., Newcomb, R.D., and Snowden, K.C. (2012). DAD2 Is an α/β Hydrolase Likely to Be Involved in the Perception of the Plant Branching Hormone, Strigolactone. Curr. Biol. *22*, 2032–2036.

Hayward, A., Stirnberg, P., Beveridge, C., and Leyser, O. (2009). Interactions between Auxin and Strigolactone in Shoot Branching Control. Plant Physiol. *151*, 400–412.

Helliwell, C.A., Chin-Atkins, A.N., Wilson, I.W., Chapple, R., Dennis, E.S., and Chaudhury, A. (2001). The Arabidopsis AMP1 Gene Encodes a Putative Glutamate Carboxypeptidase. Plant Cell *13*, 2115–2125.

Ho, M.S., Ou, C., Chan, Y.–., Chien, C.-T., and Pi, H. (2008). The utility F-box for protein destruction. Cell. Mol. Life Sci. *65*, 1977–2000.

Hubbard, L., McSteen, P., Doebley, J., and Hake, S. (2002). Expression patterns and mutant phenotype of teosinte branched1 correlate with growth suppression in maize and teosinte. Genetics *162*, 1927–1935.

Ishikawa, S., Maekawa, M., Arite, T., Onishi, K., Takamure, I., and Kyozuka, J. (2005). Suppression of tiller bud activity in tillering dwarf mutants of rice. Plant Cell Physiol. *46*, 79–86.

Janssen, B.J., Drummond, R.S., and Snowden, K.C. (2014). Regulation of axillary shoot development. Curr. Opin. Plant Biol. *17*, 28–35.

Jiang, L., Liu, X., Xiong, G., Liu, H., Chen, F., Wang, L., Meng, X., Liu, G., Yu, H., Yuan, Y., et al. (2013). DWARF 53 acts as a repressor of strigolactone signalling in rice. Nature *504*, 401–405.

Jiang, Y., Duan, Y., Yin, J., Ye, S., Zhu, J., Zhang, F., Lu, W., Fan, D., and Luo, K. (2014). Genome-wide identification and characterization of the Populus WRKY transcription factor family and analysis of their expression in response to biotic and abiotic stresses. J. Exp. Bot. 10.1093/jxb/eru381.

Johnson, X., Brcich, T., Dun, E.A., Goussot, M., Haurogné, K., Beveridge, C.A., and Rameau, C. (2006). Branching Genes Are Conserved across Species. Genes Controlling a Novel Signal in Pea Are Coregulated by Other Long-Distance Signals. Plant Physiol. *142*, 1014–1026.

Kadereit, J.W., Körner, C., Kost, B., and Sonnewald, U. (2014). Strasburger − Lehrbuch der Pflanzenwissenschaften (Springer-Verlag).

Kagiyama, M., Hirano, Y., Mori, T., Kim, S.-Y., Kyozuka, J., Seto, Y., Yamaguchi, S., and Hakoshima, T. (2013). Structures of D14 and D14L in the strigolactone and karrikin signaling pathways. Genes Cells *18*, 147–160.

Kalousek, P., Buchtová, D., Balla, J., Reinöhl, V., Procházka, S., and others (2014). Cytokinins and polar transport of auxin in axillary pea buds. Acta Univ. Agric. Silvic. Mendel. Brun. *58*, 79–88.

Kapulnik, Y., Delaux, P.-M., Resnick, N., Mayzlish-Gati, E., Wininger, S., Bhattacharya, C., Séjalon-Delmas, N., Combier, J.-P., Bécard, G., Belausov, E., et al. (2010). Strigolactones affect lateral root formation and root-hair elongation in Arabidopsis. Planta *233*, 209–216.

Kearse, M., Moir, R., Wilson, A., Stones-Havas, S., Cheung, M., Sturrock, S., Buxton, S., Cooper, A., Markowitz, S., Duran, C., et al. (2012). Geneious Basic: An integrated and

extendable desktop software platform for the organization and analysis of sequence data. Bioinformatics *28*, 1647–1649.

Kebrom, T.H., Burson, B.L., and Finlayson, S.A. (2006). Phytochrome B Represses Teosinte Branched1 Expression and Induces Sorghum Axillary Bud Outgrowth in Response to Light Signals. Plant Physiol. *140*, 1109–1117.

Keller, T., Abbott, J., Moritz, T., and Doerner, P. (2006). Arabidopsis REGULATOR OF AXILLARY MERISTEMS1 controls a leaf axil stem cell niche and modulates vegetative development. Plant Cell *18*, 598–611.

Kleine-Vehn, J., Wabnik, K., Martinière, A., Łangowski, Ł., Willig, K., Naramoto, S., Leitner, J., Tanaka, H., Jakobs, S., Robert, S., et al. (2011). Recycling, clustering, and endocytosis jointly maintain PIN auxin carrier polarity at the plasma membrane. Mol. Syst. Biol. *7*, 540.

Kohlen, W., Charnikhova, T., Liu, Q., Bours, R., Domagalska, M.A., Beguerie, S., Verstappen, F., Leyser, O., Bouwmeester, H., and Ruyter-Spira, C. (2011). Strigolactones are transported through the xylem and play a key role in shoot architectural response to phosphate deficiency in nonarbuscular mycorrhizal host Arabidopsis. Plant Physiol. *155*, 974–987.

Kohlen, W., Charnikhova, T., Lammers, M., Pollina, T., Tóth, P., Haider, I., Pozo, M.J., de Maagd, R.A., Ruyter-Spira, C., Bouwmeester, H.J., et al. (2012). The tomato CAROTENOID CLEAVAGE DIOXYGENASE8 (SlCCD8) regulates rhizosphere signaling, plant architecture and affects reproductive development through strigolactone biosynthesis. New Phytol. *196*, 535–547.

Kudo, T., Kiba, T., and Sakakibara, H. (2010). Metabolism and Long-distance Translocation of Cytokinins. J. Integr. Plant Biol. *52*, 53–60.

Lamesch, P., Berardini, T.Z., Li, D., Swarbreck, D., Wilks, C., Sasidharan, R., Muller, R., Dreher, K., Alexander, D.L., Garcia-Hernandez, M., et al. (2011). The Arabidopsis Information Resource (TAIR): improved gene annotation and new tools. Nucleic Acids Res. 10.1093/nar/gkr1090.

Ledger, S.E., Janssen, B.J., Karunairetnam, S., Wang, T., and Snowden, K.C. (2010). Modified CAROTENOID CLEAVAGE DIOXYGENASE8 expression correlates with altered branching in kiwifruit (Actinidia chinensis). New Phytol. *188*, 803–813.

Lewis, J.M., Mackintosh, C.A., Shin, S., Gilding, E., Kravchenko, S., Baldridge, G., Zeyen, R., and Muehlbauer, G.J. (2008). Overexpression of the maize Teosinte Branched1 gene in wheat suppresses tiller development. Plant Cell Rep. *27*, 1217–1225.

Liang, J., Zhao, L., Challis, R., and Leyser, O. (2010). Strigolactone regulation of shoot branching in chrysanthemum (Dendranthema grandiflorum). J. Exp. Bot. *61*, 3069–3078.

Lin, H., Wang, R., Qian, Q., Yan, M., Meng, X., Fu, Z., Yan, C., Jiang, B., Su, Z., Li, J., et al. (2009). DWARF27, an Iron-Containing Protein Required for the Biosynthesis of Strigolactones, Regulates Rice Tiller Bud Outgrowth. Plant Cell *21*, 1512–1525.

Ljung, K. (2013). Auxin metabolism and homeostasis during plant development. Dev. Camb. Engl. *140*, 943–950.

Ljung, K., Bhalerao, R.P., and Sandberg, G. (2001). Sites and homeostatic control of auxin biosynthesis in Arabidopsis during vegetative growth. Plant J. *28*, 465–474.

Long, J., and Barton, M.K. (2000). Initiation of Axillary and Floral Meristems in Arabidopsis. Dev. Biol. *218*, 341–353.

Long, J.A., Moan, E.I., Medford, J.I., and Barton, M.K. (1996). A member of the KNOTTED class of homeodomain proteins encoded by the STM gene of Arabidopsis. Nature *379*, 66–69.

López-Ráez, J.A., Charnikhova, T., Gómez-Roldán, V., Matusova, R., Kohlen, W., De Vos, R., Verstappen, F., Puech-Pages, V., Bécard, G., Mulder, P., et al. (2008). Tomato strigolactones are derived from carotenoids and their biosynthesis is promoted by phosphate starvation. New Phytol. *178*, 863–874.

López-Ráez, J.A., Kohlen, W., Charnikhova, T., Mulder, P., Undas, A.K., Sergeant, M.J., Verstappen, F., Bugg, T.D.H., Thompson, A.J., Ruyter-Spira, C., et al. (2010). Does abscisic acid affect strigolactone biosynthesis? New Phytol. *187*, 343–354.

Lu, S., Sun, Y.-H., Shi, R., Clark, C., Li, L., and Chiang, V.L. (2005). Novel and mechanical stress-responsive MicroRNAs in Populus trichocarpa that are absent from Arabidopsis. Plant Cell *17*, 2186–2203.

Lu, Z., Yu, H., Xiong, G., Wang, J., Jiao, Y., Liu, G., Jing, Y., Meng, X., Hu, X., Qian, Q., et al. (2013). Genome-Wide Binding Analysis of the Transcription Activator IDEAL PLANT ARCHITECTURE1 Reveals a Complex Network Regulating Rice Plant Architecture. Plant Cell *25*, 3743–3759.

Mangnus, E.M., and Zwanenburg, B. (1992). Tentative molecular mechanism for germination stimulation of Striga and Orobanche seeds by strigol and its synthetic analogs. J. Agric. Food Chem. *40*, 1066–1070.

Martín-Trillo, M., and Cubas, P. (2010). TCP genes: a family snapshot ten years later. Trends Plant Sci. *15*, 31–39.

Martín-Trillo, M., Grandío, E.G., Serra, F., Marcel, F., Rodríguez-Buey, M.L., Schmitz, G., Theres, K., Bendahmane, A., Dopazo, H., and Cubas, P. (2011). Role of tomato BRANCHED1-like genes in the control of shoot branching: A BRC1-like gene controls shoot branching in tomato. Plant J. *67*, 701–714.

Mashiguchi, K., Sasaki, E., Shimada, Y., Nagae, M., Ueno, K., Nakano, T., Yoneyama, K., Suzuki, Y., and Asami, T. (2009). Feedback-regulation of strigolactone biosynthetic genes and strigolactone-regulated genes in Arabidopsis. Biosci. Biotechnol. Biochem. *73*, 2460–2465.

Matusova, R., Rani, K., Verstappen, F.W.A., Franssen, M.C.R., Beale, M.H., and Bouwmeester, H.J. (2005). The Strigolactone Germination Stimulants of the Plant-

Parasitic Striga and Orobanche spp. Are Derived from the Carotenoid Pathway. Plant Physiol. *139*, 920–934.

McSteen, P., and Leyser, O. (2005). Shoot Branching. Annu. Rev. Plant Biol. *56*, 353–374.

Minakuchi, K., Kameoka, H., Yasuno, N., Umehara, M., Luo, L., Kobayashi, K., Hanada, A., Ueno, K., Asami, T., Yamaguchi, S., et al. (2010). FINE CULM1 (FC1) works downstream of strigolactones to inhibit the outgrowth of axillary buds in rice. Plant Cell Physiol. *51*, 1127–1135.

Miyawaki, K., Matsumoto-Kitano, M., and Kakimoto, T. (2004). Expression of cytokinin biosynthetic isopentenyltransferase genes in Arabidopsis: tissue specificity and regulation by auxin, cytokinin, and nitrate. Plant J. *37*, 128–138.

Müller, D., and Leyser, O. (2011). Auxin, cytokinin and the control of shoot branching. Ann. Bot. *107*, 1203–1212.

Müller, D., Waldie, T., Miyawaki, K., To, J.P.C., Melnyk, C.W., Kieber, J.J., Kakimoto, T., and Leyser, O. (2015). Cytokinin is required for escape but not release from auxin mediated apical dominance. Plant J. Cell Mol. Biol. *82*, 874–886.

Nakamura, H., Xue, Y.-L., Miyakawa, T., Hou, F., Qin, H.-M., Fukui, K., Shi, X., Ito, E., Ito, S., Park, S.-H., et al. (2013). Molecular mechanism of strigolactone perception by DWARF14. Nat. Commun. *4*.

Napoli, C. (1996). Highly Branched Phenotype of the Petunia dad1-1 Mutant Is Reversed by Grafting. Plant Physiol. *111*, 27–37.

Navaud, O., Dabos, P., Carnus, E., Tremousaygue, D., and Hervé, C. (2007). TCP Transcription Factors Predate the Emergence of Land Plants. J. Mol. Evol. *65*, 23–33.

Nicotra, A.B., Atkin, O.K., Bonser, S.P., Davidson, A.M., Finnegan, E.J., Mathesius, U., Poot, P., Purugganan, M.D., Richards, C.L., Valladares, F., et al. (2010). Plant phenotypic plasticity in a changing climate. Trends Plant Sci. *15*, 684–692.

Nordström, A., Tarkowski, P., Tarkowska, D., Norbaek, R., Åstot, C., Dolezal, K., and Sandberg, G. (2004). Auxin regulation of cytokinin biosynthesis in Arabidopsis thaliana: A factor of potential importance for auxin–cytokinin-regulated development. Proc. Natl. Acad. Sci. U. S. A. *101*, 8039–8044.

Paciorek, T., Zažímalová, E., Ruthardt, N., Petrášek, J., Stierhof, Y.-D., Kleine-Vehn, J., Morris, D.A., Emans, N., Jürgens, G., Geldner, N., et al. (2005). Auxin inhibits endocytosis and promotes its own efflux from cells. Nature *435*, 1251–1256.

Palatnik, J.F., Allen, E., Wu, X., Schommer, C., Schwab, R., Carrington, J.C., and Weigel, D. (2003). Control of leaf morphogenesis by microRNAs. Nature *425*, 257–263.

Panigrahi, B.M., and Audus, L.J. (1966). Apical Dominance in Vicia faba. Ann. Bot. *30*, 457–473.

Parniske, M. (2008). Arbuscular mycorrhiza: the mother of plant root endosymbioses. Nat. Rev. Microbiol. *6*, 763–775.

Pierik, R., and Wit, M. de (2014). Shade avoidance: phytochrome signalling and other aboveground neighbour detection cues. J. Exp. Bot. *65*, 2815–2824.

Pieterse, C.M.J., Van der Does, D., Zamioudis, C., Leon-Reyes, A., and Van Wees, S.C.M. (2012). Hormonal Modulation of Plant Immunity. Annu. Rev. Cell Dev. Biol. *28*, 489–521.

Plett, J.M., Daguerre, Y., Wittulsky, S., Vayssières, A., Deveau, A., Melton, S.J., Kohler, A., Morrell-Falvey, J.L., Brun, A., Veneault-Fourrey, C., et al. (2014). Effector MiSSP7 of the mutualistic fungus Laccaria bicolor stabilizes the Populus JAZ6 protein and represses jasmonic acid (JA) responsive genes. Proc. Natl. Acad. Sci. U. S. A. *111*, 8299–8304.

Prasad, T.K., Li, X., Abdel-Rahman, A.M., Hosokawa, Z., Cloud, N.P., Lamotte, C.E., and Cline, M.G. (1993). Does Auxin Play a Role in the Release of Apical Dominance by Shoot Inversion in Ipomoea nil? Ann. Bot. *71*, 223–229.

Prusinkiewicz, P., Crawford, S., Smith, R.S., Ljung, K., Bennett, T., Ongaro, V., and Leyser, O. (2009). Control of bud activation by an auxin transport switch. Proc. Natl. Acad. Sci. *106*, 17431–17436.

Rasmussen, A., Mason, M.G., De Cuyper, C., Brewer, P.B., Herold, S., Agusti, J., Geelen, D., Greb, T., Goormachtig, S., Beeckman, T., et al. (2012). Strigolactones suppress adventitious rooting in Arabidopsis and pea. Plant Physiol. *158*, 1976–1987.

Reddy, S.K., Holalu, S.V., Casal, J.J., and Finlayson, S.A. (2013). Abscisic acid regulates axillary bud outgrowth responses to the ratio of red to far-red light. Plant Physiol. *163*, 1047–1058.

Regier, N., and Frey, B. (2010). Experimental comparison of relative RT-qPCR quantification approaches for gene expression studies in poplar. BMC Mol. Biol. *11*, 57.

Remigereau, M.-S., Lakis, G., Rekima, S., Leveugle, M., Fontaine, M.C., Langin, T., Sarr, A., and Robert, T. (2011). Cereal Domestication and Evolution of Branching: Evidence for Soft Selection in the Tb1 Orthologue of Pearl Millet (Pennisetum glaucum [L.] R. Br.). PLoS ONE *6*, e22404.

Remphrey, W.R., and Powell, G.R. (1985). Crown architecture of Larix laricina saplings: sylleptic branching on the main stem. Can. J. Bot. *63*, 1296–1302.

Rohde, A., and Bhalerao, R.P. (2007). Plant dormancy in the perennial context. Trends Plant Sci. *12*, 217–223.

Ruttink, T., Arend, M., Morreel, K., Storme, V., Rombauts, S., Fromm, J., Bhalerao, R.P., Boerjan, W., and Rohde, A. (2007). A Molecular Timetable for Apical Bud Formation and Dormancy Induction in Poplar. Plant Cell *19*, 2370–2390.

Ruyter-Spira, C., Kohlen, W., Charnikhova, T., van Zeijl, A., van Bezouwen, L., de Ruijter, N., Cardoso, C., Lopez-Raez, J.A., Matusova, R., Bours, R., et al. (2011). Physiological

effects of the synthetic strigolactone analog GR24 on root system architecture in Arabidopsis: another belowground role for strigolactones? Plant Physiol. *155*, 721–734.

Sachs, T. (1968). On the Determination of the Pattern of Vascular Tissue in Peas. Ann. Bot. *32*, 781–790.

Sachs, T. (1981). The Control of the Patterned Differentiation of Vascular Tissues. In Advances in Botanical Research, H.W. Woolhouse, ed. (Academic Press), pp. 151–262.

Sachs, T. (2000). Integrating Cellular and Organismic Aspects of Vascular Differentiation. Plant Cell Physiol. *41*, 649–656.

Sachs, T., and Thimann, K.V. (1964). Release of Lateral Buds from Apical Dominance. Nature *201*, 939–940.

Sachs, T., and Thimann, K.V. (1967). The Role of Auxins and Cytokinins in the Release of Buds From Dominance. Am. J. Bot. *54*, 136–144.

de Saint Germain, A., Ligerot, Y., Dun, E.A., Pillot, J.-P., Ross, J.J., Beveridge, C.A., and Rameau, C. (2013). Strigolactones Stimulate Internode Elongation Independently of Gibberellins. Plant Physiol. *163*, 1012–1025.

Salmon, J., Ward, S.P., Hanley, S.J., Leyser, O., and Karp, A. (2014). Functional screening of willow alleles in Arabidopsis combined with QTL mapping in willow (Salix) identifies SxMAX4 as a coppicing response gene. Plant Biotechnol. J. *12*, 480–491.

Sambrook, J., and Russell, D.W. (2000). Molecular Cloning: A Laboratory Manual, 3 Vol. (Cold Spring Harbor, N.Y: Cold Spring Harbor Laboratory).

Sauer, M., Balla, J., Luschnig, C., Wisniewska, J., Reinöhl, V., Friml, J., and Benková, E. (2006). Canalization of auxin flow by Aux/IAA-ARF-dependent feedback regulation of PIN polarity. Genes Dev. *20*, 2902–2911.

Scarascia-Mugnozza, G.E., Isebrands, J.G., Hinckley, T.M., and Stettler, R.F. (1989). Dynamics of light interception, leaf area and biomass production in Populus clones in the establishment year. Ann. For. Sci. *46*, 515–518.

Schwab, R., Ossowski, S., Riester, M., Warthmann, N., and Weigel, D. (2006). Highly specific gene silencing by artificial microRNAs in Arabidopsis. Plant Cell *18*, 1121–1133.

Seto, Y., and Yamaguchi, S. (2014). Strigolactone biosynthesis and perception. Curr. Opin. Plant Biol. *21*, 1–6.

Seto, Y., Sado, A., Asami, K., Hanada, A., Umehara, M., Akiyama, K., and Yamaguchi, S. (2014). Carlactone is an endogenous biosynthetic precursor for strigolactones. Proc. Natl. Acad. Sci. *111*, 1640–1645.

Shaobing Peng, G.S.K. (2008). Progress in ideotype breeding to increase rice yield potential. Field Crops Res. *108*, 32–38.

Shimizu-Sato, S., Tanaka, M., and Mori, H. (2008). Auxin–cytokinin interactions in the control of shoot branching. Plant Mol. Biol. *69*, 429–435.

Shinohara, N., Taylor, C., and Leyser, O. (2013). Strigolactone Can Promote or Inhibit Shoot Branching by Triggering Rapid Depletion of the Auxin Efflux Protein PIN1 from the Plasma Membrane. PLoS Biol *11*, e1001474.

Snow, R. (1937). On the Nature of Correlative Inhibition. New Phytol. *36*, 283–300.

Snowden, K.C., Simkin, A.J., Janssen, B.J., Templeton, K.R., Loucas, H.M., Simons, J.L., Karunairetnam, S., Gleave, A.P., Clark, D.G., and Klee, H.J. (2005). The Decreased apical dominance1/Petunia hybrida CAROTENOID CLEAVAGE DIOXYGENASE8 gene affects branch production and plays a role in leaf senescence, root growth, and flower development. Plant Cell *17*, 746–759.

Sorefan, K., Booker, J., Haurogné, K., Goussot, M., Bainbridge, K., Foo, E., Chatfield, S., Ward, S., Beveridge, C., Rameau, C., et al. (2003). MAX4 and RMS1 are orthologous dioxygenase-like genes that regulate shoot branching in Arabidopsis and pea. Genes Dev. *17*, 1469–1474.

Spinelli, S.V., Martin, A.P., Viola, I.L., Gonzalez, D.H., and Palatnik, J.F. (2011). A mechanistic link between STM and CUC1 during Arabidopsis development. Plant Physiol. *156*, 1894–1904.

Stafstrom, J.P., and Sarup, V.B. (2000). Development of supernumerary buds from the axillary meristem of pea, Pisum sativum (Fabaceae). Aust. J. Bot. *48*, 271–278.

Stanga, J.P., Smith, S.M., Briggs, W.R., and Nelson, D.C. (2013). SUPPRESSOR OF MORE AXILLARY GROWTH2 1 Controls Seed Germination and Seedling Development in Arabidopsis. Plant Physiol. *163*, 318–330.

Steinkellner, S., Lendzemo, V., Langer, I., Schweiger, P., Khaosaad, T., Toussaint, J.-P., and Vierheilig, H. (2007). Flavonoids and Strigolactones in Root Exudates as Signals in Symbiotic and Pathogenic Plant-Fungus Interactions. Molecules *12*, 1290–1306.

Stirnberg, P., van De Sande, K., and Leyser, H.M.O. (2002). MAX1 and MAX2 control shoot lateral branching in Arabidopsis. Dev. Camb. Engl. *129*, 1131–1141.

Stirnberg, P., Furner, I.J., and Ottoline Leyser, H.M. (2007). MAX2 participates in an SCF complex which acts locally at the node to suppress shoot branching. Plant J. *50*, 80–94.

Sussex, I.M., and Kerk, N.M. (2001). The evolution of plant architecture. Curr. Opin. Plant Biol. *4*, 33–37.

Takeda, T., Suwa, Y., Suzuki, M., Kitano, H., Ueguchi-Tanaka, M., Ashikari, M., Matsuoka, M., and Ueguchi, C. (2003). The OsTB1 gene negatively regulates lateral branching in rice. Plant J. Cell Mol. Biol. *33*, 513–520.

Tamura, K., Peterson, D., Peterson, N., Stecher, G., Nei, M., and Kumar, S. (2011). MEGA5: molecular evolutionary genetics analysis using maximum likelihood, evolutionary distance, and maximum parsimony methods. Mol. Biol. Evol. *28*, 2731–2739.

Tanaka, M., Takei, K., Kojima, M., Sakakibara, H., and Mori, H. (2006). Auxin controls local cytokinin biosynthesis in the nodal stem in apical dominance. Plant J. *45*, 1028–1036.

Teichmann, T., and Muhr, M. (2015). Shaping plant architecture. Front. Plant Sci. *6*, 233.

Thimann, K.V. (1937). On the Nature of Inhibitions Caused by Auxin. Am. J. Bot. *24*, 407–412.

Thimann, K.V., and Skoog, F. (1933). Studies on the Growth Hormone of Plants: III. The Inhibiting Action of the Growth Substance on Bud Development. Proc. Natl. Acad. Sci. U. S. A. *19*, 714–716.

Thimann, K.V., and Skoog, F. (1934). On the Inhibition of Bud Development and other Functions of Growth Substance in Vicia Faba. Proc. R. Soc. Lond. Ser. B Contain. Pap. Biol. Character *114*, 317–339.

Torres-Vera, R., García, J.M., Pozo, M.J., and López-Ráez, J.A. (2014). Do strigolactones contribute to plant defence? Mol. Plant Pathol. *15*, 211–216.

Turnbull, C.G.N., Raymond, M.A.A., Dodd, I.C., and Morris, S.E. (1997). Rapid increases in cytokinin concentration in lateral buds of chickpea (Cicer arietinum L.) during release of apical dominance. Planta *202*, 271–276.

Tuskan, G.A., Difazio, S., Jansson, S., Bohlmann, J., Grigoriev, I., Hellsten, U., Putnam, N., Ralph, S., Rombauts, S., Salamov, A., et al. (2006). The genome of black cottonwood, Populus trichocarpa (Torr. & Gray). Science *313*, 1596–1604.

Umehara, M., Hanada, A., Yoshida, S., Akiyama, K., Arite, T., Takeda-Kamiya, N., Magome, H., Kamiya, Y., Shirasu, K., Yoneyama, K., et al. (2008). Inhibition of shoot branching by new terpenoid plant hormones. Nature *455*, 195–200.

Vieten, A., Vanneste, S., Wisniewska, J., Benková, E., Benjamins, R., Beeckman, T., Luschnig, C., and Friml, J. (2005). Functional redundancy of PIN proteins is accompanied by auxin-dependent cross-regulation of PIN expression. Dev. Camb. Engl. *132*, 4521–4531.

Waldie, T., McCulloch, H., and Leyser, O. (2014). Strigolactones and the control of plant development: lessons from shoot branching. Plant J. *79*, 607–622.

Wang, Y., and Li, J. (2008). Molecular basis of plant architecture. Annu. Rev. Plant Biol. *59*, 253–279.

Wang, Q., Kohlen, W., Rossmann, S., Vernoux, T., and Theres, K. (2014a). Auxin Depletion from the Leaf Axil Conditions Competence for Axillary Meristem Formation in Arabidopsis and Tomato. Plant Cell *26*, 2068–2079.

Wang, Y., Sun, S., Zhu, W., Jia, K., Yang, H., and Wang, X. (2013). Strigolactone/MAX2-Induced Degradation of Brassinosteroid Transcriptional Effector BES1 Regulates Shoot Branching. Dev. Cell *27*, 681–688.

Wang, Y., Wang, J., Shi, B., Yu, T., Qi, J., Meyerowitz, E.M., and Jiao, Y. (2014b). The Stem Cell Niche in Leaf Axils Is Established by Auxin and Cytokinin in Arabidopsis. Plant Cell *26*, 2055–2067.

Ward, S.P., Salmon, J., Hanley, S.J., Karp, A., and Leyser, O. (2013). Using Arabidopsis to Study Shoot Branching in Biomass Willow. Plant Physiol. *162*, 800–811.

Waters, M.T., Brewer, P.B., Bussell, J.D., Smith, S.M., and Beveridge, C.A. (2012a). The Arabidopsis ortholog of rice DWARF27 acts upstream of MAX1 in the control of plant development by strigolactones. Plant Physiol. *159*, 1073–1085.

Waters, M.T., Nelson, D.C., Scaffidi, A., Flematti, G.R., Sun, Y.K., Dixon, K.W., and Smith, S.M. (2012b). Specialisation within the DWARF14 protein family confers distinct responses to karrikins and strigolactones in Arabidopsis. Development *139*, 1285–1295.

White, J. (1979). The Plant as a Metapopulation. Annu. Rev. Ecol. Syst. *10*, 109–145.

Wilkins, O., Nahal, H., Foong, J., Provart, N.J., and Campbell, M.M. (2009). Expansion and Diversification of the Populus R2R3-MYB Family of Transcription Factors. Plant Physiol. *149*, 981–993.

Wisniewska, J., Xu, J., Seifertová, D., Brewer, P.B., Ruzicka, K., Blilou, I., Rouquié, D., Benková, E., Scheres, B., and Friml, J. (2006). Polar PIN localization directs auxin flow in plants. Science *312*, 883.

Woo, H.R., Chung, K.M., Park, J.H., Oh, S.A., Ahn, T., Hong, S.H., Jang, S.K., and Nam, H.G. (2001). ORE9, an F-box protein that regulates leaf senescence in Arabidopsis. Plant Cell *13*, 1779–1790.

Xie, X., Yoneyama, K., and Yoneyama, K. (2010). The strigolactone story. Annu. Rev. Phytopathol. *48*, 93–117.

Yang, F., Wang, Q., Schmitz, G., Müller, D., and Theres, K. (2012). The bHLH protein ROX acts in concert with RAX1 and LAS to modulate axillary meristem formation in Arabidopsis. Plant J. Cell Mol. Biol. *71*, 61–70.

Yoneyama, K., Xie, X., Kusumoto, D., Sekimoto, H., Sugimoto, Y., Takeuchi, Y., and Yoneyama, K. (2007). Nitrogen deficiency as well as phosphorus deficiency in sorghum promotes the production and exudation of 5-deoxystrigol, the host recognition signal for arbuscular mycorrhizal fungi and root parasites. Planta *227*, 125–132.

Yoneyama, K., Xie, X., Yoneyama, K., and Takeuchi, Y. (2009). Strigolactones: structures and biological activities. Pest Manag. Sci. *65*, 467–470.

Žádníková, P., and Simon, R. (2014). How boundaries control plant development. Curr. Opin. Plant Biol. *17*, 116–125.

Zhao, L.-H., Zhou, X.E., Wu, Z.-S., Yi, W., Xu, Y., Li, S., Xu, T.-H., Liu, Y., Chen, R.-Z., Kovach, A., et al. (2013). Crystal structures of two phytohormone signal-transducing α/β hydrolases: karrikin-signaling KAI2 and strigolactone-signaling DWARF14. Cell Res. *23*, 436–439.

Zhou, F., Lin, Q., Zhu, L., Ren, Y., Zhou, K., Shabek, N., Wu, F., Mao, H., Dong, W., Gan, L., et al. (2013). D14-SCFD3-dependent degradation of D53 regulates strigolactone signalling. Nature *504*, 406–410.

Zwanenburg, B., and Mwakaboko, A.S. (2011). Strigolactone analogues and mimics derived from phthalimide, saccharine, p-tolylmalondialdehyde, benzoic and salicylic acid as scaffolds. Bioorg. Med. Chem. *19*, 7394–7400.

Zwanenburg, B., Mwakaboko, A.S., Reizelman, A., Anilkumar, G., and Sethumadhavan, D. (2009). Structure and function of natural and synthetic signalling molecules in parasitic weed germination. Pest Manag. Sci. *65*, 478–491.

7 Appendix

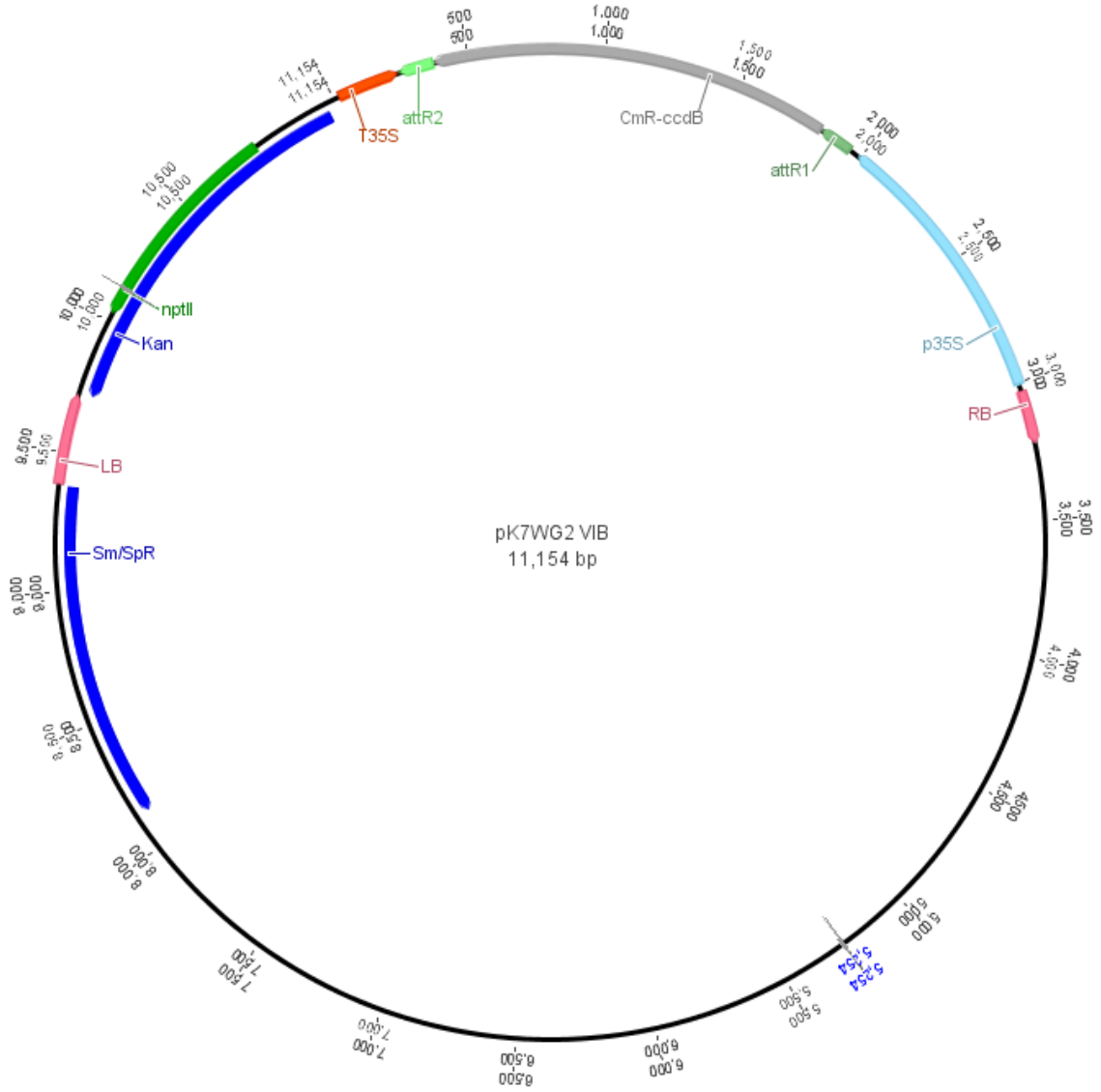

Fig. 7.1 Vector map of the binary Gateway vector pK7WG2. The vector was used as destination vector for cloning of the amiRNA constructs via an LR reaction. The T-DNA (flanked by left and right border sequences, LB and RB) contains the Gateway cassette (*CmR-ccdB*) flanked by *attR* sites, to be replaced with the gene of interest. Expression is driven by the CaMV 35S promoter (*p35S*) and terminated by the CaMV 35S terminator (*T35S*). A kanamycin resistance cassette for plant selection (*Kan*), including a separate promoter and terminator together with the *NPTII* kanamycin resistance gene, is also present on the T-DNA. For selection of bacteria, a spectinomycine resistance gene (*Sm/SpR*) is present on the vector backbone.

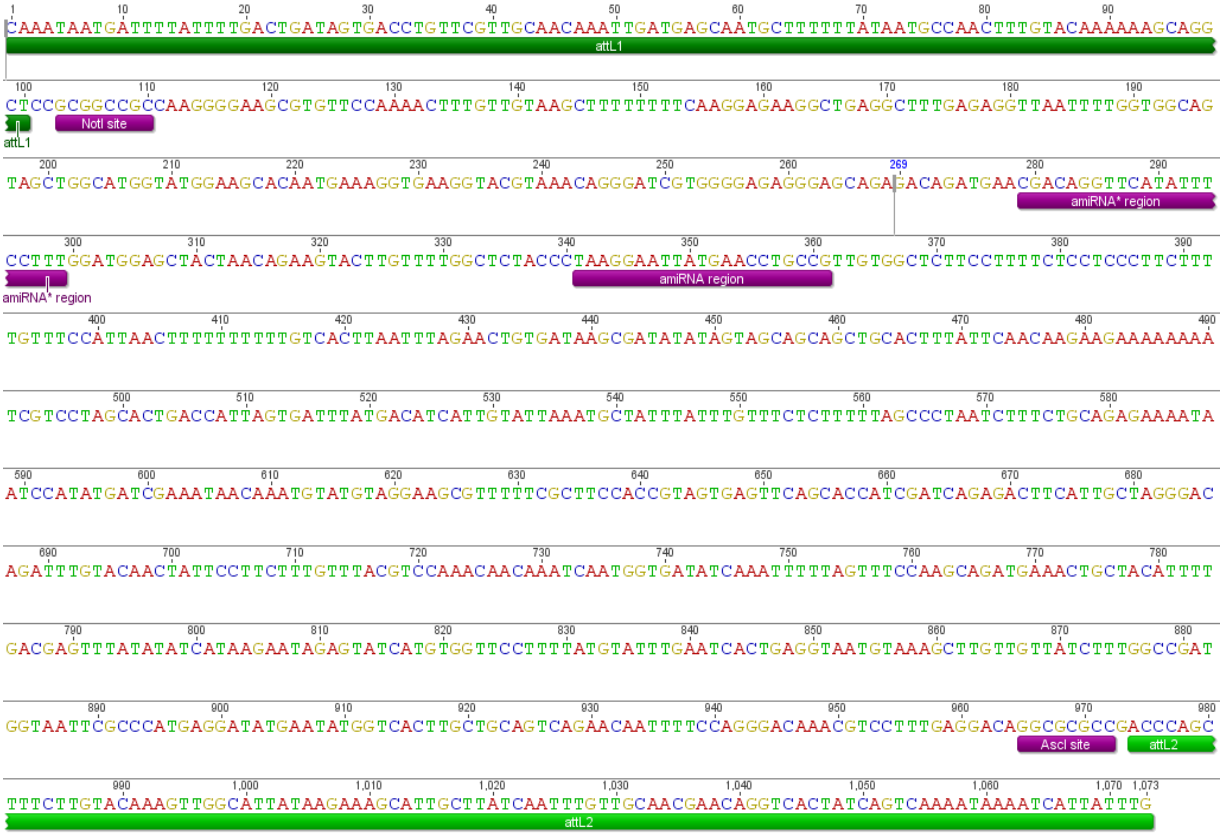

Fig. 7.2 Example for an amiRNA construct. The construct is flanked by *attL* sites for Gateway cloning as well as restriction sites for optional restriction-ligation cloning, as indicated. The amiRNA sequence is based on the natural *P. trichocarpa microRNA408* sequence. The *amiRNA* and *amiRNA** regions, which define the amiRNA target, were designed according to Tab. 2.6. The given example shows the sequence of *amiMAX4-1+2*.

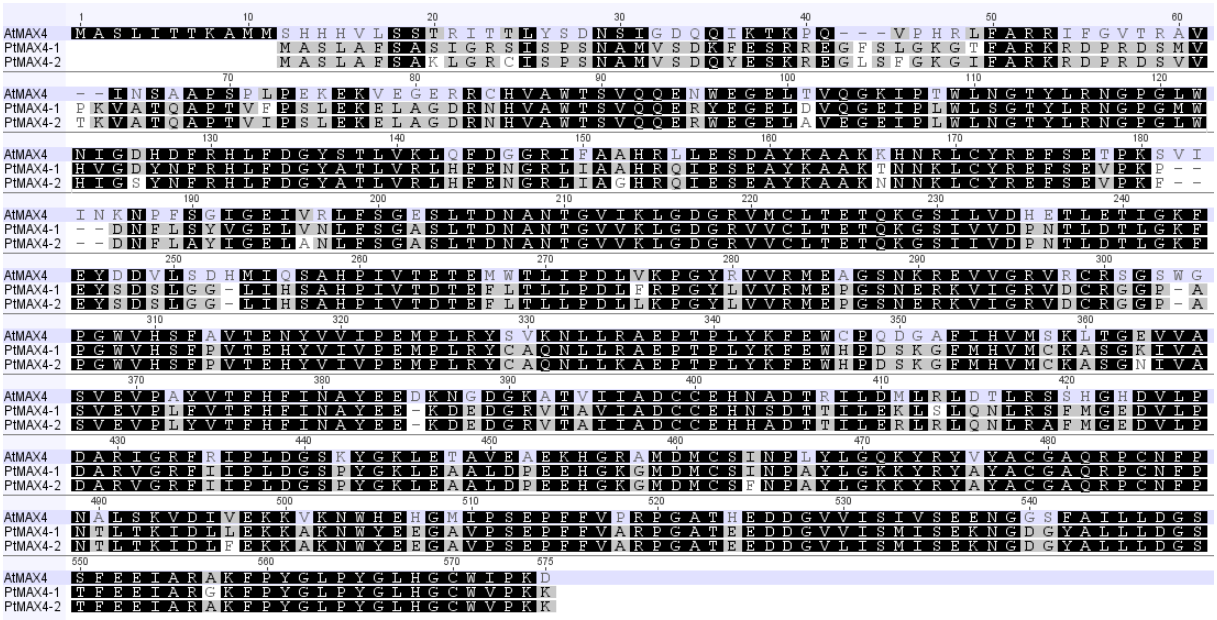

Fig. 7.3 Sequence alignment of *Arabidopsis MAX4* and its poplar orthologs *PtMAX4-1* and *PtMAX4-2*. Black background indicates similarity in all three sequences. The alignment was done using the Geneious 7.1.7 software. Sequences are noted in 5'-3' orientation.

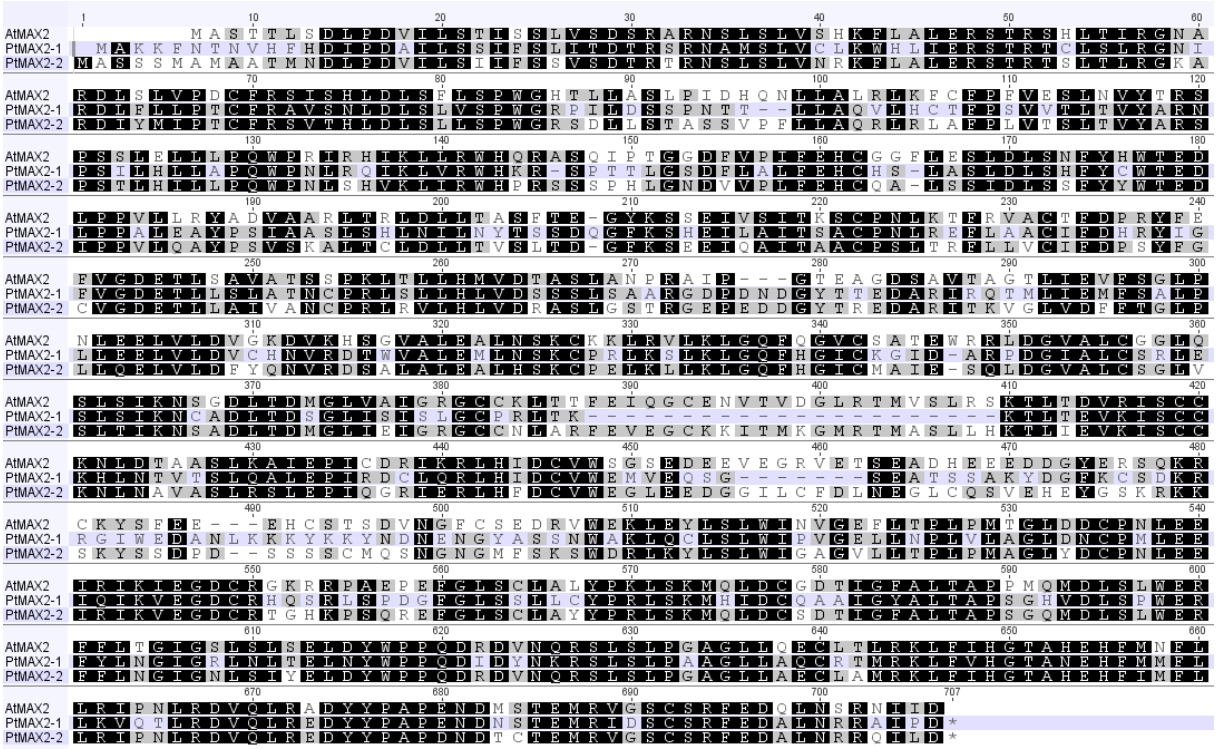

Fig. 7.4 Sequence alignment of *Arabidopsis MAX2* and its poplar orthologs *PtMAX2-1* and *PtMAX2-2*. Black background indicates similarity in all three sequences. The alignment was done using the Geneious 7.1.7 software. Sequences are noted in 5'-3' orientation.

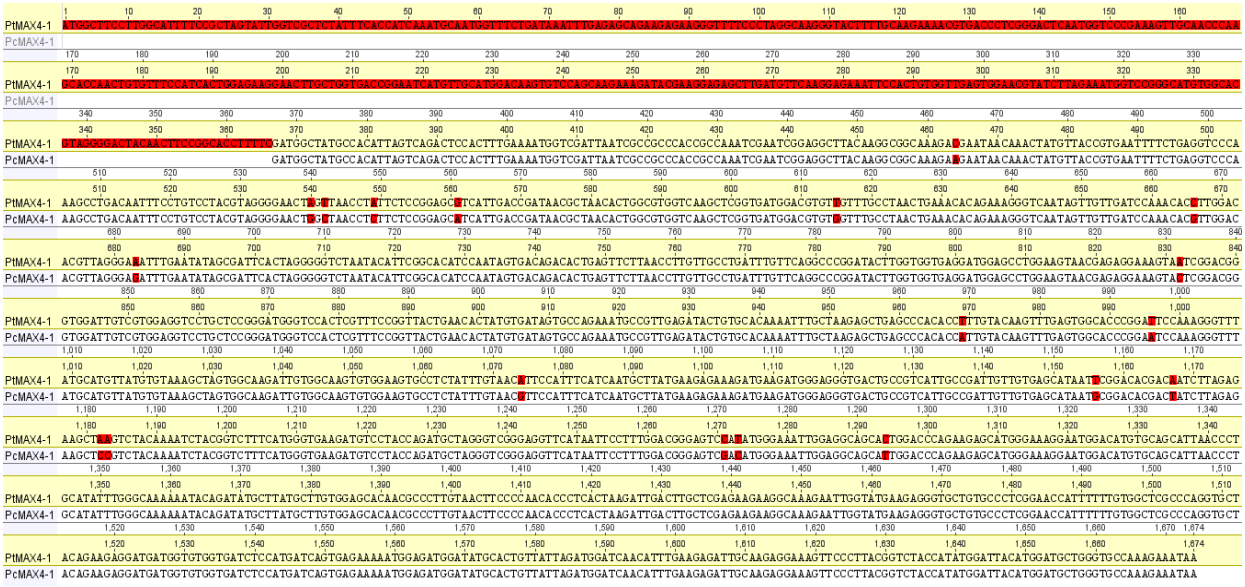

Fig. 7.5 DNA sequence alignment of *P. trichocarpa* (*Pt*) and *P.* x *canescens* (*Pc*) sequences of *MAX4-1*. The *Pc* sequence was obtained from a genomic clone. It was manually spliced and aligned with the *Pt* CDS to show only the relevant part of the gene. The 5' part of *PcMAX4-1* is missing since a full-length clone could not be obtained. Alignment was done using the Geneious 7.1.7 software. Sequences are noted in 5'-3' orientation. Red background indicates sequence differences.

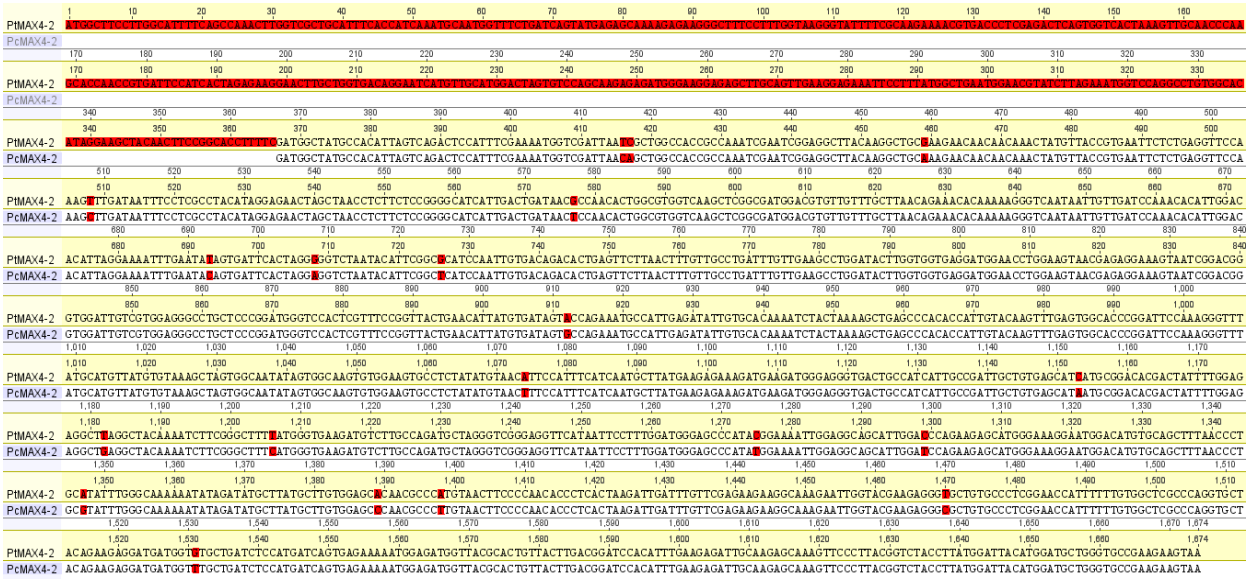

Fig. 7.6 DNA sequence alignment of *P. trichocarpa* (*Pt*) and *P.* x *canescens* (*Pc*) sequences of *MAX4-2*. The *Pc* sequence was obtained from a genomic clone. It was manually spliced and aligned with the *Pt* CDS to show only the relevant part of the gene. The 5' part of *PcMAX4-2* is missing since a full-length clone could not be obtained. Alignment was done using the Geneious 7.1.7 software. Sequences are noted in 5'-3' orientation. Red background indicates sequence differences.

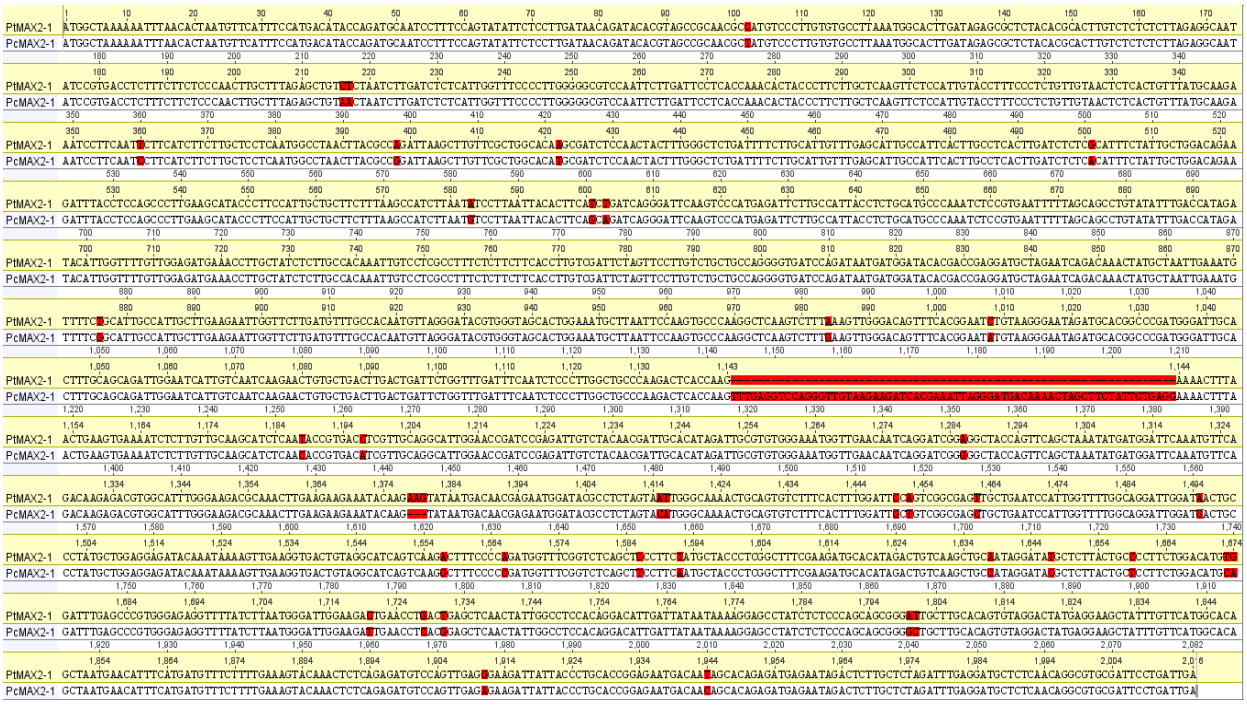

Fig. 7.7 DNA sequence alignment of *P. trichocarpa* (*Pt*) and *P.* x *canescens* (*Pc*) sequences of *MAX2-1*. Alignment was done using the Geneious 7.1.7 software. Sequences are noted in 5'-3' orientation. Red background indicates sequence differences.

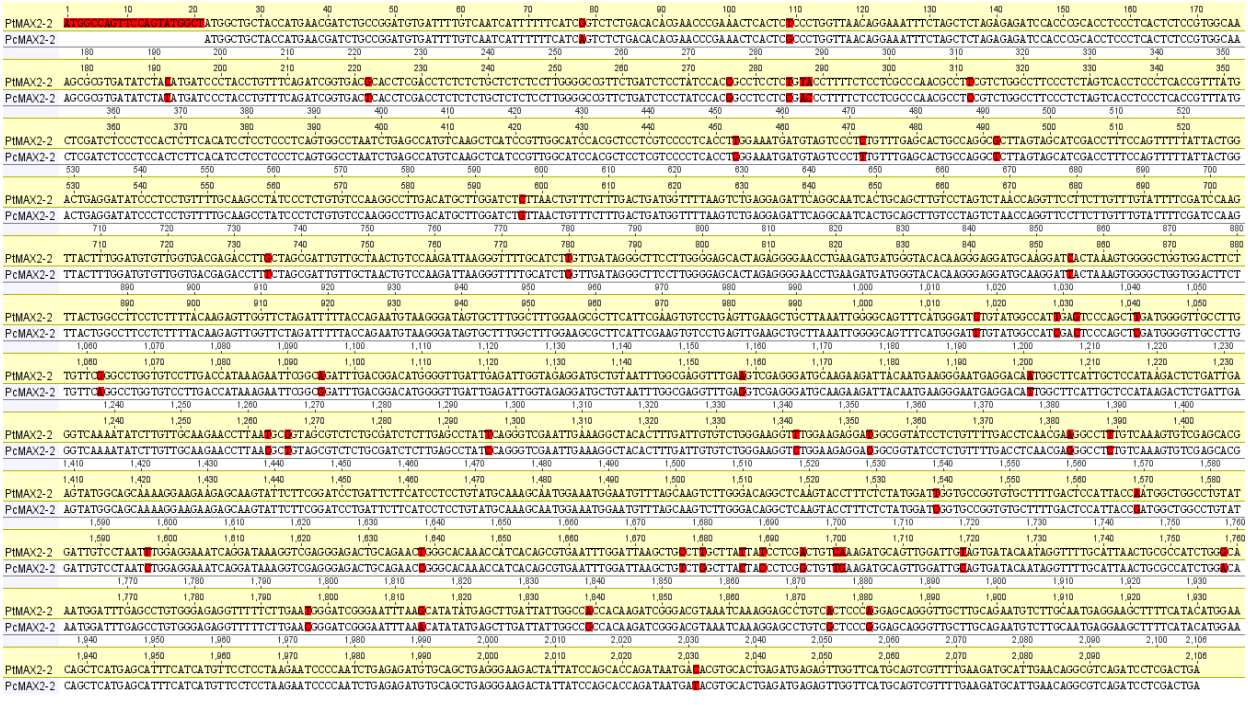

Fig. 7.8 DNA sequence alignment of *P. trichocarpa* (*Pt*) and *P.* x *canescens* (*Pc*) sequences of *MAX2-2*. Alignment was done using the Geneious 7.1.7 software. Sequences are noted in 5'-3' orientation. Red background indicates sequence differences.

Tab. 7.1 Overview about the transgenic *MAX4* and *MAX2* knockdown lines generated in this work. The amiRNA constructs were designed to target the two orthologs of each gene individually as well as simultaneously. The number of lines is given as the number of positive lines tested by PCR plus the number of lines positive in PCR, but containing residual *Agrobacterium*, e.g. "13+4". The latter therefore cannot be fully confirmed by PCR to be transgenic. A detailed list of all lines is given. Lines containing residual *Agrobacterium* are underlined. Lines grown and phenotyped under greenhouse-conditions are marked **bold**.

Construct	Target(s)	Number of independent transgenic lines and line abbreviations	
amiMAX4-1	*MAX4-1*	13+4	**T16#1A; T16#2A; T16#4A; T16#6B;** T16#8A; **T16#9A; T16#11A; T16#14A; T16#16A; T16#17A; T16#18A;** T16#23A; **T16#28A;** T16#30A; T16#31A; **T16#34A; T16#37A**
amiMAX4-2	*MAX4-2*	14+1	**T18#1B;** T18#4A; T18#5A; **T18#8A; T18#9A; T18#10A; T18#11A; T18#13A; T18#15A;** T18#16A; **T18#18A; T18#19B; T18#20A; T18#21A; T18#24A**
amiMAX4-1+2	*MAX4-1* *MAX4-2*	14+2	**T14#1A; T14#4A; T14#5B; T14#6A; T14#7A; T14#8A; T22#2A; T22#3A; T22#5A; T22#7C; T22#8A; T22#9A; T22#10A; T22#13A; T22#15A; T22#17A**
amiMAX2-1	*MAX2-1*	14+4	T19#1A; T19#2A; T19#3A; T19#4A; **T19#5B;** T19#6A; **T19#10B;** T19#13A; T19#14A; T19#16A; T19#20A; T19#21A; T19#22A; T19#23A; **T19#24B;** T19#28A; T19#34A; T19#36A
amiMAX2-2	*MAX2-2*	14+4	T20#1A; T20#3B; T20#4A; T20#5A; T20#6A; T20#7A; T20#8A; T20#10B; **T20#11A;** T20#13A; T20#14C; T20#15A; T20#16A; **T20#21A; T20#22A;** T20#23A; T20#24A ; T20#32A
amiMAX2-1+2	*MAX2-1* *MAX2-2*	12+0	T8#A; T8#B; T15#1A; T15#10A; T15#11A; **T15#15A;** T15#16A; T15#17A; T15#21A; **T15#23A; T15#25A; T15#28A**

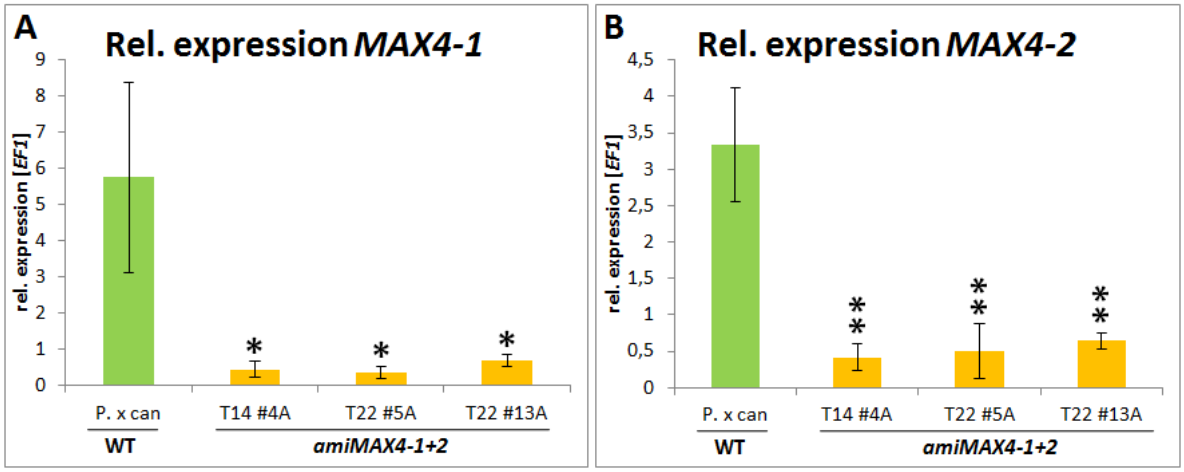

Fig. 7.9 Expression analysis of *MAX4-1* (A) and *MAX4-2* (B) in representative *amiMAX4-1+2* lines. Repetition of analysis. Expression levels were analyzed in the *P.* x *canescens* wild type and three representative *amiMAX4-1+2* double knockdown lines. Expression was normalized against the reference gene *EF1*. n= 3-5. Error bars indicate standard deviation. Asterisks indicate significant differences compared to the wild type (*P.* x *can*) according to Student's *t*-test. One and two asterisks indicate $p<0.05$ and $p<0.01$, respectively.

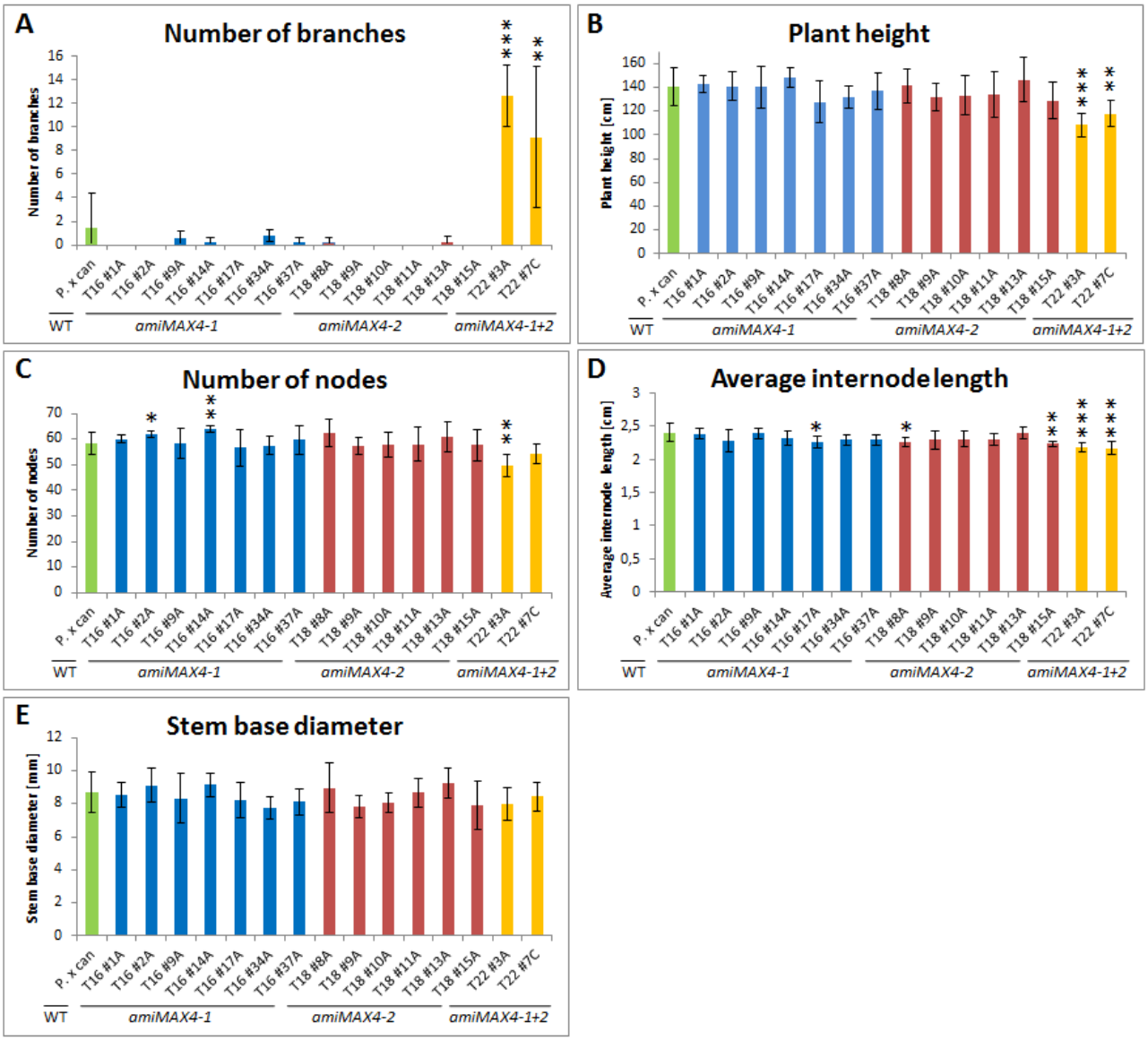

Fig. 7.10 Architectural traits of additional *amiMAX4* lines. The number of branches (A), the plant height (B), the number of nodes (C), the average internode length (D) and the stem base diameter (E) of additional *amiMAX4* lines were measured in greenhouse-grown plants. n= 4-10. Error bars indicate standard deviation. Asterisks indicate significant differences compared to the wild type (*P.* x *can*) according to Student's *t*-test. One, two and three asterisks indicate p<0.05, p<0.01 and p<0.001, respectively.

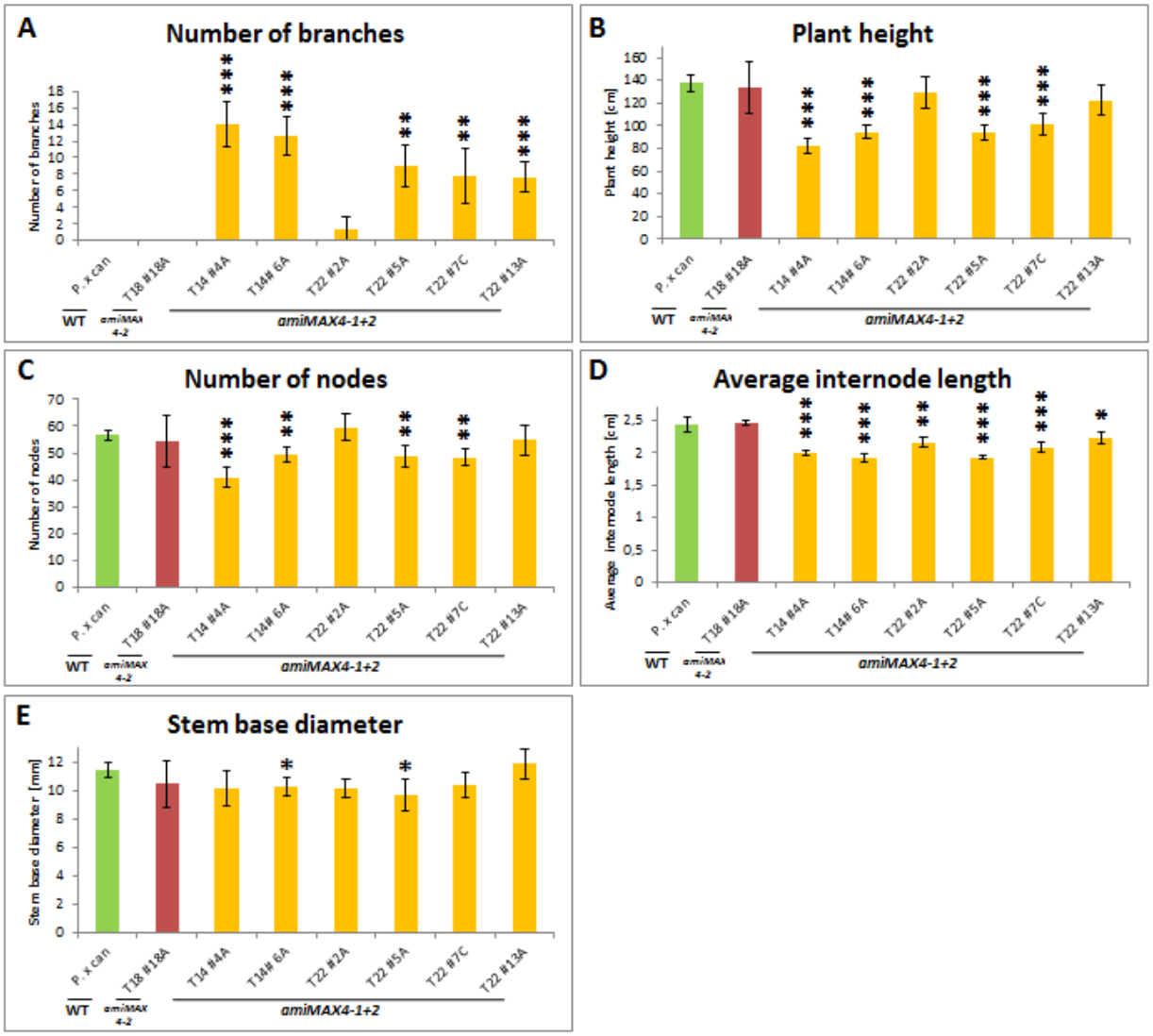

Fig. 7.11 Architectural traits of *amiMAX4* lines. Repetition of phenotyping for representative lines. The number of branches (A), the plant height (B), the number of nodes (C), the average internode length (D) and the stem base diameter (E) of selected *amiMAX4* lines were determined in 3.5 months old greenhouse-grown plants. n= 5, except for T22 #2A where n=3. Error bars indicate standard deviation. Asterisks indicate significant differences compared to the wild type (*P.* x *can*) according to Student's *t*-test. One, two and three asterisks indicate p<0.05, p<0.01 and p<0.001, respectively.

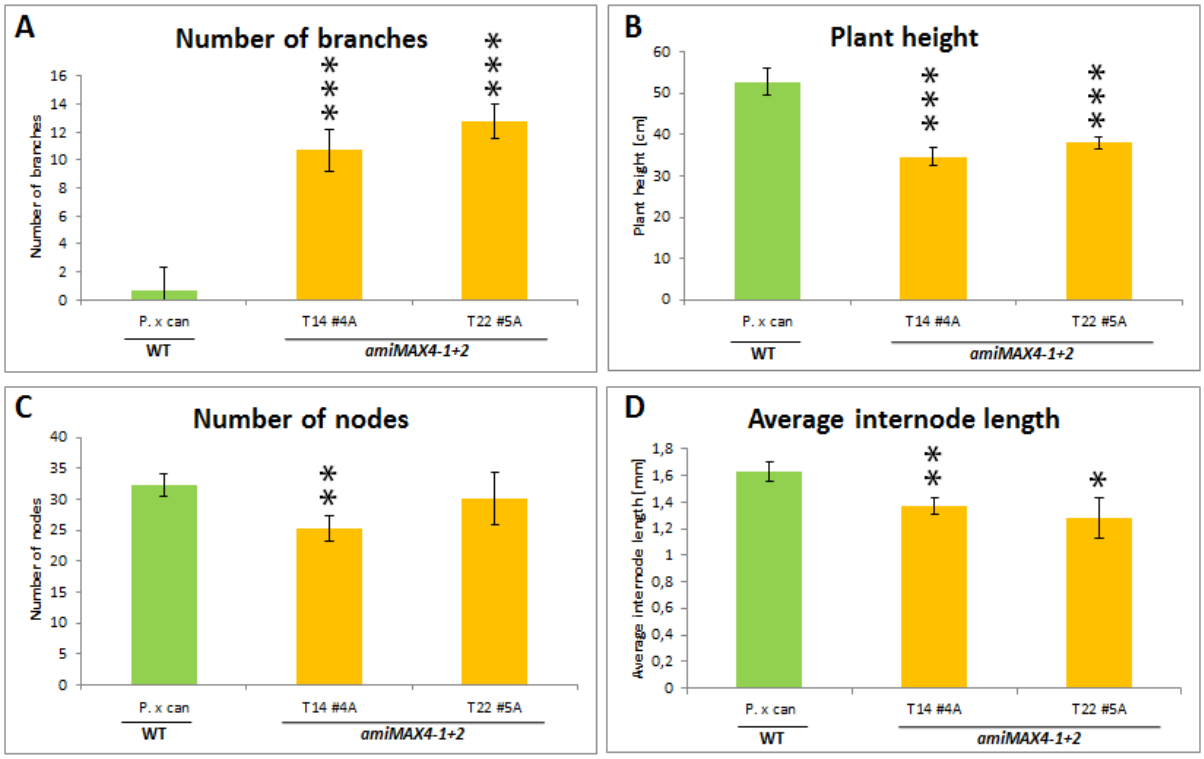

Fig. 7.12 Architectural traits of representative *amiMAX4* lines, grown in growth chamber conditions (replicate 1/2). The number of branches (A), the plant height (B), the number of nodes (C) and the average internode length (D) were determined. n= 3-6. Error bars indicate standard deviation. Asterisks indicate significant differences compared to the wild type (*P.* x *can*) according to Student's *t*-test. One, two and three asterisks indicate p<0.05, p<0.01 and p<0.001, respectively.

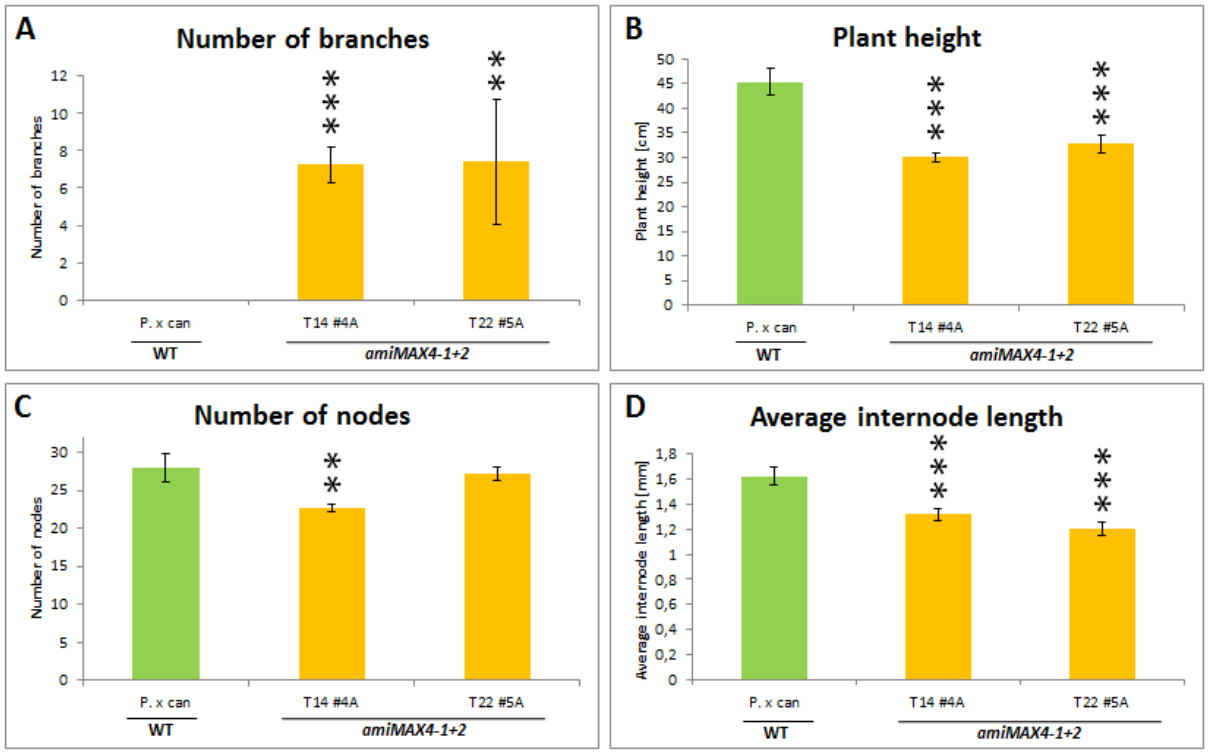

Fig. 7.13 Architectural traits of representative *amiMAX4* lines, grown in a growth chamber conditions (replicate 2/2). The number of branches (A), the plant height (B), the number of nodes (C) and the average internode length (D) were determined. n= 4-5. Error bars indicate standard deviation. Asterisks indicate significant differences compared to the wild type (*P.* x *can*) according to Student's *t*-test. One, two and three asterisks indicate $p<0.05$, $p<0.01$ and $p<0.001$, respectively.

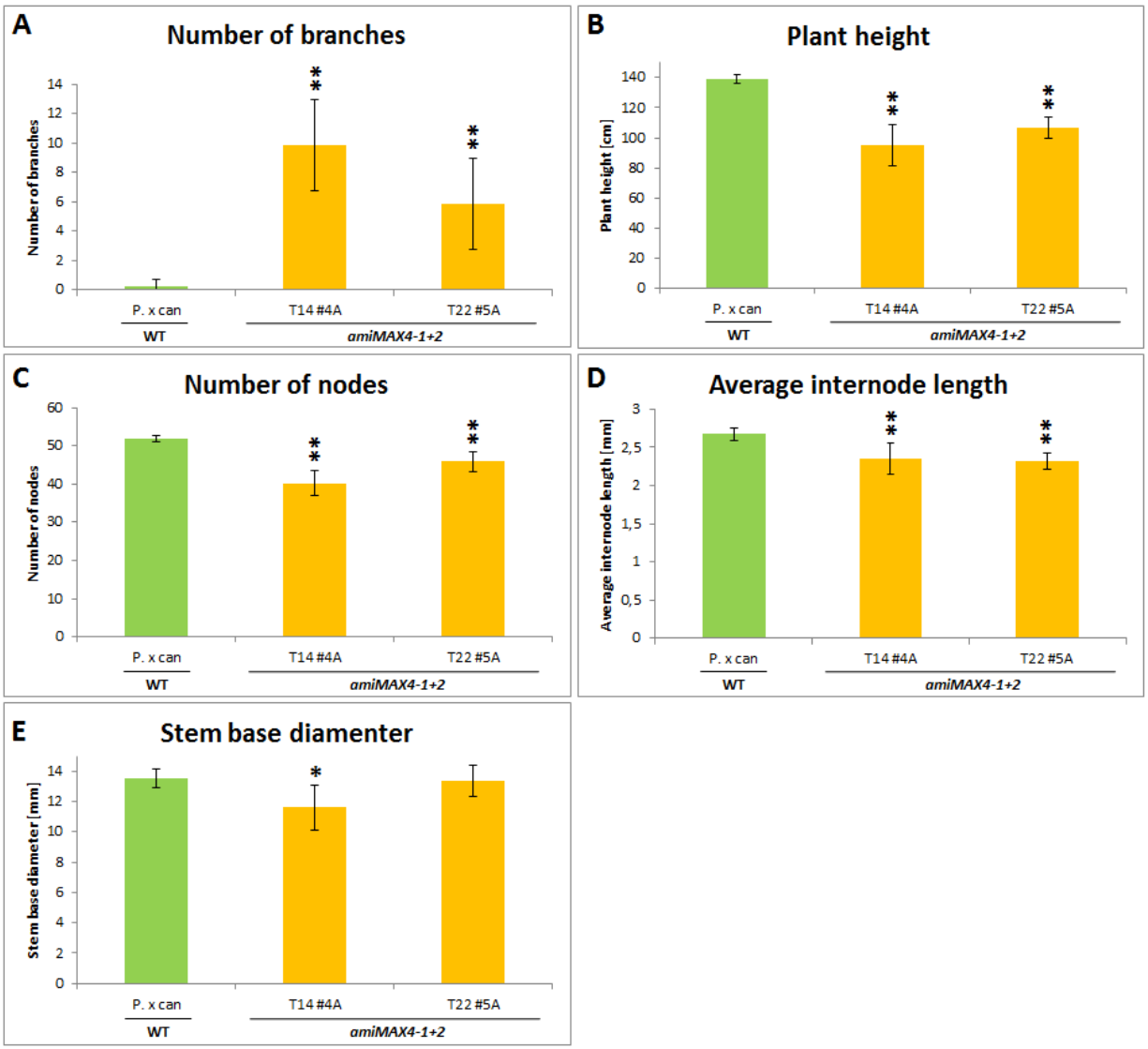

Fig. 7.14 Architectural traits of representative *amiMAX4* lines grown under outdoor conditions. The number of branches (A), the plant height (B), the number of nodes (C), the average internode length (D) and the stem base diameter (E) were determined after the first growing season. n= 4-8. Error bars indicate standard deviation. Asterisks indicate significant differences compared to the wild type (*P.* x *can*) according to Student's *t*-test. One and two asterisks indicate $p<0.05$ and $p<0.01$, respectively.

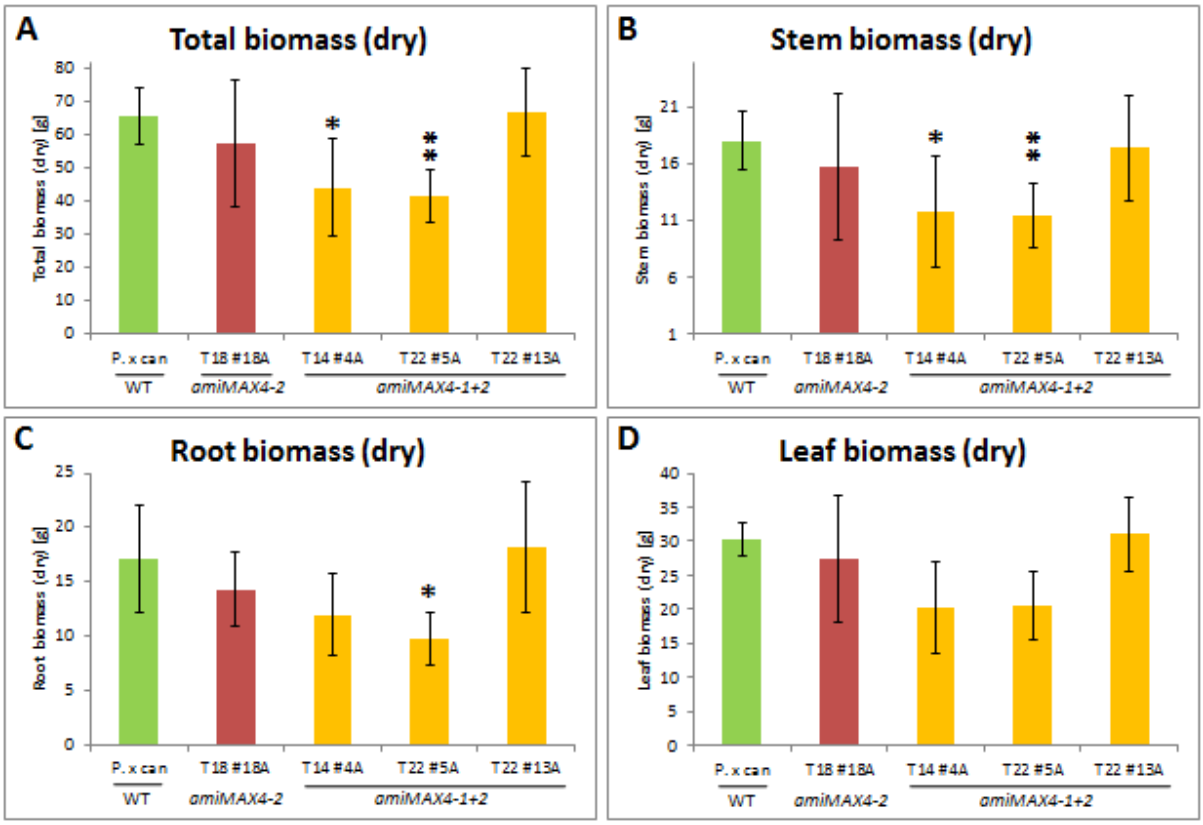

Fig. 7.15 Biomass parameters of *amiMAX4* lines: repetition of phenotyping for selected lines. The total dry biomass of the plants (A), as well as the separate dry weights of the stem (including branches) (B), the roots (C) and the leaves (including leaves from the branches) (D), were determined. n= 5. Error bars indicate standard deviation. Asterisks indicate significant differences compared to the wild type (*P.* x *can*) according to Student's *t*-test. One and two asterisks indicate $p<0.05$ and $p<0.01$, respectively.

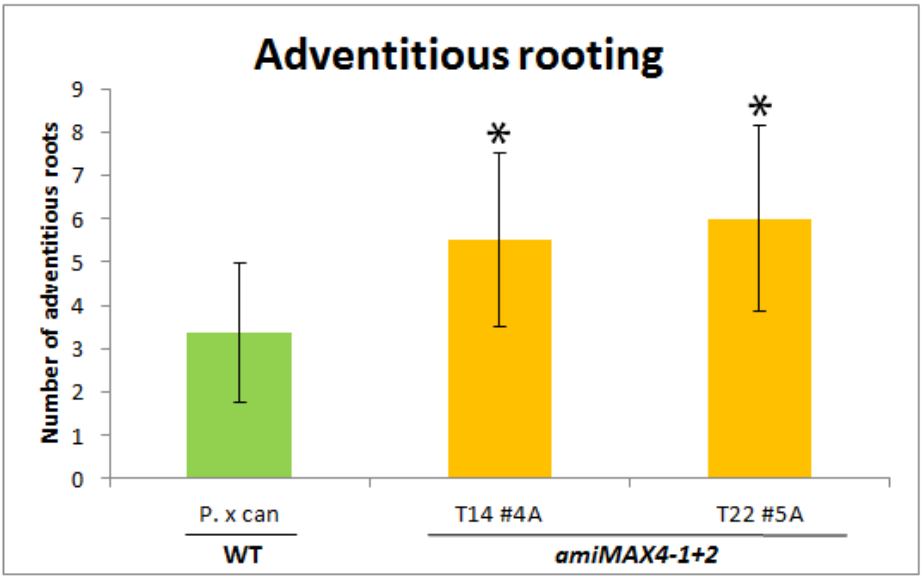

Fig. 7.16 Adventitious rooting in representative *amiMAX4-1+2* lines. Repetition of phenotyping. The number of adventitious roots was counted for *in vitro* grown cuttings of the representative *amiMAX4-1+2* lines T14 #4A and T22 #5A as well as the *P.* x *canescens* wild type. Cuttings were 7 weeks old. n=8. Error bars indicate standard deviation. Asterisks indicate significant differences compared to the wild type according to Student's t-test with $p<0.05$.

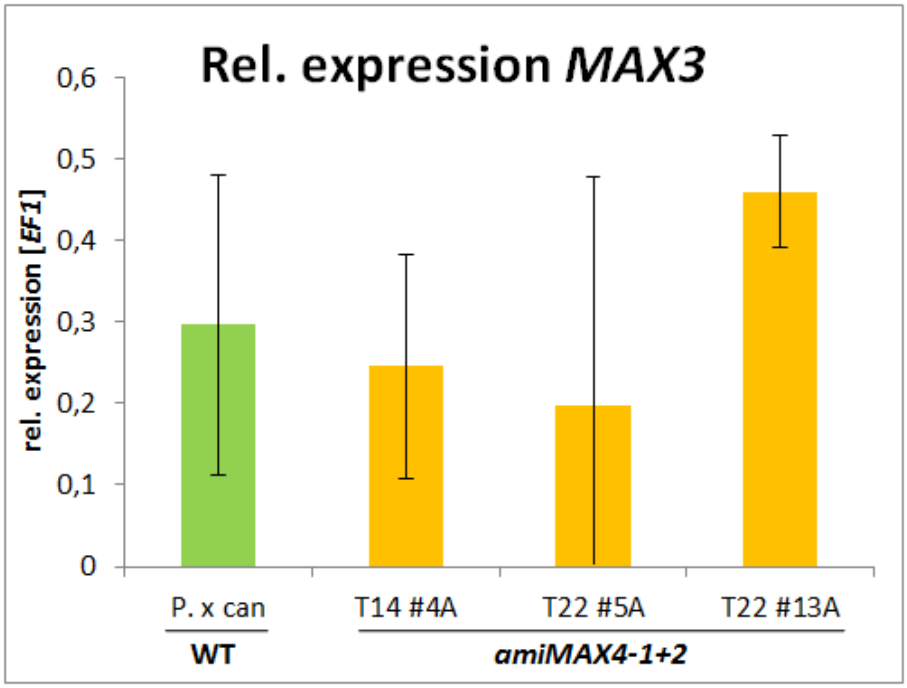

Fig. 7.17 Expression analysis of *MAX3* in representative *amiMAX4-1+2* lines. Repetition of analysis. Expression levels were analyzed in the *P.* x *canescens* wild type and three representative *MAX4-1+2* double knockdown lines. Expression was normalized against the reference gene *EF1*. n= 3-5, except for T22 #5A where n=2. Error bars indicate standard deviation. A Student's *t*-test did not reveal any significant differences between *amiMAX4-1+2* lines and the wild type.

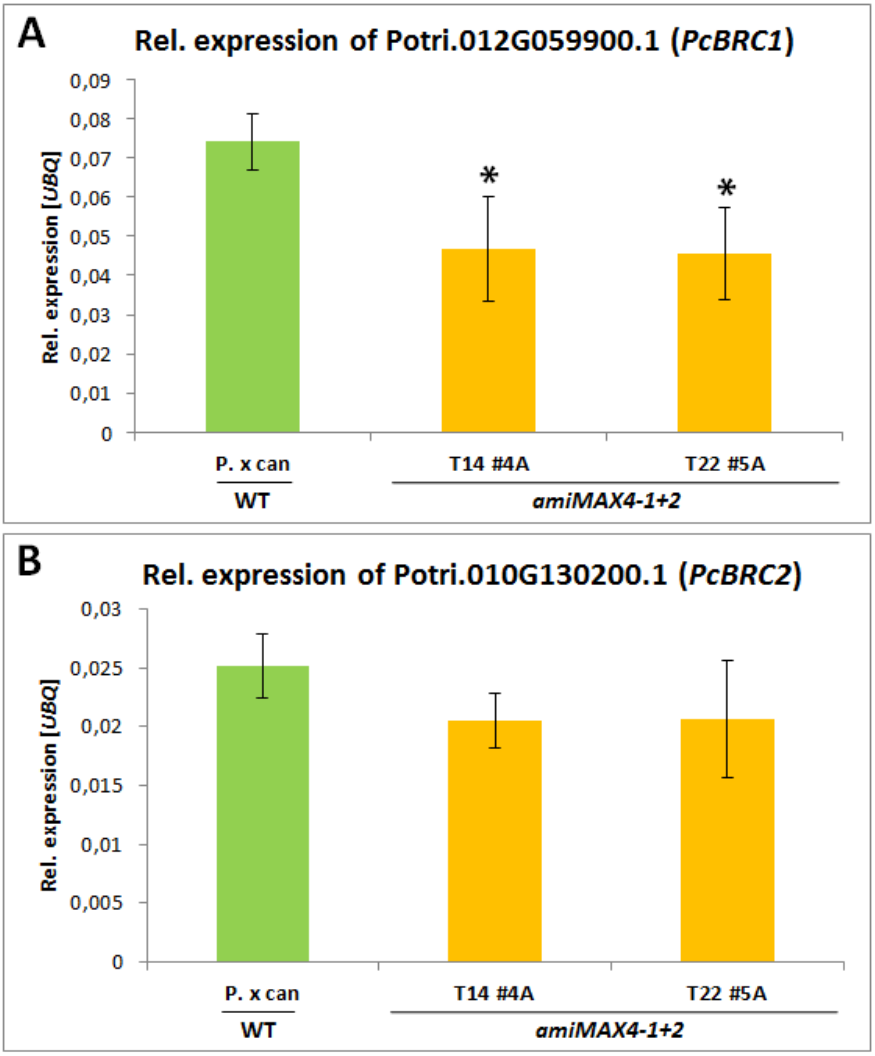

Fig. 7.18 Expression of putative *P.* x *canescens BRC1* (A) and *BRC2* (B) orthologs in dormant axillary buds of greenhouse-grown plants. Repetition of analysis. Expression was determined in the wild type (*P.* x *can*) and two representative *amiMAX4-1+2* double knockdown lines. Expression was normalized against the reference gene *UBQ*. n= 3-4. Error bars indicate standard deviation. Asterisks indicate significant differences compared to the wild type according to Student's t-test with $p<0.05$.

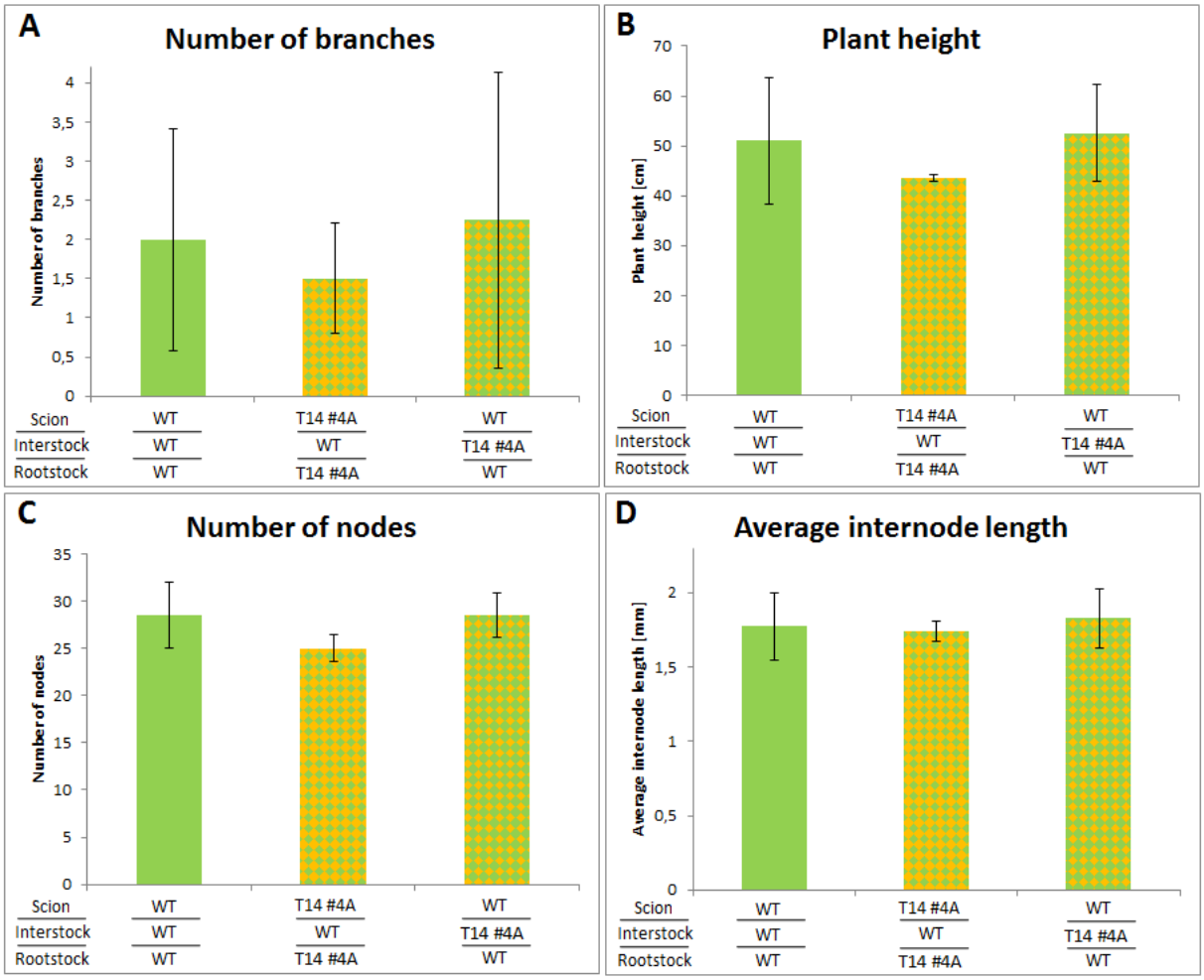

Fig. 7.19 **Architectural traits of interstock-grafted poplar plants.** For grafting, the *P.* x *canescens* wild type as well as the representative *amiMAX4-1+2* line T14 #4A were used. The upper label indicates the genotype of the scion, the middle label shows the genotype of the interstock and the lower label specifies the genotype of the rootstock. The genotypes are also highlighted by the coloring of the bars. The number of branches (A), the plant height (B), the number of nodes (C) and the average internode length (D) were determined for greenhouse-grown plants. n= 2-4. Error bars indicate standard deviation. A Student's *t*-test did not reveal any significant differences between all grafting combinations.

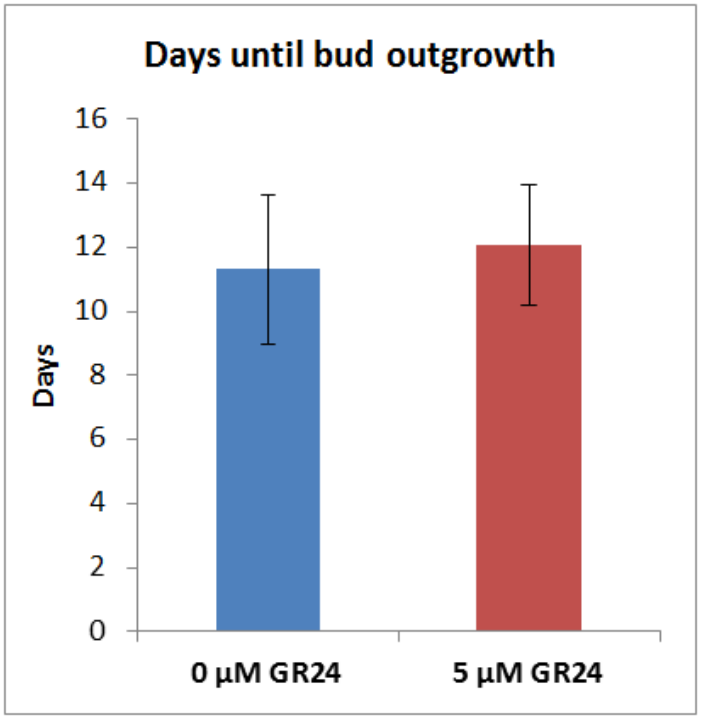

Fig. 7.20 Bud outgrowth of *P.* x *canescens* stem cuttings after 5 µM GR24 treatment. Repetition of experiment. The time point from preparation of the cuttings until outgrowth of their bud was recorded on medium containing no (0 µM) or 5 µM GR24. n=24-29. Error bars indicate standard deviation. A Student's *t*-test did not result in any significant difference between mock- and GR24-treated cuttings.

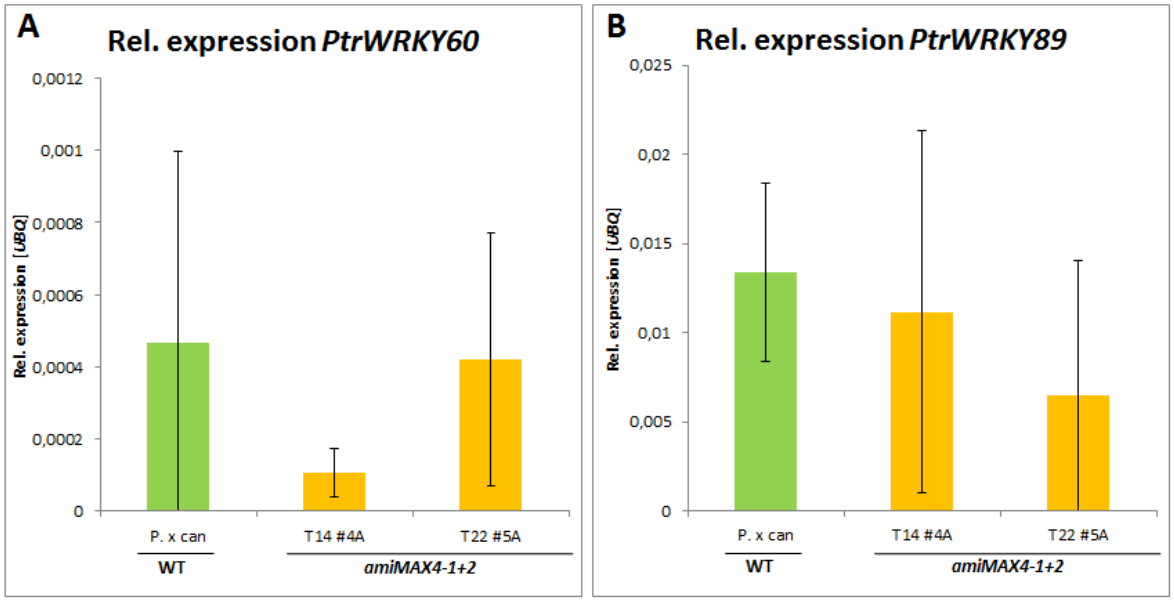

Fig. 7.21 Relative expression of the SA-marker genes *PtrWRKY60* (Potri.018G019700) (A) and *PtrWRKY89* (Potri.006G109100) (B). Expression levels were analyzed in the *P.* x *canescens* wild type and the representative *amiMAX4-1+2* lines T14 #4A and T22 #5A. Expression was normalized against the reference gene *UBQ*. n= 3-4. Error bars indicate standard deviation. A Student's *t*-test did not result in any significant differences between the *amiMAX4-1+2* lines compared to the wild type.

Acknowledgements

First of all, I like to thank everybody who supported me during my doctoral studies, also those people who I may have forgot to mention below.

I would like to sincerely thank PD Dr. Thomas Teichmann for giving me the opportunity to work on this interesting project and for the excellent supervision. His relaxed way of supervision was highly appreciable. I was free in developing my ideas as well as planning, executing and evaluating my work independently, but he was always available for fruitful discussions and advice, whenever this was required. Thanks a lot!

I thank Prof. Dr. Andrea Polle and Jun. Prof. Dr. Cynthia Gleason for being members of my examination board, as well as for providing helpful comments and suggestions concerning the project as members of my thesis committee.
Thanks to Prof. Dr. Volker Lipka for giving me the opportunity to work in his department and being member of my examination board.
Furthermore, I also like to thank the other members of my examination board, Prof. Dr. Christiane Gatz and Prof. Dr. Stefan Jakobs.

I like to thank the members of the "poplar lab". Nele Prüfer provided excellent technical assistance throughout the experiments and affectionately took care of the poplar *in vitro* culture (her "babies" ☺). Elisabeth Störzel, Benedikt Franke and Greta Niemann participated in the project during their Bachelor's theses and generated valuable results.

I like to thank all previous and current members of the Lipka lab for the very friendly working atmosphere and collaboration. Thank you Anja Auspurg, Sina Bargahn, Jan Erwig, Benedikt Franke, Dr. René Fuchs, Bianca Genenncher, Dr. Hassan Ghareeb, Felicitas Glasenapp, Ronja Hacke, Katharina Hanika, Ludmilla Heck-Hrarti, Melanie Klenke, Dr. Michaela Kopischke, Samuel Kroll, Stefan Kusch, Sabine Laukamm, Prof. Dr. Volker Lipka, Susanne Meester, Christopher Meusel, Greta Niemann, Dr. Elena Petutschnig, Nele Prüfer, Dr. Michael Reusche, Dr. Charlotte Roth, Gabriele Schauermann, Inga Sjuts, Dimitri Stepanets, Marnie Stolze, Elisabeth Störzel, PD Dr. Thomas Teichmann, Karin Thole, Jekaterina Truskina, Uwe Wedemeyer, Dr. Marcel Wiermer, Sabine Wolfarth and Yvonne Ziegler.

Thanks to the neighbors from the Gleason lab for the pleasant atmosphere, too: Birthe Barke, Prof. Dr. Cynthia Gleason, Natthanon Leelarasamee, Dr. Martin Muthreich, Frederik Polzin, Rania Saleh and Dr. Jan Utermark.
I really enjoyed the past three years.

Furthermore, I thank the gardeners of the institute for support during plant cultivation in the greenhouse, most notably Felicitas Glasenapp, Uwe Wedemeyer and Susanne Meester. Thanks to Prof. Dr. Andrea Polle and the gardener Marianne Smiatacz for providing greenhouse space at the forestry institute and taking care of the plants.

Thanks to Dr. Dennis Janz for support with the statistical analysis.

I thank Tobias Brügmann and Prof. Dr. Matthias Fladung for showing me how to successfully produce transgenic poplar lines (it worked- finally ☺), and all the other members of the PopMASS consortium for the good collaboration.

I thank the BMBF for funding of the project. Additional funding was provided by the GGNB. The latter also provided helpful skills- and methods courses, as well as industry excursions. It was an appreciable platform for exchange with other doctoral students from different fields, encouraging the organization of annual retreats and the “Cells Stammtisch”.

Last but not least, I thank my family and friends for support throughout my whole studies. You were backing me up whenever I needed support.

Vielen Dank!

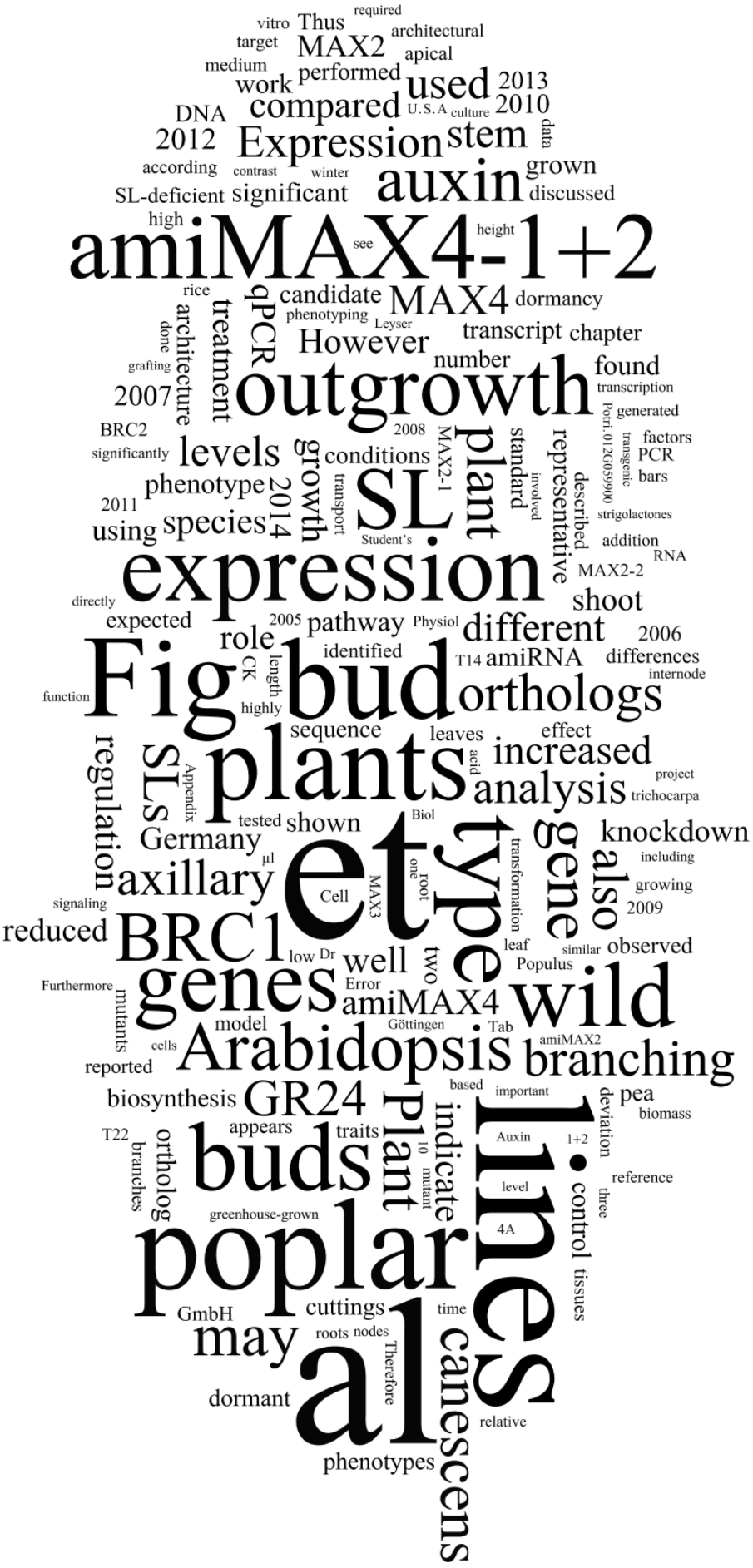
required
vitro
Thus
architectural
target
MAX2
apical
medium
performed
work
used
2013
compared
U.S.A
culture
2010
DNA
2012
Expression
stem
data
according
contrast
winter
auxin
grown
SL-deficient
significant
discussed
high
amiMAX4-1+2
see
height
rice
qPCR
candidate
MAX4
dormancy
phenotyping
Leyser
architecture
done
treatment
However
transcript
chapter
grafting
number
found
2007
outgrowth
transcription
Potri.012G059900
generated
BRC2
2008
MAX2-1
standard
factors
significantly
levels
growth
conditions
representative
PCR
transgenic
phenotype
2014
transport
SL
plant
involved
bars
described
2011
using
species
Student's
strigolactones
addition
RNA
expression
MAX2-2
directly
shoot
expected
2005
pathway
Physiol
different
2006
role
identified
T14
amiRNA
differences
internode
Fig
bud
orthologs
function
CK
length
highly
sequence
leaves
effect
plants
increased
regulation
SLs
Appendix
acid
analysis
project
trichocarpa
tested
shown
Biol
Germany
knockdown
µl
type
gene
axillary
one
root
Cell
MAX3
transformation
including
also
growing
signaling
2009
reduced
BRC1
low
Dr
well
two
leaf
similar
observed
Furthermore
Error
Populus
genes
amiMAX4
wild
mutants
model
Göttingen
Tab
cells
amiMAX2
Arabidopsis
branching
reported
based
important
biosynthesis
GR24
pea
deviation
biomass
lines
Plant
indicate
appears
traits
Auxin
1+2
T22
buds
orthologs
branches
10
mutant
level
reference
three
greenhouse-grown
4A
control
tissues
poplar
GmbH
cuttings
time
may
roots
nodes
Therefore
canescens
dormant
relative
phenotypes